Strength and Resistivity Properties of Fouled Ballast

By

Madan Neupane

Bachelor of Civil Engineering, Institute of Engineering,

Tribhuvan University, Nepal, 2007

Submitted to
The Department of Civil, Environmental, and Architectural Engineering and
Graduate Faculty of the University of Kansas in partial fulfillment of the requirements for the degree of Master of Science

……

Dr. Robert L. Parsons, Chairperson

Committee Members

……..

Dr. Jie Han

…….

Dr. Anil Misra

Date Defended: 01/07/2015

The Thesis Committee for Madan Neupane certifies that this is the approved version of the following thesis:

Strength and Resistivity Properties of Fouled Ballast

……

Dr. Robert L. Parsons, Chairperson

Committee Members

……..

Dr. Jie Han

…….

Dr. Anil Misra

Date Approved: 01/07/2015

Dedicated to my parents,

Keshab Prasad Neupane and Mrs. Indira Devi Neupane

Abstract

Maintaining rail track in good condition is essential for ensuring the overall performance and safety of railway operations. Track support, structural integrity, and effectiveness of the foundation structure depend on the characteristics and performance of the ballast and sub-ballast layers. The ballast of the rail track may be fouled due to intrusion of fine particles from outside the ballast as well as particles produced within the layer due to breakage over time. This fouling can cause track support degradation and permanent settlement. Studies show that about one third of the total freight operation cost is invested for the track maintenance. Therefore, methods for locating and characterizing fouling that are faster, more effective, and less expensive would be valuable to the industry. Since there are limited methods for fouling detection and these methods are time consuming, tedious and require significant manpower; a simple approach of identification of ballast fouling within a few minutes at low cost is discussed in this report.

Stone dust from ballast degradation caused by wear and tear of the ballast; intrusion of coal dust due to spillage from train cars; and extrusion of fine particles from the subgrade are the major contributors to ballast fouling. These particles have the capability to retain moisture and hence reduce the friction between ballast particles. Previous studies show that the fouled ballast electrical resistivity and hydraulic conductivity have certain relationships that can be used to define the amount of fouling of the ballast. The fouling agents retain moisture which acts as the medium of electrical conductivity, since there is almost no flow of electricity through the air voids or solid ballast particles of the ballast layer. So, it is proposed that ballast fouling be estimated by measuring the resistivity of the ballast. Static modulus, resilient modulus and California bearing ratio (CBR) were also investigated to determine the impact of the ballast fouling on strength properties.

A vertical probe was designed at the University of Kansas (KU); Civil, Environmental and Architectural Engineering department to measure the resistivity of the fouled ballast. The probe was tested using both horizontal and vertical configurations and worked well for estimating resistivity using the fall of potential method. Forty-eight test samples of fouled ballast were prepared in a box of almost 11 cubic feet size with different degrees of fouling and with various moisture contents. Resistivity tests using a Wenner 4 probe array in horizontal alignment and fall of potential method with a vertical probe and vertical alignment were carried out. Also, the light weight deflectometer (LWD) test for the measurement of resilient modulus, static plate loading test for determination of static modulus, and dynamic cone penetration (DCP) test for California bearing ratio (CBR) estimation were carried out.

The results from the vertical probe were consistent on most of the test samples when the Wenner 4 point array method. A boundary moisture content – termed as optimum moisture content for resistivity (OMCR) was determined. The OMCR values were 6% for subgrade soil fouled ballast, 5% for Gardner track ballast dust fouled ballast, and 5.5% of coal dust fouled ballast. The resistivity of the fouled ballast can be estimated for moisture contents greater than OMCR. The resilient modulus, static modulus and the CBR of the ballast decreased significantly for moisture contents greater than OMCR. Static and resilient moduli peaked near the OMCR for all types of fouling while the CBR was constant to slightly increasing with moisture content up to the OMCR.

Acknowledgements

I would like to express my deepest gratitude to my advisor, Professor Robert L. Parsons, for giving me the opportunity to work on this research and for guiding me personally as well as professionally to meet the academic challenges. His tutelage always guides and motivates me to strive for and achieve useful skills for my future careers. I would also like to express my deep appreciation to Professors Jie Han and Anil Misra for their valuable suggests and feedback on the development and completion of this thesis and for serving as members on my examining committee.

I would like to thank Mid-America Transportation Center (MATC) for providing financial support for this research. I am also grateful to Mr. Hank Lees of BNSF for proving the fouled sample ballast needed for the test and Michael A. Wnek of BNSF for coordinating and guiding in field trip. I would also like to thank Mr. Matthew Maksimowicz, Eric Nicholson, and David Woody for their technical support. I would also like to express my thanks to Mr. Zachary Aaron Brady (undergraduate research assistant), Krisna Prasad Ghimire, Deep K. Khatri, Jun Geo and other individuals who contributed to the completion of this research thesis both directly and indirectly and for their help in the physical testing. The authors would like to express their appreciations to the organizations and the individuals for their help and support.

Finally, I would like to thank my family and friends for their endless supports and love.

Table of Contents

ABSTRACT ..... **II**

ACKNOWLEDGEMENTS ..... **IV**

TABLE OF CONTENTS ..... **V**

LIST OF TABLES ..... **XI**

LIST OF FIGURES ..... **XIII**

CHAPTER ONE: INTRODUCTION **1**

1.1. BACKGROUND 1

1.2. PROBLEM STATEMENT 2

1.3. RESEARCH OBJECTIVE 4

1.4. (FUKUE, MINATOA, HORIBE, & TAYA, 1999) RESEARCH METHODOLOGY 4

1.5. THESIS ORGANIZATION 5

CHAPTER TWO: LITERATURE REVIEW **7**

2.1. INTRODUCTION OF FOULED BALLAST 7

2.2. EFFECTS OF FOULED BALLAST 8

2.3. RESISTIVITY OF FOULING AGENTS 11

2.4. MEASUREMENT MODULE OF ELECTRICAL RESISTANCE OF FOULED BALLAST 14

2.5. RESISTANCE MEASUREMENT OF FOULED BALLAST AT LAB AND FIELD 18

2.6. FACTORS AFFECTING SOIL RESISTIVITY 19

2.7. RESILIENT MODULUS OF BALLAST 21

2.8. CALIFORNIA BEARING RATIO (CBR) OF BALLAST 22

2.9. SHEAR STRENGTH PROPERTIES OF BALLAST 23

CHAPTER THREE: DETERMINATION OF MATERIAL PROPERTIES 25

3.1. ENGINEERING PROPERTIES OF CLEAN BALLAST 25

3.1.1. General Information about Ballast 25

3.1.2. Gradation of Clean Ballast 27

3.1.3. Other Engineering Properties 28

3.2. ENGINEERING PROPERTIES OF SUBGRADE SOIL 30

3.2.1. General Information about Subgrade Soil 30

3.2.2. Gradation of Subgrade Soil 31

3.2.3. Other Engineering Properties of Subgrade Soil 32

3.3. ENGINEERING PROPERTIES OF COAL DUST 32

3.3.1. General Information about Coal Dust 32

3.3.2. Gradation of Coal Dust 34

3.3.3. Other Engineering Properties of Coal Dust 35

3.4. ENGINEERING PROPERTIES OF GARDNER TRACK BALLAST DUST 36

3.4.1. General Information about Gardner Track Ballast Dust 36

3.4.2. Gradation of Gardner Track Ballast Dust 37

3.4.3. Other Engineering Properties of Gardner Track Ballast Dust 38

3.5. COMPARISON OF BASIC ENGINEERING PROPERTIES OF FOULING AGENTS 39

3.6. ELECTRICAL RESISTIVITY OF FOULING AGENTS 41

3.6.1. Small Box Resistivity Test of Fouling Materials 41

3.6.2. Sample Preparation and Testing 43

3.6.3. Resistivity Test Results 44

3.7. ENGINEERING PROPERTIES OF FIELD BALLAST 44

3.7.1. General 44

3.7.2. Gradation of the Ballast and Fouling Index 45
3.7.3. Field Moisture Content 47
3.8. QUANTIFICATION OF FOULED BALLAST 47

CHAPTER FOUR: TEST SETUP AND DATA COLLECTION 49

4.1. LAB TEST SET UP FOR MOISTURE VARIATION SAMPLE 49
4.1.1 Sample Descriptions 49
4.1.2 Calculation of Fouling Index of ballast samples 50
4.1.3 Mixing Procedure 51
4.1.4 Box Filling Procedure and Compaction 52
4.1.5 Bulk Density Calculation 53
4.1.6 Tests Sequence and Tests Location 53
4.2. HORIZONTAL PROBE RESISTANCE MEASUREMENT 55
4.2.1 Construction of Horizontal Probe 55
4.2.2 AEMC Ground Resistance Tester 56
4.2.3 Horizontally Aligned Probe Resistance Measurement by Wenner Four Point Method 57
4.2.4 Horizontally aligned Probe Resistance Measurement by Single Electrode Method 57
4.3. VERTICAL PROBE RESISTANCE MEASUREMENT 58
4.3.1 Construction of Vertical Probe 58
4.3.2 Vertical Probe Resistance Measurement by Three Point Method 62
4.4. RESILIENT MODULUS MEASUREMENT BY LWD 63
4.4.1 Light Weight Deflectometer 63
4.4.2 Modulus Measurement by LWD Method 65
4.5. CALIFORNIA BEARING RATIO (CBR) MEASUREMENT BY DCP 65
4.5.1 Dynamic Cone Penetrometer 65
4.5.2 California Bearing Ratio (CBR) Estimation by DCP 65

4.6. STIFFNESS MODULUS DETERMINATION BY STATIC PLATE LOADING TEST 67
4.6.1 Static Plate Loading Test 67
4.6.2 Plate Loading Test Procedure 68
4.7. CBR CALCULATION BY VERTICAL PROBE AFTER CORRELATION WITH DCP 69
4.8. MOISTURE CONTENT AND DRY DENSITY OF THE MIX 70
4.9. OPTIMUM MOISTURE CONTENT FOR FOULED SAMPLES 70
4.10. FIELD TEST PROCEDURE 71
4.10.1 General Comments about Field Testing 71
4.10.2 Resistance Measurement by Ground Tester 73
4.10.3 Dynamic Cone Penetration Test 73
4.10.4 Light Weight Deflectometer Test 74

CHAPTER FIVE: RESULTS AND DISCUSSION 75

5.1. ASSUMPTIONS OF ANALYSIS 75
5.2. TEST RESULTS OF CLEAN BALLAST 75
5.2.1. Moist and Dry Density 75
5.2.2. Resistivity of Clean Ballast 76
5.2.3. CBR, Static Modulus, and Resilient Modulus of Clean Ballast 76
5.2.4. Discussion of Test Results of Clean Ballast 77
5.3. DRY DENSITY OF FOULED BALLAST 77
5.3.1. Test Result of Dry Densities of Fouled Ballast 77
5.3.2. Discussion of Test Results of Dry Densities of Fouled Samples 80
5.4. BOUNDARY EFFECT OF RESISTIVITY TEST ON TEST BOX 81
5.4.1. Test Result of Boundary Effect of Resistivity on Test Box 81
5.4.2. Discussion on Boundary Effect of Resistivity on Test Box 87
5.5. RESULT OF RESISTIVITY TESTING BY THE WENNER FOUR POINT METHOD 88

5.5.1. Resistivity Test Result - Subgrade Soil Fouled Ballast 88
5.5.2. Resistivity Test Results – Gardner Track Ballast Dust Fouled Ballast..... 90
5.5.3. Resistivity Test Result – Coal Dust Fouled Ballast..... 92
5.5.4. Validity of Resistivity Data from 2 Point Method for Horizontal Probe 94
5.5.5. Comparison of Resistivity for Fouled Ballast with Different Fouling Agents 96
5.5.6. Discussion of Resistivity by Wenner 4 Point Method of Fouled Ballast..... 98
5.6. VALIDITY OF VERTICAL RESISTIVITY TESTER BY FALL OF POTENTIAL METHOD..... 100
5.6.1. Validity of Vertical Probe for Subgrade Material in Open Space..... 100
5.6.2. Validity of Vertical Probe on Test Sample of Fouled Ballast 102
5.6.3. Discussion of Validity of Vertical Resistivity Tester 107
5.7. VARIATION OF CBR OF BALLAST DUE TO CHANGE IN MOISTURE CONTENT 107
5.7.1. CBR for Different Percentages of Fouling for Various Fouling Agents..... 107
5.7.2. CBR Comparison of Different Fouling Agents for the Same Percentage of Fouling 110
5.7.3. Discussion of CBR of Fouled Ballast 113
5.8. RESILIENT MODULUS OF FOULED BALLAST DUE TO VARIATIONS OF MOISTURE..... 113
5.8.1. Resilient Modulus for Different Percentages of Fouling for Various Fouling Agents 113
5.8.2. Resilient Modulus Comparison of Various Fouled Ballasts..... 116
5.8.3. Discussion of Resilient Modulus versus Moisture Content..... 118
5.9. STATIC MODULUS OF FOULED BALLAST RELATIONSHIP WITH MOISTURE CONTENT 119
5.9.1. Variation of Static Modulus with Moisture Content for Subgrade Soil..... 119
5.9.2. Variation of Static Modulus with Moisture Content for Gardner Track Ballast Dust..... 123
5.9.3. Variation of Static Modulus with Moisture Content for Coal Dust..... 127
5.9.4. Comparison of Static Modulus for Different Fouling Agents 131
5.9.5. Discussion of Static Modulus of Fouled Ballast 134
5.10. CORRELATION OF STRENGTH PROPERTIES OF FOULED BALLAST 134
5.10.1. Correlation of Resilient Modulus and Static Modulus of Fouled Ballast 134

5.10.2. Correlation of Resilient Modulus and CBR for Fouled Ballast 135
5.10.3. Correlation of Static Modulus and CBR of Fouled Ballast 136
5.10.4. Discussion of Correlation of Strength Properties 137
5.11. RESULT OF PROCTOR TEST 137
5.12. FIELD TEST RESULTS 140
5.11.1. Resistivity Test Results 140
5.11.2. Test Results of DCP 141
5.11.3. Test Result of LWD 144
5.11.4. Discussion of Field Test 144
CHAPTER SIX: CONCLUSIONS AND RECOMMENDATIONS 146
6.1 INTRODUCTION 146
6.2 DRY DENSITY TEST OF FOULED BALLAST 146
6.3 RESISTIVITY ANALYSIS 147
6.3.1. Horizontal Probe Resistivity 147
6.3.2. Vertical Probe Resistivity 149
6.4 CBR TEST 149
6.5 RESILIENT MODULUS 150
6.6 STATIC MODULUS 151
6.7 CORRELATION OF CBR, STATIC MODULUS, AND RESILIENT MODULUS 151
6.8 FIELD TEST 152
6.9 RECOMMENDATIONS 152
BIBLIOGRAPHY 154

List of Tables

TABLE 2-1: RECOMMENDED BALLAST GRADATION (MANUAL FOR RAILWAY ENGINEERING, AREMA 2010) 7

TABLE 2-2: TYPICAL RESISTIVITY VALUES OF SOME SOILS (G.F. TAGG, 1964) 12

TABLE 2-3 RESISTIVITY CHART FOR 0 - 24 HOURS FOR DIFFERENT FOULED BALLAST (RAHMAN, 2014) 14

TABLE 3-1 ENGINEERING PROPERTIES OF CLEAN BALLAST 28

TABLE 3-2 SPECIFIC GRAVITY AND WATER ABSORPTIONS OF DIFFERENT GRADED SAMPLES 30

TABLE 3-3 ENGINEERING PROPERTIES OF SUBGRADE SOIL 32

TABLE 3-4 COMPOSITION OF TEST COAL DUST 33

TABLE 3-5 GRADATION CALCULATION TABLE FOR COAL DUST 34

TABLE 3-6 ENGINEERING PROPERTIES OF COAL DUST 35

TABLE 3-7 ENGINEERING PROPERTIES OF GARDNER TRACK BALLAST DUST 38

TABLE 3-8 COMPARISON OF ENGINEERING PROPERTIES OF FOULING AGENTS 39

TABLE 3-9 FIELD BALLAST DISTRIBUTION PROPERTIES AT SITE A OF MIDLAND RAILWAY TRACK, KANSAS 46

TABLE 3-10 FIELD BALLAST DISTRIBUTION PROPERTIES AT SITE B OF MIDLAND RAILWAY TRACK, KANSAS 47

TABLE 3-11 FIELD MOISTURE CONTENT OF BALLAST AT MIDLAND RAILWAY TRACK, KANSAS 47

TABLE 3-12 BALLAST FOULING CLASSIFICATION BASED ON FI 48

TABLE 4-1 COEFFICIENT OF FOULING INDEX CALCULATION BASED ON SIEVE ANALYSIS 50

TABLE 4-2 FOULING INDEX CALCULATION FOR DIFFERENT SAMPLES 50

TABLE 4-3 ENGINEERING PROPERTIES OF THE W1 TOOL STEEL USED FOR HORIZONTAL PROBES 55

TABLE 4-4 GENERAL FEATURES OF AEMC GROUND TESTER 56

TABLE 4-5 ENGINEERING PROPERTIES OF THE STEEL USED FOR SENSOR PROBE 60

TABLE 4-6 ENGINEERING PROPERTIES OF THE STEEL USED FOR SENSOR PROBE 60

TABLE 5-1 MOIST AND DRY DENSITY OF CLEAN BALLAST 75

TABLE 5-2 CBR, RESILIENT MODULUS, AND STATIC MODULUS OF CLEAN BALLAST 77

TABLE 5-3 FOULED BALLAST DRY DENSITIES FOR DIFFERENT TYPES OF FOULED BALLAST 78

TABLE 5-4 COMPARISON OF RESISTIVITY FOR VARIOUS % FOULING OF SUBGRADE SOIL FOULED BALLAST 90

TABLE 5-5 RESISTIVITY OF VARIOUS % FOULING OF GARDNER TRACK BALLAST DUST FOULED BALLAST 92

TABLE 5-6 RESISTIVITY COMPARISON FOR DIFFERENT % FOULING FOR COAL DUST FOULED BALLAST 94

TABLE 5-7 RESISTANCE MEASUREMENT BY HORIZONTAL AND VERTICAL PROBE ARRANGEMENTS 101

TABLE 5-8 COMPARISON OF RESISTIVITY IN HORIZONTAL AND VERTICAL ALIGNMENTS AT 10% FOULING 103

TABLE 5-9 COMPARISON OF RESISTIVITY IN HORIZONTAL AND VERTICAL ALIGNMENTS AT 20% FOULING 104

TABLE 5-10 COMPARISON OF RESISTIVITY IN HORIZONTAL AND VERTICAL ALIGNMENTS AT 30% FOULING 105

TABLE 5-11 COMPARISON OF RESISTIVITY IN HORIZONTAL AND VERTICAL ALIGNMENTS AT 40% FOULING 106

TABLE 5-12 STIFFNESS OF SUBGRADE FOULED BALLAST WITH VARIOUS MOISTURE CONTENTS 121

TABLE 5-13 STIFFNESS OF GARDNER TRACK DUST FOULED BALLAST WITH VARIOUS MOISTURE CONTENTS 125

TABLE 5-14 STIFFNESS OF COAL DUST FOULED BALLAST WITH VARIOUS MOISTURE CONTENTS 129

TABLE 5-15 FIELD RESISTIVITY DATA OF MIDLAND RAILROAD TRACK 141

TABLE 5-16 CBR OF SITES FROM FIELD TEST BY DCP METHOD 144

TABLE 5-17 RESILIENT MODULUS OF FIELD SITES FROM LWD METHOD 144

List of Figures

FIGURE 2-1: SCHEMATIC DIAGRAM OF THE TRACK SUBSTRUCTURE (MODIFIED AFTER SELIG & WATERS, 1994) 8

FIGURE 2-2 SKETCH OF FOULED BALLAST LAYER AFTER PIT INVESTIGATION (READ ET AL, 2010) 10

FIGURE 2-3 FOULED BALLAST LAYER AFTER PIT INVESTIGATION (A) PLAN (B) SECTION (READ ET AL. 2010) 10

FIGURE 2-4: PATHWAYS ON SOIL ELECTRICAL CONDUCTANCE (RHOADES ET AL., 1989) 12

FIGURE 2-5 RESISTIVITY MEASUREMENT TEST SET UP BY WENNER 4 POINT METHOD (RAHMAN, 2014) 13

FIGURE 2-6 SCHEMATIC DIAGRAM OF SIMPLE GROUND RESISTANCE MEASUREMENT 15

FIGURE 2-7 SIMPLIFIED DIAGRAM OF GROUND RESISTANCE MEASUREMENT WITH SINGLE POLE (DATTA ET AL) 16

FIGURE 2-8 CONCEPTUAL DIAGRAM OF 4 ELECTRODE METHOD (AFTER FRANK WENNER) 17

FIGURE 2-9 RESISTANCE MEASUREMENT BY FALL OF POTENTIAL (USER MANUAL-4620, AEMC INSTRUMENTS) 17

FIGURE 2-10: SCHEMATIC DIAGRAM OF LARGE SCALE RESISTIVITY TEST (AFTER RAHMAN SETUP) 18

FIGURE 2-11: RESISTIVITY OF FOULED BALLAST AT THE 18TH HOUR VERSUS FOULING INDEX (AJ RAHMAN) 19

FIGURE 3-1 SCHEMATIC DIAGRAM OF BALLAST CLEANING ARRANGEMENT 25

FIGURE 3-2 BALLAST RECYCLING (A) WIRE SIEVE AND POND FOR SIEVING (B) SIEVING PROCEDURE 26

FIGURE 3-3 GRADATION CURVE OF BALLAST BEFORE WASHING (WITHOUT CLEANING) AND AFTER WASHING 27

FIGURE 3-4 GRADATION CURVE OF TEST BALLAST AND AREMA SPECIFIED BALLAST 28

FIGURE 3-5 SPECIFIC GRAVITY DETERMINATION OF BALLAST (A) SOAKING OF DIFFERENT SIZES OF BALLAST (B) & (C) FINDING SATURATED WEIGHT OF BALLAST (D) FINDING SUBMERGED WEIGHT OF BALLAST 29

FIGURE 3-6 REMOVAL OF TOP SOIL FOR EXTRACTING SUBGRADE SOIL AS FOULING AGENT 31

FIGURE 3-7 PARTICLE SIZE DISTRIBUTION OF SUBGRADE SOIL 31

FIGURE 3-8 PROCTOR CURVE OF SUBGRADE SOIL 32

FIGURE 3-9 COLLECTION AND GRINDING OF COAL (A) COAL STORE YARDS AND COLLECTION (B) GRINDING ARRANGEMENT OF COAL AT THE LABORATORIES OF THE UNIVERSITY OF KANSAS 34

FIGURE 3-10 GRADATION CURVE OF COAL DUST 35

FIGURE 3-11 PROCTOR CURVE FOR COAL DUST 36

FIGURE 3-12 WATER DRAIN OUT ARRANGEMENT AFTER WASHING GARDNER TRACK BALLAST DUST 37

FIGURE 3-13 GRADATION CURVE FOR GARDNER TRACK BALLAST DUST 38

FIGURE 3-14 PROCTOR CURVE OF GARDNER TRACK BALLAST DUST 39
FIGURE 3-15 COMPARISON OF PARTICLE SIZE DISTRIBUTION OF FOULING AGENTS 40
FIGURE 3-16 COMPARISON OF OPTIMUM MOISTURE CONTENT OF FOULING AGENTS 41
FIGURE 3-17 SCHEMATIC DIAGRAM OF SMALL TEST BOX FOR RESISTIVITY 42
FIGURE 3-18 TEST BOX CONSTRUCTED AT KU 42
FIGURE 3-19 SAMPLE PREPARATION AND TESTING FOR RESISTIVITY DETERMINATION 43
FIGURE 3-20 RESISTIVITY OF FOULING AGENTS 44
FIGURE 3-21 PARTICLE SIZE DISTRIBUTION AT SITE A OF MIDLAND RAILWAY TRACK, KANSAS 45
FIGURE 3-22 PARTICLE SIZE DISTRIBUTION AT SITE B OF MIDLAND RAILWAY TRACK, KANSAS 46
FIGURE 4-1 TYPES OF SAMPLES FOR TEST 49
FIGURE 4-2 MIXING PROCEDURE STARTED FROM TOP LEFT CORNER RUNNING COUNTERCLOCKWISE 51
FIGURE 4-3 ARTIFICIALLY FOULED BALLAST READY TO GO INTO TEST BOX (A) CRUSHED STONE FOULED (B) SUBGRADE SOIL FOULED (C) COAL DUST FOULED 51
FIGURE 4-4 BOX FILLING PROCEDURE - STARTS TOP LEFT CORNER PROGRESSES COUNTERCLOCKWISE 52
FIGURE 4-5 FILLING PROCEDURE (A) COMPACTION OF SAMPLE (B) WEIGHING BEFORE POURING TO BOX 53
FIGURE 4-6 TEST LOCATION FOR LWD TEST, DCP TEST AND PLATE LOADING TEST 54
FIGURE 4-7: TEST LOCATIONS FOR HORIZONTAL AND VERTICAL ALIGNED PROBE METHOD (FIGURE NOT TO SCALE) 54
FIGURE 4-8 SCHEMATIC HORIZONTAL PROBE UNIT FOR WENNER FOUR POINT METHOD 55
FIGURE 4-9 HORIZONTAL PROBE UNIT FOR WENNER FOUR POINT METHOD 56
FIGURE 4-10 SCHEMATIC CONNECTION DIAGRAM OF AEMC GROUND TESTER (WWW.AEMC.COM) 56
FIGURE 4-11 RESISTANCE MEASUREMENT BY WENNER FOUR POINT METHOD WITH AMCE TESTER 57
FIGURE 4-12 FOULED BALLAST RESISTANCE MEASUREMENT BY SINGLE PROBE METHOD 58
FIGURE 4-13 CONCEPT OF RESISTANCE MEASUREMENT FROM FALL OF POTENTIAL METHOD (WWW.AEMC.COM) 59
FIGURE 4-14 RESISTANCE MEASUREMENT MODEL OF FALL OF POTENTIAL METHOD FOR VERTICAL PROBE 59
FIGURE 4-15 CONCEPTUAL DIAGRAM OF VERTICAL PROBE 60
FIGURE 4-16 CONSTRUCTION OF VERTICAL PROBE (A) VERTICAL PROBE (B) CONSTRUCTION OF SENSOR SECTION (C) JOINT MECHANISM OF CONDUCTOR AND INSULATOR MATERIALS 62

FIGURE 4-17 (A) SCHEMATIC DIAGRAM OF ZORN 3000 LWD (B) ACTUAL PHOTO OF ZORN 3000 LWD USED IN LAB (WWW.ZORN-INSTRUMENTS.COM) 63
FIGURE 4-18 SCHEMATIC DIAGRAM OF DCP 66
FIGURE 4-19 PLATE LOADING TEST SET UP 68
FIGURE 4-20 LAYER DEPTH OF VERTICAL PROBE FOR CALIBRATION WITH DCP (SECTION MM IN FIGURE 4.7) 69
FIGURE 4-21 PROCTOR TEST PROCEDURE AT LAB 71
FIGURE 4-22 LOCATION MAP OF THE TEST SITES (WWW.MAPS.GOOGLE.COM) 72
FIGURE 4-23 TESTS LOCATION AT FIELD TEST (NOT TO SCALE) 72
FIGURE 4-24 FIELD PROCEDURE OF RESISTIVITY MEASUREMENT AT SITE B (PARALLEL TO TRACK) 73
FIGURE 5-1 UNIT LOAD VERSUS DEFLECTION CURVE BY STATIC PLATE LOADING TEST OF CLEAN BALLAST 76
FIGURE 5-2 DRY DENSITY VERSUS PERCENTAGE FOULING FOR DIFFERENT TYPES OF FOULED BALLAST 79
FIGURE 5-3 DRY DENSITY DETERMINATION FROM SMALL BOX TEST 80
FIGURE 5-4 BOUNDARY EFFECT STUDY FOR RESISTIVITY - 10% FOULED WITH SUBGRADE SOIL 82
FIGURE 5-5 BOUNDARY EFFECT STUDY FOR RESISTIVITY - 20% FOULED WITH SUBGRADE SOIL 83
FIGURE 5-6 BOUNDARY EFFECT STUDY FOR RESISTIVITY – 30% FOULED WITH SUBGRADE SOIL 83
FIGURE 5-7 BOUNDARY EFFECT STUDY FOR RESISTIVITY – 40% FOULED WITH SUBGRADE SOIL 84
FIGURE 5-8 BOUNDARY EFFECT STUDY FOR RESISTIVITY - 10% FOULED WITH TRACK DUST 84
FIGURE 5-9 BOUNDARY EFFECT STUDY FOR RESISTIVITY - 20% FOULED WITH TRACK DUST 85
FIGURE 5-10 BOUNDARY EFFECT STUDY FOR RESISTIVITY - 30% FOULED WITH TRACK DUST 85
FIGURE 5-11 BOUNDARY EFFECT STUDY FOR RESISTIVITY - 40% FOULED WITH TRACK DUST 86
FIGURE 5-12 BOUNDARY EFFECT STUDY FOR RESISTIVITY - 10% FOULED WITH COAL DUST 86
FIGURE 5-13 BOUNDARY EFFECT STUDY FOR RESISTIVITY - 20% FOULED WITH COAL DUST 87
FIGURE 5-14 BOUNDARY EFFECT STUDY FOR RESISTIVITY - 30% FOULED WITH COAL DUST 87
FIGURE 5-15 RESISTIVITY OF SUBGRADE SOIL FOULED BALLAST FOR DIFFERENT MOISTURE CONTENTS 89
FIGURE 5-16 RESISTIVITY OF SUBGRADE SOIL FOULED BALLAST FOR VARIOUS MC (ZOOM IN VIEW) 89
FIGURE 5-17 RESISTIVITY OF GARDNER TRACK DUST FOULED BALLAST FOR DIFFERENT MOISTURE CONTENTS 91
FIGURE 5-18 RESISTIVITY OF GARDNER TRACK DUST FOULED BALLAST FOR VARIOUS MC (ZOOM IN VIEW) 91
FIGURE 5-19 RESISTIVITY OF COAL DUST FOULED BALLAST FOR DIFFERENT MOISTURE CONTENTS 93

FIGURE 5-20 RESISTIVITY OF COAL DUST FOULED BALLAST FOR VARIOUS MC (ZOOM IN VIEW) 93
FIGURE 5-21 RESISTIVITY BY 2 & 4 POINT METHODS FOR SUBGRADE SOIL FOULED BALLAST 95
FIGURE 5-22 RESISTIVITY BY 2 POINT & WENNER METHODS OF GARDNER TRACK DUST FOULED BALLAST 95
FIGURE 5-23 RESISTIVITY BY 2 POINT & 4 POINT METHODS FOR COAL DUST FOULED BALLAST 96
FIGURE 5-24 COMPARISON OF RESISTIVITY FOR DIFFERENT FOULED BALLAST AT 10% FOULING BY WEIGHT 96
FIGURE 5-25 COMPARISON OF RESISTIVITY FOR DIFFERENT FOULED BALLAST AT 20% FOULING BY WEIGHT 97
FIGURE 5-26 COMPARISON OF RESISTIVITY FOR DIFFERENT FOULED BALLAST AT 30% FOULING BY WEIGHT 97
FIGURE 5-27 COMPARISON OF RESISTIVITY FOR DIFFERENT FOULED BALLAST AT 40% FOULING BY WEIGHT 98
FIGURE 5-28 SKETCH OF VERTICAL PROBE RESISTANCE CHECK BY FALL OF POTENTIAL METHOD 100
FIGURE 5-29 FIELD SETUP OF HORIZONTAL VERSUS VERTICAL RESISTANCE MEASUREMENT 101
FIGURE 5-30 RESISTANCE VS DEPTH ON SUBGRADE SOIL BY VERTICAL AND HORIZONTAL PROBES 102
FIGURE 5-31 COMPARISON OF RESISTIVITY USING HORIZONTAL AND VERTICAL ALIGNMENTS AT 10% FOULING 103
FIGURE 5-32 COMPARISON OF RESISTIVITY USING HORIZONTAL AND VERTICAL ALIGNMENTS AT 20% FOULING 104
FIGURE 5-33 COMPARISON OF RESISTIVITY USING HORIZONTAL AND VERTICAL ALIGNMENTS AT 30% FOULING 105
FIGURE 5-34 COMPARISON OF RESISTIVITY BY HORIZONTAL AND VERTICAL ALIGNMENTS AT 40% FOULING 106
FIGURE 5-35 MOISTURE CONTENT VERSUS CBR FOR SUBGRADE SOIL FOULED BALLAST 108
FIGURE 5-36 MOISTURE CONTENT VERSUS CBR FOR GARDNER TRACK DUST FOULED BALLAST 109
FIGURE 5-37 MOISTURE CONTENT VERSUS CBR FOR COAL DUST FOULED BALLAST 110
FIGURE 5-38 MOISTURE CONTENT VERSUS CBR AT 10% FOULING WITH DIFFERENT FOULING AGENTS 111
FIGURE 5-39 MOISTURE CONTENT VERSUS CBR AT 20% FOULING WITH DIFFERENT FOULING AGENTS 112
FIGURE 5-40 MOISTURE CONTENT VERSUS CBR AT 30% FOULING WITH DIFFERENT FOULING AGENTS 112
FIGURE 5-41 MOISTURE CONTENT VERSUS CBR AT 40% FOULING WITH DIFFERENT FOULING AGENTS 113
FIGURE 5-42 RESILIENT MODULUS VS MC FOR SUBGRADE SOIL FOULED BALLAST 114
FIGURE 5-43 RESILIENT MODULUS VS MC FOR GARDNER TRACK DUST FOULED BALLAST 115
FIGURE 5-44 RESILIENT MODULUS VS MC FOR COAL DUST FOULED BALLAST 115
FIGURE 5-45 RESILIENT MODULUS VS MC FOR 10% FOULING FOR FOULED BALLAST WITH DIFFERENT AGENTS 116
FIGURE 5-46 RESILIENT MODULUS VS MC FOR 20% FOULING FOR FOULED BALLAST WITH DIFFERENT AGENTS 117
FIGURE 5-47 RESILIENT MODULUS VS MC FOR 30% FOULING FOR FOULED BALLAST WITH DIFFERENT AGENTS 117

FIGURE 5-48 RESILIENT MODULUS VS MC FOR 40% FOULING FOR FOULED BALLAST WITH DIFFERENT AGENTS..... 118
FIGURE 5-49 UNIT LOAD VERSUS DEFLECTION CURVE OF 10% FOULED BY SUBGRADE SOIL AT VARIOUS MC..... 119
FIGURE 5-50 UNIT LOAD VERSUS DEFLECTION CURVE OF 20% FOULED BY SUBGRADE SOIL AT VARIOUS MC..... 120
FIGURE 5-51 UNIT LOAD VERSUS DEFLECTION CURVE OF 30% FOULED BY SUBGRADE SOIL AT VARIOUS MC..... 120
FIGURE 5-52 UNIT LOAD VERSUS DEFLECTION CURVE OF 40% FOULED BY SUBGRADE SOIL AT VARIOUS MC..... 121
FIGURE 5-53 STIFFNESS OF SUBGRADE FOULED BALLAST WITH VARIOUS MOISTURE CONTENTS..... 122
FIGURE 5-54 STATIC MODULUS OF SUBGRADE FOULED BALLAST WITH VARIOUS MOISTURE CONTENTS..... 122
FIGURE 5-55 UNIT LOAD VERSUS DEFLECTION CURVE OF 10% FOULED BY GARDNER TRACK DUST..... 123
FIGURE 5-56 UNIT LOAD VERSUS DEFLECTION CURVE OF 20% FOULED BY GARDNER TRACK DUST..... 124
FIGURE 5-57 LOAD VERSUS DEFLECTION CURVE OF 30% FOULED BY GARDNER TRACK DUST..... 124
FIGURE 5-58 UNIT LOAD VERSUS DEFLECTION CURVE OF 40% FOULED BY GARDNER TRACK DUST..... 125
FIGURE 5-59 STIFFNESS OF GARDNER TRACK DUST FOULED BALLAST WITH VARIOUS MOISTURE CONTENTS..... 126
FIGURE 5-60 STATIC MODULUS OF GARDNER TRACK BALLAST DUST FOULED BALLAST..... 126
FIGURE 5-61 UNIT LOAD VERSUS DEFLECTION CURVE OF 10% FOULED BALLAST BY COAL DUST..... 128
FIGURE 5-62 UNIT LOAD VERSUS DEFLECTION CURVE OF 20% FOULED BALLAST BY COAL DUST..... 128
FIGURE 5-63 UNIT LOAD VERSUS DEFLECTION CURVE OF 30% FOULED BALLAST BY COAL DUST..... 129
FIGURE 5-64 STIFFNESS OF COAL DUST FOULED BALLAST WITH VARIOUS MOISTURE CONTENTS..... 130
FIGURE 5-65 STATIC MODULUS OF COAL DUST FOULED BALLAST WITH VARIOUS MOISTURE CONTENTS..... 131
FIGURE 5-66 COMPARISON OF STATIC MODULUS VERSUS MC AT 10% FOULING..... 132
FIGURE 5-67 COMPARISON OF STATIC MODULUS VERSUS MC AT 20% FOULING..... 132
FIGURE 5-68 COMPARISON OF STATIC MODULUS VERSUS MC AT 30% FOULING..... 133
FIGURE 5-69 COMPARISON OF STATIC MODULUS VERSUS MC AT 40% FOULING..... 133
FIGURE 5-70 CORRELATION OF RESILIENT MODULUS AND STATIC MODULUS OF FOULED BALLAST..... 135
FIGURE 5-71 CORRELATION OF RESILIENT MODULUS AND CBR OF FOULED BALLAST..... 136
FIGURE 5-72 CORRELATION OF STATIC MODULUS AND CBR OF FOULED BALLAST..... 136
FIGURE 5-73 DRY DENSITIES VERSUS MOISTURE CONTENT OF SUBGRADE SOIL FOULED BALLAST..... 138
FIGURE 5-74 DRY DENSITIES VERSUS MOISTURE CONTENT OF GARDNER TRACK DUST FOULED BALLAST..... 138
FIGURE 5-75 DRY DENSITIES VERSUS MOISTURE CONTENT OF COAL DUST FOULED BALLAST..... 139

FIGURE 5-76 OPTIMUM DRY DENSITIES VERSUS PERCENTAGE FOULING BY WEIGHT 140

FIGURE 5-77 DEPTH VERSUS PENETRATION INDEX FOR SITE LOCATION A 142

FIGURE 5-78 DEPTH VERSUS PENETRATION INDEX FOR SITE LOCATION B 143

Chapter One: Introduction

1.1. Background

The United States freight rail system operates throughout the 48 continuous states and is the safest, most affordable, and most reliable rail system in the world. The freight rail networks work together on their nearly 140,000–mile system to deliver economic growth, support job creation, and to provide huge environmental benefits by reducing highway gridlock and providing clearer air (AAR, Overview of America's Freight Railroads, 2014). About 70% of the railroad network is used by both freight and passenger trains. Maintaining tracks in good condition is a critical need, as good track conditions are the only sustainable means for ensuring the overall performance and safety of railway operations. Track conditions are governed by the rate of deterioration of geometry, track buckling potential, and overall track support degradation and integrity. Among these, track support, structural integrity, and performance of the overall structure depend on the characteristics and performance of the ballast and sub-ballast layers.

Excessive ballast fouling in the railroad substructure is detrimental to the operation of the railroad track and its structural capacity. The early detection of ballast fouling is of great importance to the safety of the rail system and its life-cycle cost-effectiveness (Leng & Al-Qadi, 2010). Track instabilities caused by track support degradation and settlement as a result of progressive fouling of ballast can be temporarily addressed by keeping the track geometry at an acceptable level through a ballast tamping maintenance action, or more permanently by cleaning the ballast and removing the fines. Studies in Australia have shown that track maintenance costs comprise about 25-35% of total freight train operation costs (Majidzadeh, 2010).

There are currently three common ways to assess ballast fouling conditions, each falling into either the destructive or non-destructive category.

Destructive method	Non-destructive method
a) Visual Inspection	c) Ground Penetrative Radar Method
b) Selective drilling / digging	

The easiest way to detect ballast fouling is with visual inspection—however, it is difficult to quantify the amount of fouling through inspection. The remaining two methods involve tedious and time-consuming field and lab work and are expensive. A portion of this thesis describes the development of a new device with the ability to determine the degree of fouling of ballast within a few minutes and with much lower cost.

1.2. Problem Statement

The speed and freight capacity of train locomotives are both continually increasing due to new innovations. However, these cost- and time-saving innovations are limited in the railroad system by existing track condition/design and maintenance costs associated with degradation of track. So, increased weight of locomotives and railcars could result in functional and/or structural failure of track. In 2010, track defects caused 32.2% of the 2079 rail accidents in the U.S. and caused $113 million in damage. Out of these track defect accidents, 622 (93%) involved the derailment of the train (FRA Annual Report, 2012). Broken rails or welds (15.3%), track geometry (7.3%), and bearing failure (5.9%) are some of the main causes of train derailments (Liu, Saat, & Barkan, 2012). A broken rail is most likely caused by the differential settlement of the track bed. Also, the geometry of the track can be distorted due to instability of the supporting base of the rail.

To prevent functional failure due to fouled substructure materials, costly ballast maintenance is routinely performed, especially on track serving heavy–axle–load unit trains – which includes the investment of millions of dollars that may also include the removal and replacement of fouled railway ballast (Ebrahimi, 2011). The Association of American Railroads (AAR) found that America's freight railroads spent $1 billion (11.0%) out of their $9.2 billion maintenance budgets for track and property in 2012, including the addition of 12.7 million cubic yards of ballast to build and maintain a rail network that is safe, reliable, efficient, and affordable (AAR, Total Annual Spending - 2012 Data, 2013). Cleaning ballast to remove fine particles and/or replacing fouled ballast are the major actions taken to correct track foundations of the railroad network.

Accumulation of fine particles within the ballast due to intrusion from the exposed surface, extrusion from subgrade soil, and wearing of ballast is the major factor that reduces the shear strength and the stability of the ballast. Water promotes soil migration by washing surface particles down into the ballast, and by softening subgrade soils that can migrate upward under the dynamic loading from passing trains. Since fine particles tend to retain moisture, addition of water to them in railroad ballast can create slurry, which can flow through the ballast layer and may accumulate. This migration fills voids within the coarse aggregates and decreases drainage, which leads to further reduction in stability due to a decrease in frictional force, subgrade attrition, and ballast deterioration, caused by the delay in dissipation of excess pore water pressure (Indraratna, Khabbaz, Salim, & Christie, 2006). Failure to quickly dissipate excess pore water pressure prevents the ballast from performing properly, safely, and effectively.

Early detection of fouling is important for maintaining track alignments to prevent slow orders and eventually rail accidents. Railroad civil engineers / geotechnical engineers are facing the

challenge of detecting and quantifying the degree of ballast fouling so that a recommended action for correction can be developed in a timely manner. The established testing methods are time consuming and costly. A new, non-destructive approach to ballast fouling detection is needed by railroad civil engineers, an approach that can compute the degree of fouling quickly in the field with limited investment and provided guidance for more detailed investigation and maintenance and rehabilitation actions.

1.3. Research Objective

The objectives of this research are discussed as follows:

- To evaluate the resistivity of fouled ballast with different fouling agents for unsaturated states (at different moisture contents).
- To propose a fouled ballast resistance measurement probe and to verify the accuracy of this probe with existing approved methods of soil resistance measurement.
- To evaluate the shear strength and modulus of fouled ballast and to study the impact of water content on fouled ballast.
- To characterize the correlation of strength parameters of fouled ballast at different fouling levels.

1.4. (Fukue, Minatoa, Horibe, & Taya, 1999) Research Methodology

The research methodology adopted for this research included the following steps:

a. Literature review of the fouling mechanisms of ballast and soil resistivity methods.
b. Testing carried out to determine the engineering properties of major fouling agents of fouled ballast, including resistivity.

c. Determination in the lab of fouled ballast resistivity using the Wenner 4-probe method with horizontal probe alignments on samples with controlled moisture content.
d. Strength testing that included dynamic cone penetration (DCP), light weight deflectometer (LWD), and plate loading tests for determination of California Bearing Ratio (CBR), resilient modulus, and static modulus of fouled ballast.
e. The vertical probe designed and constructed at the University of Kansas (KU), which can measure the soil resistivity by fall of potential method, was evaluated in lab.
f. Fouling detection at filed by resistivity method as well as strength determination by above mentioned test.

1.5. Thesis Organization

Following are the details of the report organization of this thesis.

Chapter One introduces the topic, including the background, problem statement, research objective, and research methodology.

Chapter Two contains a detailed literature review on the cause and effect of ballast fouling, resistivity measurement methods of fouled ballast, factors affecting the soil resistivity, static and resilient moduli of ballast, and CBR of ballast.

Chapter Three describes the gradation and other engineering properties of clean ballast as well as other fouling materials used in this research. This chapter includes the quantification of the properties of the ballast and fouling materials used in this research.

Chapter Four discusses the detailed methodology of measurement in this study. This includes the method of preparation of samples. Measurement of resistivity by the four probe and fall of

potential methods are also discussed. The details about the Dynamic Cone Penetration (DCP) test, Light Weight Deflectometer (LWD) test, and Plate Loading Test are discussed.

Chapter Five discusses the results obtained after data analysis. It also compares results of different samples prepared in different proportions of various types of fouling materials.

Chapter Six contains a discussion of the conclusions reached based on the findings of this research and recommendations for the direction of further study on this subject.

Chapter Two: Literature Review

2.1. Introduction of Fouled Ballast

Ballast is a free draining granular material that plays a crucial role in transmitting and distributing the induced cyclic train loading to the underlying sub-ballast and subgrade at a reduced and acceptable stress level (Selig & Waters, 1994). The recommended gradations of the railroad ballast should have 100% passing through the 3" (76 mm) sieve and no more than 5% passing Sieve no 8 (2.36 mm) as recommended by American Railway Engineering and Maintenance-of-way Association (AREMA) (AREMA manual for railway engineering, 2010). The detail of the ballast gradation is given in table 2.1.

Table 2-1: Recommended Ballast Gradation (Manual for Railway Engineering, AREMA 2010)

Size No	**Nominal Sieve size**	**Percent Passing**									
		3"	2.5"	2"	1.5"	1"	0.75"	0.5"	0.375"	No. 4	No. 8
24	2.5" – 0.75"	100	90-100	-	25-60	-	0-10	0-5	-	-	-
25	2.5" – d "	100	80-100	60-85	50-70	25-50		5-20	0-10	0-3	
3	2" – 1"	-	100	95-100	35-70	0-15	-	0-5	-	-	-
4A	2.0" – 0.75"	-	100	90-100	60-90	10-35	0-10	-	0-3	-	-
4	1.5" – 0.75"	-	-	100	90-100	20-55	0-15	-	0-5	-	-
5	1" – d "	-	-	-	100	90-100	40-75	15-35	0-15	0-5	-
57	1" – No 4	-	-	-	100	95-100	-	25-60	-	0-10	0-5
Note: Gradation Numbers 24, 25, 3, 4A and 4 are main line ballast materials. Gradation Numbers 5 and 57 are yard ballast materials.											

Good ballast is characterized by strength, toughness, durability, stability, drainability, cleanability, workability, availability, least purchase price, resistance to deformation and overall economy (Hay, 1982). A strong, well-drained ballast layer is an important factor in the reliability and efficiency of rail track performance. The typical railroad section is given in figure 2.1.

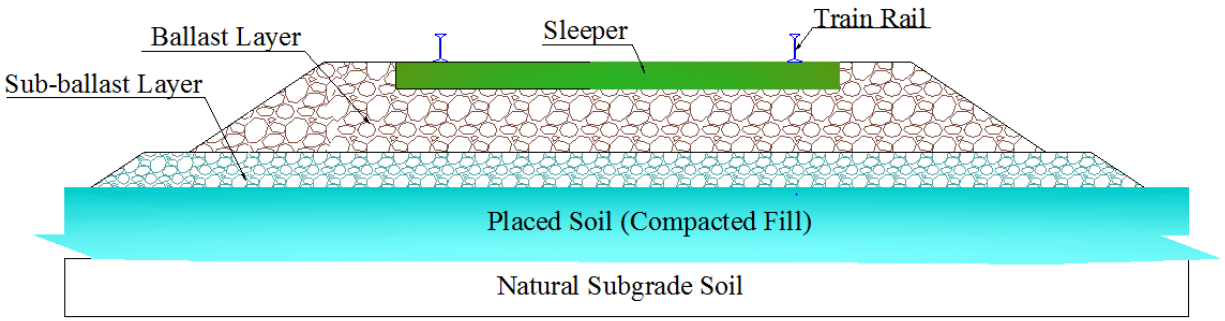

Figure 2-1: Schematic Diagram of the Track Substructure (Modified after Selig & Waters, 1994)

The load bearing strength of the ballast is determined by frictional interlocking. Drainage is provided by the void spaces between the interlocking particles, and ballast particles with hard, durable and angular shapes and rough surface texture are necessary for strength. The major benefits of the ballast are its drainage properties and resilient behavior for repeated load applications. It is also commonly used due to its relatively low cost of construction and maintenance.

As the applied ballast ages, it fouls progressively and the fouling material fills the voids between coarse particles. Based on a study carried out at the University of Massachusetts; about 76% of ballast fouling is caused by ballast breakdown, 13% by infiltration from sub-ballast, 7% by infiltration from the ballast surface, 3% from subgrade intrusion and 1% is related to the tie wear (Selig & Waters, 1994).

2.2. Effects of Fouled Ballast

The fine particles have the capability to retain moisture and may prevent it from passing through. Ultimately, the fine particles from the broken ballast, intruded coal dust, and extruded subgrade soil particles can become slurry fines when mixed with a sufficient amount of water. This slurry can flow throughout the ballast layer. This migration can fill voids within the coarse aggregates

and decrease drainage, which can lead to further accumulation of particles to hinder drainage and reduction in stability due to loss of friction, subgrade attrition, and ballast deterioration due to delay in dissipation of excess pore water pressure (Indraratna, Khabbaz, Salim, & Christie, 2006). This creates serviceability problems in the superstructure.

Wallace (Wallace, 2003) and Rahman (Rahman, Parsons, Han, & Glavinich, 2014) found that an increase in the percentage of fines resulted in a decrease in hydraulic conductivity and thus, the drainage capacity of the ballast, with silt and clay particles having much more effect than sand particles. Due to continuous wear and tear of ties with ballast, a pocket of very fine dust forms beneath the tie. These fines may be added with coal dust intrusion from the surface or/and the fine subgrade soil extrusion from subgrade. Viscous slurry beneath the ties is created due to the combination of water and fine particles. As a result, a mud spot forms when the slurry is pushed up around the ties at the time of loading. Read et.al (Read, Hyslip, McDaniel, & Lees, 2010) investigated the substructure of track at Norfolk Southern mainline sites to determine the root causes of localized mud–fouled ballast deterioration and associated track roughness due to degradation of track geometry - and concluded that the middle layer fouled ballast is denser than the top layer fouled ballast with mud slurry. There was a bottom layer composed of medium stiff moist clay. The subgrade was the most plastic clay, being moderately stiff at the surface and with increasing stiffness below the surface. The finding of Read et al (2010) is described on figure 2.2 and corresponding finding is given in figure 2.3.

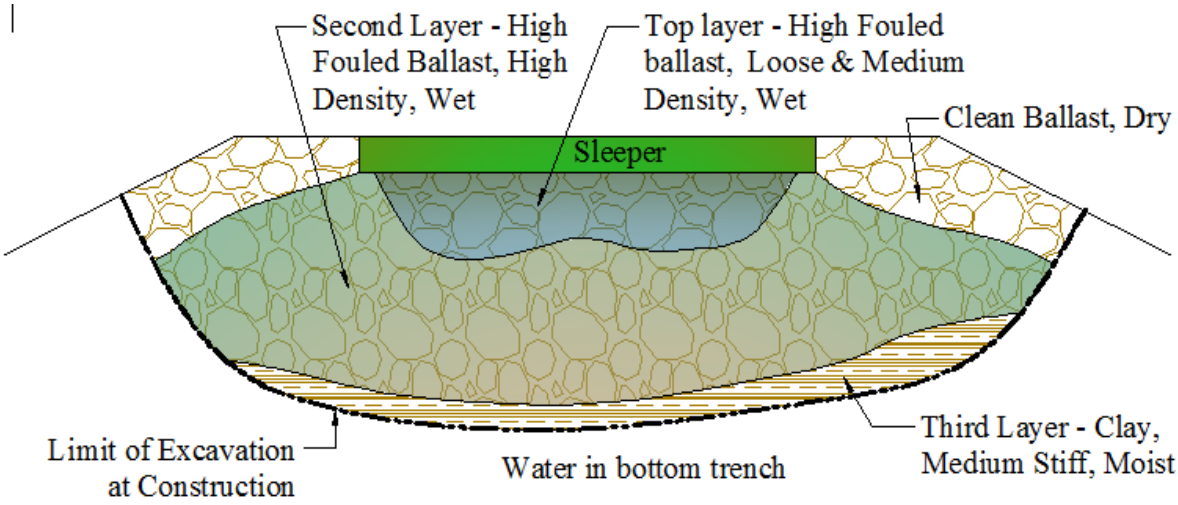

Figure 2-2 Sketch of Fouled Ballast Layer after Pit Investigation (Read et al, 2010)

Figure 2-3 Fouled Ballast Layer after Pit Investigation (a) plan (b) section (Read et al. 2010)

Read et al (2010) concluded that external drainage at the sites appeared to be adequate to remove water from the right-of-way; however, the internal drainage of the ballast section was inadequate to drain water laterally to the ditches. Furthermore, the ballast particles had become rounded due to abrasion that lessened the interlocking strength of the ballast layer and allowed increased track deflection, which caused increased rail and tie bending stresses and fatigue and may compromise track stability.

Track stability related failures vary from rapid deterioration with little warning to slow and progressive deterioration. Visual evidence that fouling is present can often be seen during required maintenance. In summary, blocked drainage caused by fouling of ballast can result in a saturated roadbed that is not stable and can rapidly deteriorate to an unsafe condition with little warning (Sussmann, Ruel, & Chrismer, 2012).

2.3. Resistivity of Fouling Agents

Soil and rock minerals - either in dust or chunk (ballast) form - are insulators and possess good electrical resistance unless they have sufficient moisture. The electrical conductance in sufficiently moist soils is primarily via the electrolytes (salts) contained in the water occupying the larger pores (Rhoades, Corwin, & Lesch, 1999). Though some types of soil minerals also contribute to current transfer through surface conduction in moist soil – this is primarily via the exchangeable cation associated with soil minerals - the amount of such types of conduction is relatively very small. Any fouling agents - crushed stone dust, coal, or clay - are a heterogeneous medium of liquid, solid, and gaseous phases. For spontaneous electrical phenomena and the behavior of the electrical field, the solid and liquid phases play an important role. The air entrapped within the fouling agent or void without water is considered a poor conductor of electricity. The above mentioned two mediums provide the three pathways of current flow namely (A) a solid pathway via soil particles that are in direct and continuous contact with one another (B) a liquid phase pathway via dissolved solids contained in the soil water occupying the large pores, and (C) the solid-liquid phase pathway primarily via exchangeable cations associated with clay minerals (Rhoades, Corwin, & Lesch, 1999).

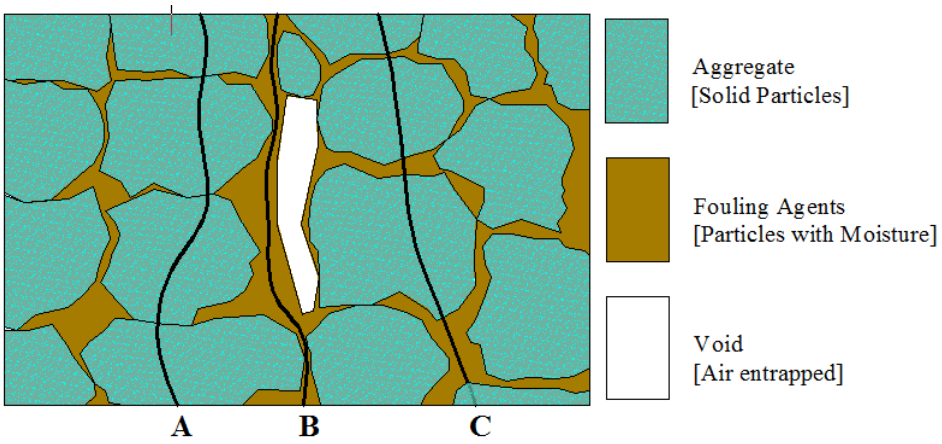

Figure 2-4: pathways on Soil Electrical Conductance (Rhoades et al., 1989)

Soil resistance is the resistance of soil to the passage of electric current. A material with high resistivity is considered to be a poor conductor. Sand, loam and crushed stone aggregate are considered to be poor conductors if they are dry. When water is present, these materials turn into a conductor, though still possessing poor conductivity as compared to copper. Therefore, the conductivity of the soil is a function of the water retained within it. Examples of the resistivities determined by Tagg (1964) of selected soil and rock materials are presented in Table 2-2.

Table 2-2: Typical Resistivity Values of Some Soils (G.F. Tagg, 1964)

Types of Soil	**Resistivity in ohm-cm**
Loam, Garden Soil etc.	500-5,000
Clays	800-5,000
Sand and Gravel	6,000-10,000
Slates, Shale, Sandstone, etc,	1,000-50,000
Crystalline rocks	20,000-1,000,000

While the type of fouling agent is very important in determining the resistivity of the soil, it is difficult to classify the fouling agents clearly because fouling material may contain different

constituents at different site. Water content is another major factor that governs the conductivity of the fouling agent. The exact value of electrical resistivity of fouling agents or fouled ballasts will almost certainly vary as the water content changes.

A.J Rahman (Rahman, Parsons, Han, & Glavinich, 2014) prepared a test box at the University of Kansas for testing the hydraulic conductivity and the electrical resistivity of the fouled ballast. The test set up is shown in figure 2.6.

Figure 2-5 Resistivity Measurement Test Set up by Wenner 4 Point Method (Rahman, 2014)

Rahman measured the resistivity of the fouled ballast with different agents using the Wenner 4 point method. He conducted a series of laboratory test of fouled ballast with three different fouling agents and measured the permeability and resistivity. After filling the test box with ballast and water he drained the water and took readings from 0 minutes (fully saturated condition) to 24 hours (partial saturation condition) at 5 minute intervals for the first 80 minutes and 40 minute to 6 hour intervals for up to 24 hours. He further observed that the resistivity increases as the fouled ballast goes from saturation to a partially saturated state. For his timeline of 24 hours, he presented the

ranges of resistivity of fouled ballast for different degrees of fouling. His results are presented in the Table 2.3.

Table 2-3 Resistivity Chart for 0 - 24 Hours for Different Fouled Ballast (Rahman, 2014)

Fouling Ratio (%)	**Resistivity Range (Ohms – cm) of Ballast Fouling with**		
	Crushed Stone Dust	Subgrade Soil	Coal Dust
10	NA	NA	27,000 - 46,000
20	42,000 – 80,000	20,000 – 24,000	16,000 - 26,000
30	32,000 – 42,000	15,000 – 20,000	12,000 – 16,700
40	12,000 – 20,000	11,000 – 15,000	7,800 - 12,000
50	8,000 – 12,000	8,000 – 9,000	6,000 - 8,000

2.4. Measurement Module of Electrical Resistance of Fouled Ballast

Soil electrical resistance is measured between probes or electrodes inserted into the ground far enough to make adequate contact. A soil may be defined as a "semi-infinite medium" for electrical conductance with only one boundary, which is the surface. The current passing from one probe to another is unconfined and follows the easiest path and spreads deeply into the ground due to the repelling action of charged ions. A simple ground resistance measurement circuit is shown in figure 2-7.

Determination of the earth resistance by the common multi-meter can be done, where one electrode is attached to a driven probe and the other probe acts as ground. Datta et al. (Datta, Basu, & Roy Chowdhury, 1967) assumed that the earth surrounding the electrode is isotropic and homogeneous; having constant resistivity and the direct current (DC) resistance along the probe is evaluated though the measurements are made with alternating current (AC).

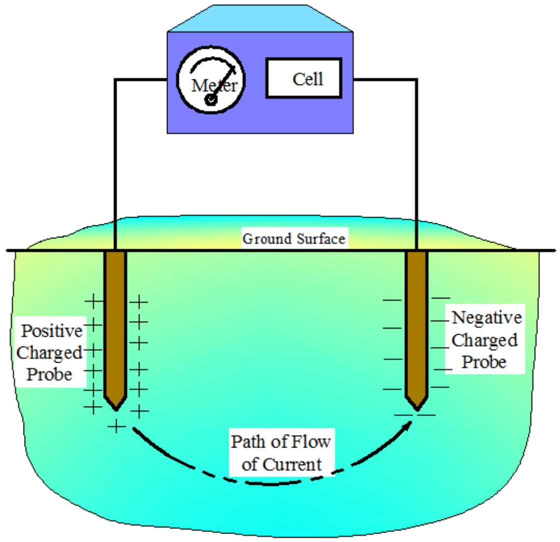

Figure 2-6 Schematic Diagram of Simple Ground Resistance Measurement

Datta et.al (Datta, Basu, & Roy Chowdhury, 1967) and Blattner (Blattner, 1982) analyzed the equation for the measurement of the earth resistance with a single rod, and the equation is given by the following

$$R = \frac{\rho}{2\pi L}\left(\ln\left(\frac{8L}{d}\right) - 1\right) \ldots\ldots\ldots\ldots\ldots\ldots\ldots\ldots\ldots\ldots\ldots\ldots\ldots\ldots\ldots\ldots\ldots\ldots\ldots\ldots\ldots\ldots\ldots\ldots\ldots 2.1$$

Where,

R = Soil Resistance in Ω

ρ = Soil Resistivity in Ωm

L = Length of rod driven in m

d = Diameter of the electrode in m

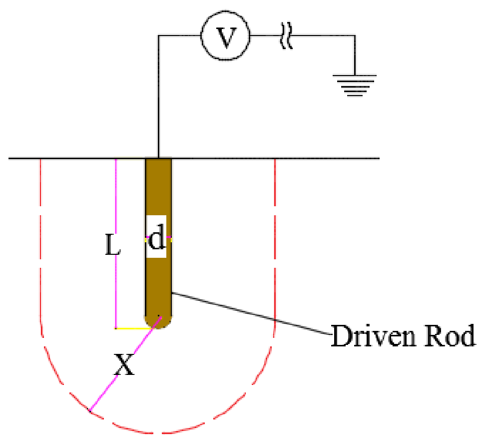

Figure 2-7 Simplified Diagram of Ground Resistance Measurement with Single Pole (Datta et al)

However, this measurement on ground presents problems because the electrodes have less contact area in relation to the overall volume of ground traversed by the current and the soil is a comparatively poor conductor – especially at the surface, where it tends to be relatively dry - as compared to metal. These effects create much higher resistance immediately around the probes than is encountered by the current in the deeper ground and may lead to an inaccurate result (Anthony, 1996).

The four electrode method with equidistance separation was introduced by Frank Wenner, which considers the effect of ground surface and contact area. If the contact conditions are poor and the current drops, then the potential measurement also drops but the ratio – the resistance – remains the same.

If the probes are inserted at the depth 'L' and are equal spacing to each other at 'a', then the soil resistance is given by;

$$R = \frac{\rho}{4\pi L}\left(1 + \frac{2a}{\sqrt{a^2 + 4L^2}} - \frac{a}{\sqrt{a^2 + L^2}}\right) \ldots\ldots\ldots\ldots\ldots\ldots\ldots\ldots\ldots\ldots .2.II$$

If L<< a, then the formula reduced to the following;

$$R = \frac{\rho}{2\pi L} \ldots\ldots\ldots\ldots\ldots\ldots\ldots\ldots\ldots\ldots\ldots\ldots\ldots .2.III$$

Where, 'ρ' is the soil resistivity.

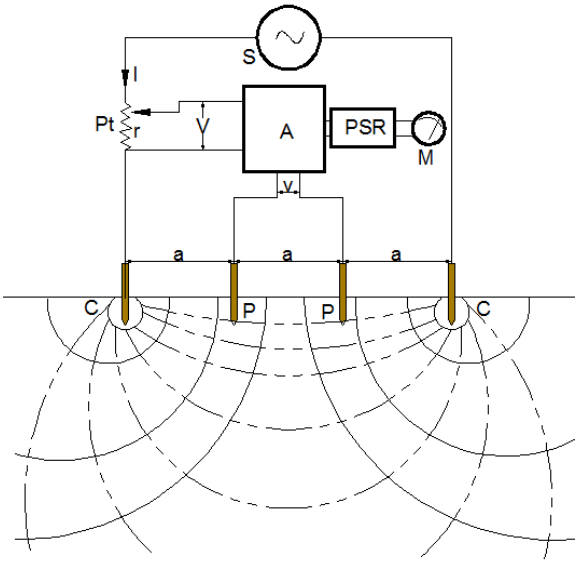

Figure 2-8 Conceptual Diagram of 4 Electrode Method (After Frank Wenner)

Fall of potential method is another well-known method for determination of soil resistivity. The relation 2.I is valid for fall of potential method. The diagrammatical representation for fall of potential method is as shown in figure 2.9.

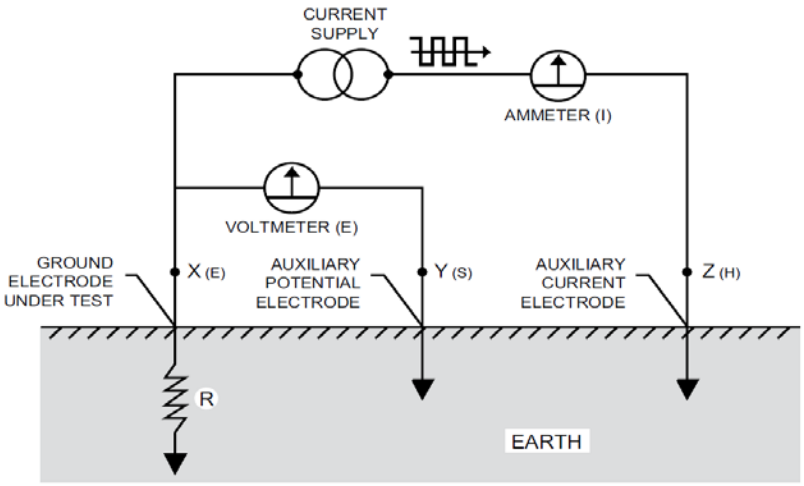

Figure 2-9 Resistance Measurement by Fall of Potential (User Manual-4620, AEMC Instruments)

2.5. Resistance Measurement of Fouled Ballast at Lab and Field

For determination of the degree of fouling of large scale sample ballast, the Wenner 4 point method was applied by Rahman (2014). Rahman measured the resistivity for thicknesses of six inches, eighteen inches, and twelve inches of fouled ballast. A wooden board with pre-drilled holes at a measured spacing was used to hold the rods during the test. Figure 2.10 illustrates the electrical resistance measurement set up done by Rahman.

The resistivity of the sample was measured using an AEMC 4620 digital ground resistance tester. As the depth of the rods was increased, the resistivity of the sample increased. The higher resistivity at greater depths was interpreted to be representative of drier materials, while the near surface materials had a lower resistivity due to the addition of water to the surface at the process of sample preparation.

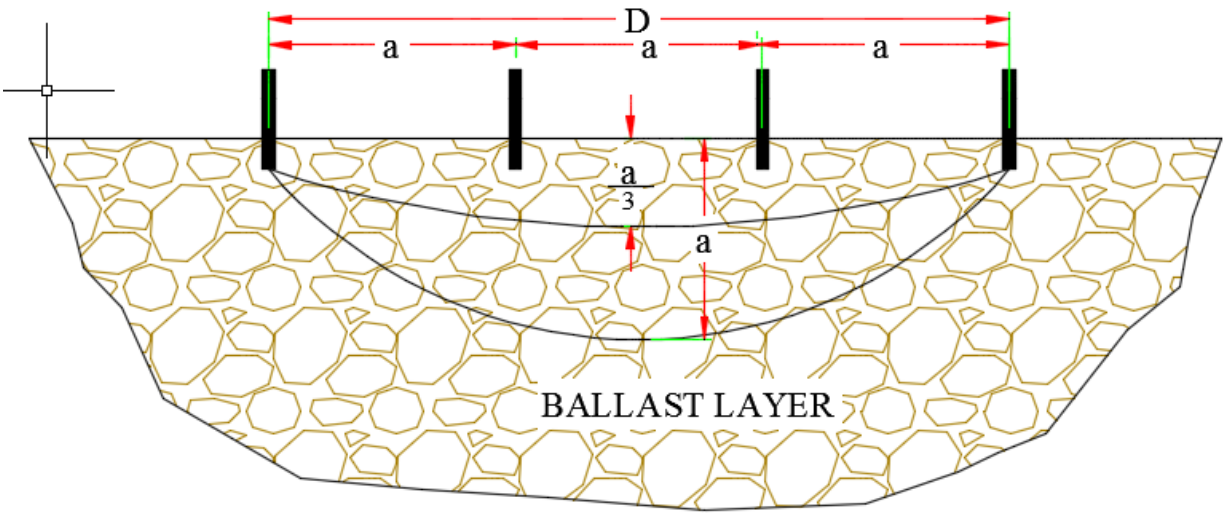

Figure 2-10: Schematic Diagram of Large Scale Resistivity Test (After Rahman Setup)

The relationship between permeability, resistivity and percentage fouling by weight was identified by AJ Rahman (2014). The test was carried out on fouled ballast obtained from

Gardner, Kansas and coal dust from Wyoming provided by Burlington Northern and Santa Fe (BNSF) Railway. During the test, permeability and resistivity were measured for materials with different fouling indices. The sample fouled materials having different fouling indices were prepared by mixing with coal dust, crushed ballast fines, or clay with clean aggregates. A relation of resistivity of the fouled ballast with the percentage fouling by weight of the fouled aggregate in is given in figure 2.11.

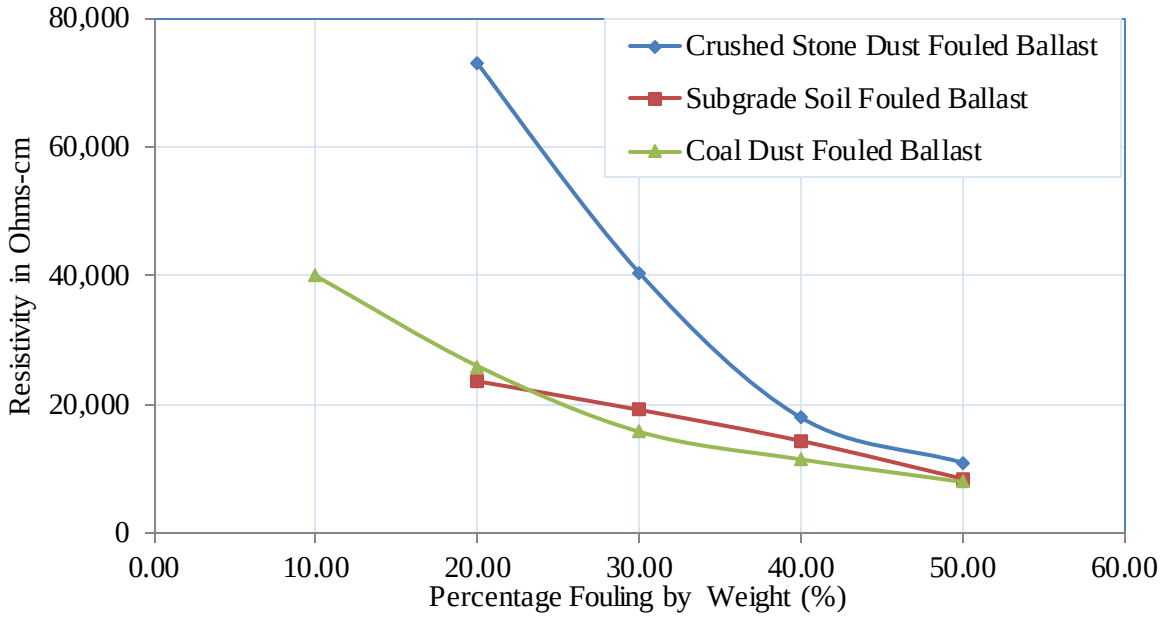

Figure 2-11: Resistivity of Fouled Ballast at the 18th Hour versus Fouling Index (AJ Rahman)

2.6. Factors Affecting Soil Resistivity

Tagg (Tagg, 1964) listed the type of soil, chemical composition of salt dissolved in the contained water, moisture content, temperature, grain size of material, grain size distribution and closeness of packing and pressure as major factors that determine the resistivity of soil. These parameters are controlled by (a) moisture content (b) temperature (c) soil type and (d) electrolyte.

Presence of water in the soil controls the electrical current flow due to the presence of electrolytic particles on the soil. Therefore, for higher water content, the electrical resistivity will be reduced. It has been reported that for water contents less than 15%, the electrical resistivity rapidly decreases with increasing water content (Samouelian, Cousin, Tabbagh, Bruand, & Richard, 2005). Tagg (Tagg, 1964) reported that the soil resistivity at first falls rapidly as the moisture content is increased, but after a value of 14 to 18% the rate of decrease becomes much less. Archie (Archie, January 1942) developed an empirical relationship between water content and electrical resistivity based on laboratory measurement of clean sandstone samples. His equation was modified to be valid for medium to coarse – grained soils. Later, Goyal et al. (Goyan, Gupta, Seth, & Singh, 1996) developed a liner relationship between the resistivity and the water content. Water content of the soil is a variable quantity and depends on weather, season of a year, nature of subsoil, and depth of water table. Soil will seldom be dry except for desert sand and rarely has a water content of more than 40% (Tagg, 1964). Since the moisture content is variable for fouled ballast layers because the moisture absorption by the fouling agent may be governed by the amount of fouling, the relationships between moisture content, resistivity and fouling and were examined as a part of this study.

Ion agitation increases with temperature when the viscosity of a fluid decreases. Thus the electrical resistivity decreases when the temperature increases (Samouelian, Cousin, Tabbagh, Bruand, & Richard, 2005). For temperatures below freezing the resistivity of the soil increases due to formation of ice (Tagg, 1964). Campbell et al. (Campbell, Bower, & Richards, 1948) found that the conductivity increased by 2.02% per degree centigrade between 15 to 35^{o}C. Therefore comparisons of electrical resistivity should be done at one standard temperature.

The major role of electrical conductivity on soil is due to presence of electrolytes or dissolved salts. Since the electrical conductivity is different for different salts, the same soil at different locations may have a different electrical resistivity if different salts are present. The salts are not conductive by themselves and need a medium of water. Since the rail track is fouled by coal dust, subgrade soil or crushed stone dust ballast, the properties of the fouled ballast are the same throughout the track for a given fouling agent unless the subgrade soil changes.

Soil types describe the nature and arrangement of solid constituents. The electrical conductivity is a function of soil particle size and the electrical charge density at the surface of the soil solids. Fukue et al. (Fukue, Minatoa, Horibe, & Taya, 1999) found that the electrical charges located at the surface of clay particles lead to greater electrical conductivity than in coarse textured soils because of the higher specific surface area. Pore geometry and void distribution generally governs the amount of air and water in the voids based on water potential. Tagg (Tagg, 1964) stated that the same general type of soil occurring in various localities is often found to have different resistivities. Therefore, soil types describe in a general way the chemical composition, grain size of material and its distribution, closeness of packing and applied pressure.

2.7. Resilient Modulus of Ballast

The resilient modulus (M_R) is the elastic modulus based on the recoverable strain under repeated loads. As ballast exhibits a nonlinear and time dependent elasto-plastic response under repeated loading, the resilient modulus is often of more interest than the elastic modulus. The resilient modulus is equal to the deviator stress (σ_d) divided by recoverable elastic strain (ε_r). The resilient modulus of railroad ballast is influenced by several parameters including stress history, load cycles and stress level; load duration, frequency and load sequence; density; grading, fines content and maximum grain size; aggregate type and particle shape; and moisture content.

Among these factors, only the influence of stress and moisture content are consistent (Lekarp, Isacsson, & Dawson, 2000) . The resilient modulus is generally taken to characterize the cyclic densification of granular aggregates commonly used in pavements and rail lines. The resilient behavior of railway track bed is complex as the properties of subgrade soil underlying the track also affect the rate of settlement and partial ballast degradation.

The magnitude of the resilient modulus is very much stress-state dependent. The resilient response of unbound granular materials greatly increases as the confining pressure increases and the magnitude of the repeated deviator stress has little effect (Selig & Waters, 1994).

2.8. California Bearing Ratio (CBR) of Ballast

Evaluation of California Bearing Ratio (CBR) value by the dynamic cone penetrometer (DCP) is useful for the determination of the bearing value of crushed stone ballast when subjected to intense repeated loading. A cone tipped rod is driven with repeated blows with a weight falling from certain height. The rate of penetration per blow is the dynamic penetration index (DPI) or penetration index (PI) and is an indicator of the type and strength of the soil. There has been little success on numerically relating dynamic PI to dry density and other parameters. Salgado and Yoon (Salgado & Yoon, 2003) found that the CBR increases while dry unit weight increases. However he proposed no exact numerical relationship. The DCP index is plotted against total depth and is correlated with CBR. The US Army Corps of Engineers recommended numerical relations that can relate the value of CBR to PI (Webster, Brown, & Porter, 1994).

Harison (Harison, 1987) describes the penetration index (PI) as a function of moisture content and dry unit weight. He found that if the moisture content increased, the penetration index first decreased and then increased after optimum moisture content of compaction curve. However,

Salgado and Yoon (Salgado & Yoon, 2003) found that the PI from DCP is very sensitive to moisture conditions and PI for a given material slightly increases with increasing moisture content. Sayers et al. (Ayers, Thompson, & Uzarski, 1989) developed a correlation between PI and the shear strength of the granular soil. He ran the test for different materials including crushed dolomitic ballast and other ballast having non plastic fines of 7.5%, 15% and 22.5% and correlated the shear strength with PI at different confining stress. The PI for granular soil, especially soils with gravel, can cause unrealistic PI measurements due to contact with the large aggregate.

2.9. Shear Strength Properties of Ballast

Ballast loses strength as the amount of fouling increases. Strength can be determined by the Large Direct Shear Test in the laboratory. Huang et.al (Huang, Tutumluer, & Dombrow, 2009) conducted a study of the strength properties of clean and fouled ballast samples fouled with coal dust, plastic clay, and mineral fillers at various percentages by weight. The result of the study showed that coal dust is the worst fouling agent based on its impact on track substructures, though all types of fouling agents cause decreasing trends in shear strength properties. Because of the increasing cohesive nature with increasing fouling percentages, plastic clay fouled samples exhibit slight increases in shear strength under both dry and wet conditions. Coal dust caused the most drastic decreases in shear strength especially for highly fouled levels. Fifteen percent of dry coal dust by weight was sufficient to cause critical fouling and decreased the ballast strength considerably (Huang, Tutumluer, & Dombrow, 2009). Rahman (Rahman, Parsons, Han, & Glavinich, 2014) conducted shear strength tests on fouled ballast samples in the large direct shear test box and modified large direct shear box at the University of Kansas and concluded that coal dust and subgrade soil caused a significant decrease in strength as compare to crushed stone dust. The

modified direct shear box test presented a clearer pattern of decreasing strength as fouling agent content increased. Also, the Modified Direct Shear test results showed lower friction angles for the same sample as compared with the Large Direct Shear Test (Rahman, Parsons, Han, & Glavinich, 2014).

Chapter Three: Determination of Material Properties

3.1. Engineering Properties of Clean Ballast

3.1.1. General Information about Ballast

The clean ballast was obtained by washing the fouled ballast from the Gardner, Kansas BNSF rail track. The schematic diagram of recycling of ballast is given in figure 3.1.

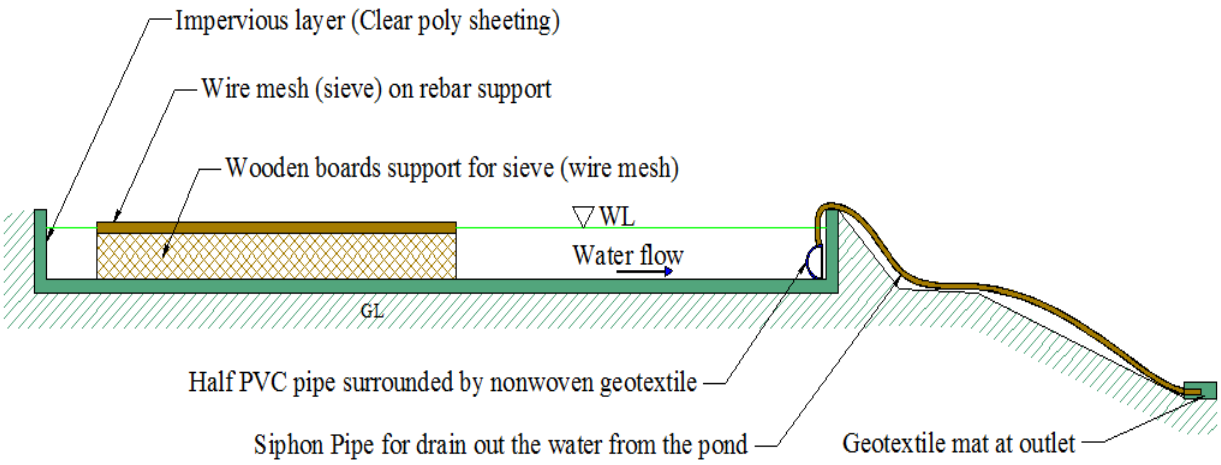

Figure 3-1 Schematic Diagram of Ballast Cleaning Arrangement

A wire mesh of 6.42 mm (C – C of the mesh) with a mesh wire diameter of 0.55 mm was used for wet sieving the materials. The clear spacing of the mesh was 5.87 mm. A mesh of 4 ft. width and 6 ft. length was constructed on a rebar frame as shown in the following figure. The 6 mil polyethylene sheeting was used for making impervious layers which were laid just above the non-woven geotextile which served as a cushion for the plastic sheet. Wooden boards of approximately 5.5 inch height (2 x 6) were placed all around the pond to make the levee for collected wash water. At the end of the pond, the outlet hose pipe was connected to the 5 ft. long and 2 inch diameter PVC pipe, which had rows of holes in one side and was wrapped with geotextile and acted as the mouth of the water outlet. The wire mesh was designed to be placed at the middle of the pond at the same height as the pond levee.

Figure 3-2 Ballast Recycling (a) Wire Sieve and Pond for Sieving (b) Sieving Procedure

The fouled ballast was spread over the wire mesh as shown in figure 3.2. Water was sprayed via hose directly on the ballast over the sieve and the sieve was shaken by hand to obtain clean ballast. Water was applied continuously until the clean water came from the bottom of the mesh. This water after washing went to the bell mouth and the outlet hose while the soil particles larger than 5.87 mm were retained in the pond.

The ballast obtained from washing was dried and the gradation of the ballast was determined. The gradation of the fouled ballast before washing and the clean ballast after washing are shown in the following figure:

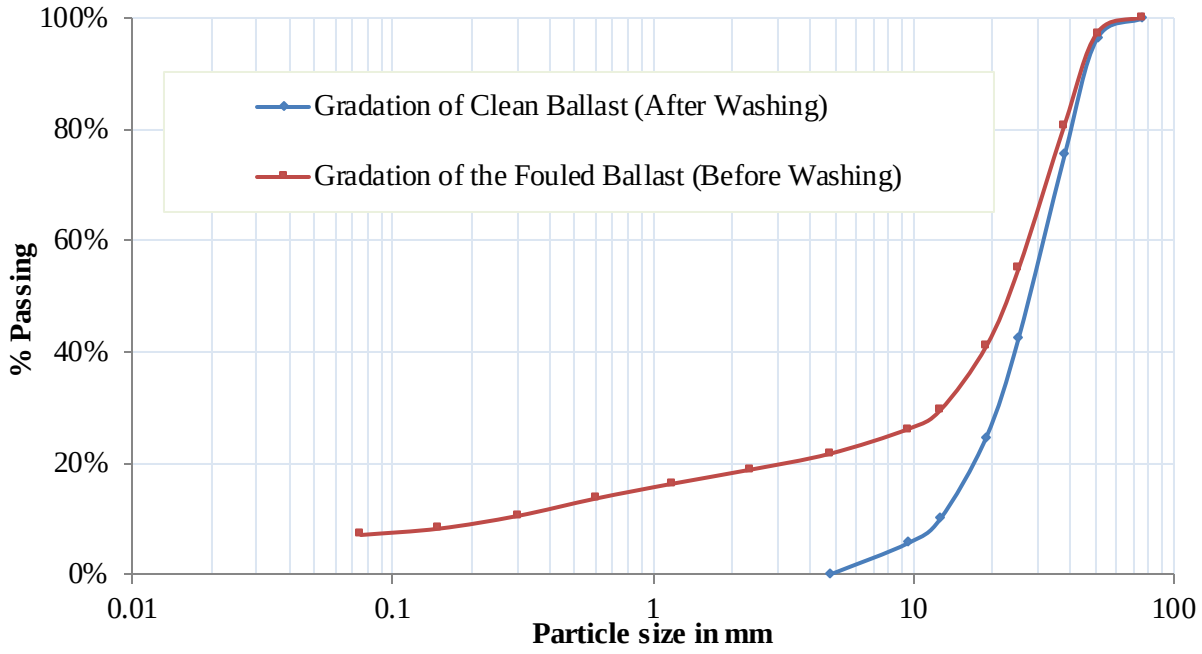

Figure 3-3 Gradation Curve of Ballast before Washing (without Cleaning) and after Washing

3.1.2. Gradation of Clean Ballast

The distribution of particle size was determined by sieve analysis in accordance with ASTM D6913-04. The result of the distribution is plotted in figures 3.3 and 3.4. A total of 61.65 lb (27.97 kg which is greater than 25 kg for maximum particle size of 50 mm) of sample was taken for the sieve analysis. The maximum size, mean size, coefficient of curvature and coefficient of uniformity of the coal dust were found to be 50 mm, 24.14 mm, 1.25 and 2.77 respectively.

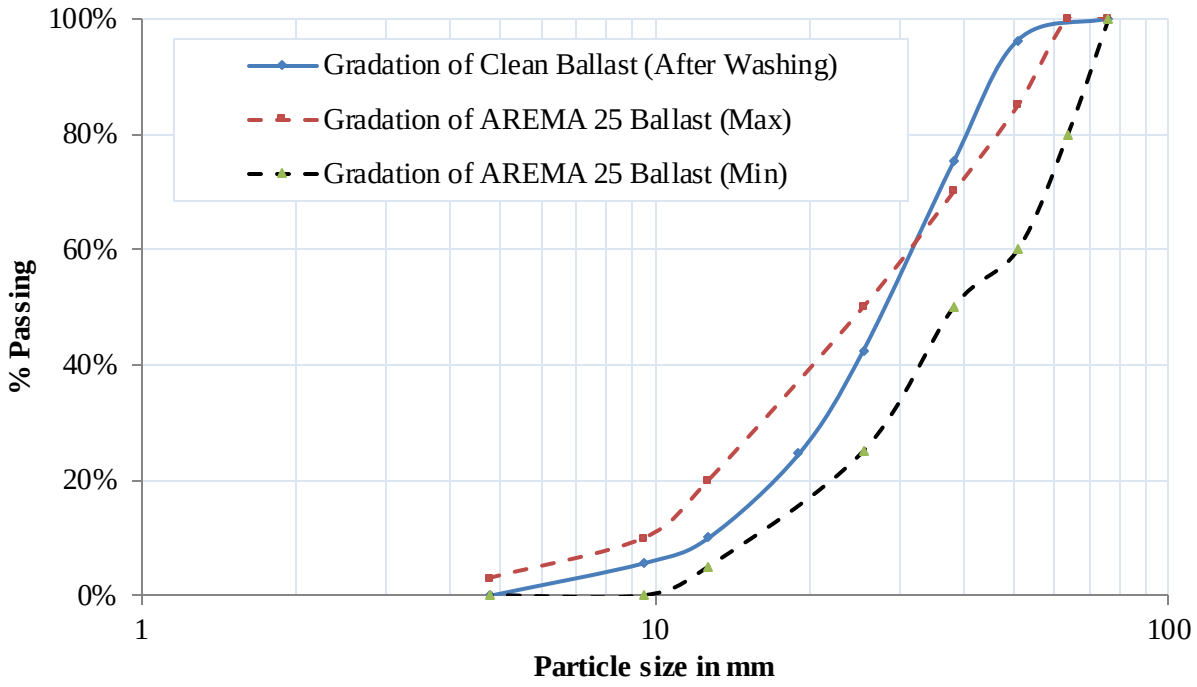

Figure 3-4 Gradation Curve of Test Ballast and AREMA Specified Ballast

3.1.3. Other Engineering Properties

The bulk specific gravity, saturated surface dry (SSD) bulk specific gravity and water absorption were measured based on ASTM C127 – 12. The results are listed in the following table.

Table 3-1 Engineering Properties of Clean Ballast

Bulk Specific Gravity	Saturated Surface Dry (SSD) Bulk Specific Gravity	Apparent Specific Gravity	Water Absorption
2.69	2.71	2.74	0.67%

The lab set up for determination of the different specific gravities of the ballast is as shown in below figure.

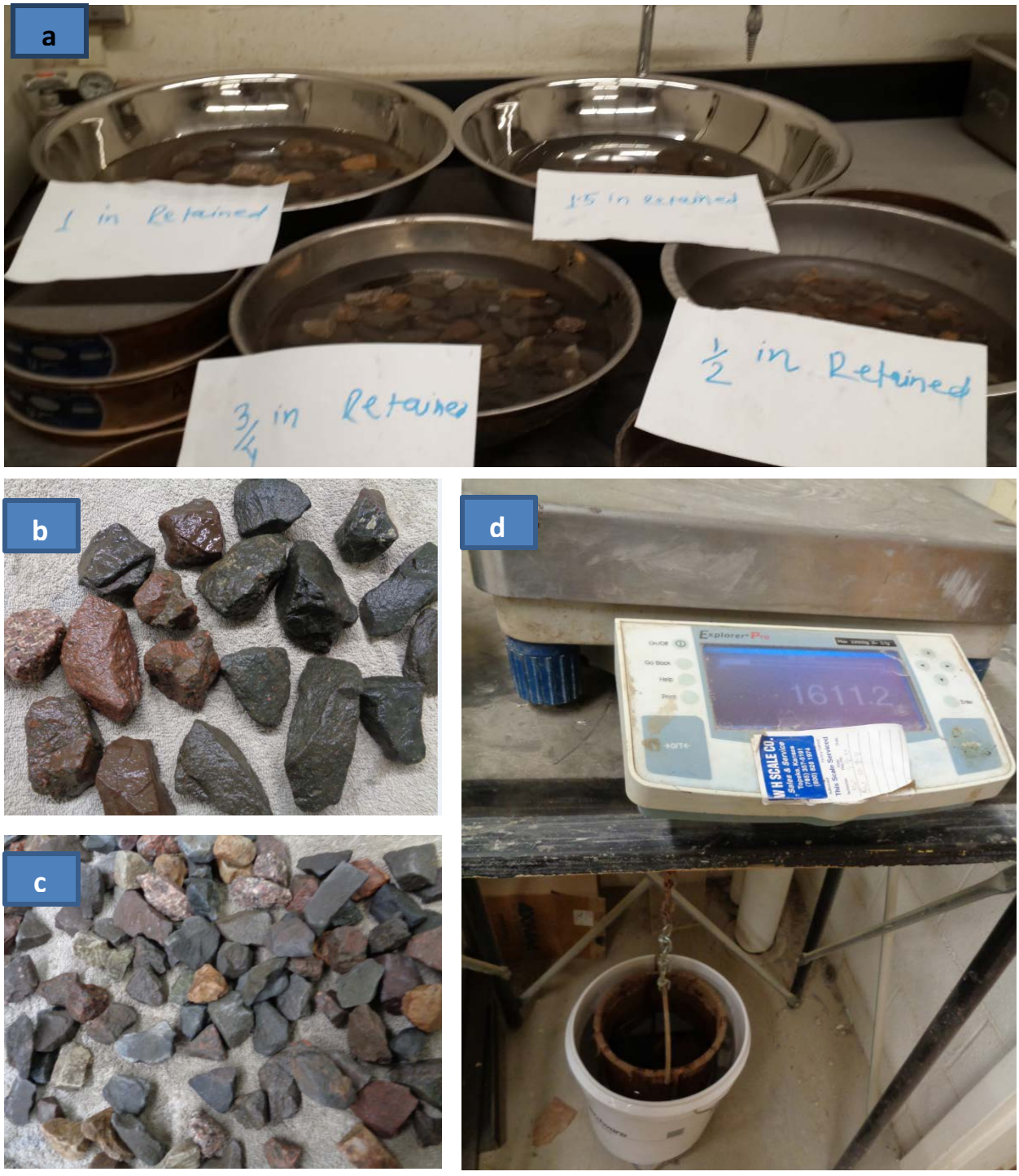

Figure 3-5 Specific Gravity Determination of Ballast (a) Soaking of Different Sizes of Ballast (b) & (c) Finding Saturated Weight of Ballast (d) Finding Submerged Weight of Ballast

Four samples of 1.5 inches retained, 1 inches retained, 3/8 inches retained and ½ inches retained ballast were used for specific gravity determination. Four different test of specific gravity of the

ballast were conducted. The ballast samples with sizes of 1.5 inches, 1 inch, ¾ inches, and ½ inches diameter were present in percentages of 20.9%, 32.8%, 17.9% and 14.6%. Since the majority of the ballast fell in these four categories, these samples were considered for finding the average specific gravity of the ballast. The average relative densities of the ballast was found by

$$G = \frac{1}{\frac{P_1}{G_1} + \frac{P_2}{G_2} + \frac{P_3}{G_3} + \frac{P_4}{G_4}} \ldots\ldots\ldots\ldots\ldots\ldots\ldots\ldots\ldots\ldots\ldots\ldots\ldots\ldots\ldots\ldots 4.II$$

Where, G_1, G_2, G_3, G_4 are the specific gravity of each size fraction

P1, P2, P3 and P4 are the mass percentage of each size fraction in original sample. The individual specific gravities and water absorptions are listed in the following table:

Table 3-2 Specific Gravity and water absorptions of Different Graded Samples

Descriptions of Items	Sample 1 1.5 in retained	Sample 2 1 in retained	Sample 3 3/4 in retained	Sample 4 1/2 in retained
Bulk Specific Gravity	2.71	2.69	2.69	2.67
SSD Specific Gravity	2.73	2.71	2.71	2.69
Apparent Specific Gravity	2.76	2.74	2.74	2.73
Water Absorption	0.57%	0.65%	0.63%	0.84%

3.2. Engineering Properties of Subgrade Soil

3.2.1. General Information about Subgrade Soil

The subgrade soil was obtained by digging a pit on northwest of the soil lab at west campus. The top 1 foot of soil was removed first in order to minimize the organic materials in the soil. The excavation was carried out with a skid loader. The photograph of the pit excavation for the subgrade soil is shown below:

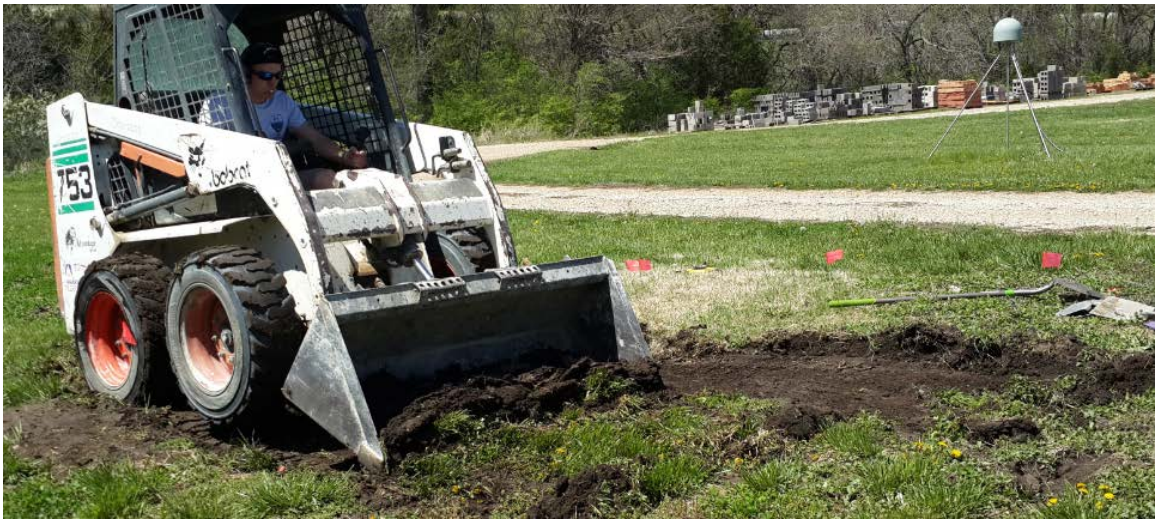

Figure 3-6 Removal of Top Soil for Extracting Subgrade Soil as Fouling Agent

3.2.2. Gradation of Subgrade Soil

The distribution of particle size was determined by hydrometer analysis in accordance with ASTM D422. The result is plotted in figure 3.7. The maximum size, mean size, coefficient of curvature and coefficient of uniformity of the subgrade soil were found to be 0.075 mm, 0.031 mm, 0.563 and 9.286 respectively.

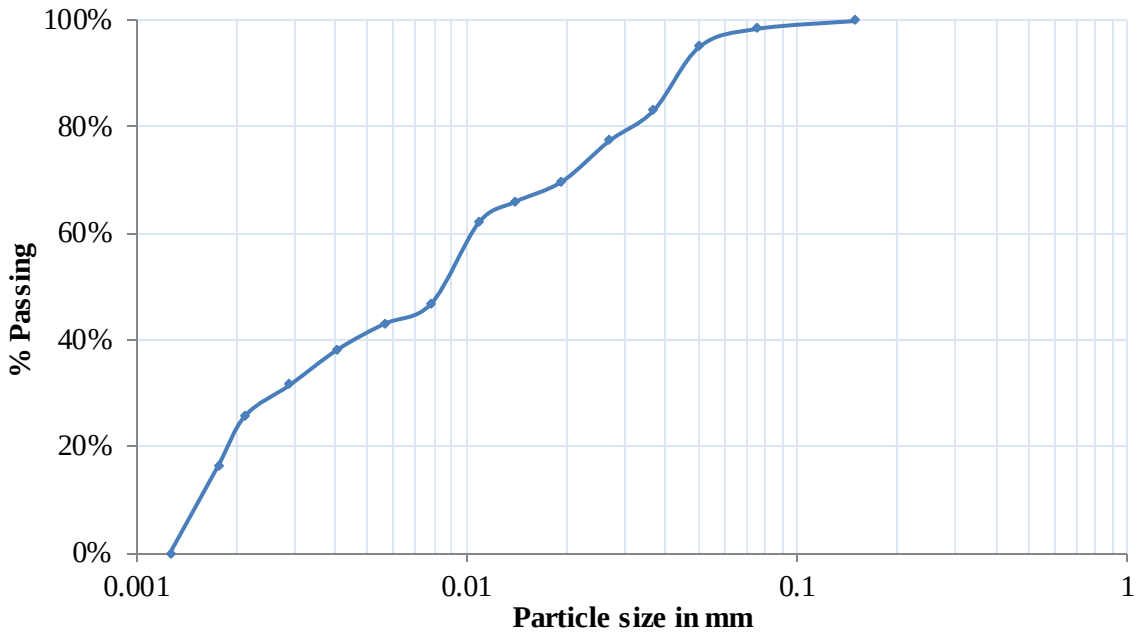

Figure 3-7 Particle Size Distribution of Subgrade Soil

3.2.3. Other Engineering Properties of Subgrade Soil

The specific gravity of the subgrade soil was determined by the water pycnometer test in accordance with ASTM D854-06. The liquid limit and plastic limit were obtained using ASTM D4318-10 and the optimum moisture content and the maximum dry density were measured using ASTM D1557-12. The results are summarized in the following table:

Table 3-3 Engineering Properties of Subgrade Soil

Specific Gravity	Liquid Limit (%)	Plastic Limit (%)	Optimum Moisture Content (%)	Maximum Dry Density (lb/ft3)
2.66	43	21	19.3%	101.2

The proctor curve for the subgrade soil used as a fouling agent in ballast was found as follows:

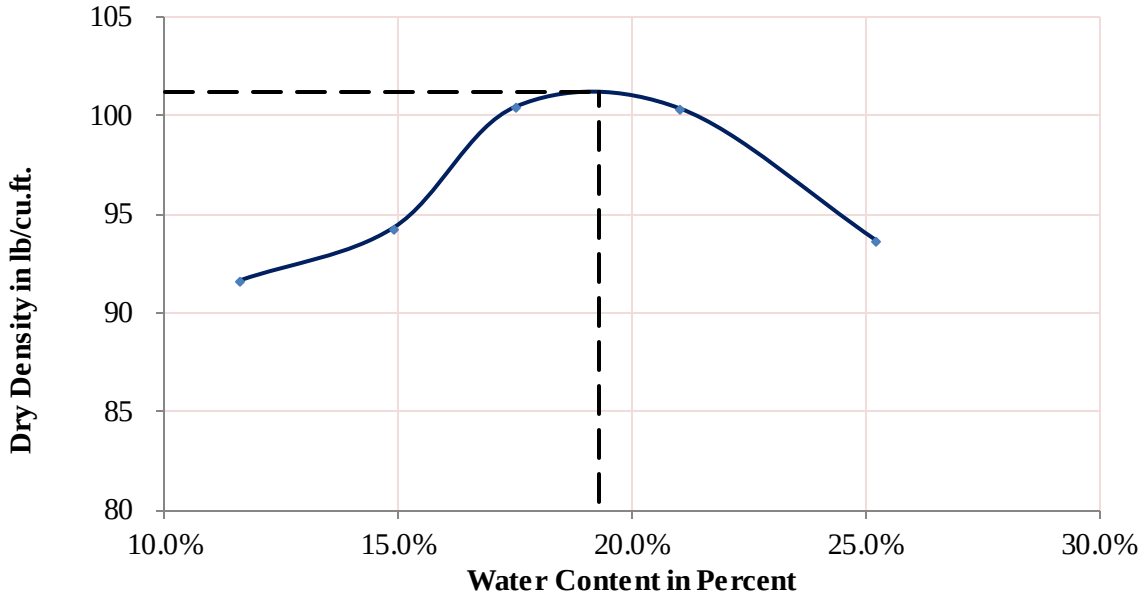

Figure 3-8 Proctor Curve of Subgrade Soil

3.3. Engineering properties of Coal Dust

3.3.1. General Information about Coal Dust

Coal consists of the remains of plant materials. Commonly measured properties of coal include heating value, ash melting temperature, sulfur and other impurities content, mechanical strength,

and other physical properties. Coal is classified as anthracite, bituminous, subbituminous and lignite based on its properties. For this research purpose, subbituminous coal was sampled because of its large application for industry - primarily to generate electricity and make coke for the steel industry. It is mostly hauled via rail. This type of coal has a carbon content ranging from 45 to 86%.

The coal used in this research was Subbituminous – C type coal. This coal originated from Wyoming's Powder River basin. This is insoluble black solid chunk coal rock up to 3 inch size and has a pH of 7. The composition of the coal is given in Table 3.4.

The chunk of coal was ground in the Los Angeles Abrasion test machine. Photographs in figure 3.9 depict the status of the coal at the yard, the grinding procedure and the coal dust obtained after grinding. The larger particles – which were not ground properly – were separated from the mix manually and the dust particles were collected.

Table 3-4 Composition of Test Coal Dust

S.N.	Ingredients	% by Weight
1.	Carbon – Fixed	32 – 41 %
2.	Carbon – Volatiles	28 – 35 %
3.	Moisture	24 – 40 %
4.	Ash	3 – 9 %
5.	Sulfur	0.1 – 1.1 %
6.	Silica	1 – 3 %

Figure 3-9 Collection and Grinding of Coal (a) Coal Store Yards and Collection (b) Grinding Arrangement of Coal at the Laboratories of the University of Kansas

3.3.2. Gradation of Coal Dust

The distribution of particle size was determined by sieve analysis in accordance with ASTM D6913-04. The result of the distribution is tabulated in table 3.5 and plotted in figure 3.10. The maximum size, mean size, coefficient of curvature and coefficient of uniformity of the coal dust were found to be 4.5 mm, 0.554 mm, 1.993 and 12.131 respectively.

Table 3-5 Gradation Calculation Table for Coal Dust

Sieve Descriptions	Sieve Nos	Mass Retained on Sieve (lb)	Cumulative Mass Retained in Sieve (lb)	Cumulative Mass Passing from Sieve (lb)	% Passing from Sieve
4.75 mm (0.187 in)	4	0.000	0.000	2.822	100.00%
2.36 mm (0.0937 in)	8	0.007	0.007	2.815	99.74%
1.18 mm (0.0469 in)	16	0.659	0.667	2.155	76.38%
0.85 mm (0.0331 in)	20	0.351	1.018	1.804	63.94%
0.60 mm (0.0234 in)	30	0.368	1.386	1.436	50.88%
0.30 mm (0.0117 in)	50	0.583	1.969	0.853	30.22%
0.15 mm (0.0059 in)	100	0.343	2.313	0.509	18.05%
0.075 mm (0.0029 in)	200	0.170	2.482	0.340	12.04%
Pan	Pan	0.340	2.822	0.000	0.00%
Total		2.822			

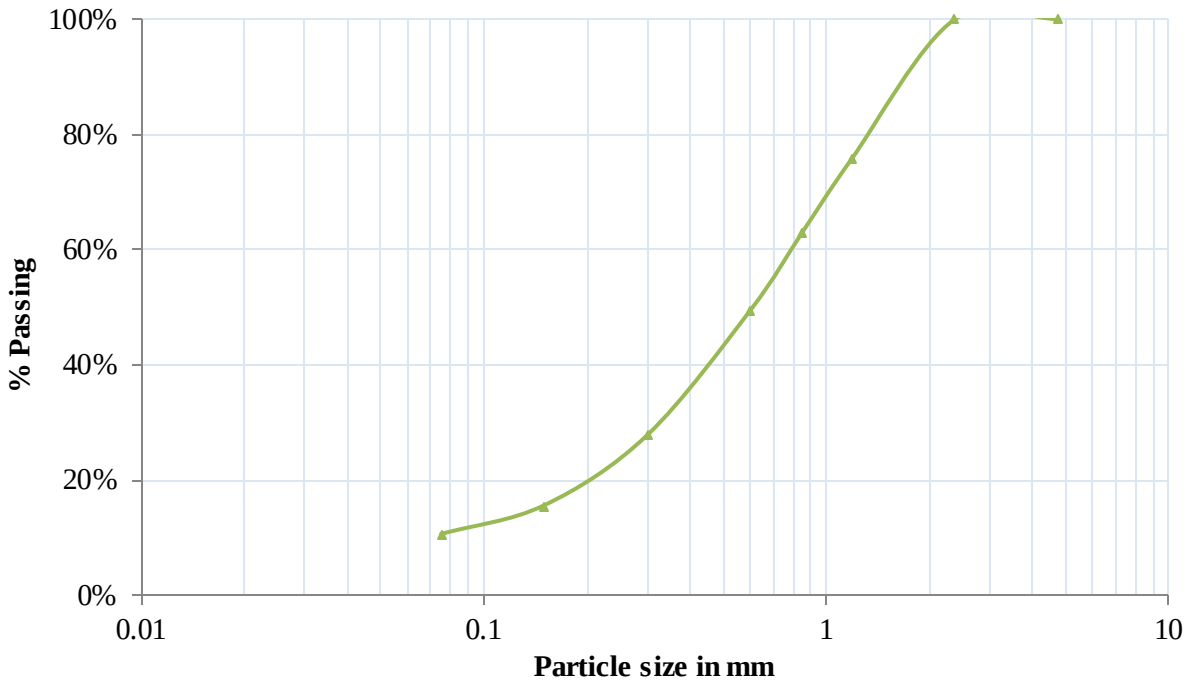

Figure 3-10 Gradation Curve of Coal Dust

3.3.3. Other Engineering Properties of Coal Dust

The specific gravity of the coal dust was determined by the water pycnometer test in accordance with ASTM D854-06. The liquid limit and plastic limit were obtained using ASTM D4318-10 and the optimum moisture content and the maximum dry density were measured using ASTM D1557-12. The results are summarized in the following table:

Table 3-6 Engineering Properties of Coal Dust

Specific Gravity	Liquid Limit (%)	Plastic Limit (%)	Optimum Moisture Content (%)	Maximum Dry Density (lb/ft3)
1.30	85	59	29.30	58.20

The proctor curve for the subbituminous coal dust used as a fouling agent in ballast was found as follows:

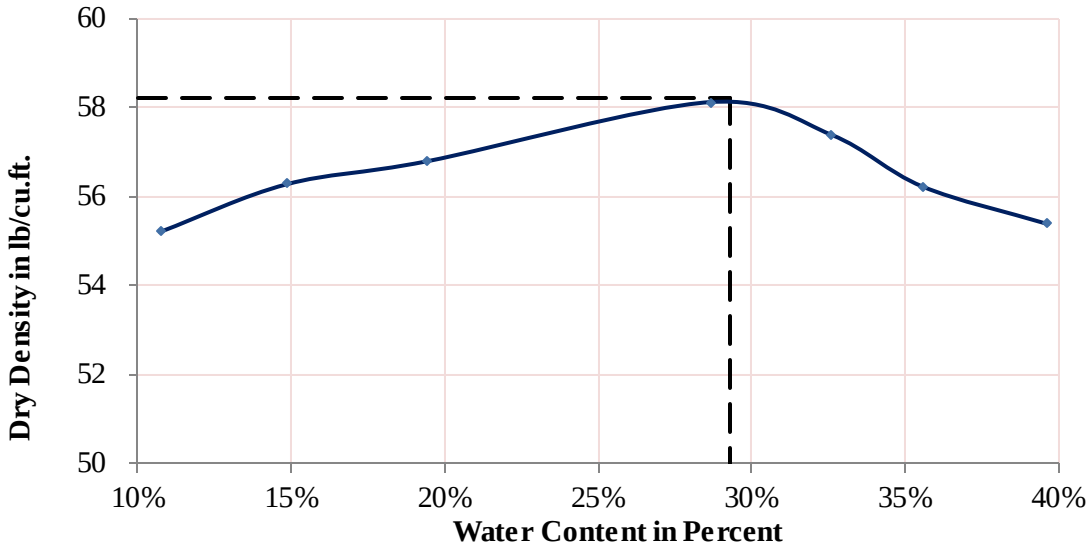

Figure 3-11 Proctor Curve for Coal Dust

This coal dust sample nearly matched to the coal sample collected from Power River Basin (PRB) Orin Line, Milepost 62.4 by Huang et.al. (2009). His sample has the specific gravity of 1.28, liquid limit of 91, plastic limit of 50, optimum moisture content of 35%, maximum dry density of 55 lb/ft^3, and percentage passing from 75 micron sieve of about 24%.

3.4. Engineering Properties of Gardner Track Ballast Dust

3.4.1. General Information about Gardner Track Ballast Dust

The Gardner track ballast dust was collected from the residuals of the ballast wash in the process of cleaning. The ballast residual that passed the 5.87 mm size wire mesh was washed with flowing water in a containment area of 10 ft. width and 16 ft. length as shown in figure 3.1 (a). The siphon was constructed at the end of pond to remove the washed water. The bell mouth of the siphon was covered with a geotextile with a 0.10 mm filtration opening size (FOS) – equivalent to 0.21 mm apparent opening size (AOS). This FOS was selected to remove most of the clay and silt particles from the mix such that the residuals contain only the Gardner track ballast dust to eliminate as much of the non-ballast source particles from the sample to compared

with the crushed stone ballast dust. A photograph and sketch of the ballast cleaning arrangement and the collection of Gardner track ballast dust are given in Figure 3-12:

Figure 3-12 Water Drain out Arrangement after Washing Gardner Track Ballast Dust

3.4.2. Gradation of Gardner Track Ballast Dust

The particle size distribution was determined by sieve analysis in accordance with ASTM D6913-04. The distribution is plotted in figure 3-13. The maximum size, mean size, coefficient of curvature and coefficient of uniformity of the Gardner track ballast dust were found to be 5.87 mm, 0.958 mm, 2.206 and 13.70 respectively.

The percentage of particles smaller than 75 micron was found to be only about 14.5% of the total mass of the fouling. The corresponding gradation curve is shown in the following figure.

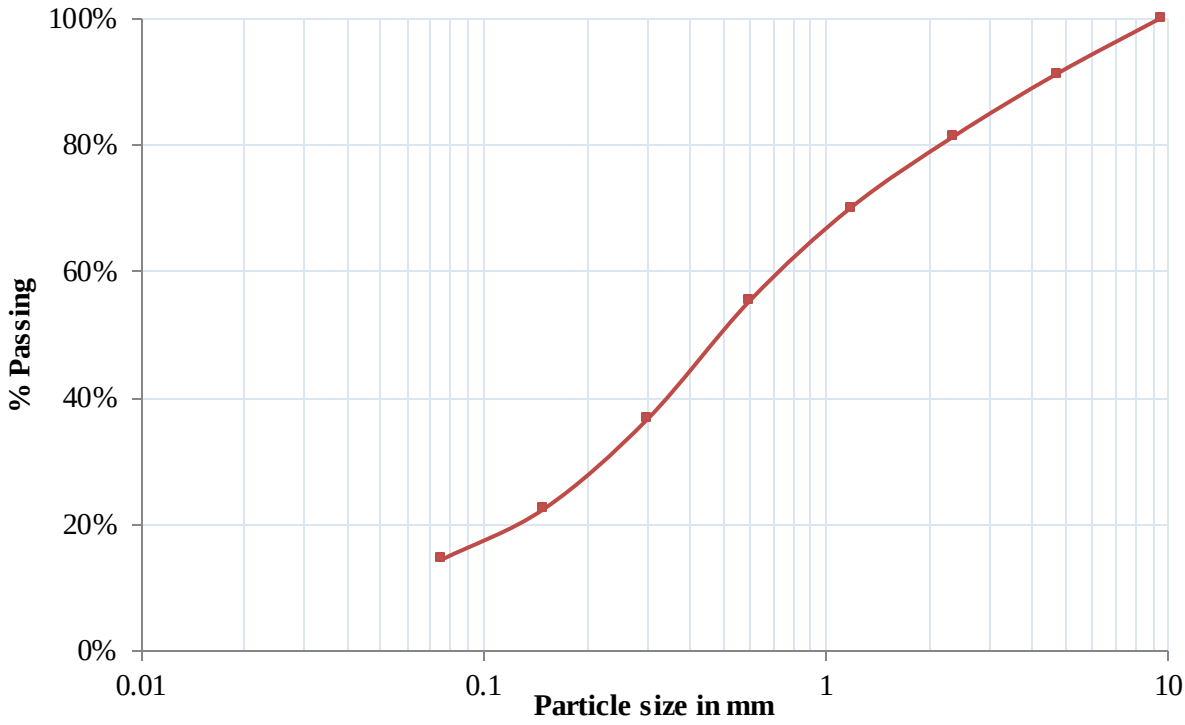

Figure 3-13 Gradation Curve for Gardner Track Ballast Dust

3.4.3. Other Engineering Properties of Gardner Track Ballast Dust

The specific gravity of the Gardner track ballast dust was determined by the water pycnometer test in accordance with ASTM D854-06. The liquid limit and plastic limit were obtained using ASTM D4318-10 and the optimum moisture content and the maximum dry density were found using ASTM D1557-12. The results are summarized here in the following table:

Table 3-7 Engineering Properties of Gardner Track Ballast Dust

Specific Gravity	Liquid Limit (%)	Plastic Limit (%)	Optimum Moisture Content (%)	Maximum Dry Density (lb/ft^3)
2.70	31	14	11.3	121.1

The proctor curve for the Gardner track ballast dust used as a ballast fouling agent was found as follows:

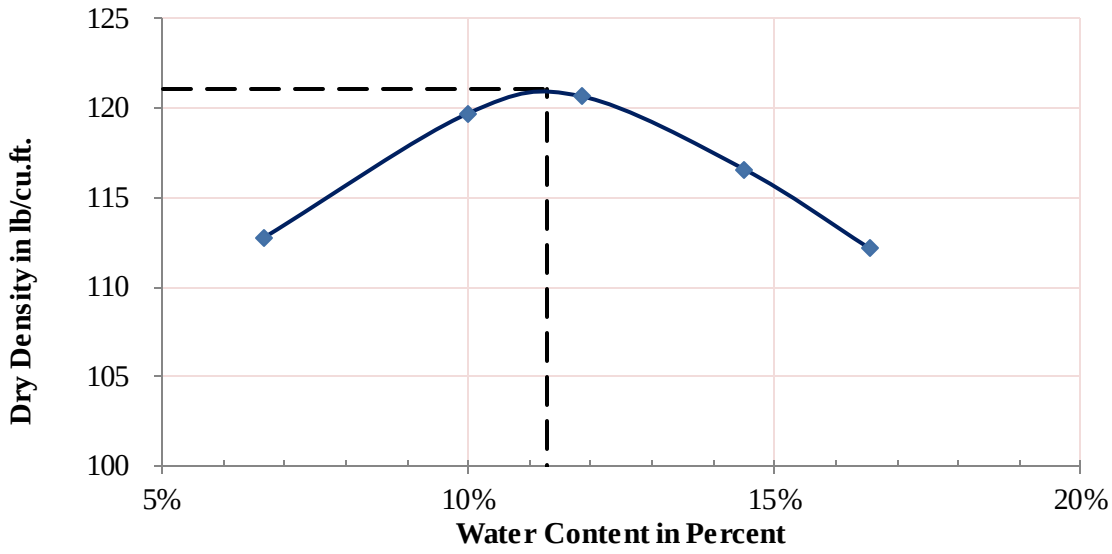

Figure 3-14 Proctor Curve of Gardner Track Ballast Dust

3.5. Comparison of Basic Engineering Properties of Fouling Agents

Table 3.8 depicts the comparison of all basic engineering properties of the fouling agents

Table 3-8 Comparison of Engineering Properties of Fouling Agents

S.N.	Descriptions of Properties	Units	Subgrade Soil	Gardner Track Ballast Dust	Coal Dust
1	Fine content (Less than 75 micron)	%	95.1	14.50	10.5
2	Maximum size of particles	mm	1.50	5.87	4.50
3	Average mean size of particles	mm	0.031	0.958	0.554
4	Coefficient of curvature (C_c)		0.563	2.206	1.993
5	Coefficient of uniformity (C_u)		9.286	13.70	12.131
6	Specific gravity		2.66	2.70	1.30
7	Liquid limit	%	43	31	85
8	Plastic limit	%	21	14	59
9	Optimum moisture content	%	19.3	11.3	29.30
10	Maximum dry density	lb/cu.ft.	101.2	121.1	58.20

The comparative graph of particle size distribution is given below in Figure 3-15. Here, the distribution shows that the particle size for Gardner track ballast dust and the coal dust are almost equal and the subgrade soil has a large percentage of very fine particles as compared to other two fouling agents.

Gardner track ballast dust had the highest maximum dry density followed by the subgrade soil and coal dust. However the optimum moisture content is just the reverse. Coal dust had a very high optimum moisture content as compared to the Gardner track ballast dust. Figure 3-16 shows the optimum moisture content versus maximum dry density graphs for these types of fouling agents.

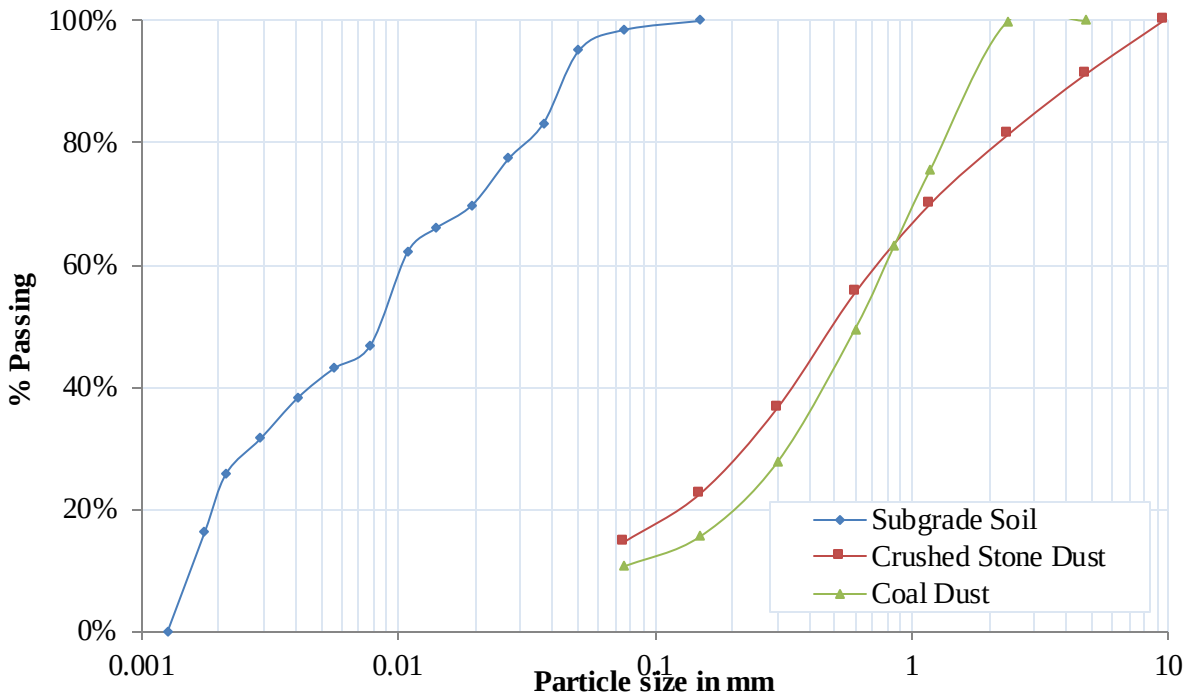

Figure 3-15 Comparison of Particle Size Distribution of Fouling Agents

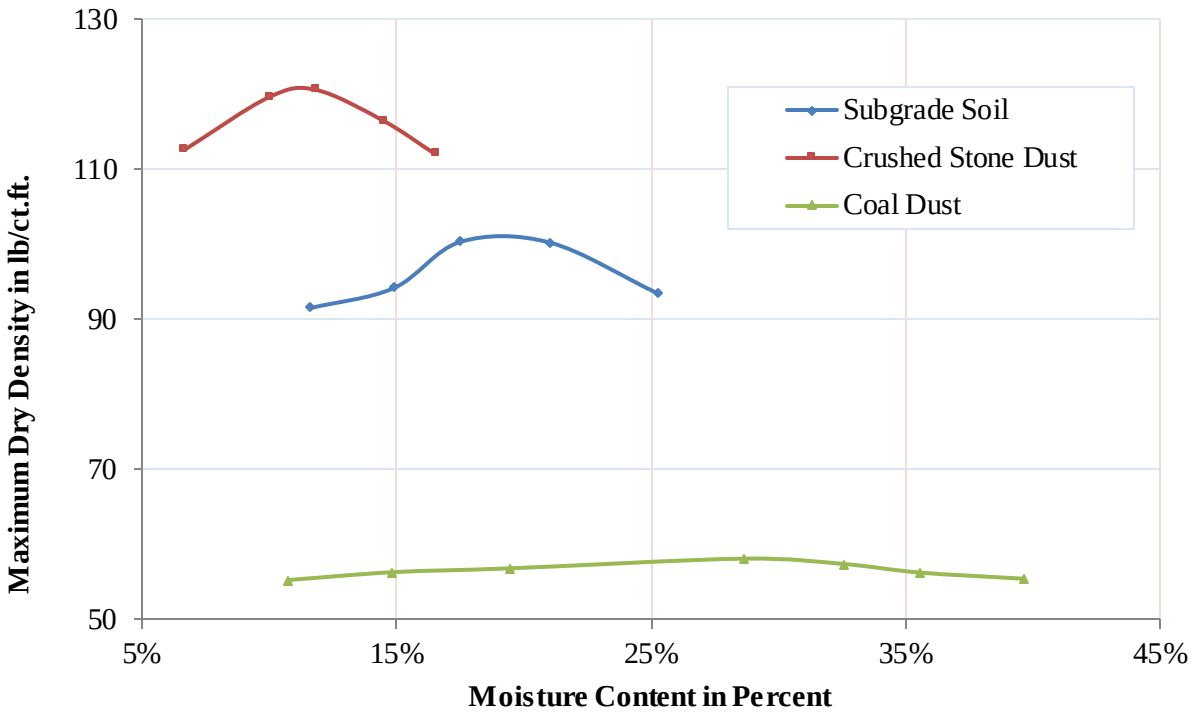

Figure 3-16 Comparison of Optimum Moisture Content of Fouling Agents

3.6. Electrical Resistivity of Fouling Agents

3.6.1. Small Box Resistivity Test of Fouling Materials

A plastic box 18 inches in length, 6 inches in width, and with a depth of 8 inches was constructed at the University of Kansas to measure the resistivity of the fouling agents in order to define their resistivity properties. The box was designed based on the four probe method of measuring the resistivity. A prototype of a larger size of the test box was constructed according to ASTM G57 and its standard test box. Copper plates 6 inch x 6 inch square were placed at the two ends of the test box. Two middle probes of diameter 0.4 inches were inserted horizontally for the length of 4.25 inches from the inner side of the wall. The schematic diagram of the box is presented in figure 3-17 and figure 3-18 shows the test box prepared at KU. The four probes of the test box were connected to the 4 probes of the ground resistance tester as directed by the manual for the ground resistivity testing meter.

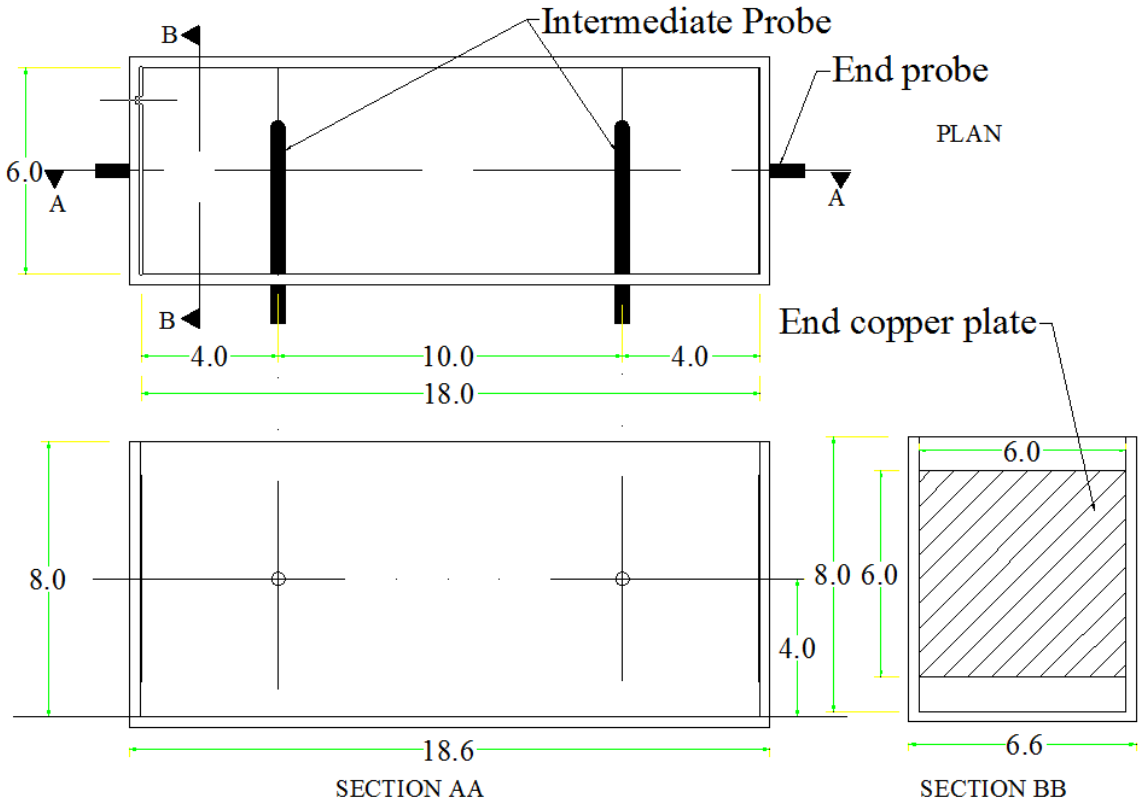

Figure 3-17 Schematic Diagram of Small Test Box for Resistivity

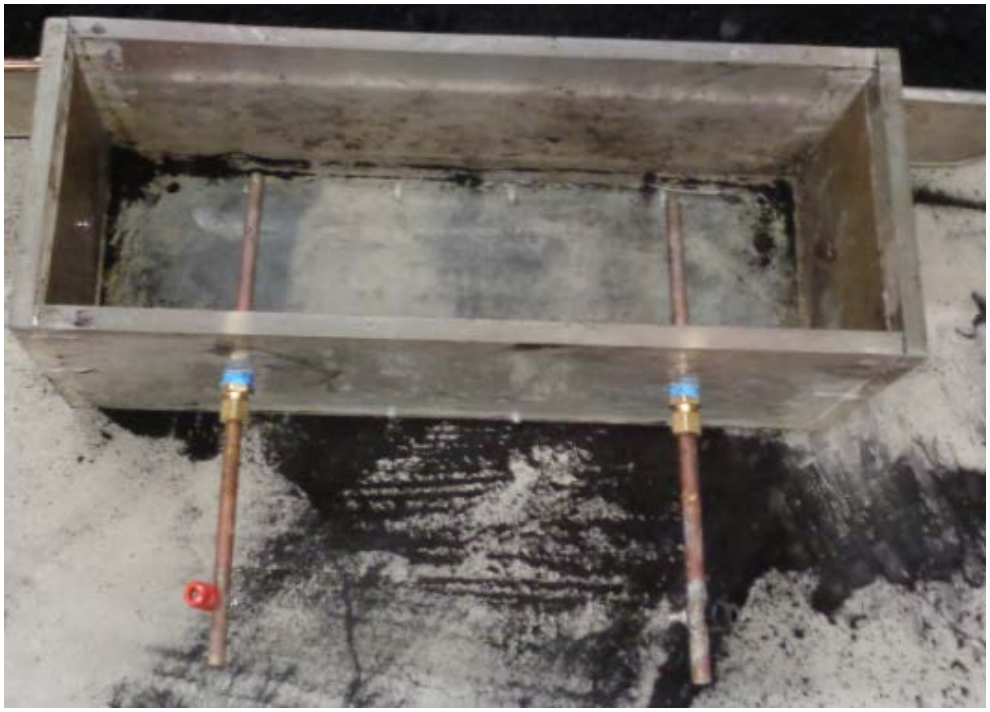

Figure 3-18 Test Box Constructed at KU

3.6.2. Sample Preparation and Testing

Three fouling agents: subgrade soil; Gardner track ballast dust; and coal dust, were dried and then crushed with a 4.9 lb (2.21 kg) compactor. The large, dried chunks were crushed into their small particle constituents. Specific amounts of water were added to these samples and then the samples were mixed uniformly. The fouling agents were placed in the designed box in three layers and compacted with the 4.9 lb (2.21 kg) compactor manually. The average depth of all the samples was 7.2 inches. Figure 3-19a illustrates the construction of the samples.

The resistivity values of the samples were measured with the AEMC ground tester. 4 point resistivity measurements were carried out. The total depths of the samples were used to calculate the densities of the samples in each test. The moisture contents of the samples were obtained using two samples for each test. The test was repeated for moisture contents representing an almost dry condition to almost the state of field capacity. Figure 3.19.b demonstrates the testing procedure of the resistivity of fouling agents in the lab.

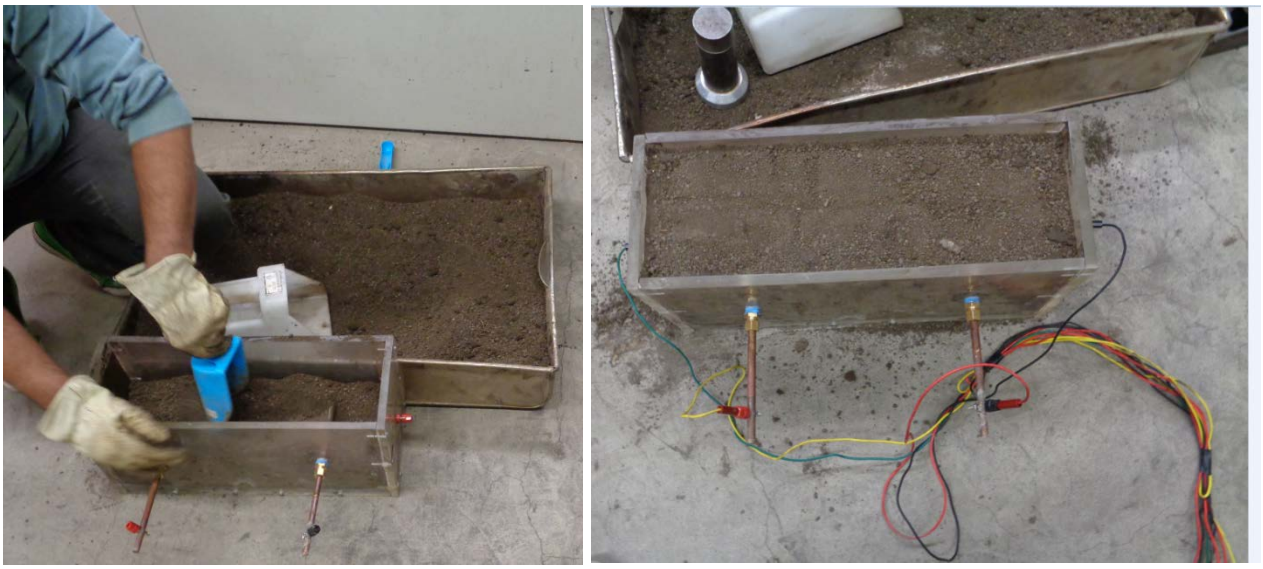

(a) (b)

Figure 3-19 Sample Preparation and Testing for Resistivity Determination

3.6.3. Resistivity Test Results

The resistivity values of the fouling materials are plotted in figure 3-20. This figure shows the resistivity of the coal dust is higher for similar water contents as compared to both subgrade soil and the Gardner track fouling dust. The subgrade soil had the lowest resistivity when the water content was at its field capacity. The coal dust had the highest resistivity at its field capacity. Minimum resistivity values for the sampled subgrade soil, the Gardner track ballast dust, and the coal dust measurements were approximately 1,800 ohm – cm, 3,400 ohm – cm, and 6,600 ohm – cm, respectively.

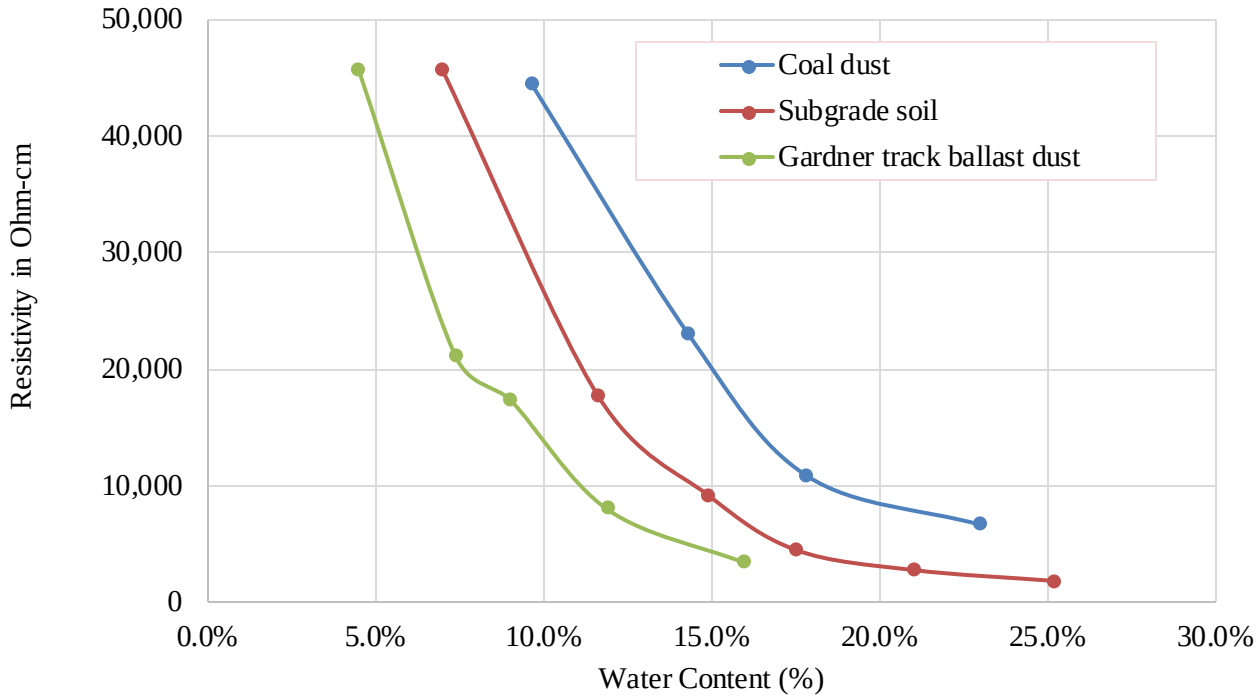

Figure 3-20 Resistivity of Fouling Agents

3.7. Engineering Properties of Field Ballast

3.7.1. General

Field testing was conducted on Midland Railway track near Baldwin, Kansas on October 21, 2013. The test field trip location and the test are discussed further in Chapter 4. The general

properties of the field ballast are discussed in this chapter. Two sites (Location A - near the crossing of Montana Road and Location B – near the crossing of US 59) were identified for sample collection and testing. At each site, two locations – the center and shoulder of the track - were chosen for collecting the samples. The following field properties are discussed hereafter in this chapter.

3.7.2. Gradation of the Ballast and Fouling Index

The ballast gradation curve for site A (near the crossing of Montana Road with rail track) is presented in figure 3.21.

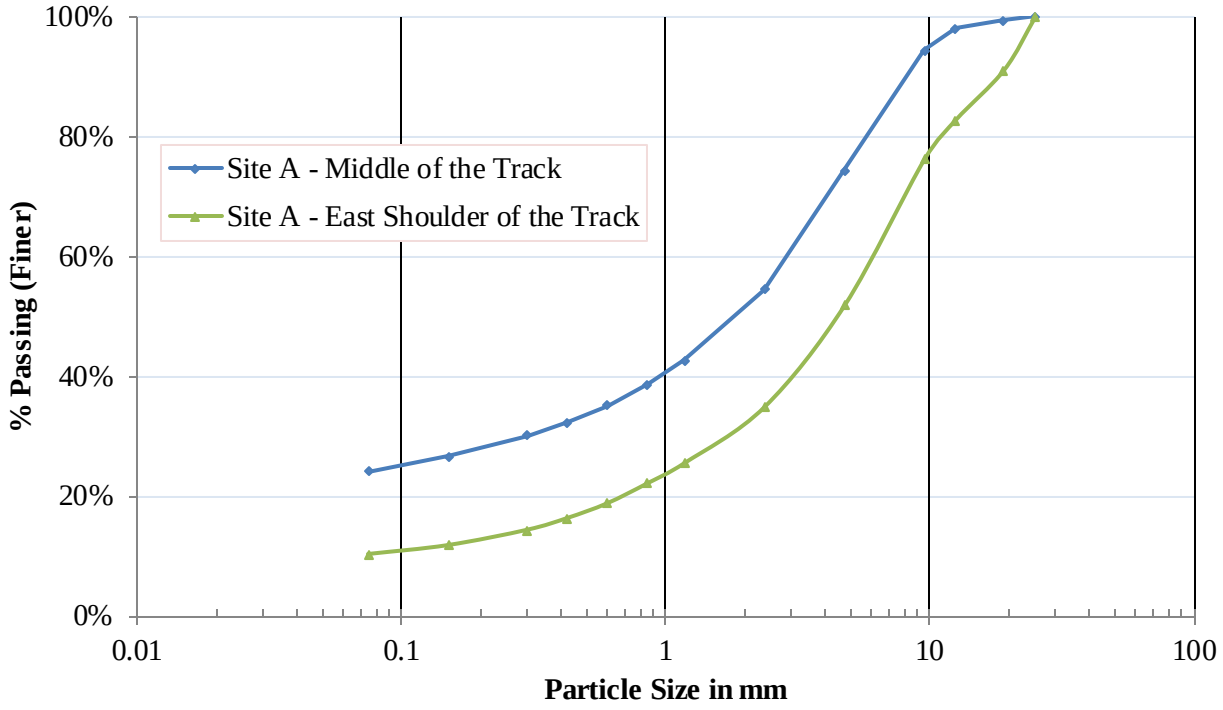

Figure 3-21 Particle Size Distribution at Site A of Midland Railway Track, Kansas

The percentage of fines was 24.1% in the center of track and 10.3% at the shoulder. The average size of the ballast, coefficient of curvature and the coefficient of uniformity of the ballast are tabulated as follows.

Table 3-9 Field Ballast Distribution Properties at Site A of Midland Railway Track, Kansas

Descriptions of Items	At the center of the track	At the shoulder of the track
Average size of the ballast (mm)	2.27	4.45
Coefficient of curvature (C_c)	4.8	7.5
Coefficient of uniformity (C_u)	467	94

Gradation curve of site B (near the crossing of US 59 with rail track) is presented in figure 3.22.

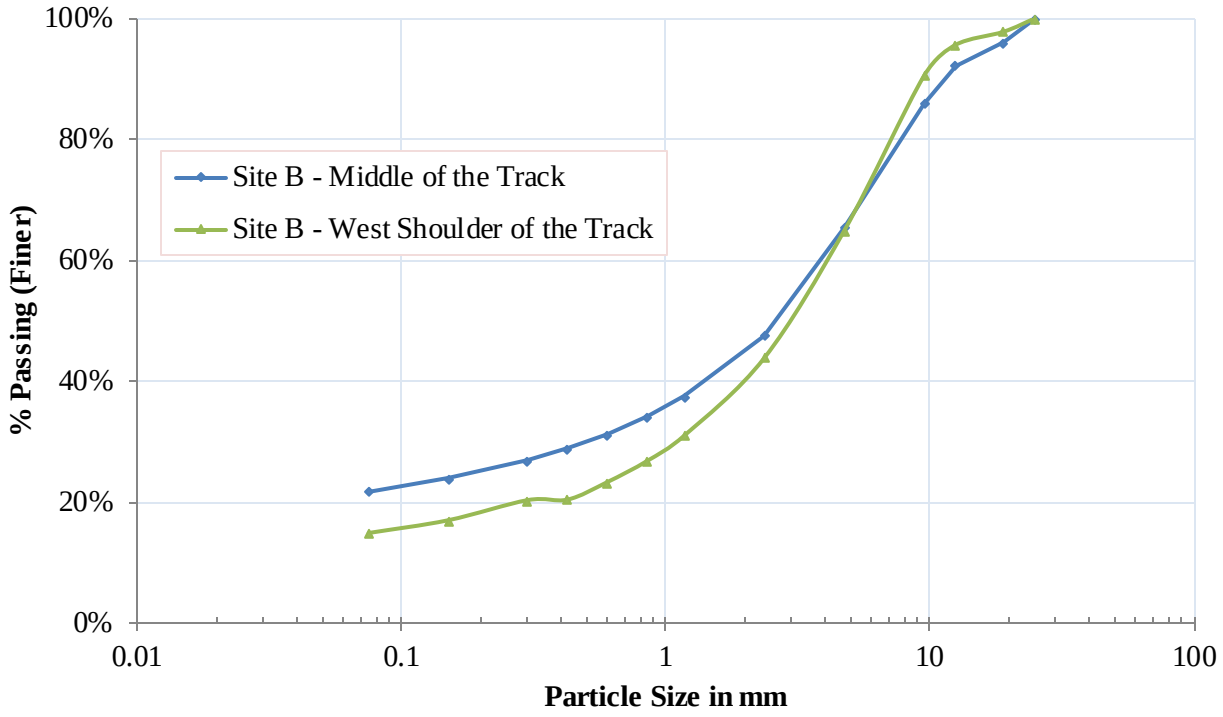

Figure 3-22 Particle Size Distribution at Site B of Midland Railway Track, Kansas

The percentage of fines was 21.8% in the center of track and 14.9% at the shoulder. The average size of the ballast, coefficient of curvature and the coefficient of uniformity of the ballast are presented in Table 3-10.

Table 3-10 Field Ballast Distribution Properties at Site B of Midland Railway Track, Kansas

Descriptions of Items	At the center of the track	At the shoulder of the track
Average size of the ballast (mm)	3.41	5.53
Coefficient of curvature (C_c)	26.4	29.7
Coefficient of uniformity (C_u)	1520	460

3.7.3. Field Moisture Content

The field moisture content was determined in accordance with ASTM D2216. Three samples of each sampling location were taken and average moisture content was calculated. The field moisture contents of the samples are presented in Table 3-11.

Table 3-11 Field Moisture Content of Ballast at Midland Railway Track, Kansas

Descriptions or Location	Site A	Site B
Central of Track	11.8%	7.5%
Shoulder of Track	10.6%	6.3%

Location A had the higher moisture content than location B and the middle part of the track had higher moisture content than the shoulder, based on these results.

3.8. Quantification of Fouled Ballast

There are several widely used methods to quantify ballast fouling level. Fouling Index, Percentage Void Contaminant, and Void Contaminant Index are three such methods. In this report, the Fouling Index proposed by Selig and Waters (1994) is used. Fouling Index (FI) is the summation of percentage by weight of material passing the 4.75 mm sieve and material passing the 0.075 mm sieve. The classification of the ballast fouling is carried out as follows:

Table 3-12 Ballast Fouling Classification Based on FI

Clean Ballast	FI < 1
Moderately Clean Ballast	1 < FI < 10
Moderately Fouled Ballast	10 < FI < 20
Fouled Ballast	20 < FI < 40
Highly Fouled Ballast	FI > 40

From the sieve analysis of the clean test ballast, the fouling index was found to be 0.2 which is almost equal to zero.

In this study, a separate term of "Percentage Fouling by Weight or Percentage Fouling" is used for ease of sample preparation. The percentage fouling by weight is the ratio of the mass of fouling agent to the ratio of the mass of the clean ballast in dry condition. The corresponding fouling index was also calculated.

Chapter Four: Test Setup and Data Collection

4.1. Lab Test Set up for Moisture Variation Sample

4.1.1 Sample Descriptions

The clean ballast obtained from washing the Gardner, Kansas fouled ballast by the wet sieving method was uniformly mixed with the different percentages by weight of the fouling agents using a skid loader. The following diagram shows the test specimen composition based on addition of fouling agents.

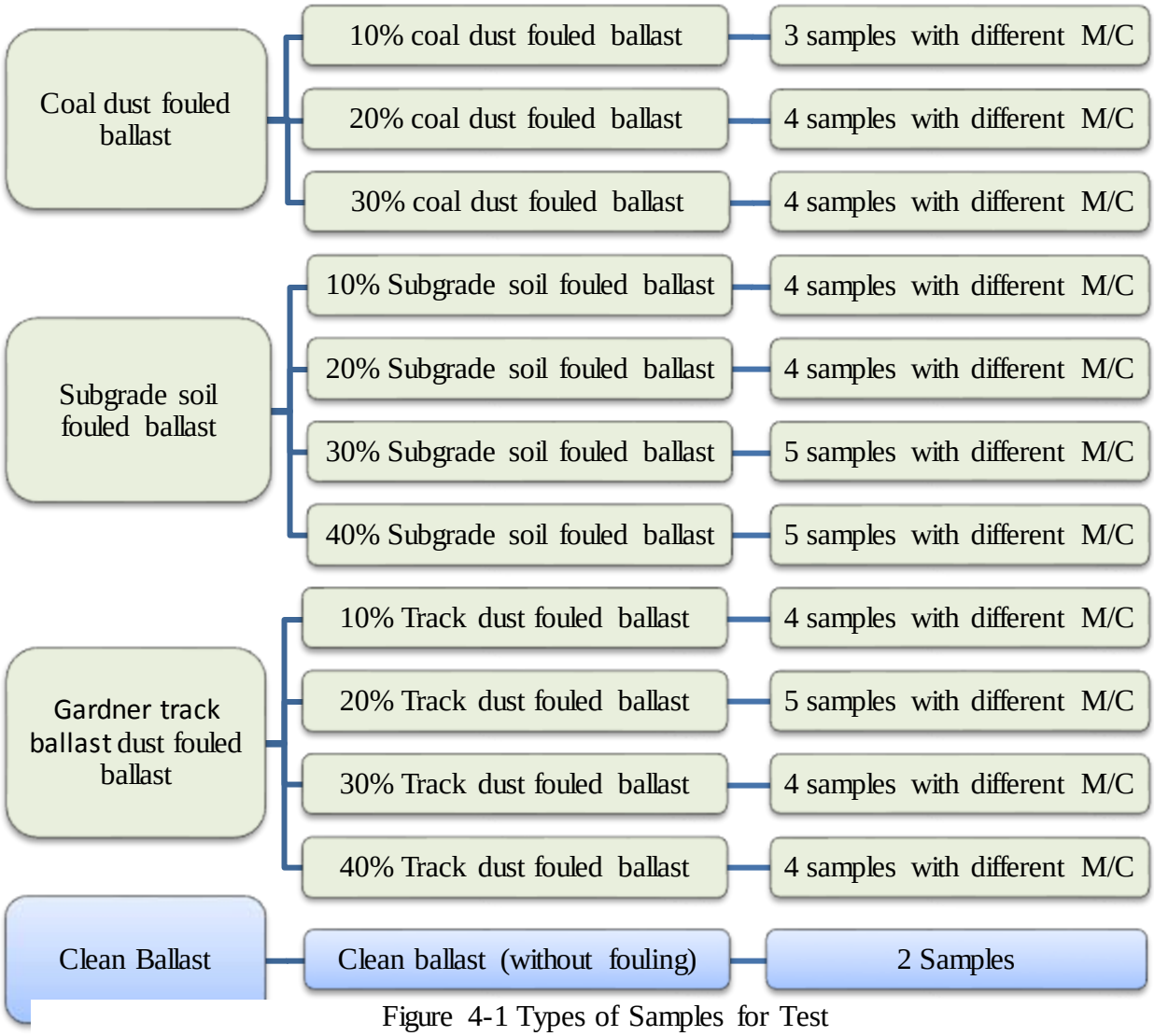

Figure 4-1 Types of Samples for Test

4.1.2 Calculation of Fouling Index of ballast samples

The ballast samples were artificially fouled by adding fouling agents for a range of proportions as mentioned in Figure 4.1. The sieve analysis of the fouling agents gave the necessary fouling index (FI) calculation coefficients as shown in the following table 4.1.

Table 4-1 Coefficient of Fouling Index Calculation Based on Sieve Analysis

Fouling Agents	Material Passing No 4 Sieve (4.75 mm) (A)	Material Passing No 200 Sieve (0.075 mm) (B)	FI Coefficient (Sum of A +B)
Coal Dust	100.00%	12.04%	1.120
Subgrade Soil	100.00%	95.14%	1.951
Gardner track Dust	91.26%	14.49%	1.058

Based on the fouling index coefficients listed in table 4.1, the fouling index (FI) of each sample is calculated and listed in Table 4.2.

Table 4-2 Fouling Index Calculation for Different Samples

Fouling Agent	Type of Fouling	Clean ballast dry wt. (lb.)	Fouling Agent by % of Clean Ballast	Added Fouled Material dry Wt.(lb.)	FI
Coal dust fouled Ballast	Moderately clean ballast	1206	10%	121	10
	Moderately fouled ballast	1204	20%	141	19
	Fouled ballast	1214	30%	364	26
Subgrade soil fouled ballast	Moderately fouled ballast	1312	10%	131	18
	Fouled ballast	1214	20%	243	33
	Highly fouled ballast	1390	30%	417	45
	Highly fouled ballast	1380	40%	559	56
Gardner track Ballast dust	Moderately clean ballast	1224	10%	122	10
	Moderately fouled ballast	1290	20%	258	18
	Fouled ballast	1287	30%	386	24
	Highly fouled ballast	1278	40%	511	31

4.1.3 Mixing Procedure

Mixing of the fouled materials with the clean ballast was carried out using a skid loader. The fouled materials were spread at the top of the clean ballast and the skid loader was used to mix the materials. A suitable amount of water was sprinkled on the materials before mixing. The fouled materials mixing process is shown in Figure 4.2.

Figure 4-2 Mixing Procedure Started from Top Left Corner Running Counterclockwise

The close views of the mixed ballast with different fouling agents are shown in Figure 4.3.

a b c

Figure 4-3 Artificially Fouled Ballast Ready to Go into Test Box (a) Crushed Stone Fouled (b) Subgrade Soil Fouled (c) Coal Dust Fouled

4.1.4 Box Filling Procedure and Compaction

The artificially fouled ballast was placed into a test box 31.75 in. (L) x 31.75 in. (B) and 20 in. (H) in four layers of approximately equal height. A total of about 18 in. of depth was filled for each test. The sample materials were weighed in a five gallon bucket before being poured into the test box and this bucket was used to transfer material from the skid loader to the test box. The attached photographs show different layers of the box filling from first layer to the fourth layer.

Figure 4-4 Box Filling Procedure - Starts Top Left Corner Progresses Counterclockwise

A load of 27.90 lb was applied for 50 drops from an average height of 20 inches for the compaction of the fouled ballast sample in each layer. The box was filled in four layers with almost equal weight in each layer and thicknesses of 3.5 to 5 inches depending up on the total height of the sample. Relevant photographs of the weighing arrangement before transferring the fouled ballast to the test box and the compaction procedure are shown below:

a b

Figure 4-5 Filling Procedure (a) Compaction of Sample (b) Weighing before Pouring to Box

4.1.5 Bulk Density Calculation

The bulk density of the sample was calculated by weighing the sample from the five gallon bucket and measuring the sample height. The box volume (V) was calculated by:

$$V = L(= 31.75\ in)xB(= 31.75\ in)xH(= varies\ depending\ on\ sample\ height) \ldots\ldots\ldots\ldots 4.I$$

The wet mass of the sample (M) was recorded using a weighing scale while filling the box. The bulk density (ρ) of the sample was calculated by the following relation:

$$\rho = \frac{M}{V} \ldots\ldots\ldots\ldots\ldots\ldots\ldots\ldots\ldots\ldots\ldots\ldots\ldots\ldots\ldots 4.II$$

The bulk density calculation sheet for all the samples are attached in the appendix 8.B.I.

4.1.6 Tests Sequence and Tests Location

The following five types of tests were conducted on the box in the following order:

I. Light weight deflectometer test

II. Dynamic cone penetrometer test

III. Horizontal probe resistance measurement

IV. Vertical probe resistance measurement

V. Plate loading test

The locations of the tests on the box are shown in the following two figures:

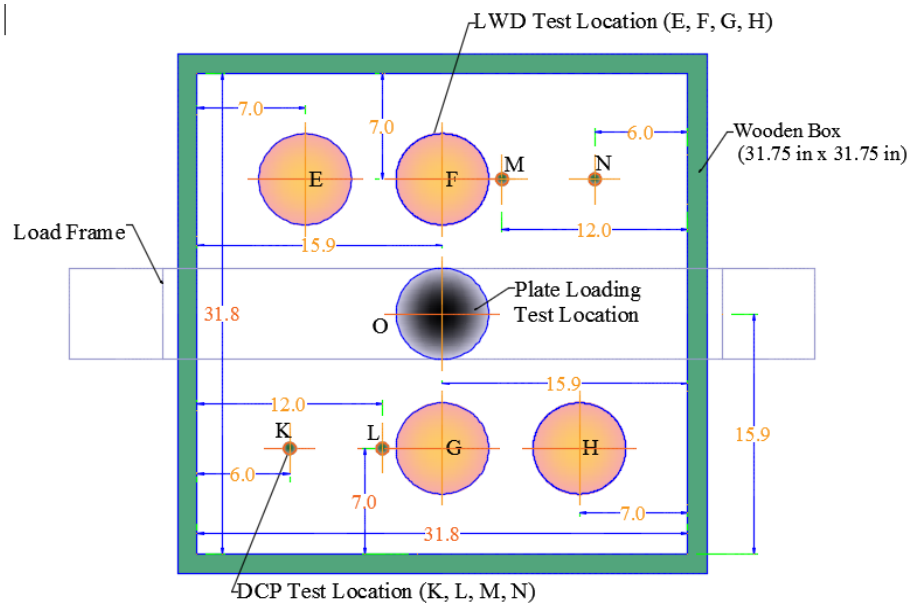

Figure 4-6 Test Location for LWD Test, DCP Test and Plate Loading Test

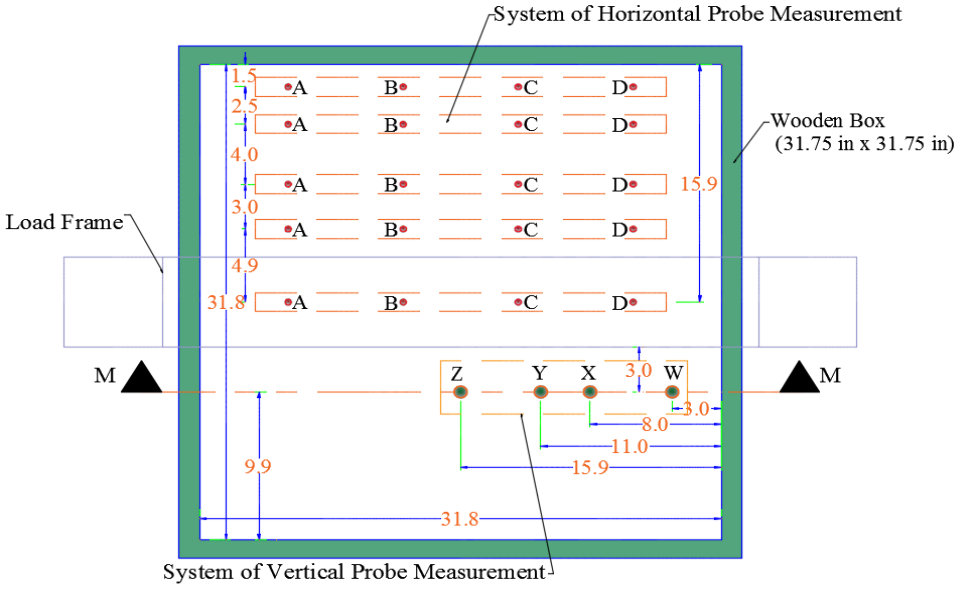

Figure 4-7: Test Locations for Horizontal and Vertical Aligned Probe Method (Figure not to scale)

4.2. Horizontal Probe Resistance Measurement

4.2.1 Construction of Horizontal Probe

The horizontal probe was constructed based on the Wenner four point method. Four probes of 4.5 inch clear penetrating depth were constructed from Ultra-Machinable W1 Tool Steel rod of with a diameter of 0.3437 in. The engineering properties of this alloy steel are given as follows:

Table 4-3 Engineering Properties of the W1 Tool Steel Used for Horizontal Probes

Rockwell Hardness	Yield Strength	Density in lb/cu.in	Type of Hardening	Electrical Resistivity at 68° F	Carbon Content
B96	50,000 psi	0.283	Water	0.00018 Ω-cm	0.95% - 1.05%

The rods were attached to a 1.25 inch thick high density polyethylene (HDPE) sheet of length 25 inch to make a single tool. Rods one inch in lengths were extended from the top of the machined HDPE section as shown in Figures 4-8 and 4-9.

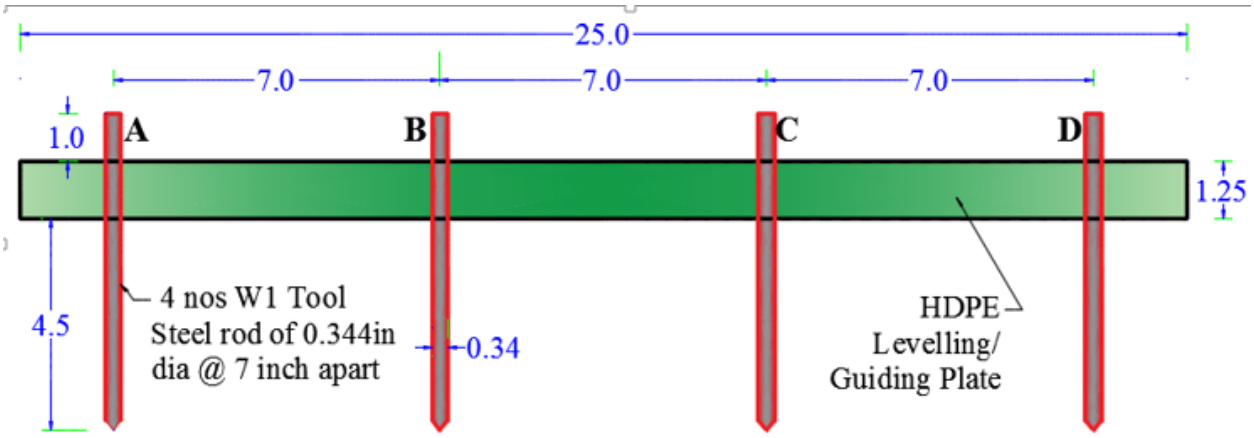

Figure 4-8 Schematic Horizontal Probe Unit for Wenner Four Point Method

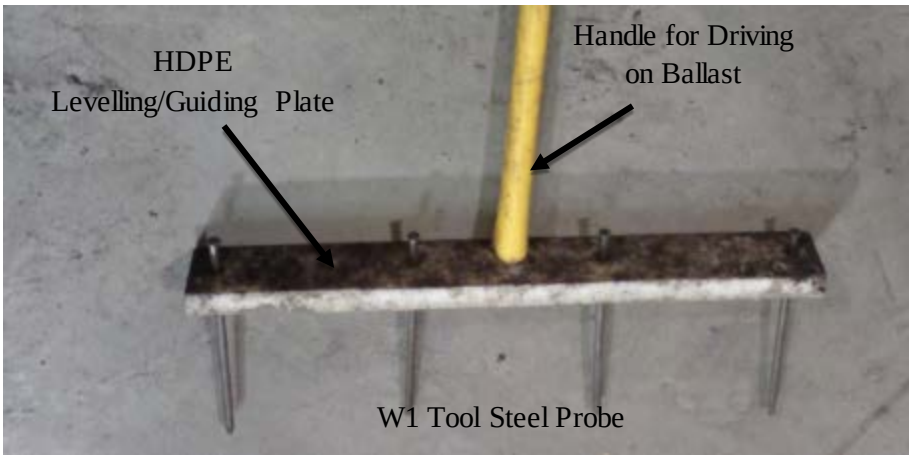

Figure 4-9 Horizontal Probe Unit for Wenner Four Point Method

4.2.2 AEMC Ground Resistance Tester

AEMC 4620 Model ground resistance tester was used for the measurement of the resistance of the ballast. The general features of the tester were as follows:

Table 4-4 General Features of AEMC Ground Tester

Measurement Range	Resolution	Test Current	Resistance Frequency	Accuracy	Response time
0 to 2000	10 mΩ to 1Ω	10mA to 0.1A	128 Hz	5%	4 to 8 sec

The schematic connection diagram of the AEMC ground tester is given as follows:

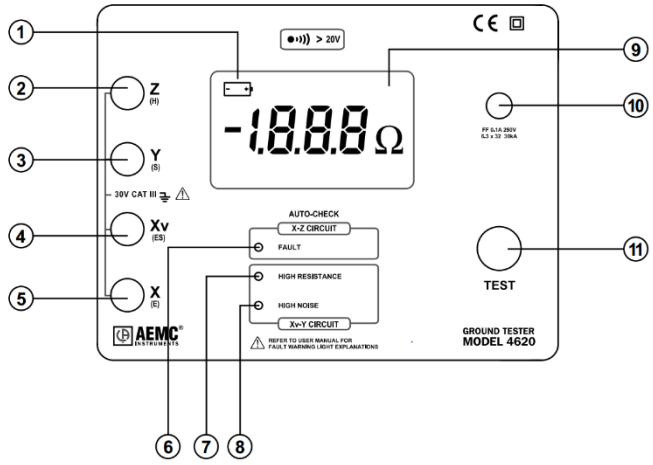

1. Battery Indicator
2. Input Terminal (Z)
3. Input Terminal (Y)
4. Input Terminal (Xv)
5. Input terminal (X)
6. X-Z Fault Indicator
7. Xv–Y High Resistance Indicator
8. Xv-Y High Noise Indicator
9. Display
10. Fuse Holder
11. Test Button
12. Test Bottom

Figure 4-10 Schematic Connection Diagram of AEMC Ground Tester (www.aemc.com)

4.2.3 Horizontally Aligned Probe Resistance Measurement by Wenner Four Point Method

These horizontally aligned probes were driven into the soil to their full depth. Due to the uneven ballast surface, 4 inches of penetration out of the 4.5 inch maximum was typically required for the fouled ballast to touch the leveling plate and was taken as the reference depth for calculation purposes.

The wires were connected from each probe to the AEMC 4620 ground tester based on the above circuit diagram and a reading was taken over a 5 to 10 second period until the reading stabilized.

Figure 4-11 illustrates the procedure for taking the horizontal probe resistance measurement by the Wenner Four Point Method using the AEMC ground tester.

Figure 4-11 Resistance Measurement by Wenner Four Point Method with AMCE Tester

4.2.4 Horizontally aligned Probe Resistance Measurement by Single Electrode Method

A simple multimeter was used to measure the resistance between horizontally aligned single electrodes. Between two electrodes, one electrode is considered as a ground and the resistance was measured with the probe. Three measurements were taken between electrodes A and B; B and C; and C and D as shown in Figure 4-12.

Figure 4-12 Fouled Ballast Resistance Measurement by Single Probe Method

For uniformity of reading, each measurement was taken either after 3 minutes of stabilization time or after the reading stabilized, whichever occurred earlier. This stabilization time was required due to the electrical noise produced in the soil at the time of measurement. The three minutes of data reading time was established as the criteria after several tests were carried out in the laboratory.

The ground resistance of the soil was mostly determined using the AEMC ground tester with the Wenner four point method. This test was carried out to provide a reference for validation of the single point method for fouled ballast resistance measurement.

4.3. Vertical Probe Resistance Measurement

4.3.1 Construction of Vertical Probe

A vertical probe was constructed at the University of Kansas. The concept of fall of potential was applied for the design of the vertical probe. The average height of the ballast varied from 17 to 19 inches with an average thickness of 18 inches. The concept of fall of potential was applied to reduce the length of probe required to penetrate the ballast layer. The conceptual drawing of the resistance measurement with a horizontal arrangement is given in Figure 4.13. Also, based on

this established concept, a model concept of effective resistance area was developed for the vertical probe and is presented in Figure 4.14.

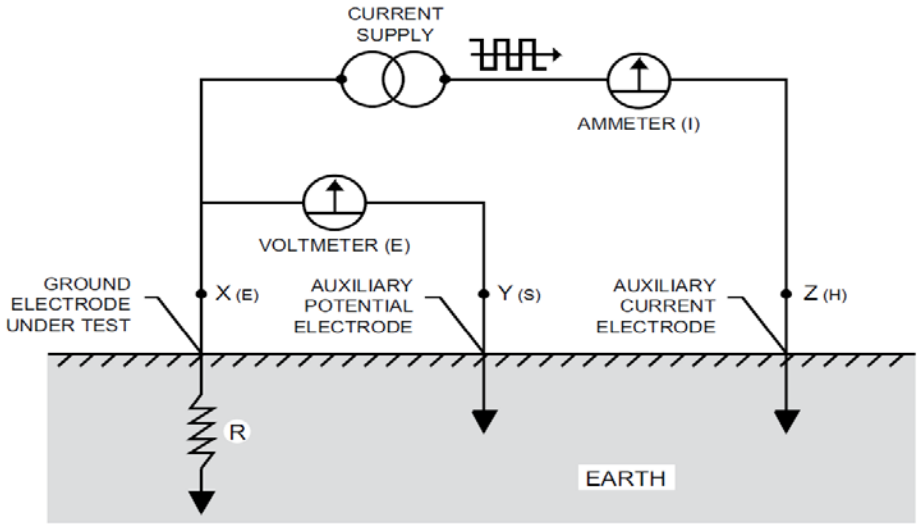

Figure 4-13 Concept of Resistance Measurement from Fall of Potential Method (www.aemc.com)

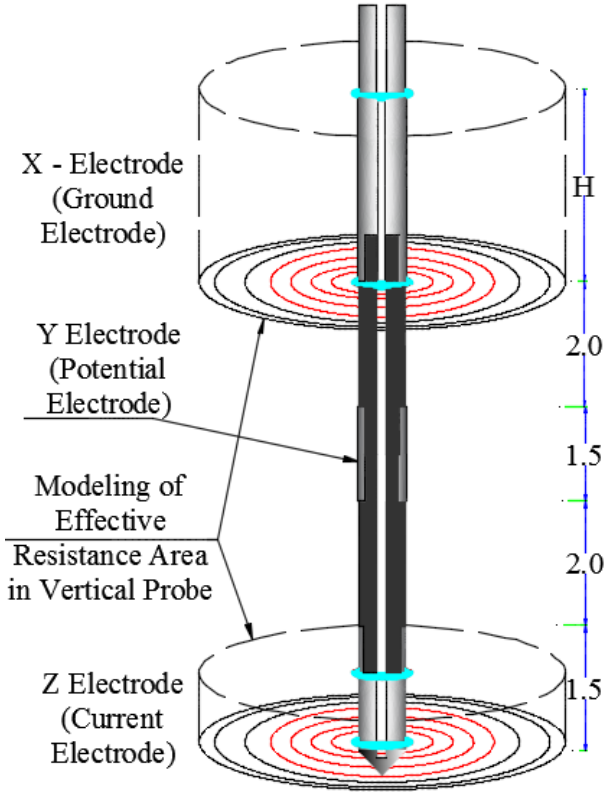

Figure 4-14 Resistance Measurement Model of Fall of Potential Method for Vertical Probe

A conceptual drawing has been prepared based on this resistance measurement model and this drawing is presented in Figure 4.15.

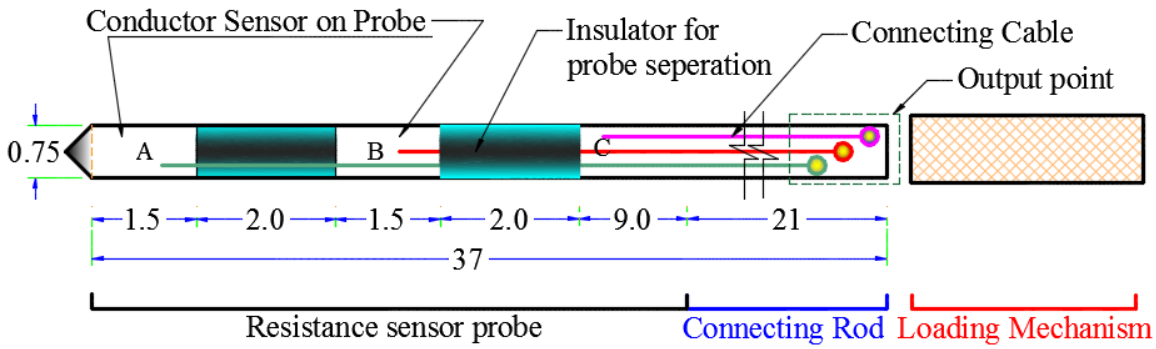

Figure 4-15 Conceptual Diagram of Vertical Probe

Steel alloy pipe of 0.75 inches (19 mm) of outer diameter was used for the construction of sensors and the connecting rod of the vertical probe. This round tube had a wall thickness of 0.035 inches (0.9 mm). The engineering properties of this alloy steel are given as follows:

Table 4-5 Engineering Properties of the Steel Used for Sensor Probe

Rockwell Hardness	Yield Strength	Internal Diameter	Type of Hardening	Electrical Resistivity	Carbon Content
C19	70,000 psi	0.68 inch	Cold Drawn	0.0000271 Ω-cm	0.27% - 0.34%

Glass Filled Black Polycarbonate (GFBP) rod of 0.75 inches (19 mm) diameter was used for creating the different zones in the probe. This black solid rod has -40° to 265° F for operating temperature. It has very good impact strength. This material is manufactured with 20% glass to provide better tensile strength such that it meets ASTM D3935 and ASTM D6098 requirements. The engineering properties of this insulation material are listed in the following table:

Table 4-6 Engineering Properties of the Steel Used for Sensor Probe

Tensile Strength	Impact Strength	Thermal Expansion	Electrical Resistivity	Density
16,000 psi	2.06	1.5×10^{-5} in/in/°F	$>10^{13}$ Ω-cm	0.048 lbs./in^3

Two high electrical resistance zones were created to separate the rod into three parts on the vertical probe as shown in the schematic diagram presented in Figure 4.15. GFBP rod was used to create the resistance zone that separated the three conductor zones from each other. These three parts act as three probes for the fall of potential method. Three wires were connected internally from different sensor zones to the output point as shown in the Figure 4.15. The diagrammatical representation of different parts of the vertical probe is given in Figure 4.15.

For better connection at the point of impact or at joints between the sensor and the electrical resistance, the GFBP was machined and inserted into the metal part completely as shown in the Figure 4.16 (c).

A load assembly of 17.6 lb was assembled with a fall height 22.6 inches to drive the probe into the ballast layer. The connection between the resistance probe and the load assembly was done with a screw system.

A rod of 0.30 inch was inserted between the different parts to tighten each other and make it solid. The rod moves from the tip of the sensor probe to the end of the connecting rod just below the connection mechanism with the loading system. This stiffening rod (tighten rod) was separated from the outer metallic sensor pipe with one PVC flexible pipe.

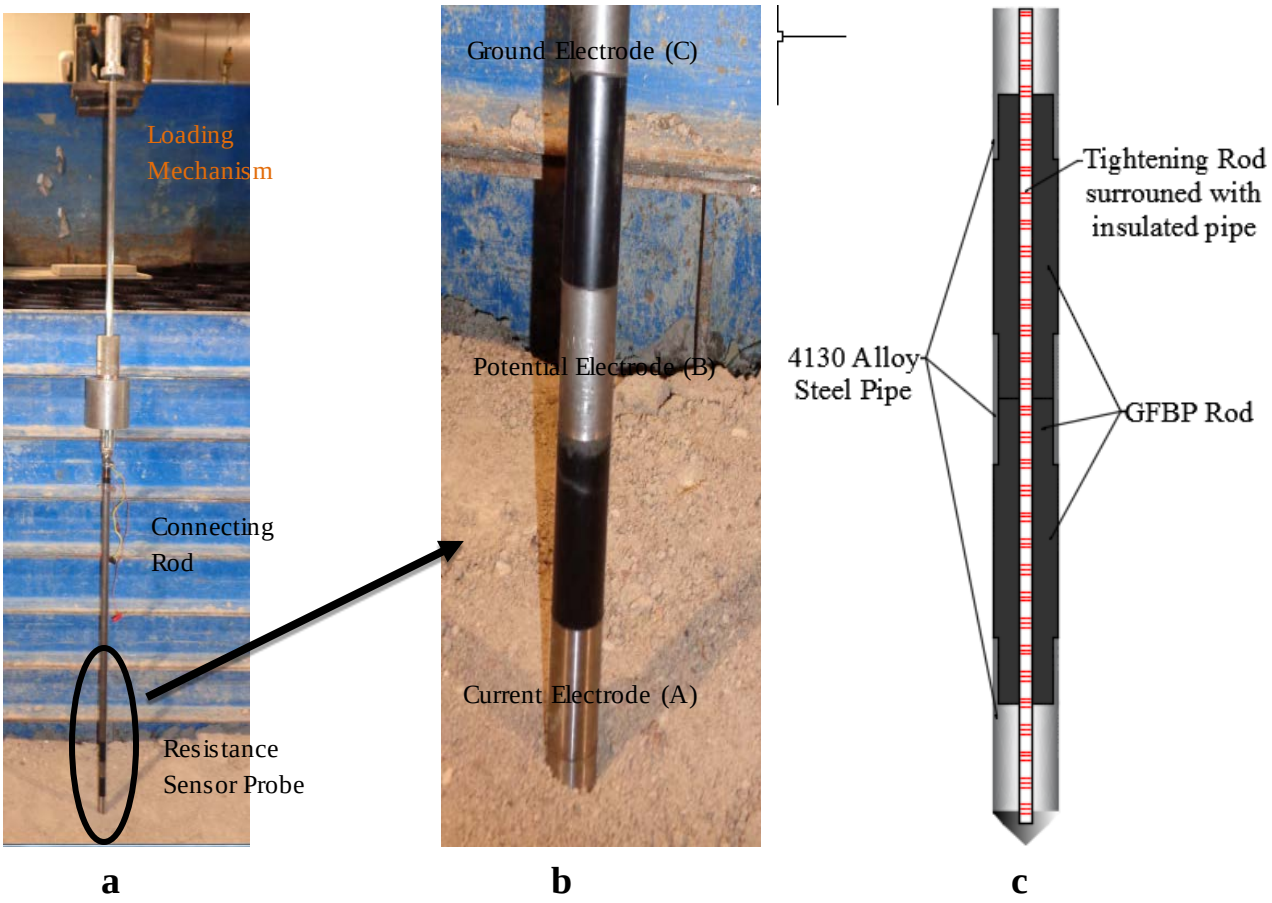

Figure 4-16 Construction of Vertical Probe (a) Vertical Probe (b) Construction of Sensor Section (c) Joint Mechanism of Conductor and Insulator Materials

4.3.2 Vertical Probe Resistance Measurement by Three Point Method

This vertical probe resistance measurement device is based on the three point method or fall of potential method. In Figure 4.16 (b), the ground electrode 'C' acts as test electrode; and 'B' and 'A' act as two probes – namely; potential probe and current probe - between which the resistance was measured. The AEMC ground resistance meter was used for the measurement of soil resistance by connecting the wires in the configuration mentioned in Figure 4.13. Here, the same 4620 AEMC Ground Tester was used for measuring the ground resistance by shorting X and Xv terminals.

4.4. Resilient Modulus Measurement by LWD

4.4.1 Light Weight Deflectometer

A ZFG 3000 Light Weight Deflectometer (LWD) was used for determination of the resilient deformation modulus and the degree of compaction of the fouled ballast sample. This ZFG 3000 LWD was manufactured by Zorn Instruments in Germany. The schematic diagram and the picture of the equipment are shown in the Figures 4.17 (a) and 4.17 (b).

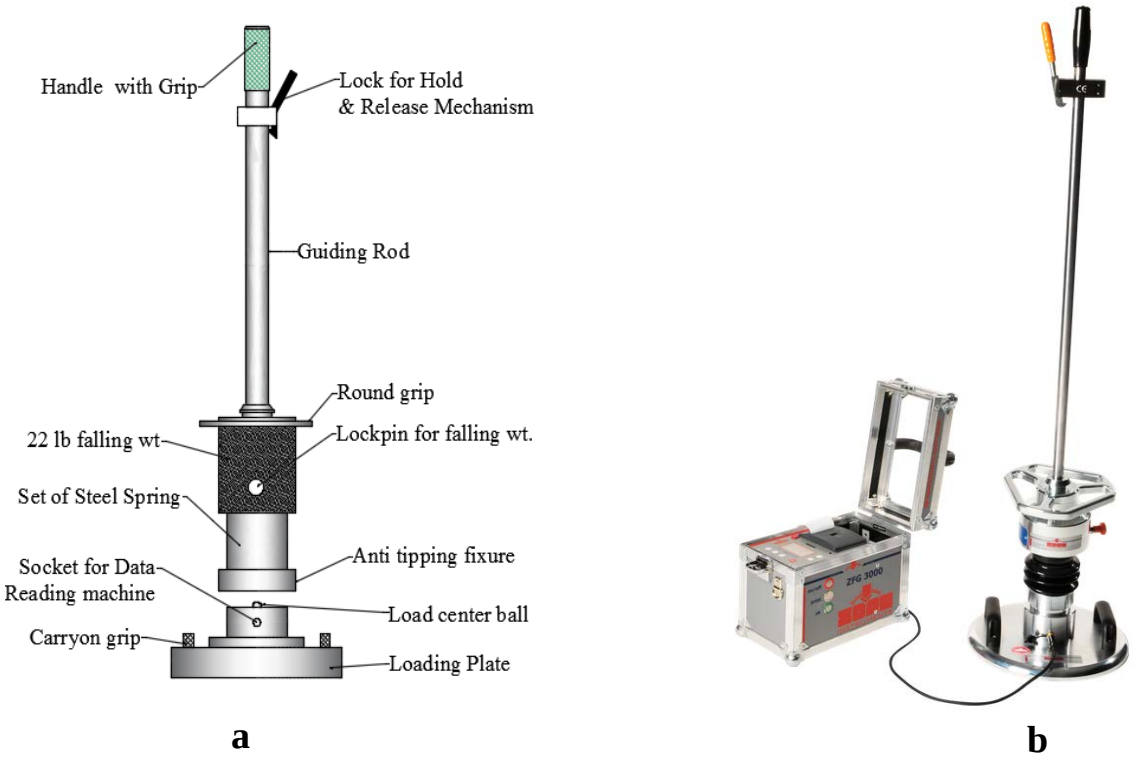

Figure 4-17 (a) Schematic Diagram of Zorn 3000 LWD (b) Actual photo of Zorn 3000 LWD Used in Lab (www.zorn-instruments.com)

The Zorn 3000 satisfies ASTM E2835-11 and ASTM E2583-07 requirements. This instrument comes with three loading plates 6 in (15 cm), 8 in (20 cm) and 12 in (30 cm) in diameter – which are loaded with 22 lb. (10 kg) of dynamic load that free falls on the guiding rod from a height of 2.4 ft. (0.73 m). The size of the plate is generally chosen based on the type of material and the thickness and stiffness of the material that is going to be tested. Typically the granular material is

tested using the 6 in. diameter plate, and flat clay and sand are tested using the large diameter plate (12 in.).

The resilient modulus is measured based on the settlement made on each drop. The relation of this modulus and the settlement after each pulse from the dynamic load is given by:

$$E_{Hd} = f * (1 - \vartheta) * \sigma * \frac{r}{s} \ldots\ldots\ldots\ldots\ldots\ldots\ldots\ldots\ldots\ldots\ldots\ldots\ldots\ldots\ldots\ldots\ldots\ldots\ldots\ldots\ldots\ldots..4.III$$

Where;

f = shape factor = 2

υ = Poisson's ratio = 0.30

σ = Pressure on plate due to dynamic loading = $\frac{M.a}{A}$

M = Free fall weight = 22 lb.

a = acceleration of the drop

A = plate area (28.27 in^2 for 6 inches diameter plate)

r = radius of the contact plate in inches = 6 inches

s = Settlement on each drop in inches

Since the samples were granular material fouled with different fouling agents and there was limited space for the test in the test box, a 6 in diameter plate was used. The setting was also adjusted based on the plate diameter selection.

4.4.2 Modulus Measurement by LWD Method

The resilient modulus was measured in four places: E, F, G and H as shown Figure 4.6. Since the compaction on two sides of the box was manually done from two different sides; left and right (upper and lower side in the Figure 4.6), the four test locations were chosen for measurement of the resilient modulus for better accuracy.

Three calibration drops were executed without taking recording a measurement. The next three successive drops were completed and the settlement measured for each drop. The resilient modulus was automatically calculated based on the settlements by the display unit attached to the LWD.

4.5. California Bearing Ratio (CBR) Measurement by DCP

4.5.1 Dynamic Cone Penetrometer

A schematic diagram of the Dynamic Cone Penetrometer (DCP) is shown in Figure 4.18. A mass of 17.6 lb. was allowed to freefall for 22.6 inches. A cone of 13/16 inches (20 mm) diameter was connected to a 39.4 inches (1000 mm) penetrating rod and driven into the sample with by the force of the falling mass. The penetrating rod was 5/8 inches (16 mm) diameter. The cone was of 60 degree convergence.

4.5.2 California Bearing Ratio (CBR) Estimation by DCP

California bearing ratio (CBR) was estimated using the dynamic cone penetration (DCP) test at four locations as shown in Figure 4.6 in accordance with ASTM D6591-03. The load drop count and successive depth of penetration was measured from the top of the average 18 inch thick sample to the bottom of the box. The relationship between CBR value for any fouled ballast samples and the penetration per blow (inches/blow) was calculated based on the US Army Corps of Engineers recommendation (Webster, Brown, & Porter, 1994) :

- For all soil except CL below CBR 10 and CH Soils – Where DCPI in mm/blow

$$\text{CBR} = \frac{292}{\text{DCPI}^{1.12}} \ldots\ldots\ldots\ldots\ldots\ldots\ldots\ldots\ldots\ldots\ldots\ldots\ldots\ldots\ldots\ldots\ldots\ldots\ldots\ldots\ldots\ldots\ldots\ldots\ldots\ldots\ldots\ldots 4.IV$$

- For CL soils with CBR<10 – Where DCPI in mm/blow

$$\text{CBR} = \frac{1}{(0.017019 \text{ x DCPI})^2} \ldots\ldots\ldots\ldots\ldots\ldots\ldots\ldots\ldots\ldots\ldots\ldots\ldots\ldots\ldots\ldots\ldots\ldots\ldots\ldots\ldots\ldots\ldots\ldots\ldots\ldots\ldots 4.V$$

- For CH Soils – Where DCPI in mm/blow

$$\text{CBR} = \frac{292}{(0.002871 \text{ x DCPI})} \ldots\ldots\ldots\ldots\ldots\ldots\ldots\ldots\ldots\ldots\ldots\ldots\ldots\ldots\ldots\ldots\ldots\ldots\ldots\ldots\ldots\ldots\ldots\ldots\ldots\ldots\ldots 4.VI$$

Where; DCP index (DCPI) is the rate of penetration (penetration in mm/blow).

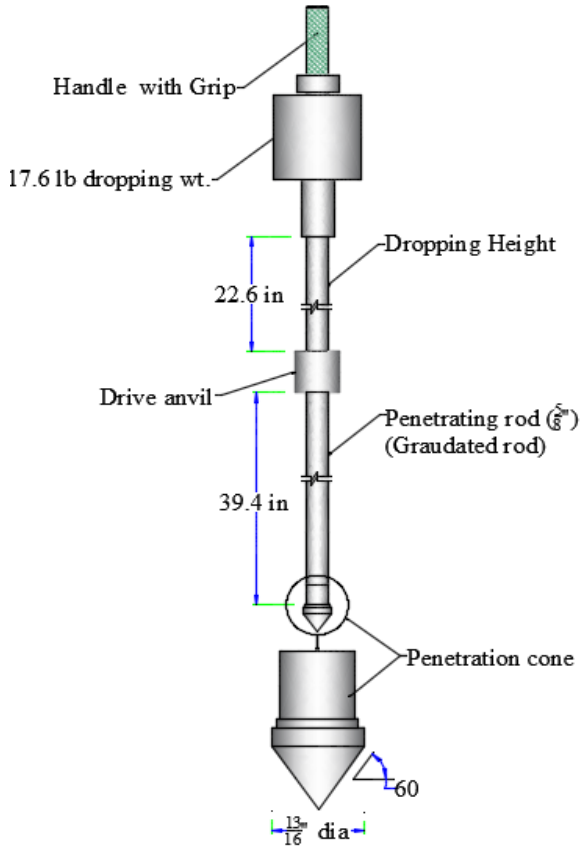

Figure 4-18 Schematic Diagram of DCP

4.6. Stiffness Modulus Determination by Static Plate Loading Test

4.6.1 Static Plate Loading Test

The static plate loading test was carried out for the determination of the stiffness of the fouled ballast. The slope of the load - displacement curve is the stiffness modulus of the fouled ballast. The variation of stiffness of fouled ballast was studied based on the type and amount of fouling materials and the moisture content.

Elastic theory explains the settlement (s) of a rigid surface plate of diameter (D) with uniform load of P applied on a semi-infinite isotropic soil characterized by Young's modulus (E_s) and Poisson's ratio (ν) as shown in equation 4.VII.

$$s = \frac{\pi}{4}\frac{DP(1-\nu^2)}{E_s} \quad \ldots\ldots 4.VII$$

From the above relation, s/P, which represents the slope of the load displacement curve, is the coefficient of subgrade reaction and is given by

$$\frac{s}{P} = \frac{\pi}{4}\frac{D(1-\nu^2)}{E_s} \quad \ldots\ldots 4.VIII$$

The small size plate loading system was used for the plate loading test. The sample box and the plate loading apparatus was previously designed and fabricated at the geotechnical laboratory at the University of Kansas. The system had a 6 inch diameter air cylinder with a maximum pressure of 120 psi to apply the load. The loading plate was 6 inches in diameter and 0.4 inches thick. The air cylinder was mounted on a steel frame and connected to a metal base which supported the sample box. The whole system was placed on casters for easy movement. Figure 4.19 shows the details of the test apparatus. A box of 31.75 inches x 31.75 inches x 20 inches effective size was constructed for preparation and containment of the sample materials.

Figures 4.7 and 4.20 show the plan and elevation of the test box used for plate loading tests. A detachable cross beam was fixed on the frame for mounting the displacement gauges that measured the displacement while loading the system. A tripartite flat steel plate was mounted on the exposed piston to measure the displacement recorded by the three displacement gauges.

Figure 4-19 Plate Loading Test Set up

4.6.2 Plate Loading Test Procedure

The loading plate was attached to the piston of the air cylinder. The dial gauges were fixed on the cross beam attached to the loading frame and were set to zero when the loading plate just touched the sample. Loads of 5, 10, 15, 20, 30, 40, 50, 60, 70, 80 and 90 psi were applied through the regulator of the air cylinder that was connected to the air compressor, and the corresponding displacements shown by the dial gauges were recorded until the dial gauge showed the constant reading at least for 3 minutes. For each loading sequence, the displacement response time was different. For drier samples the displacement time period was shorter. For

higher loading, the displacement time period was longer. The test was stopped before it reached maximum load if the displacement exceeded 0.4 inch (10 mm).

4.7. CBR Calculation by Vertical Probe after Correlation with DCP

The vertical resistance probe was driven into the fouled ballast sample with a certain counted number of drops for standardizing the vertical probe with DCP. The dynamic load that drove the sensor rod into the fouled ballast samples was the same as that of the DCP with a dynamic mass of 17.6 lbs. and a free fall distance of 22.6 in. From the top of the sample, the number of drops required reaching depths of 3.2 inches (8.1 cm), 6.4 inches (16.3 cm), 9.6 inches (24.4 cm), 12.8 inches (32.5 cm) and 16 inches (40.6 cm) were recorded. For easy recording purposes, the permanent markings were placed at the above mentioned heights of the vertical probe from the probe tip. Figure 4-20 shows the level of the penetration for CBR calibration of the vertical probe in the ballast.

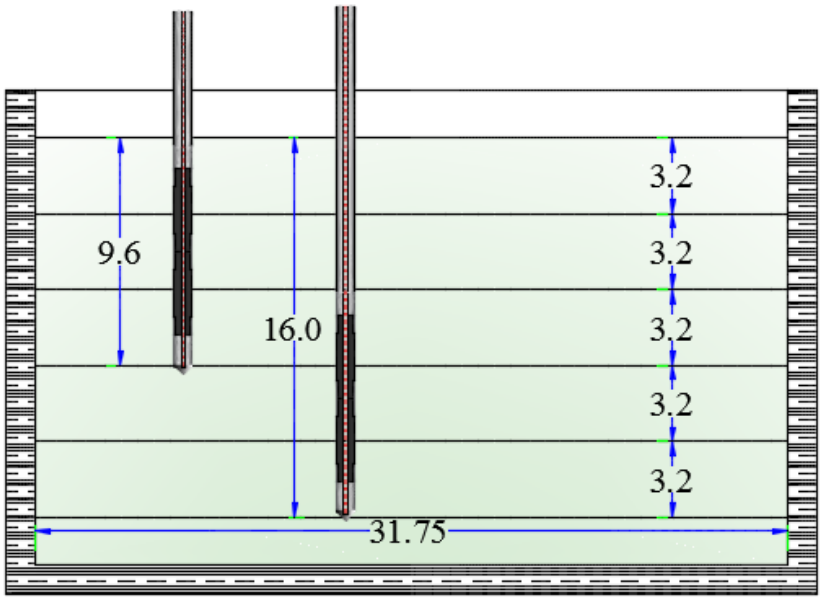

Figure 4-20 Layer Depth of Vertical Probe for Calibration with DCP (Section MM in Figure 4.7)

4.8. Moisture Content and Dry Density of the Mix

The test box was unloaded after testing was complete. Two moisture samples were taken from the unloaded sample for determination of the moisture content of the sample. The first moisture sample was taken at a depth of 8 inches from the top of the sample layer and a second moisture sample was taken 16 inches below the surface of the sample layer. The average of these two moisture contents was considered the moisture content of the whole sample. For more accurate results for the large granular soil mix, all samples taken weighed more than 4.5 lb.

The dry density of the soil samples were calculated based on moisture content and the bulk density as follows:

$$Dry\ Density(\rho_d) = \frac{\left(Bulk\ density\ (\rho)\right)}{\left(1 + Water\ content\ (w)\right)} \ldots\ldots\ldots\ldots\ldots\ldots\ldots\ldots\ldots\ldots\ldots\ldots\ldots\ldots\ldots\ldots 4.IX$$

4.9. Optimum Moisture Content for Fouled Samples

The optimum moisture content of the fouled ballast samples was determined using the standard proctor test using a 6-inch diameter mold. Fifty-six blows with a 5.5 lbf rammer were completed for compaction of each of the three layers of each sample. The proctor test was carried out based on ASTM D698. The compaction was carried out with an automatic rammer. The test was completed for 11 samples with varying fouling materials and percentages by weight. The test procedure is presented in the following figure.

Due to the large particles within the ballast, it was difficult to level the top of the mold after compaction. Judgment was applied for estimating the appropriate volume of the ballast. Also, the elongated ballast samples with more than 2.5 inch were removed from the samples. The fouled samples were mixed by hand with a small shovel and transferred to the mold at the test set up.

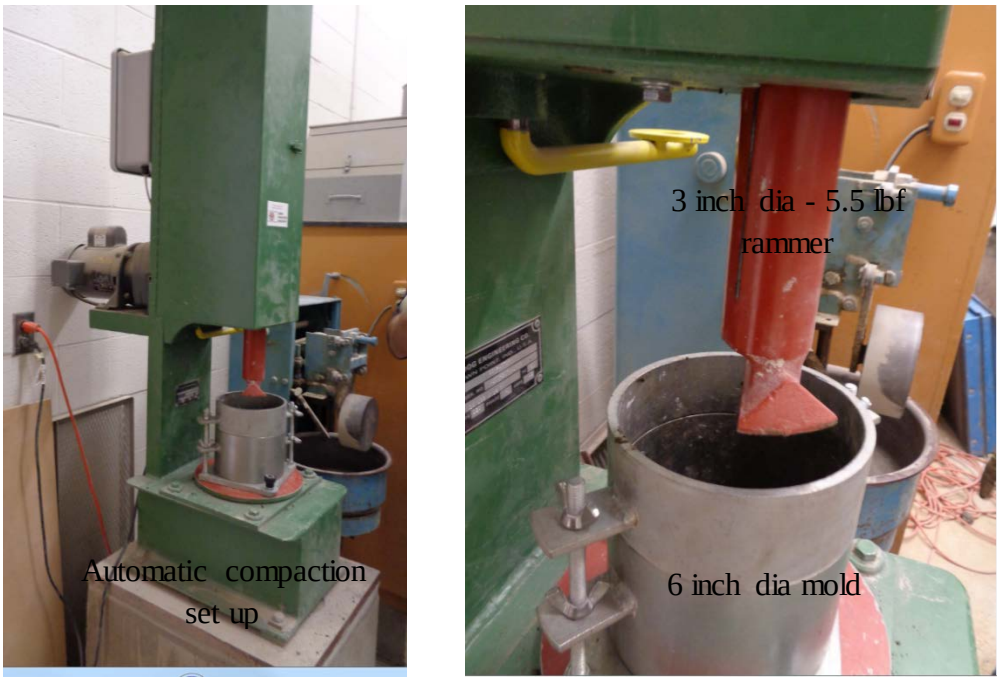

Figure 4-21 Proctor Test Procedure at Lab

4.10. Field Test Procedure

4.10.1 General Comments about Field Testing

The field tests were carried out on the track of Midland Railway operated from Baldwin City to Ottawa Junction, Kansas. The track was originally constructed in 1867. This vintage railway is operated by Midland Railway Historical Association as an excursion train through Eastern Kansas farmland and woods. The sites are approximately 17 miles south of the University of Kansas.

The test locations are given in Figure 4-22, taken from Google Maps and Figure 4-23. The two test locations were marked in the field after a site visit of the track. These two locations represented the fouled section of the ballast. The first location (site A) was on the north side of the crossing of rail track with Montana road while the second site (site B) was on the north side of the crossing of US 59 and the railway.

Figure 4-22 Location Map of the Test Sites (www.maps.google.com)

Figure 4.23 represents the test locations on both of sites.

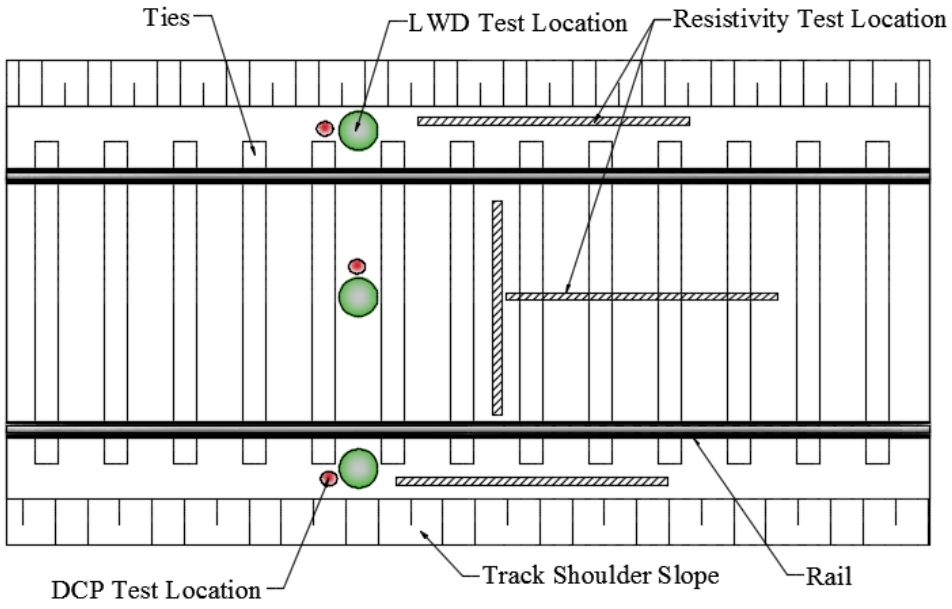

Figure 4-23 Tests Location at Field Test (not to scale)

4.10.2 Resistance Measurement by Ground Tester

The AEMC ground tester was used to measure the resistance of the ballast layer. Resistivity was measured based on a Wenner 4 probe array with probe spacing of 1 ft., 1.5 ft., 2 ft., 3 ft., and 4 ft. Because the ballast was assumed to have a depth of 2 feet, the resistivity data of 1 ft. and 1.5 ft. were taken for resistivity calculation proposes. For both sites (site A and site B), the resistivity of ballast between the rail track (middle of the track) parallel to rails and parallel to ties was measured. The resistivity of the east shoulder was measured for site A and west shoulder was measured for site B. The test locations are shown in figure 4.22 and 4.23.

Figure 4-24 Field Procedure of Resistivity Measurement at Site B (Parallel to Track)

4.10.3 Dynamic Cone Penetration Test

Two dynamic cone penetration (DCP) tests were conducted at each site. The DCP described in chapter 4.5.1 was used for field testing. The test locations for site A were at the center of the railroad and the east side shoulder. The test locations for site B were at the center of the track and the west side shoulder.

4.10.4 Light Weight Deflectometer Test

Two light weight deflectometer (LWD) tests were conducted at each site. The LWD described in chapter 4.4.1 was used for field testing. The test locations for site A were at the center of the railroad and the east side shoulder. The test locations for site B were at the center of the track and the west side shoulder.

Chapter Five: Results and Discussion

5.1. Assumptions of Analysis

The following assumptions were made during test procedures and the data analyses:

I. The fouling of the ballast is uniform.

II. The clean ballast and the fouled ballast are both isotropic.

III. The fouled ballast composition is a linearly elastic material.

IV. Poisson's Ratio of both the clean and the fouled ballast is 0.3.

5.2. Test Results of Clean Ballast

5.2.1. Moist and Dry Density

Two samples were taken for moisture and maximum density determination. Table 5.1 represents the test density of the clean ballast in the test box. The moisture contents of the two samples were 0.78% and 0.81%, respectively, and the corresponding wet densities were 110.3 lb/ft^3 and 111.8 lb/ft^3, respectively. The average dry density of the clean ballast samples was 110.1 lb/ft^3.

Table 5-1 Moist and Dry Density of Clean Ballast

Sample Descriptions	Date	Wet density in lb/ft^3	Moisture Content in %	Dry Density in lb/ft^3
Sample One	6/11/2014	110.3	0.78%	109.4
Sample Two	11/22/2014	111.8	0.81%	110.9
Average				110.1

The bulk specific gravity of the clean ballast was determined to be 2.69, and the height of the above-mentioned ballast samples were 18.67 inch and 18.66 inch, respectively. The average void ratios of the clean ballast were calculated as 0.55 and 0.53, respectively.

5.2.2. Resistivity of Clean Ballast

The range of the AEMC ground tester was up to 2,000 Ω. The resistance of clean ballast was above the range of the ground tester for both samples. Hence, the resistivity values of the clean ballast samples were greater than 440,000 Ω-cm in the above mentioned two moisture content samples.

5.2.3. CBR, Static Modulus, and Resilient Modulus of Clean Ballast

The stiffness values (k) for the ballast samples were determined to be 319.2 psi/inch and 341.4 psi/inch, which are the slopes of the load deflection curves of static plate loading test. The average stiffness of the clean ballast was 330.3 psi/inch. The following graph represents the load deflection curves for two samples of the ballast and corresponding stiffness calculations.

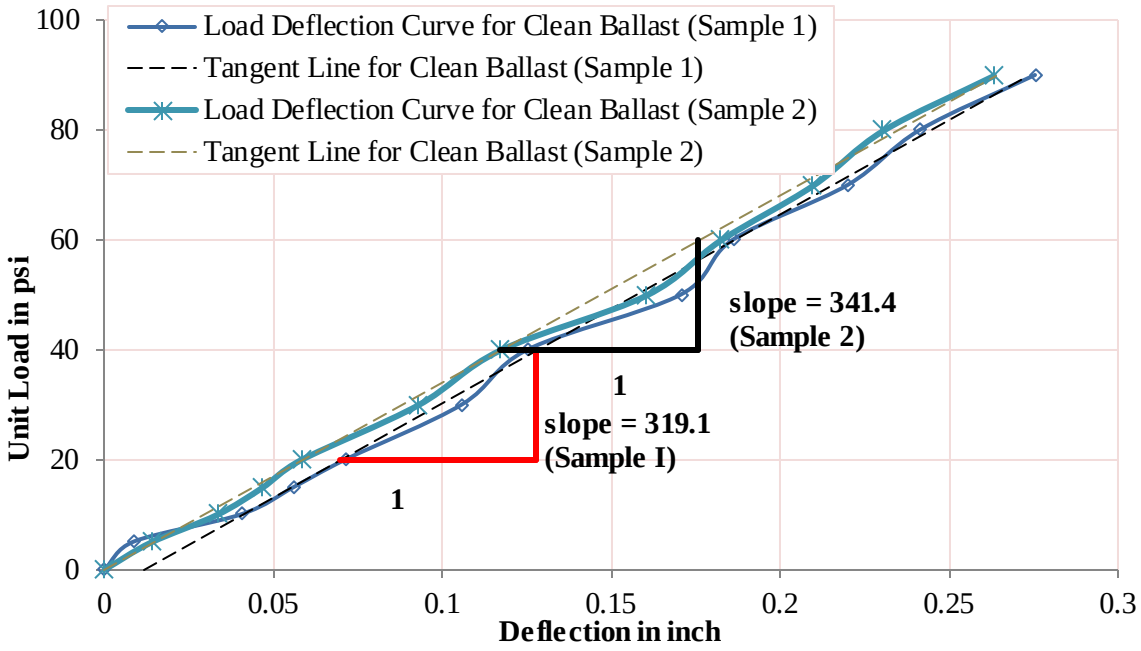

Figure 5-1 Unit Load versus Deflection Curve by Static Plate Loading Test of Clean Ballast

The static modulus of the clean ballast was determined to be 1,368 psi and 1,464 psi from the plate loading tests. The average CBR from DCP tests and the average resilient modulus from the LWD tests of the ballast are listed in Table 5.2 for both samples.

Table 5-2 CBR, Resilient Modulus, and Static Modulus of Clean Ballast

Descriptions	CBR	Resilient Modulus in psi	Static Modulus in psi
Test Method	DCP Test	LWD Test	Plate Loading Test
Sample 1	11.9	2,821	1,369
Sample 2	11.8	2,204	1,464
Average	11.9	2,512	1,416

Ratios of resilient modulus to static modulus are 2.06 for sample 1 and 1.50 for sample 2.

5.2.4. Discussion of Test Results of Clean Ballast

The average dry density of clean ballast was found to be 110.1 lb/ft^3 and the corresponding void ratio was 0.54. The resistivity of the clean ballast sample was very high and was out of range of the equipment deployed for the test. The average stiffness of the clean ballast sample was 330.3 psi. Between the above mentioned two samples, sample 1 showed slightly higher values of CBR, resilient and static moduli. The average values of CBR, resilient, and static moduli were determined to be 11.9, 2,512 psi and 1,115 psi.

5.3. Dry Density of Fouled Ballast

5.3.1. Test Result of Dry Densities of Fouled Ballast

The dry densities of the fouled ballast samples were calculated from the wet densities and corresponding moisture contents. Table 5.3 shows the average dry densities of each type of fouled ballast. Figure 5.2 shows the corresponding average dry density based on type of fouling.

Here the average dry density represents the averages of different moisture content samples for the corresponding fouling category.

Table 5-3 Fouled Ballast Dry Densities for Different Types of Fouled Ballast

Descriptions	Type of Fouling	Average Dry Unit Weight in lb/ft^3
Subgrade soil fouled ballast	10%	122.1
	20%	130.6
	30%	126.3
	40%	124.8
Gardner track ballast dust fouled ballast	10%	123.5
	20%	128.4
	30%	132.9
	40%	127.9
Coal dust fouled ballast	10%	120.5
	20%	118.9
	30%	116.6

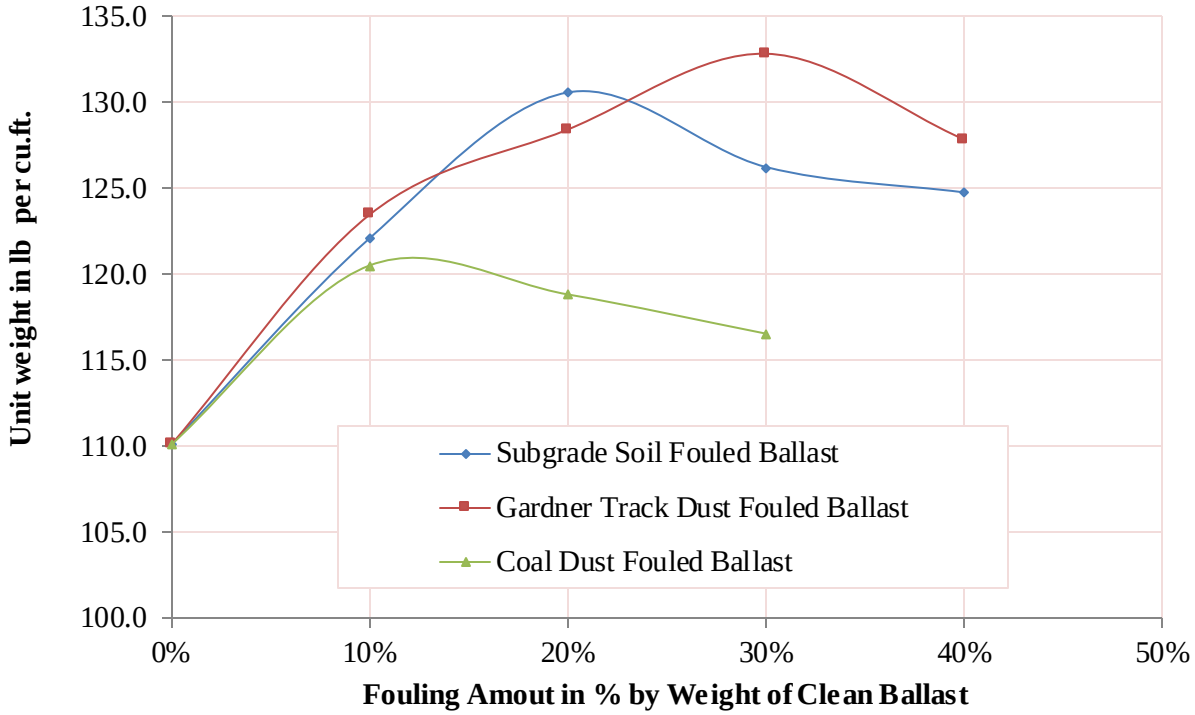

Figure 5-2 Dry Density versus Percentage Fouling For Different Types of Fouled Ballast

In Figure 5.2, the density of subgrade soil fouled ballast peaked at 20% fouling while the maximum value of the Gardner track ballast dust fouled ballast and coal dust fouled ballast peaked at 30% and 10% fouling, respectively.

At 10% fouling, the three types of fouled ballast have almost equal unit weights while the maximum unit weight of fouled ballast is obtained with Gardner track ballast dust fouled ballast at 132.9 lb/ft^3. The density of coal fouled ballast decreases with increasing fouling material by weight from 10% to 30%. A peak value was obtained for Gardner track ballast dust fouled ballast and the subgrade soil ballast while increasing the fouling materials from 10% and 40% for each mixture.

No relationship was observed between moisture content and dry density for clean or fouled ballast (Proctor curve). A cross check of ballast density was carried out separately with the smaller box shown in Figure 5.3. Samples composed of three layers of equal height were uniformly compacted to a total height of almost 7.5 inch. The size of the box was 21 x 21 inches.

Figure 5-3 Dry Density Determination from Small Box Test

The dry density of samples fouled with 30% and 40% Gardner track ballast dust was determined for two samples and was observed to be 133.3 lb/ft^3 and 128.4 lb/ft^3, respectively. These densities are close to the previous densities obtained from the test box, 132.9 lb/ft^3 and 127.9 lb/ft^3 respectively.

5.3.2. Discussion of Test Results of Dry Densities of Fouled Samples

Densities of the different moisture content samples for the same percentage fouling by weight were taken into consideration for determination of average density. Densities varied with moisture content and there was no clearly defined relationship observed between moisture content and dry density for any of the fouled ballast mixtures.

Gardner track ballast dust fouled ballast had the highest dry densities followed by the subgrade soil fouled ballast and coal fouled ballast for a particular percentage of fouling by weight. Densities of Gardner track ballast dust fouled ballast varied from 122.1 lb/ft^3 to 130.6 lb/ft depending upon the amount of fouling. The maximum dry density of Gardner track ballast dust fouled ballast was 132.9 at 30% fouling by weight and the minimum value was 123.5 lb/ft^3. The coal fouled ballast density decreased as the percentage of fouling increased from 10% to 30% fouling by weight. A cross check of densities from the small box test were valid for 30% and 40% by weight of Gardner track ballast dust fouled ballast and were very near to the previous test results.

5.4. Boundary Effect of Resistivity Test on Test Box

5.4.1. Test Result of Boundary Effect of Resistivity on Test Box

The resistivity of the fouled ballast was calculated using the relationship mentioned in equation 2.II from the resistance obtained from the ground resistance tester. Resistivity measurements for a series of fouled ballast moistures are shown in Figures 5.4 through 5.14. The resistivity calculated from the data obtained by the Wenner four point method shows that the resistivity changed substantially for measurements 1.5 inches and 4 inches from the boundary. However, the resistivity measured for 8 inches, 11 inches, and 15.88 inches experienced significantly less deviation.

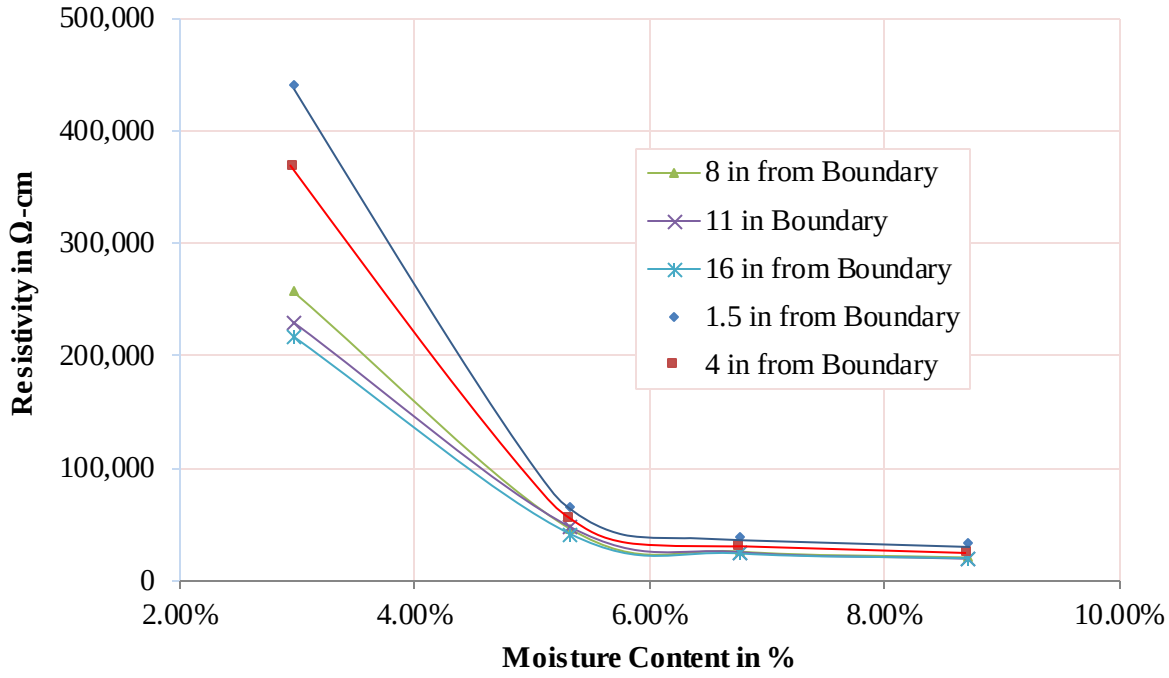

Figure 5-4 Boundary Effect Study for Resistivity - 10% Fouled with Subgrade Soil

Figure 5.4 shows the resistivity of 10% fouled ballast with subgrade soil. The resistivity measured at 1.5 in and 4 in from the boundary was substantially higher that values measured at distances of 8 in, 11 in and 16 in.

The overall trends in Figures 5.5 through 5.7 are similar to Figure 5.4, however the resistivity measurements in Figure 5.5 at different distances from boundary at 2.34% MC are almost identical. This is due to inability of reading the resistance (out of limit of the resistance measurement of the AEMC 4620 Instrument).

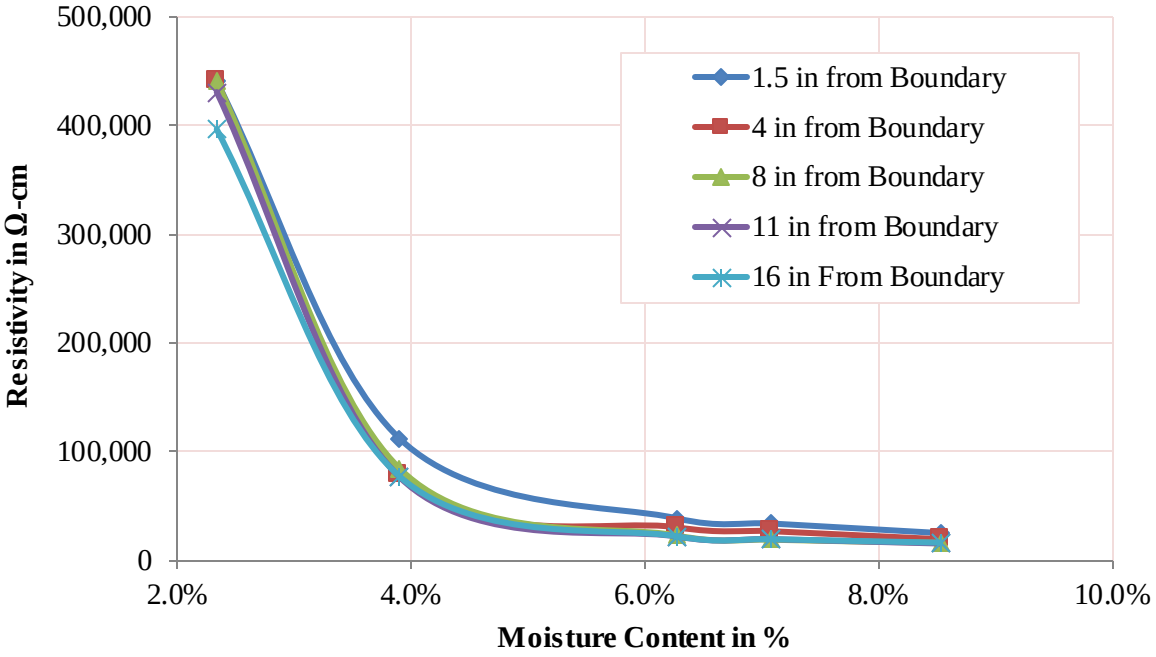

Figure 5-5 Boundary Effect Study for Resistivity - 20% Fouled with Subgrade Soil

In both figures, resistivity measurements for 1.5 inches and 4 inches deviated significantly from those for 8 inches, 11 inches, and 15.88 inches.

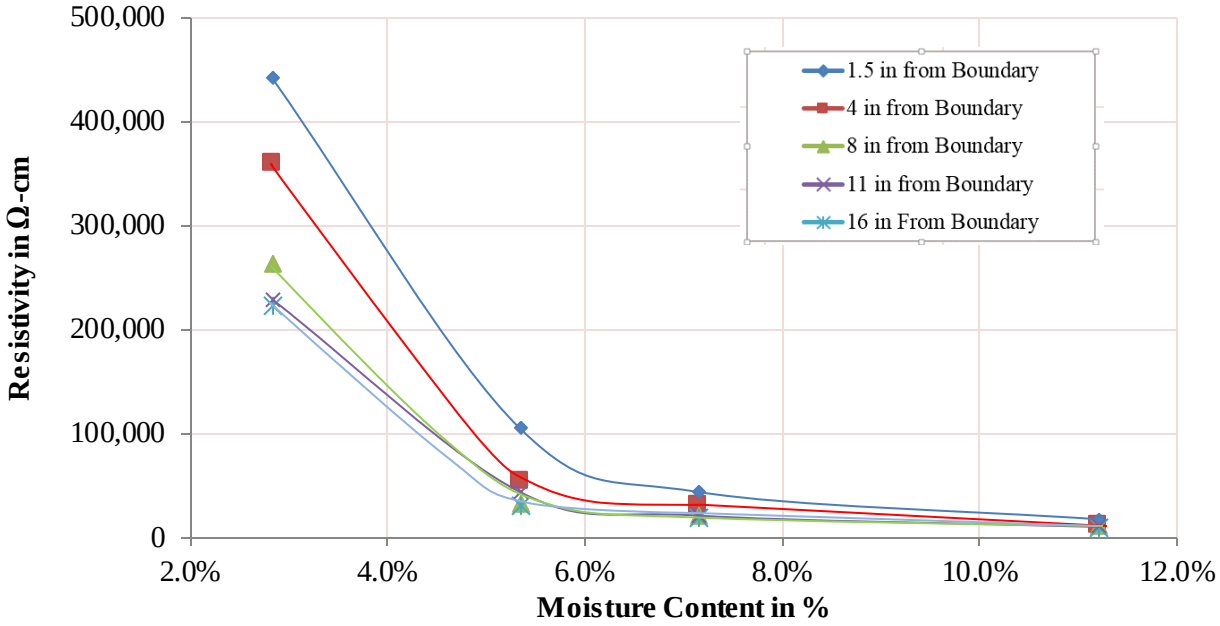

Figure 5-6 Boundary Effect Study for Resistivity – 30% Fouled with Subgrade Soil

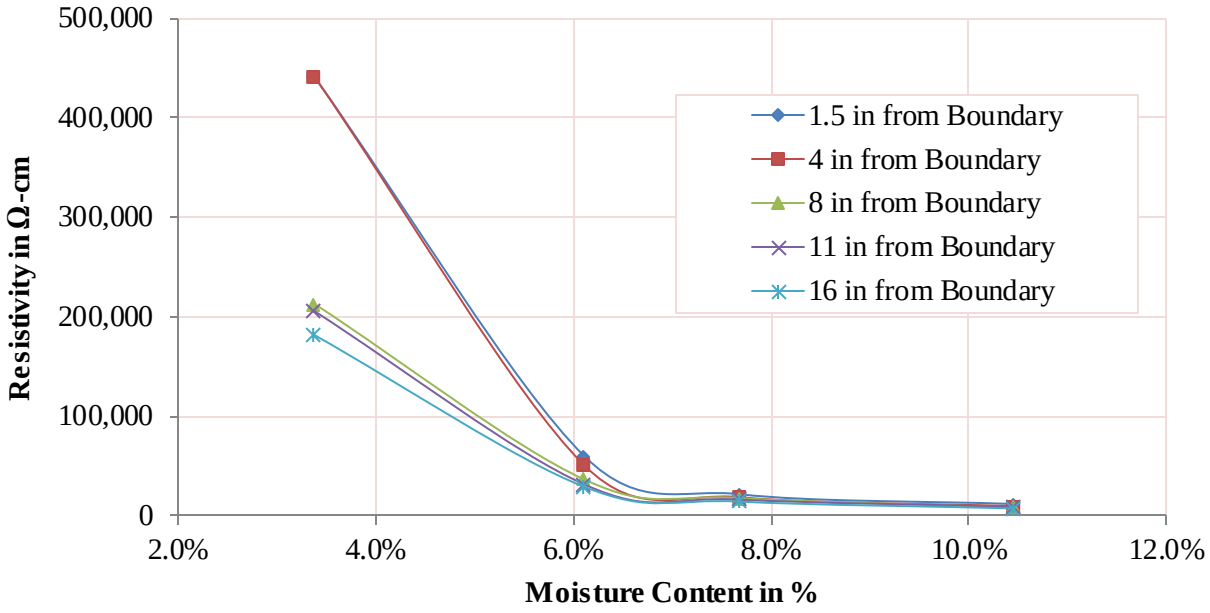

Figure 5-7 Boundary Effect Study for Resistivity – 40% Fouled with Subgrade Soil

The resistivity of the Gardner track ballast dust fouled ballast was measured at different moisture contents and an analysis of boundary effects on soil resistance measurement was conducted. The corresponding results are shown in Figure 5-8 through 5.11.

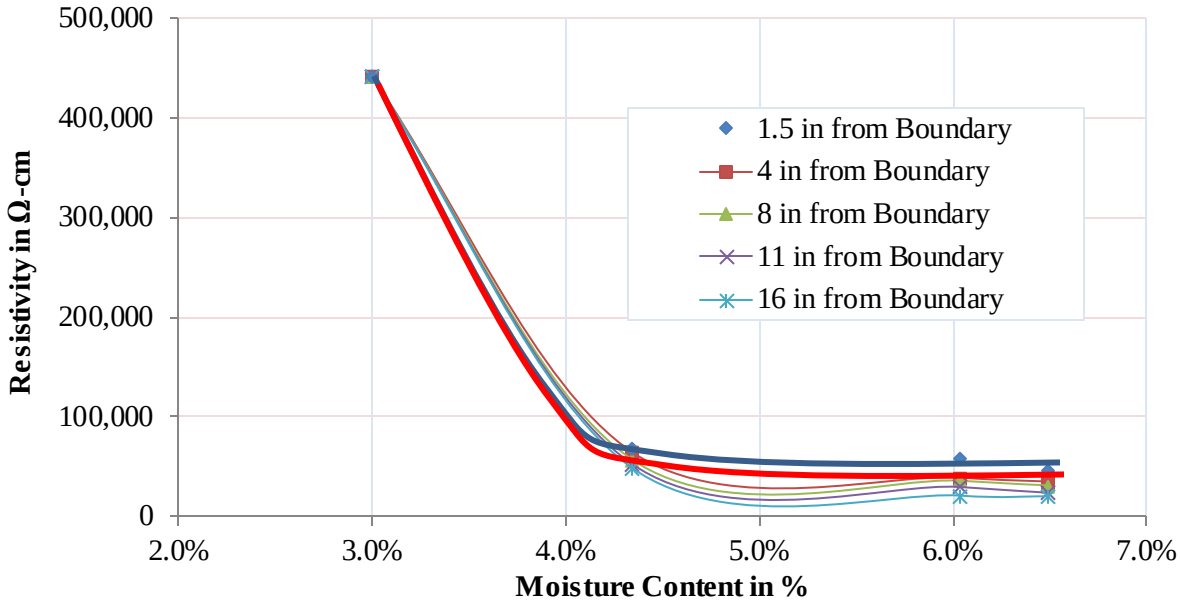

Figure 5-8 Boundary Effect Study for Resistivity - 10% Fouled with Track Dust

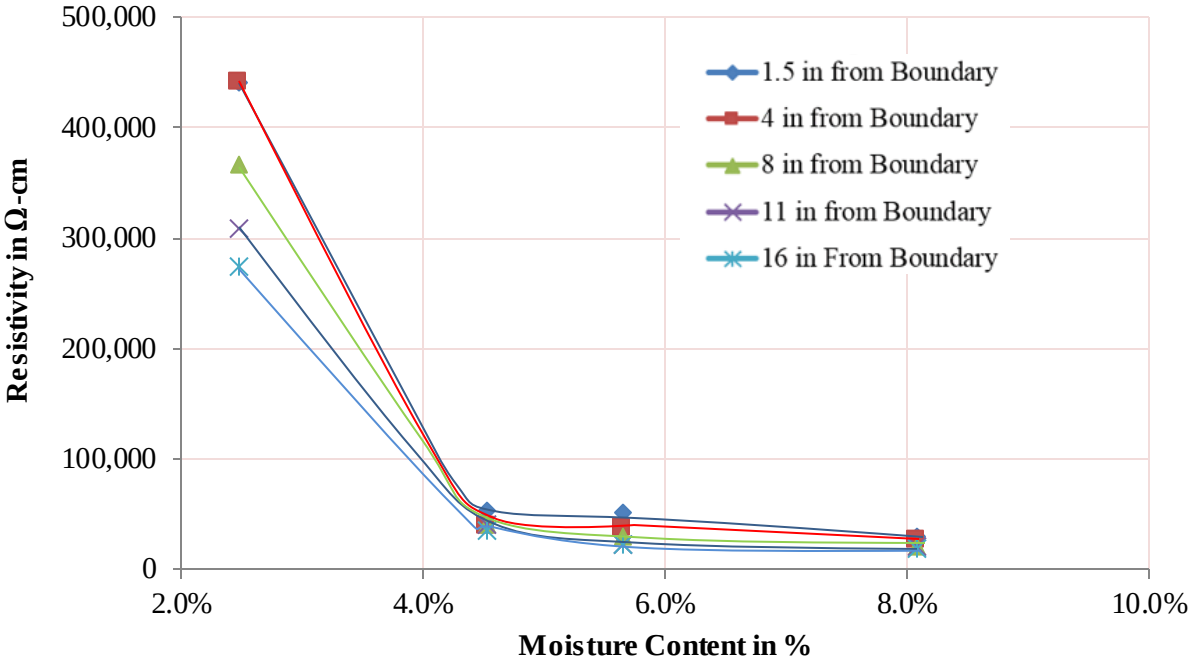

Figure 5-9 Boundary Effect Study for Resistivity - 20% Fouled with Track Dust

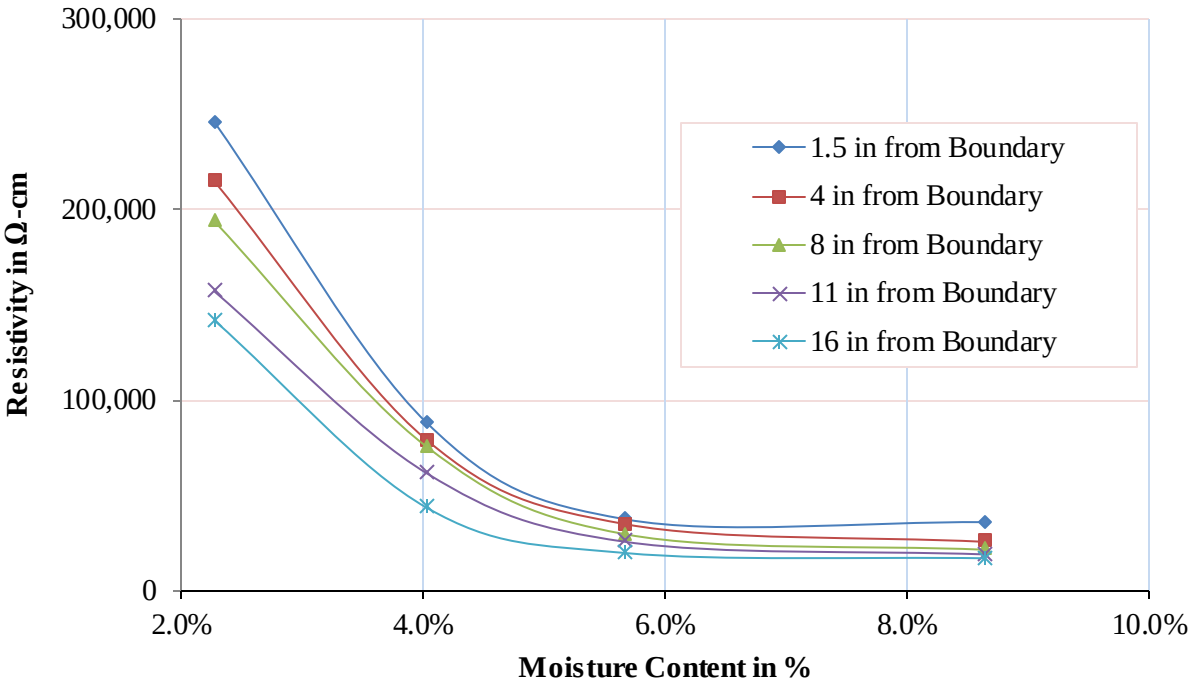

Figure 5-10 Boundary Effect Study for Resistivity - 30% Fouled with Track Dust

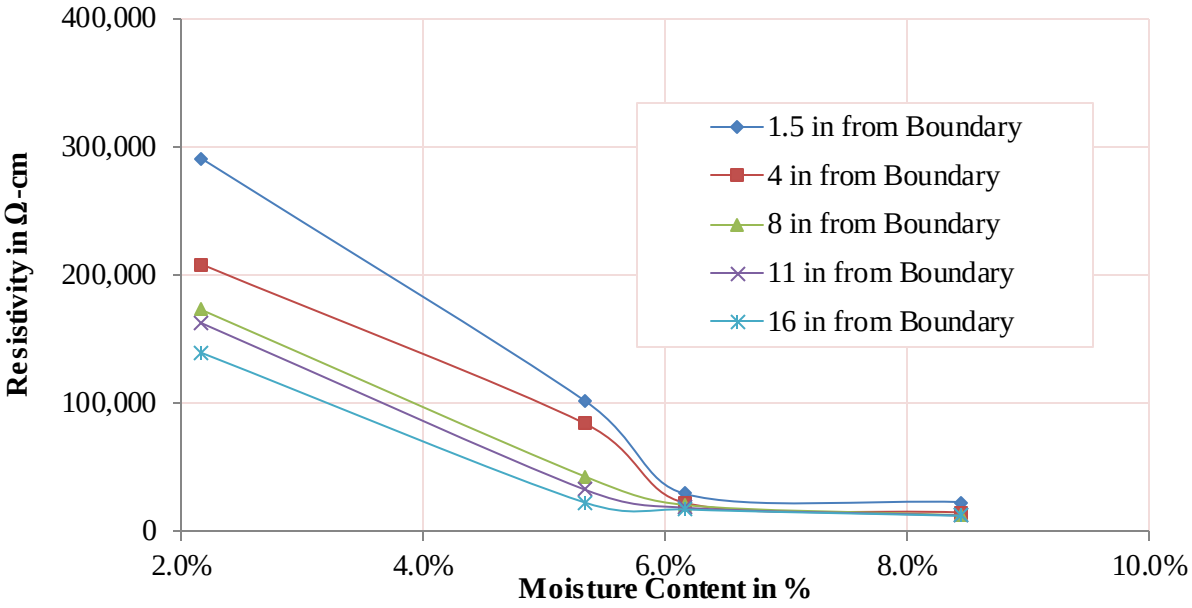

Figure 5-11 Boundary Effect Study for Resistivity - 40% Fouled with Track Dust

The test procedure was repeated for coal dust, and the effect of close boundaries on resistivity measurement was studied. The corresponding results are given in the figures 5-12 through 5.14.

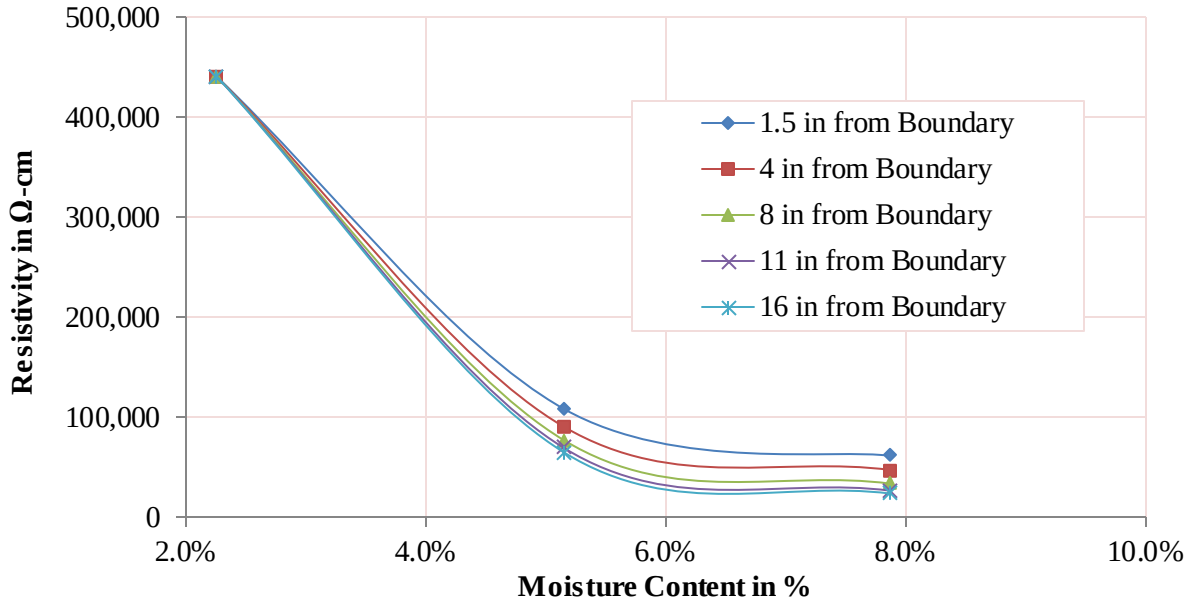

Figure 5-12 Boundary Effect Study for Resistivity - 10% Fouled with Coal Dust

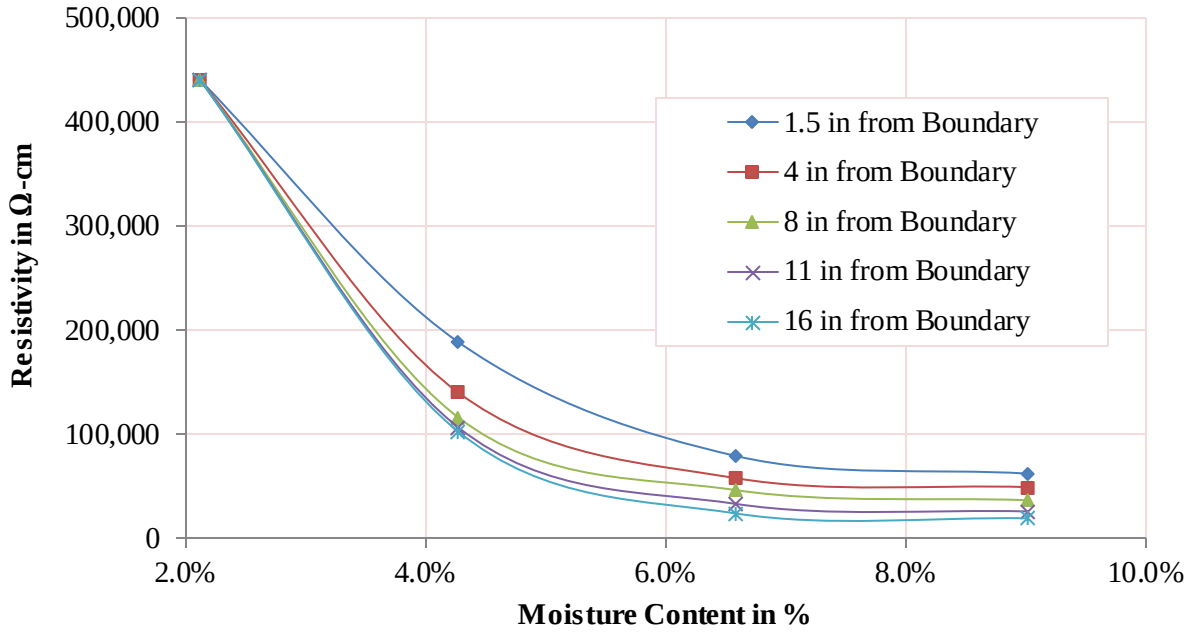

Figure 5-13 Boundary Effect Study for Resistivity - 20% Fouled with Coal Dust

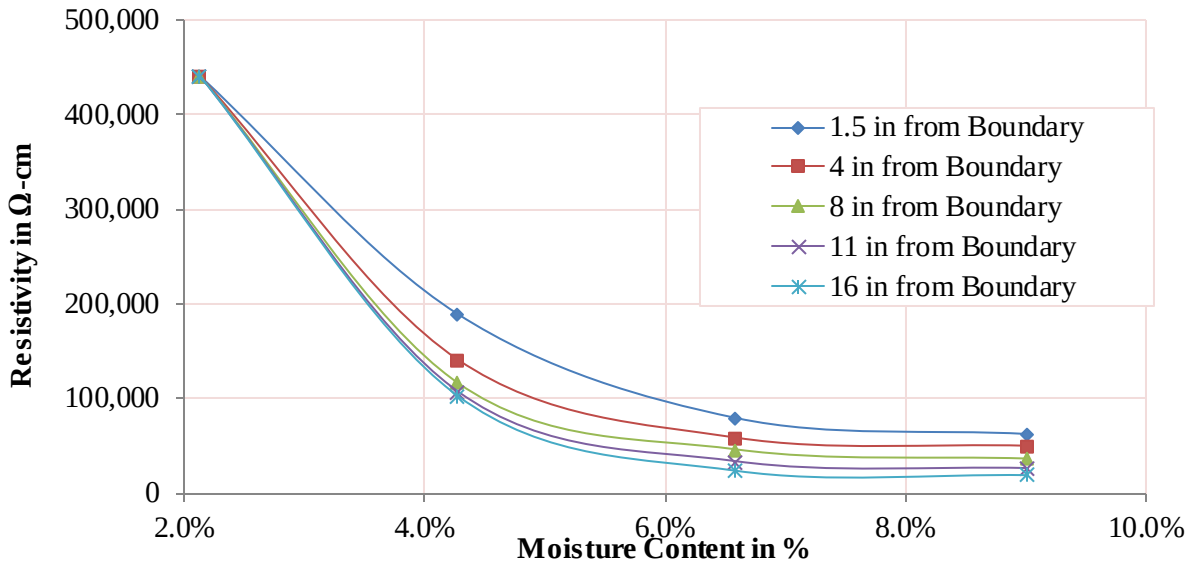

Figure 5-14 Boundary Effect Study for Resistivity - 30% Fouled with Coal Dust

5.4.2. Discussion on Boundary Effect of Resistivity on Test Box

Since the test box was a poor conductor of electricity, the boundary of the test box caused an elevated reading for resistivity up to a distance 8 inches from the boundary – which was slightly

greater than the probe spacing of 7 inches. The length of the probes may be the controlling distance for the boundary effect. If the probe spacing was lower, the boundary effect distance may be lower. Moreover, the penetration depth of the probe was 4 inches, and the effect was negligible at twice the penetration depth. Hence, the boundary effect is likely a function of the probe spacing and the penetration depth of probes.

It was observed that the variations of resistivity for subgrade soil due to the boundary effect were lower as compared to Gardner track ballast dust fouled ballast and coal dust fouled ballast. This suggests that if the medium is a comparatively good conductor, there is less effect from the boundary.

5.5. Result of Resistivity Testing by the Wenner Four Point Method

5.5.1. Resistivity Test Result - Subgrade Soil Fouled Ballast

Figure 5.15 and 5.16 presents the test results of resistivity of subgrade soil fouled ballast for different percentages of fouling by weight. Figure 5.16 is a close-up view of figure 5.15.

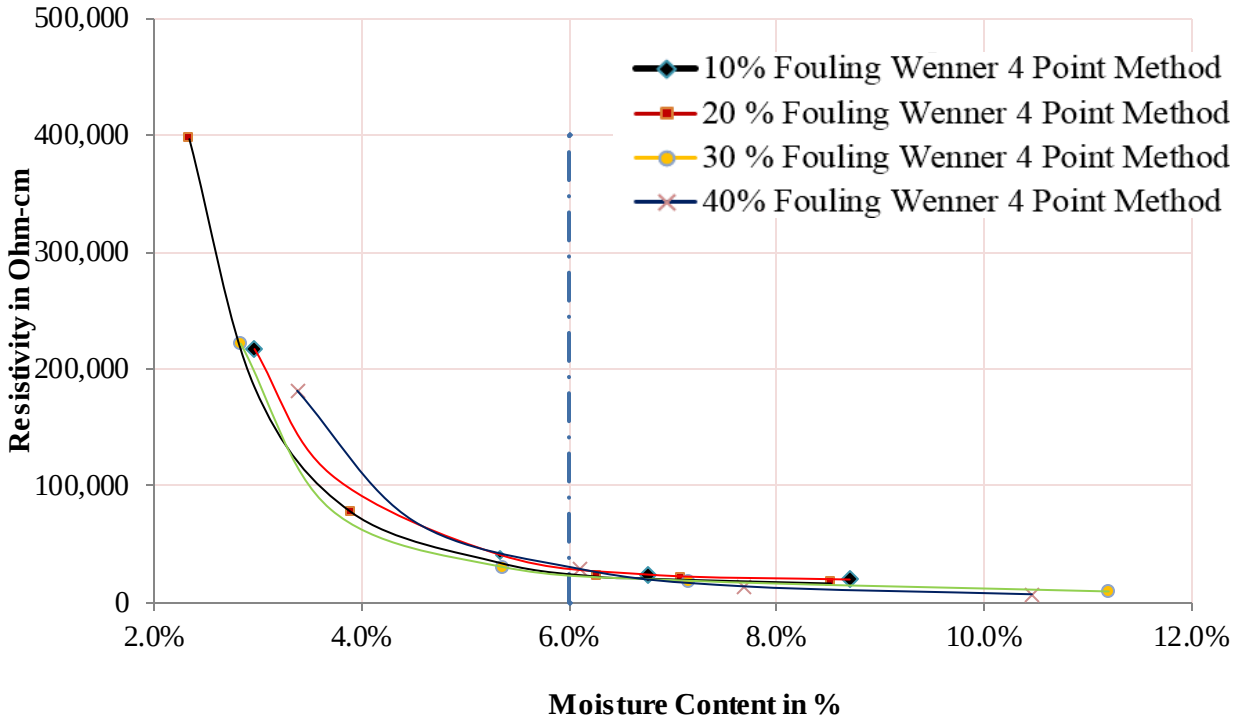

Figure 5-15 Resistivity of Subgrade Soil Fouled Ballast for Different Moisture Contents

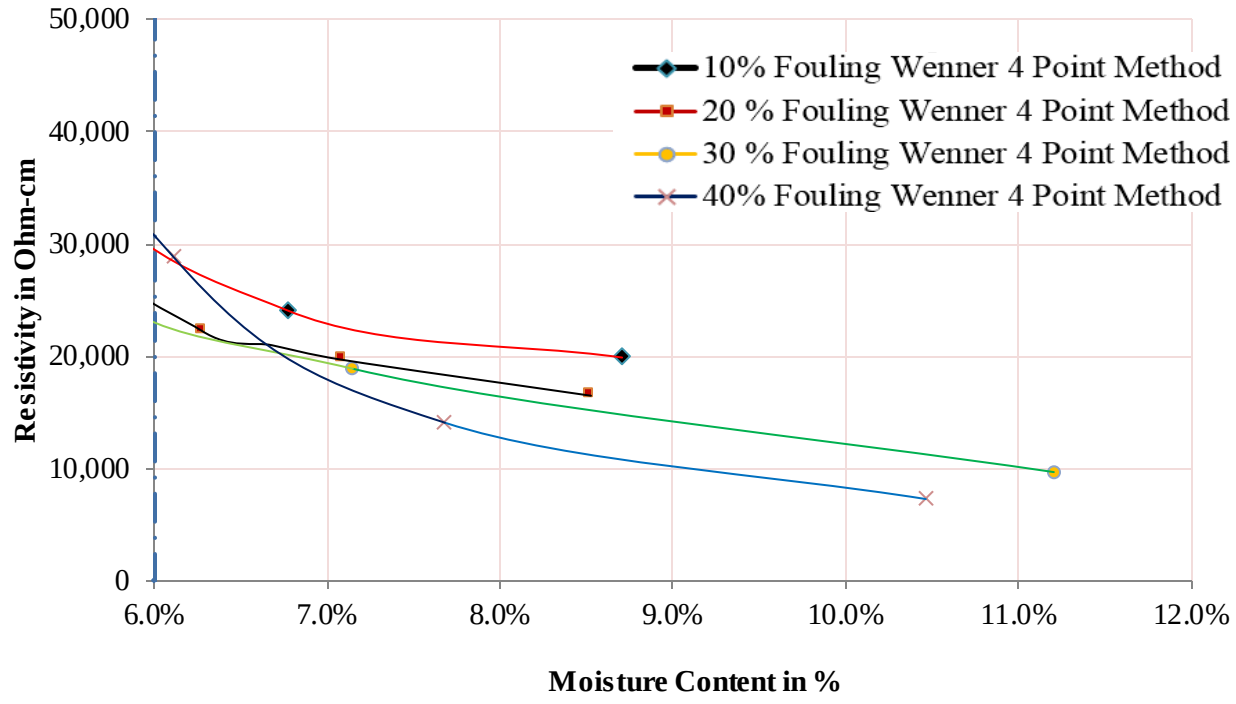

Figure 5-16 Resistivity of Subgrade Soil Fouled Ballast for Various MC (Zoom In View)

Here, the subgrade soil fouled ballast with 10% fouling material reached a near-constant resistivity at 8.5% moisture content, while the subgrade soil fouled ballast with 40% fouling material reached a near-constant resistivity at 10.5% moisture content. Based on these results, the subgrade soil fouled ballast was observed to have the following range of resistivity values:

Table 5-4 Comparison of Resistivity for Various % Fouling of Subgrade Soil Fouled Ballast

Type of Fouling	Fouling Index	Range of Resistivity from OMCR (6%) to field capacity state [Ω-cm]	Resistivity Range for Rahman (2014) Ω-cm
10% by weight	18	20,000 - 29,000	NA
20% by weight	33	16,000 - 27,000	20,000 – 24,000
30% by weight	45	10,000 - 23,000	15,000 – 20,0000
40% by weight	56	8,000 - 20,000	11,000 – 15,000

Note: NA = Not available.

Hence, the resistivity of the fouled ballast with subgrade soil is very sensitive to moisture contents less than 6%. For more than 6% moisture up to the approximately field capacity state, where the field capacity is the amount of soil moisture (water content) after the excess water has drained away, was less sensitive; however the resistivity varied slightly depending upon the actual moisture content.

5.5.2. Resistivity Test Results – Gardner Track Ballast Dust Fouled Ballast

Figures 5.17 and 5.18 present the resistivity test results for Gardner track ballast dust fouled ballast for different percentages of fouling by weight. Figure 5.18 is the close-up view of figure 5.17. Gardner track ballast dust fouled ballast reaches the field capacity state for a lower moisture content than the subgrade fouled ballast. For 10% fouling by weight, the resistivity dropped to the level of a saturated soil at about 6.5% of water content, while for 40% fouling by

weight, the resistivity of the fouled ballast almost dropped to the level of a saturated soil at about 8.5% moisture content.

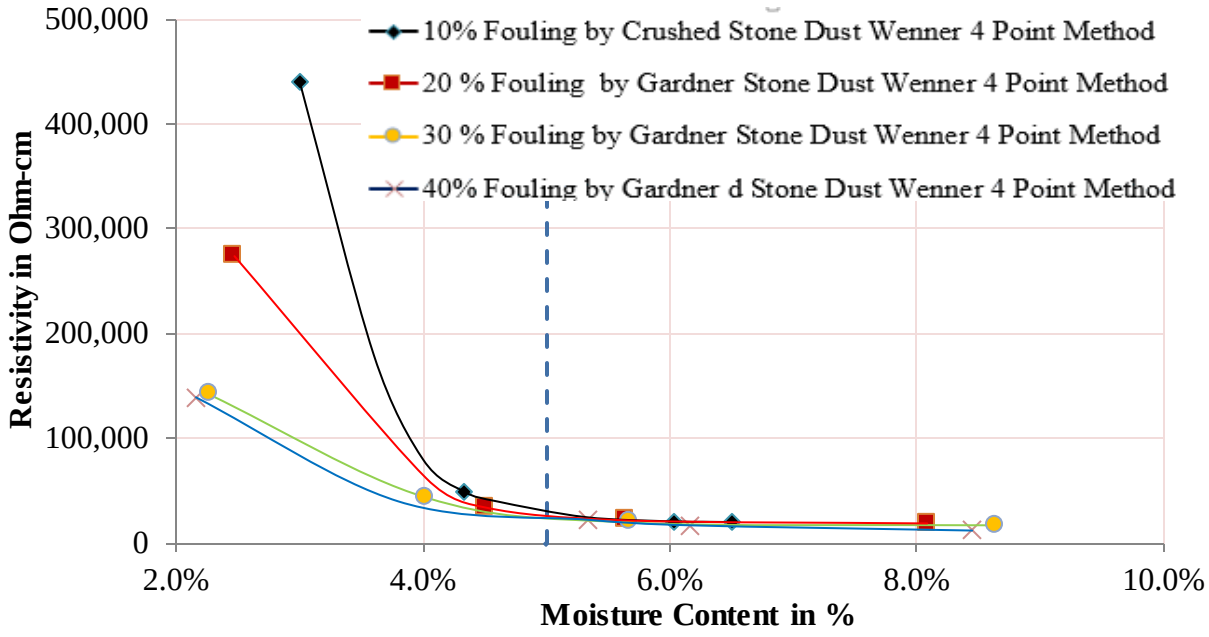

Figure 5-17 Resistivity of Gardner Track Dust Fouled Ballast for Different Moisture Contents

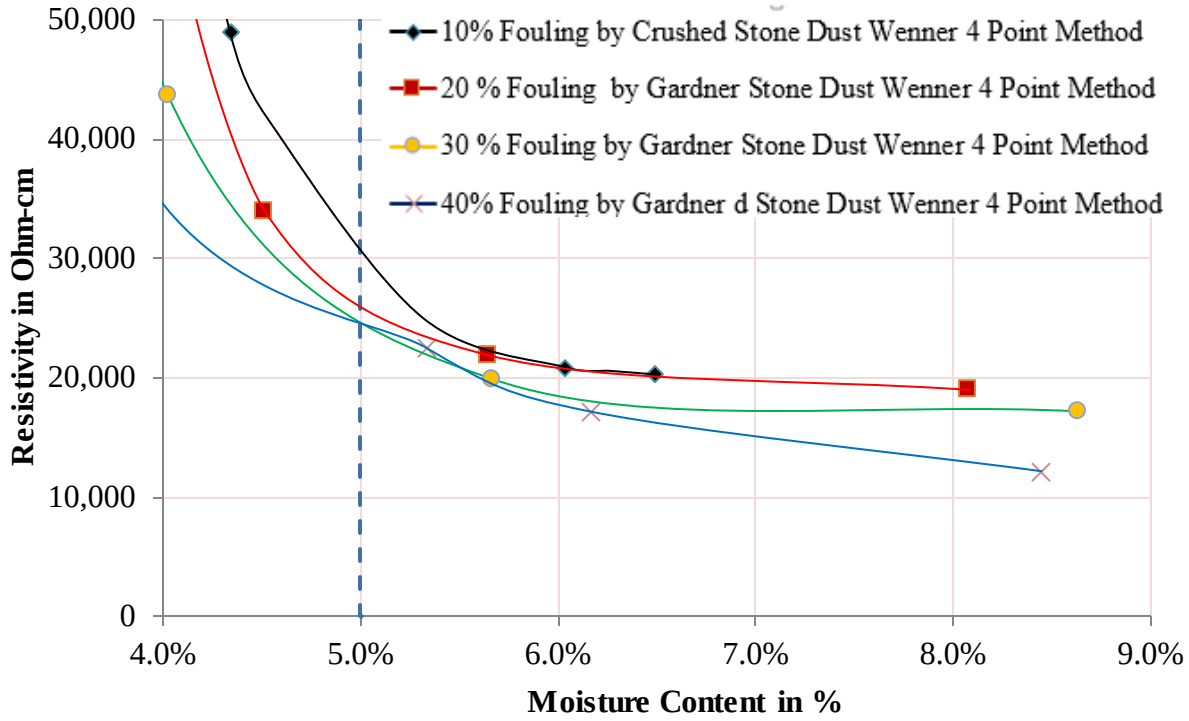

Figure 5-18 Resistivity of Gardner Track Dust Fouled Ballast for Various MC (Zoom In View)

The Gardner track dust fouled ballast was observed to have the ranges of resistivity shown in Table 5-5.

Table 5-5 Resistivity of Various % Fouling of Gardner Track Ballast Dust Fouled Ballast

Type of Fouling	Fouling Index	Range of Resistivity from OMCR (5%) to field capacity state [Ω-cm]	Resistivity Range for A.J Rahman Test Set up Ω-cm
10% by weight	10	20,000 - 30,000	NA
20% by weight	18	18,500 - 24,500	42,000 – 80,000
30% by weight	24	17,000 - 23,000	32,000 – 42,0000
40% by weight	30	13,000 - 23,000	12,000 – 20,000

Note: NA = Not available.

As shown in graphs 5.17 and 5.18, the resistivity of the fouled ballast with Gardner track ballast dust is very sensitive to moisture contents less than 5.5%. For 5.5% up to the saturated condition, the resistivity of the ballast is less sensitive and the graph is almost parallel to the x axis. However, the resistivity varies slightly depending upon the amount of moisture content.

Present test results are considerably lower as compared to Rahman results, because of presence of finer particles significantly in Gardner track fouled ballast as compared to the ballast dust sampled in previous study.

5.5.3. Resistivity Test Result – Coal Dust Fouled Ballast

Figure 5.19 and 5.20 presents the test results for the resistivity of coal dust fouled ballast at different percentages of fouling by weight. Figure 5.20 is the close view of figure 5.19.

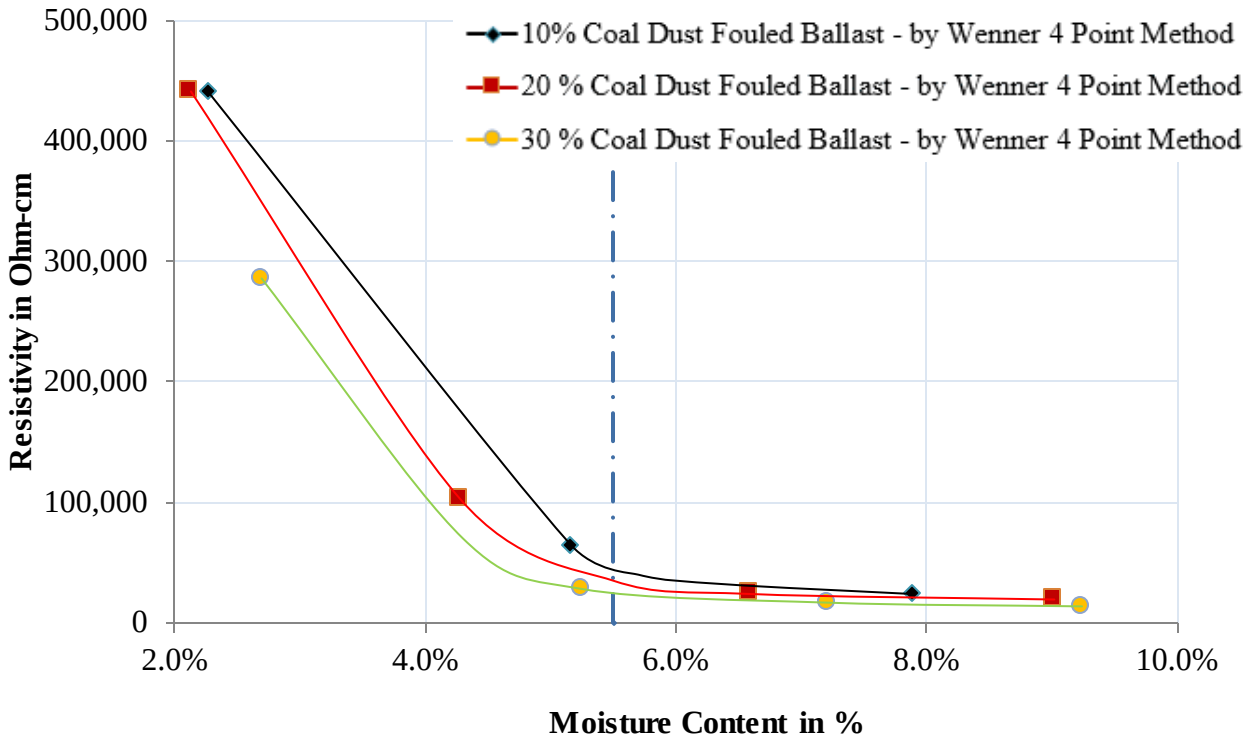

Figure 5-19 Resistivity of Coal Dust Fouled Ballast for Different Moisture Contents

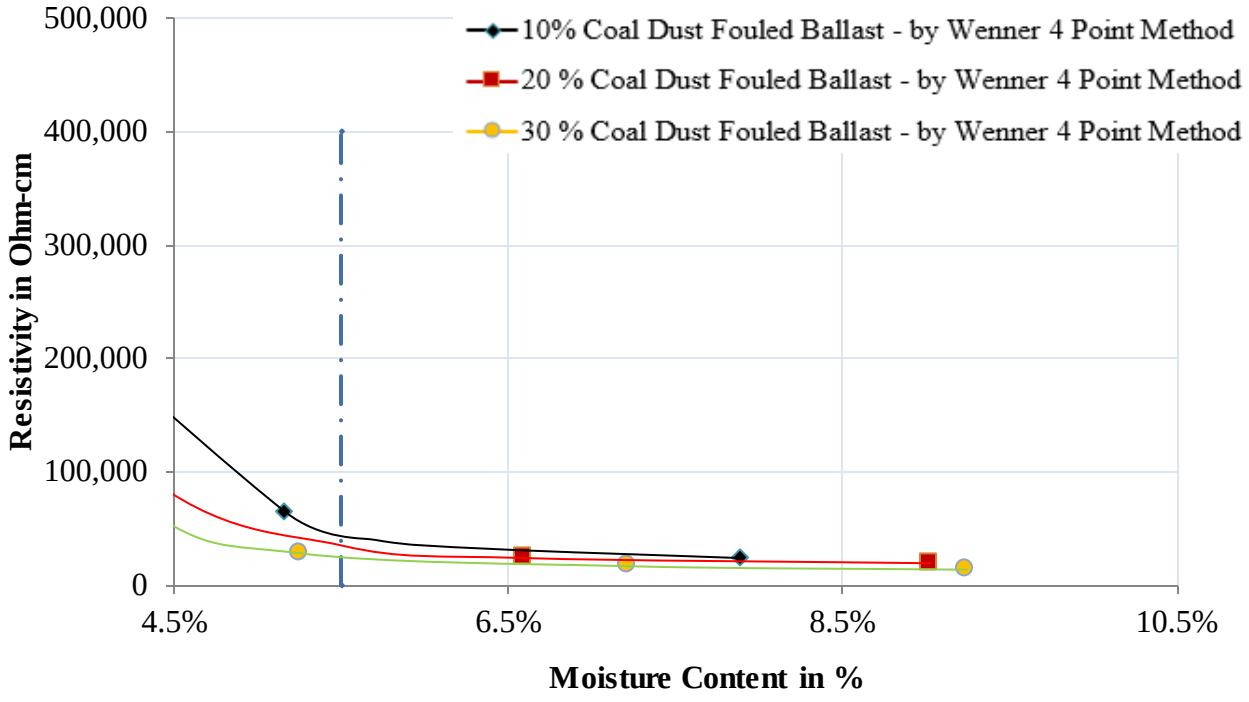

Figure 5-20 Resistivity of Coal Dust Fouled Ballast for Various MC (Zoom In View)

From the graphs 5.19 and 5. 20, the coal dust fouled ballast is shown to have the following ranges of resistivity:

Table 5-6 Resistivity Comparison for Different % Fouling for Coal Dust Fouled Ballast

Type of Fouling	Fouling Index	Range of Resistivity from OMCR (6%) to field capacity state [Ω-cm]	Resistivity Range for Rahman (2014) Ω-cm
10% by weight	10	21,000 - 40,000	27,000 - 46,000
20% by weight	19	20,000 - 34,000	16,000 - 26,000
30% by weight	26	15,000 - 21,000	12,000 -16,700

In the above graph, the resistivity of the coal dust fouled ballast is very sensitive to moisture contents less than 5%. For moisture contents of 5% up to the saturated condition, the resistivity of the ballast is less sensitive. However, the resistivity varies slightly depending on the amount of moisture content.

5.5.4. Validity of Resistivity Data from 2 Point Method for Horizontal Probe

The resistance of the fouled ballast measured by simple multimeter was plotted against moisture content of the fouled ballast along with the resistivity obtained from Wenner 4-point Method. The resistivity obtained from simple multimeter is higher than that of the resistivity obtained from Wenner 4-point Method. So, this method of measurement was discontinued for measuring the resistivity of the fouled ballast. Figures 5.21, 5.22, and 5.23 show the resistivity versus moisture content obtained by the Wenner 4-point Method and the 2 point method by simple multimeter for subgrade soil fouled ballast, Gardner track ballast dust fouled ballast, and coal dust fouled ballast, respectively, for different percentages of fouling.

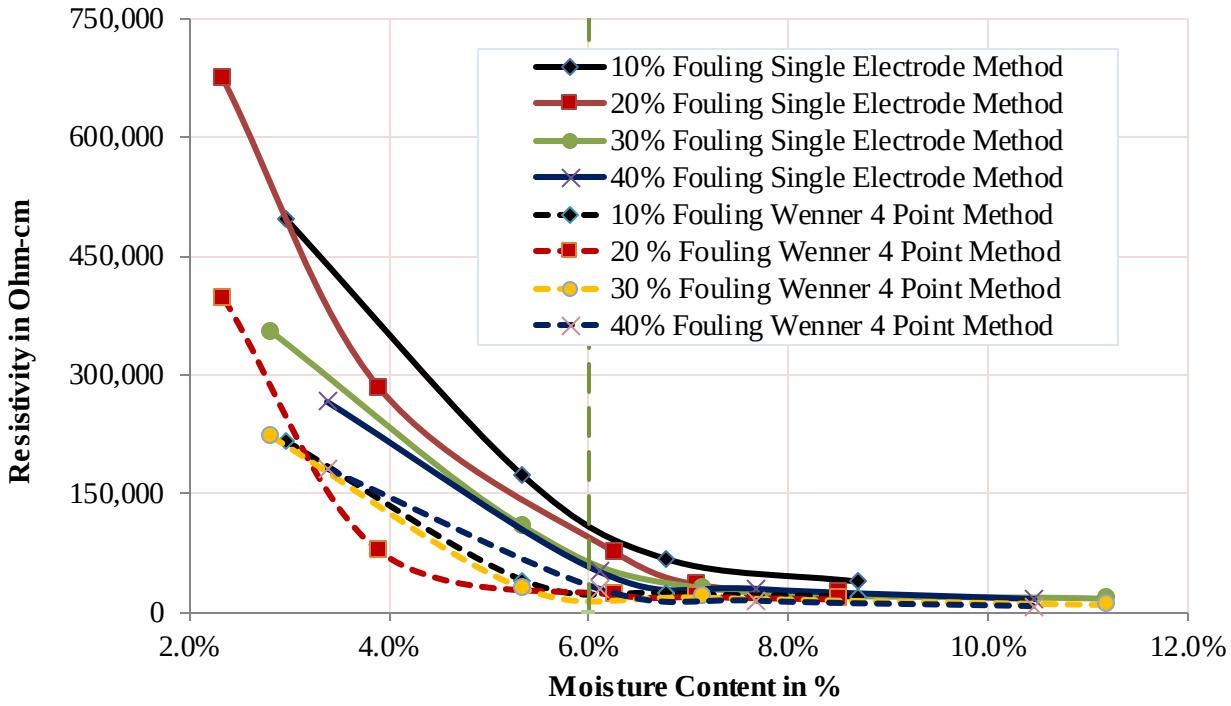

Figure 5-21 Resistivity by 2 & 4 Point Methods for Subgrade Soil Fouled Ballast

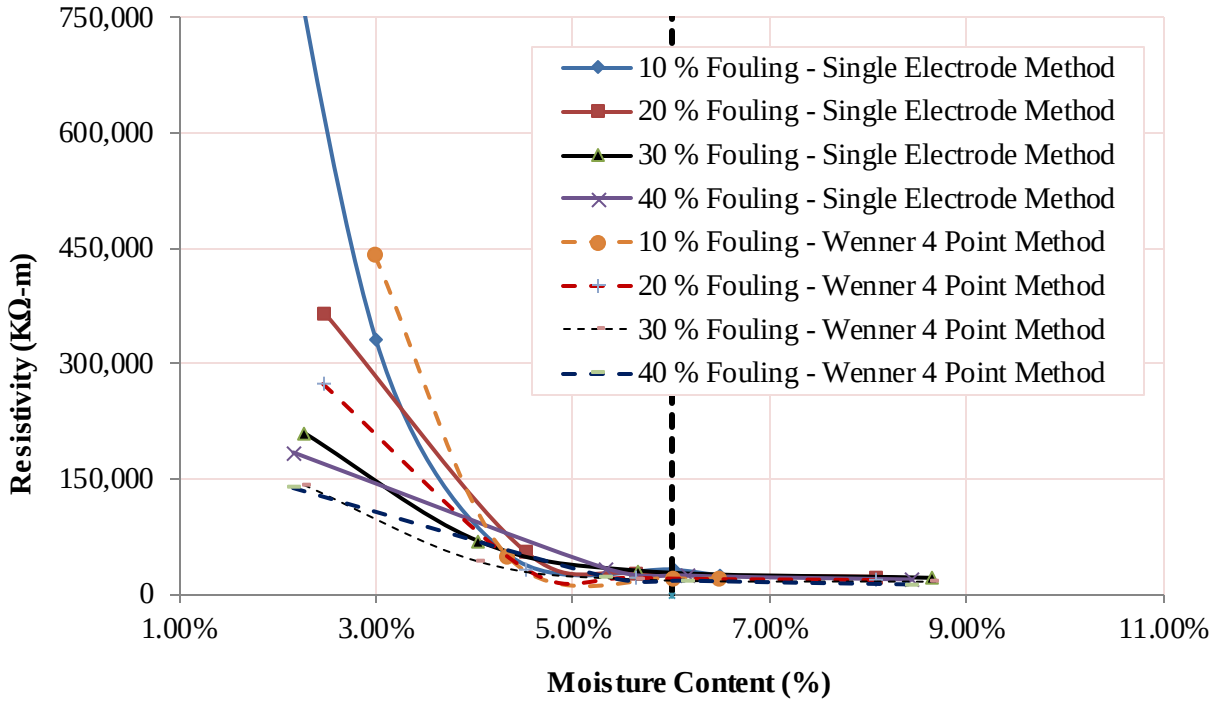

Figure 5-22 Resistivity by 2 Point & Wenner Methods of Gardner Track Dust Fouled Ballast

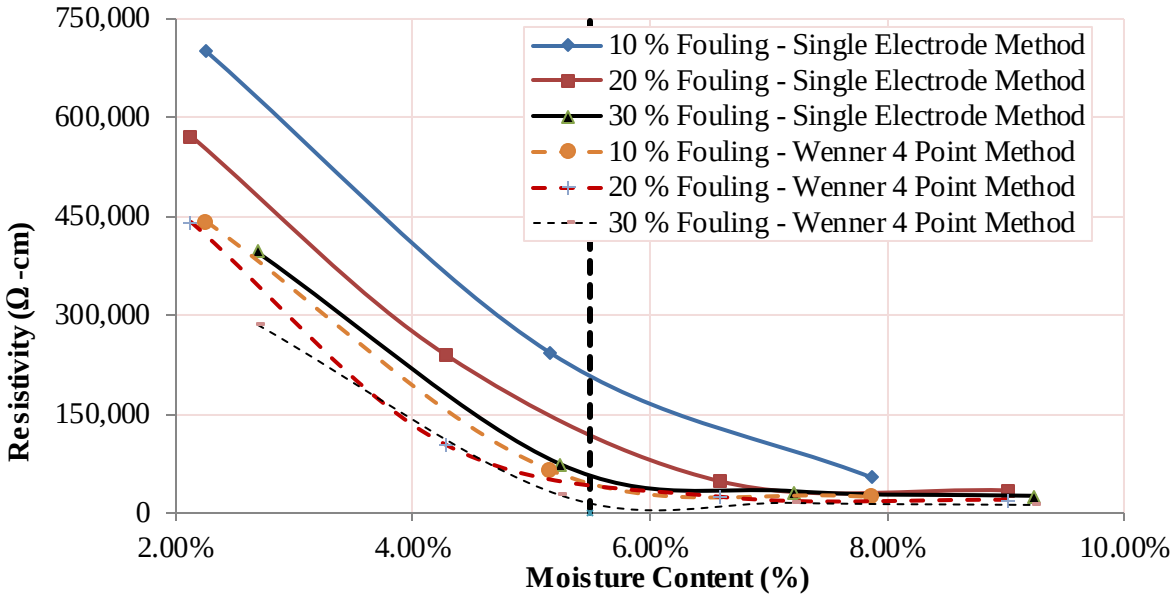

Figure 5-23 Resistivity by 2 Point & 4 Point Methods for Coal Dust Fouled Ballast

5.5.5. Comparison of Resistivity for Fouled Ballast with Different Fouling Agents

Figures 5.24 to 5.27 show a comparison of resistivity of fouled ballast with different types of fouling materials for the same fouling percentages by weight.

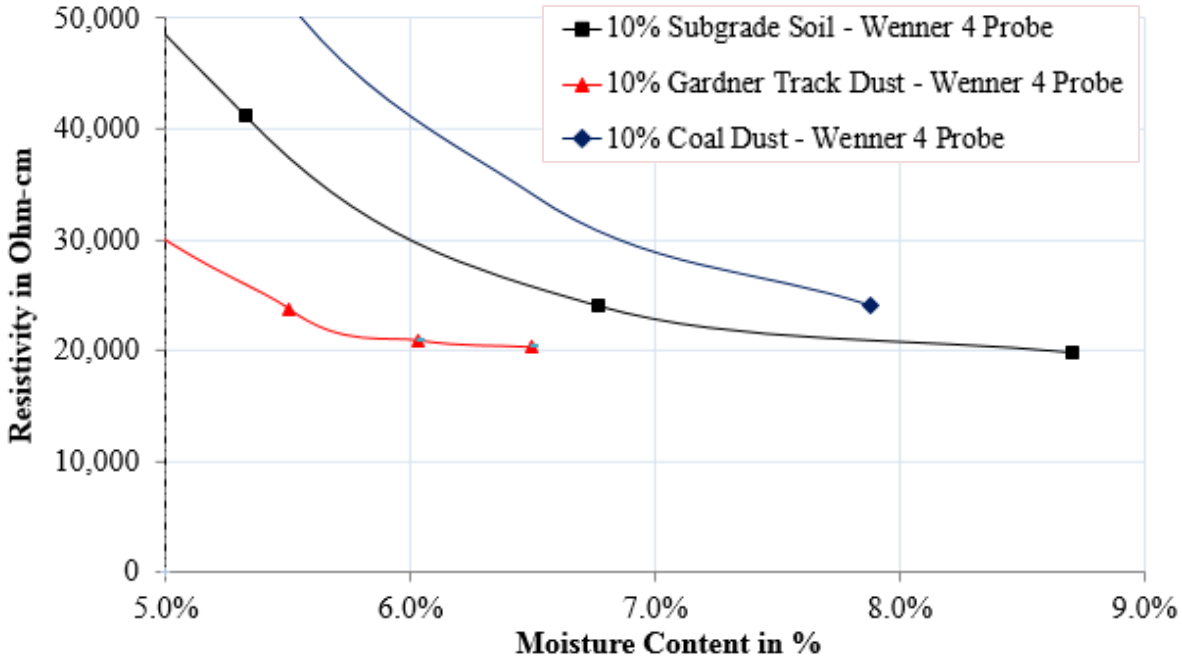

Figure 5-24 Comparison of Resistivity for Different Fouled Ballast at 10% Fouling by Weight

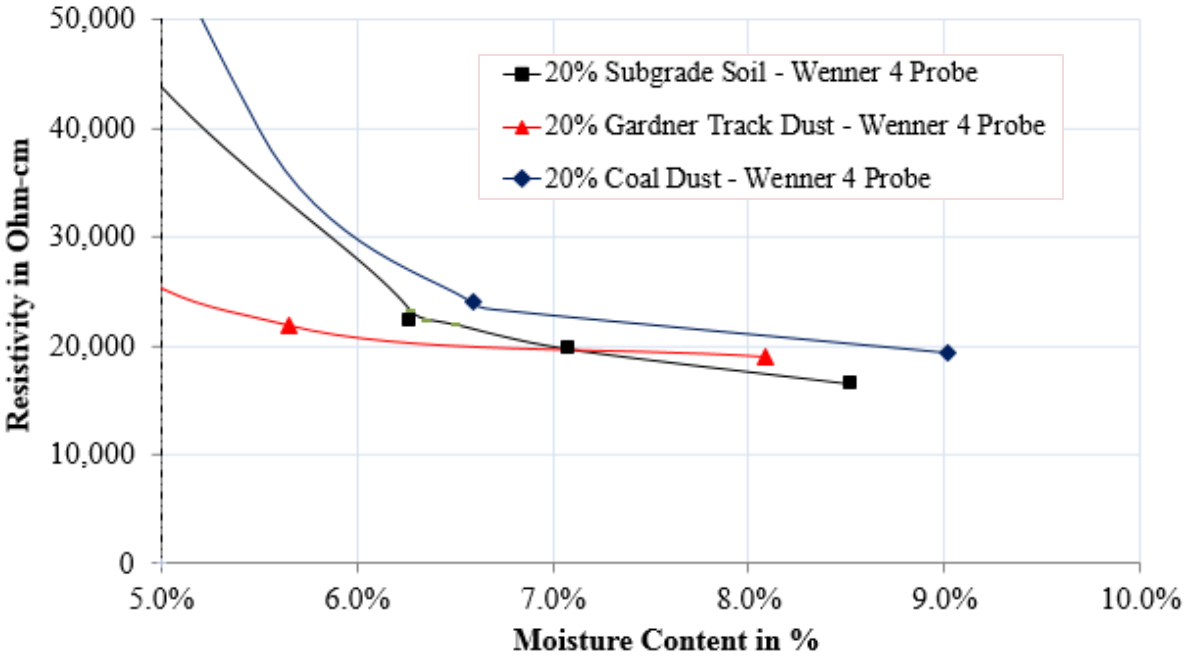

Figure 5-25 Comparison of Resistivity for Different Fouled Ballast at 20% Fouling by Weight

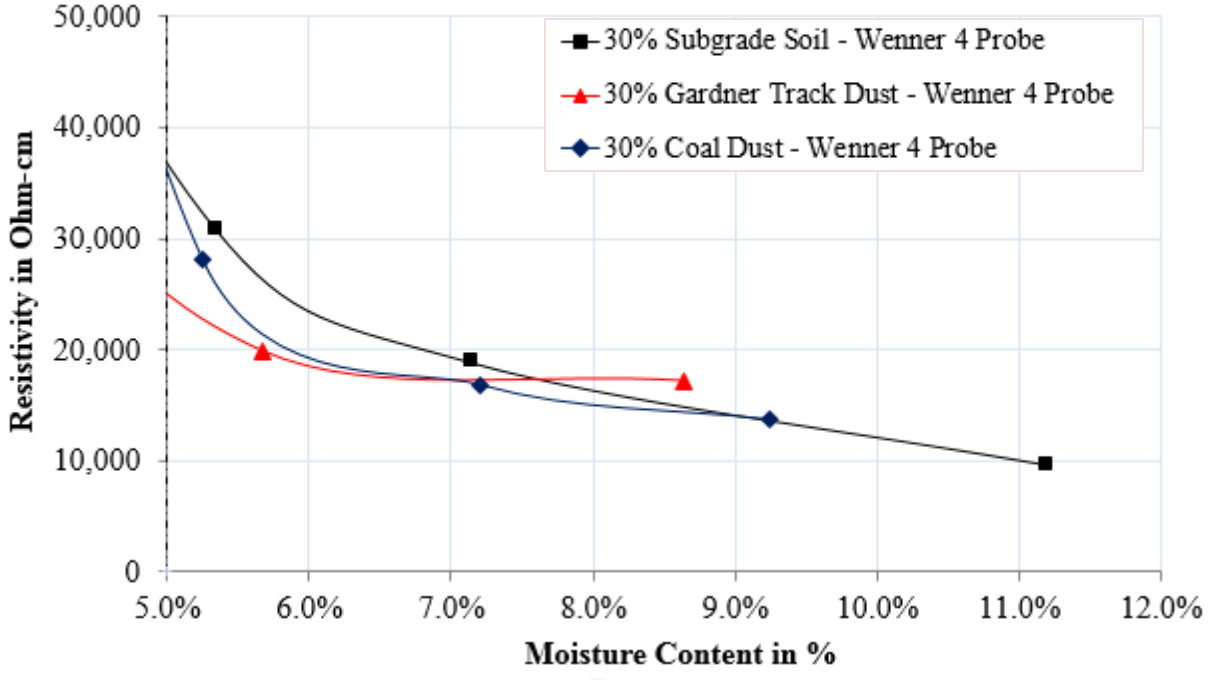

Figure 5-26 Comparison of Resistivity for Different Fouled Ballast at 30% Fouling by Weight

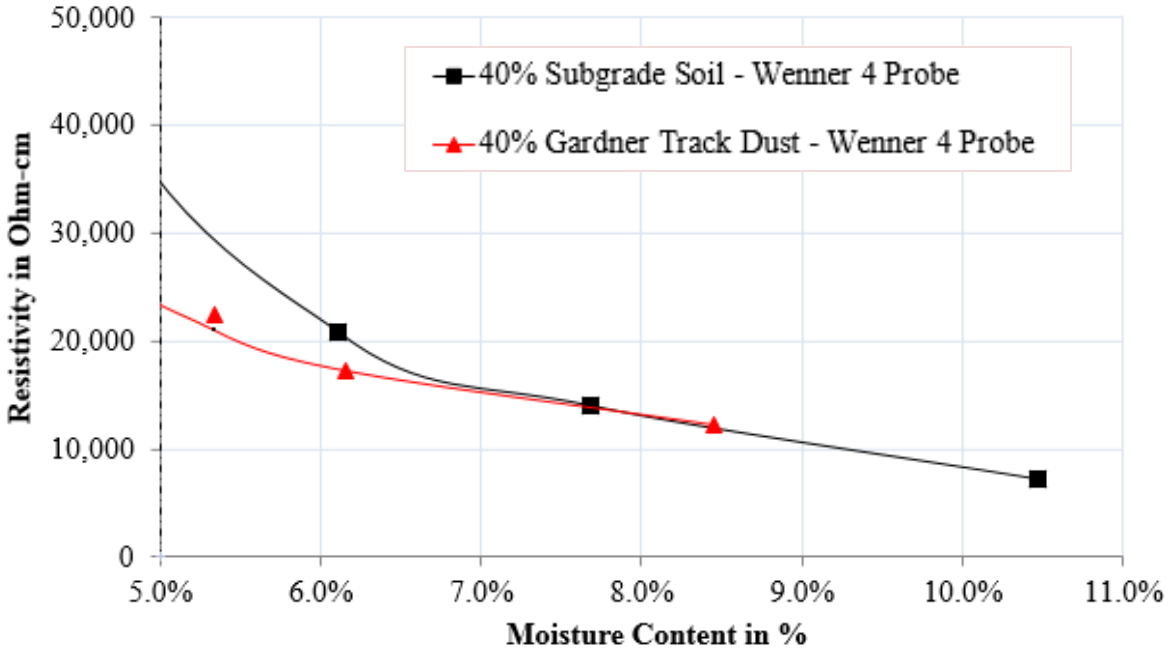

Figure 5-27 Comparison of Resistivity for Different Fouled Ballast at 40% Fouling by Weight

The above four graphs show that the Gardner track ballast dust fouled ballast possesses lower resistance than both subgrade soil fouled ballast and coal dust fouled ballast for similar moisture contents and similar amounts of fouling by weight. However, for the moisture contents at approximately field capacity level, the resistivity of subgrade soil fouled ballast is lower than both Gardner track ballast dust fouled ballast and coal dust fouled ballast.

5.5.6. Discussion of Resistivity by Wenner 4 Point Method of Fouled Ballast

The resistivity of fouled ballast was recorded in the presence of moisture. The trend of resistivity was decreasing for increasing amount of fouling. There was a boundary value of moisture content, above which the resistivity of fouled ballast was almost constant. This boundary value of moisture content was of 6% for subgrade soil fouled ballast, 5% for Gardner track ballast dust fouled ballast and 5.5% for coal dust fouled ballast. These boundary values moisture content are termed as "Optimum Moisture Content for Resistivity (OMCR)". These OMCRs were averages

of moisture content and a slight variation might occur depending upon the fouling amount. If the percentage fouling by weight was higher, the boundary values of moisture content were slightly higher as mentioned above and if the percentage fouling by weight was lower, the boundary values of moisture content were slightly lower as mentioned above.

Resistivity data were compared for moisture content higher than OMCR. The tests showed that resistivity of subgrade soil fouled ballast was found to be 8,000 Ω-cm to 29,000 Ω-cm depending up on the amount of fouling and percentage of moisture content higher than OMCR. Similarly, the resistivity of Gardner track ballast fouled ballast was found to be 13,000 Ω-cm to 30,000 Ω-cm depending up on the amount of fouling and percentage of moisture content higher than OMCR. The resistivity of coal fouled ballast was even higher as compared to previous two fouling agents and the values ranged from 15,000 Ω-cm to 40,000 Ω-cm. A clear range of resistivity was observed for each type of fouling and varied with the amount of fouling.

The resistivity data obtained by the single point method with the help of a simple multimeter were not very accurate when compared with the actual resistivity data obtained from Wenner 4 point method. These data were higher than the resistivity determined by the Wenner method.

For the same amount of percentage fouling by weight, the coal dust fouled ballast experienced higher resistivity while subgrade soil fouled ballast experienced lower resistivity at moisture contents near field capacity. However, for moisture contents lower than field capacity, the Gardner track ballast fouled ballast for 10% fouling by weight had a lower value of resistivity as compared to subgrade soil fouled ballast, since it has lower value of OMCR and goes to the field capacity state at a lower moisture content.

5.6. Validity of Vertical Resistivity Tester by Fall of Potential Method

5.6.1. Validity of Vertical Probe for Subgrade Material in Open Space

The vertical probe designed at the University of Kansas was inserted into the ground at different depths and used to measure the resistance by fall of potential method with the AEMC resistance meter in the vertical arrangement. At the same time, fall of potential measurements were carried out horizontally for probe spacing D equal to 3 ft. and 4.5 ft. as shown in figures 5.28 and 5.29. The same probe was used for measuring the resistance for the horizontal alignment as well as vertical alignment. The resistance was measured for the subgrade soil at different depths of the probe. The results of the resistance measurements by vertical probe and horizontal probe were generally consistent, depending upon the depth. For shallow depths the resistance was very high due to insufficient contact between the measuring rod and the ground. Insufficient contact was observed to affect readings for depths up to 11.0 inches.

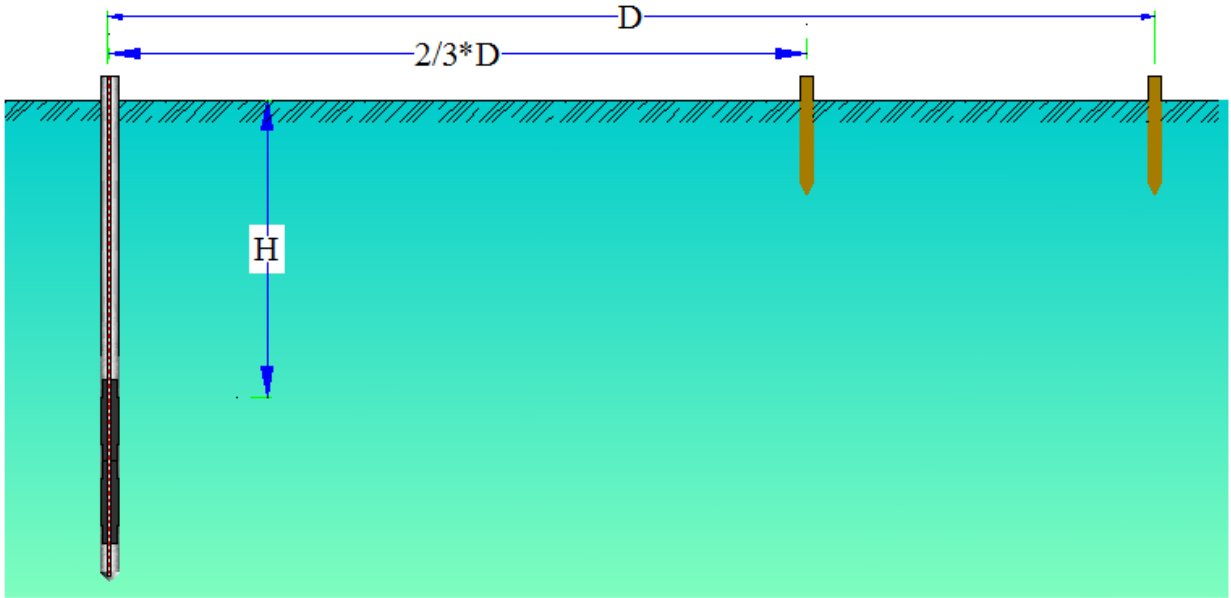

Figure 5-28 Sketch of Vertical Probe Resistance Check by Fall of Potential Method

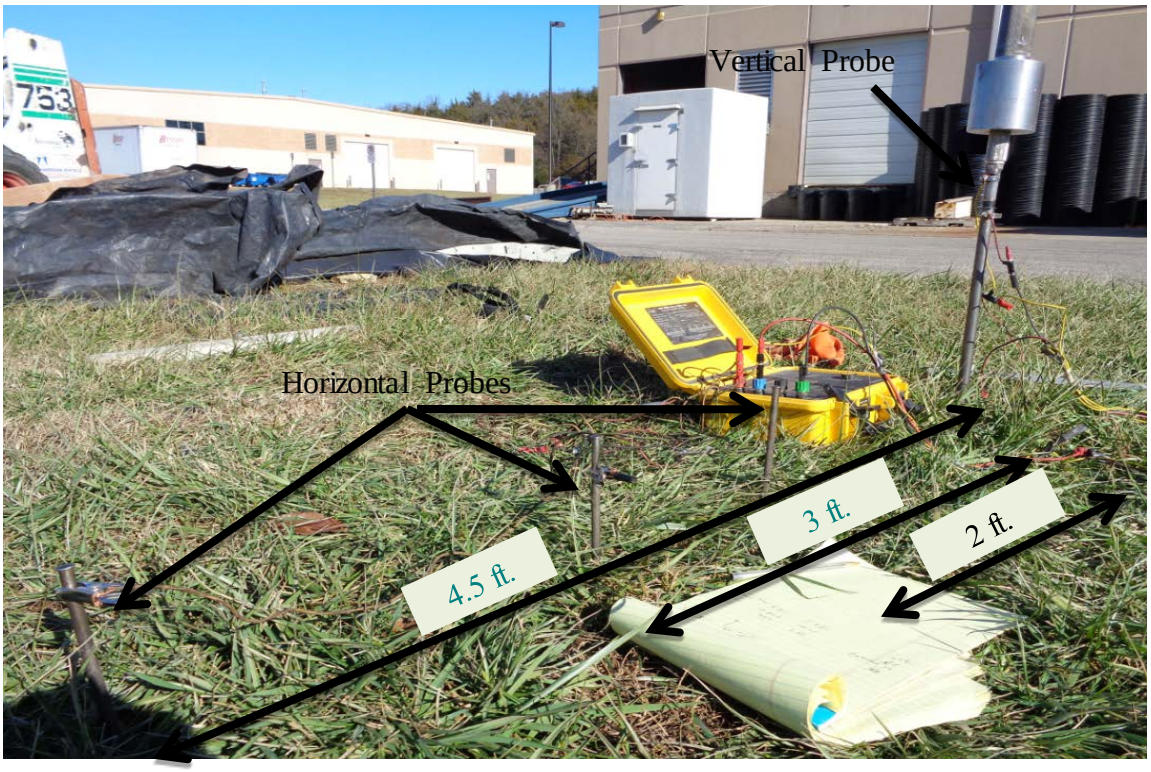

Figure 5-29 Field Setup of Horizontal versus Vertical Resistance Measurement

Table 5-7 Resistance Measurement by Horizontal and Vertical Probe Arrangements

Distance in Inches		Reading of Resistance in Ω		
Distance from reference to GS	Penetration depth of vertical probe (H)	Vertical probe	Fall of potential method, D = 3 ft.	Fall of potential method, D = 4.5 ft.
25.0	4.0	253.0	284.0	280.0
23.0	6.0	152.0	178.2	174.0
21.0	8.0	102.1	126.3	121.8
19.0	10.0	72.7	93.3	89.2
18.0	11.0	61.3	76.2	76.4
17.0	12.0	55.7	71.7	69.2
15.0	14.0	48.7	63.5	59.0
10.5	18.5	35.0	48.9	44.2

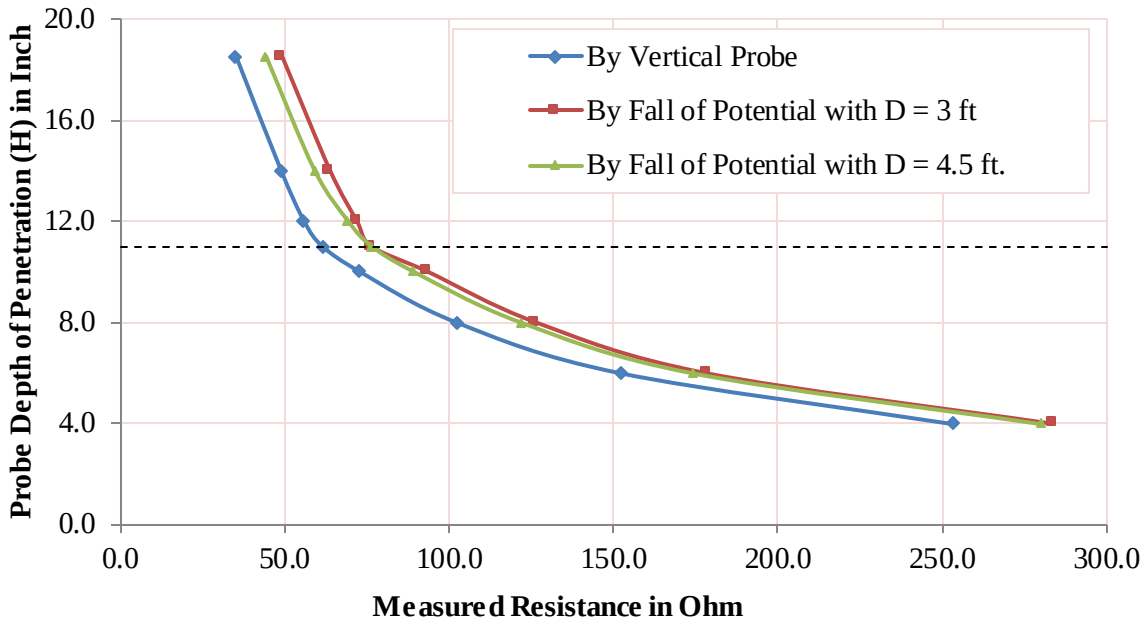

Figure 5-30 Resistance vs Depth on Subgrade Soil by Vertical and Horizontal Probes

The effective probe depth of penetration was 11 inches for the case of ballast resistance measurements at the box test. Therefore, the resistance for up to 11 inches of penetration was measured. The apparent resistance at that point was nearly identical for the fall of potential method and the vertical probe. As shown in Figure 5-30, if the rod depth is small, the resistance seems to be very large; however this result is likely to be a function of poor contact between the rod and ground. The resistance measured below the 11 inch penetration depth varies slightly.

5.6.2. Validity of Vertical Probe on Test Sample of Fouled Ballast

Tables 5.8 to 5.11 show the resistivities obtained using the Wenner 4-point Method by horizontal probe and fall of potential method by vertical probe for different fouling amounts by weight for different moisture contents on the test sample. Also, Figures 5.31 to 5.34 show comparisons of resistivity for different amounts of fouling using the Wenner 4-point Method with horizontally aligned probes and the fall of potential method measured with the vertical probe developed at KU.

Table 5-8 Comparison of Resistivity in Horizontal and Vertical Alignments at 10% Fouling

Subgrade Soil Fouled Ballast	Moisture Content	3.0%	5.3%	6.8%	8.7%	
	Wenner 4-point Method	223,500	44,700	25,100	20,000	
	Fall of Potential Method	NA	NA	37,100	16,900	
Gardner Track Ballast Dust Fouled Ballast	Moisture Content	1.6%	3.0%	4.3%	6.0%	6.5%
	Wenner 4-point Method	NA	NA	48,900	20,900	20,300
	Fall of Potential Method	NA	NA	NA	NA	26,300
Coal Dust Fouled Ballast	Moisture Content	2.3%	5.3%	7.9%		
	Wenner 4-point Method	NA	65,200	24,000		
	Fall of Potential Method	NA	55,200	32,000		

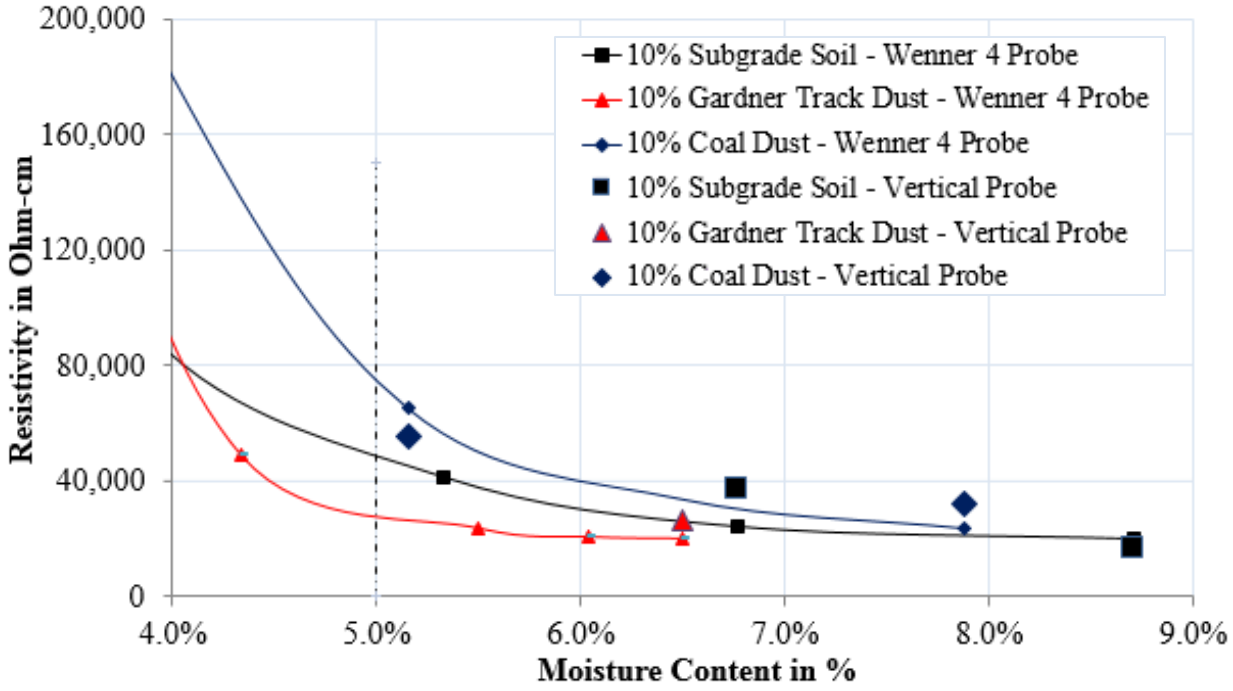

Figure 5-31 Comparison of Resistivity using Horizontal and Vertical Alignments at 10% Fouling

Table 5-9 Comparison of Resistivity in Horizontal and Vertical Alignments at 20% Fouling

Subgrade Soil Fouled Ballast	Moisture Content	2.3%	3.9%	6.3%	7.1%	8.5%
	Wenner 4-point Method	422,900	79,300	22,600	19,600	16,200
	Fall of Potential Method	NA	NA	35,300	16,200	13,600
Gardner Track Dust Fouled Ballast	Moisture Content	2.5%	4.5%	5.7%	8.6%	
	Wenner 4-point Method	274,000	33,900	21,900	17,200	
	Fall of Potential Method	NA	51,167	42,080	19,850	
Coal Dust Fouled Ballast	Moisture Content	2.1%	5.3%	7.2%	9.2%	
	Wenner 4-point Method	285,700	28,200	16,800	13,700	
	Fall of Potential Method	NA	93,500	49,600	27,800	

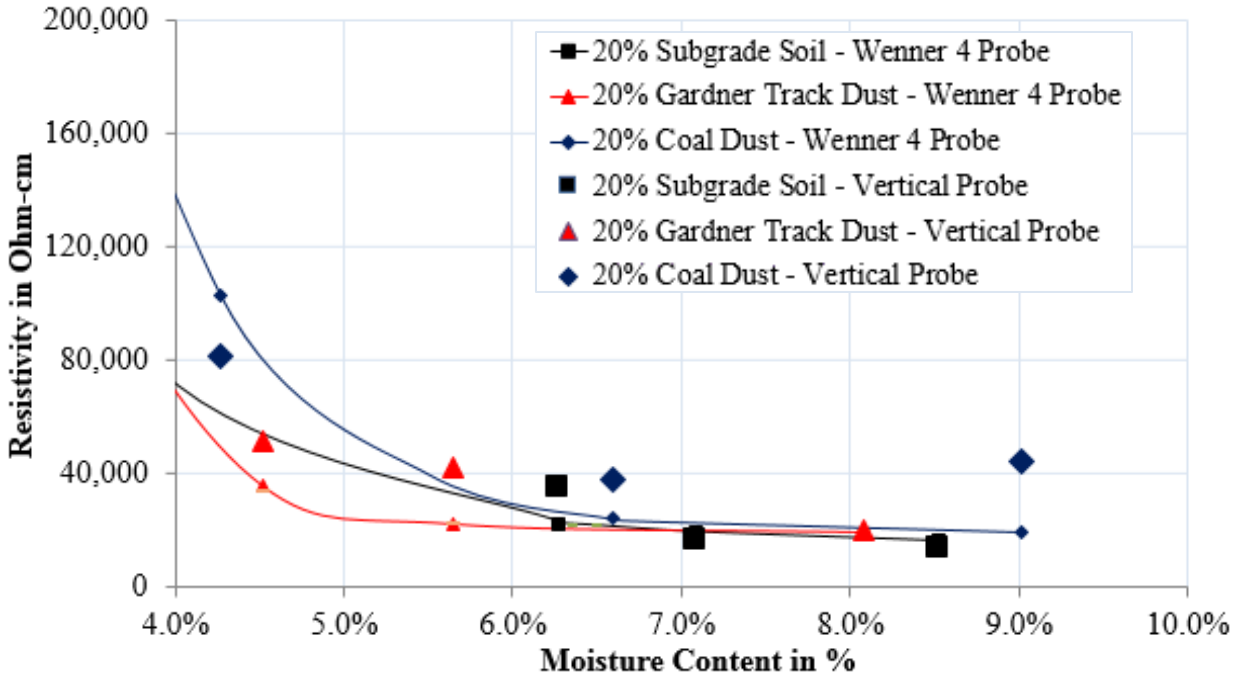

Figure 5-32 Comparison of Resistivity using Horizontal and Vertical Alignments at 20% Fouling

Table 5-10 Comparison of Resistivity in Horizontal and Vertical Alignments at 30% Fouling

Subgrade Soil Fouled Ballast	Moisture Content	2.8%	5.4%	7.2%	11.2%
	Wenner 4-pointMethod	237,800	35,400	20,500	10,100
	Fall of Potential Method	NA	33,100	23,300	13,200
Gardner Track Dust Fouled Ballast	Moisture Content	2.3%	4.0%	5.7%	8.6%
	Wenner 4-point Method	141,900	43,600	19,900	17,200
	Fall of Potential Method	NA	42,100	23,400	11,200
Coal Dust Fouled Ballast	Moisture Content	2.7%	5.3%	7.2%	9.2%
	Wenner 4-point Method	285,700	28,200	16,800	13,700
	Fall of Potential Method	NA	93,500	49,600	27,800

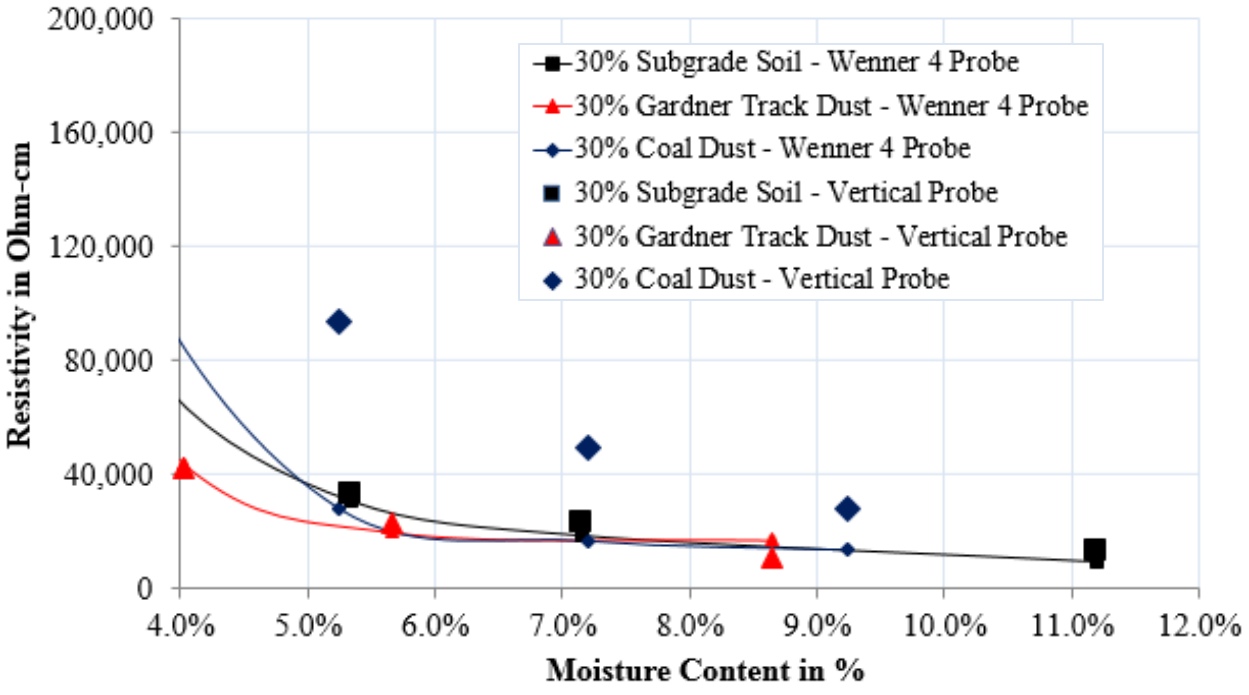

Figure 5-33 Comparison of Resistivity using Horizontal and Vertical Alignments at 30% Fouling

Table 5-11 Comparison of Resistivity in Horizontal and Vertical Alignments at 40% Fouling

Subgrade Soil Fouled Ballast	Moisture Content	3.4%	6.1%	7.7%	10.5%
	Wenner 4-point Method	199,800	32,100	16,000	8,200
	Fall of Potential Method	NA	36,800	24,600	12,600
Gardner Track Dust Fouled Ballast	Moisture Content	2.2%	5.3%	6.2%	8.5%
	Wenner 4-point Method	1-39,300	22,500	17,200	12,200
	Fall of Potential Method	NA	33,600	17,500	10,800

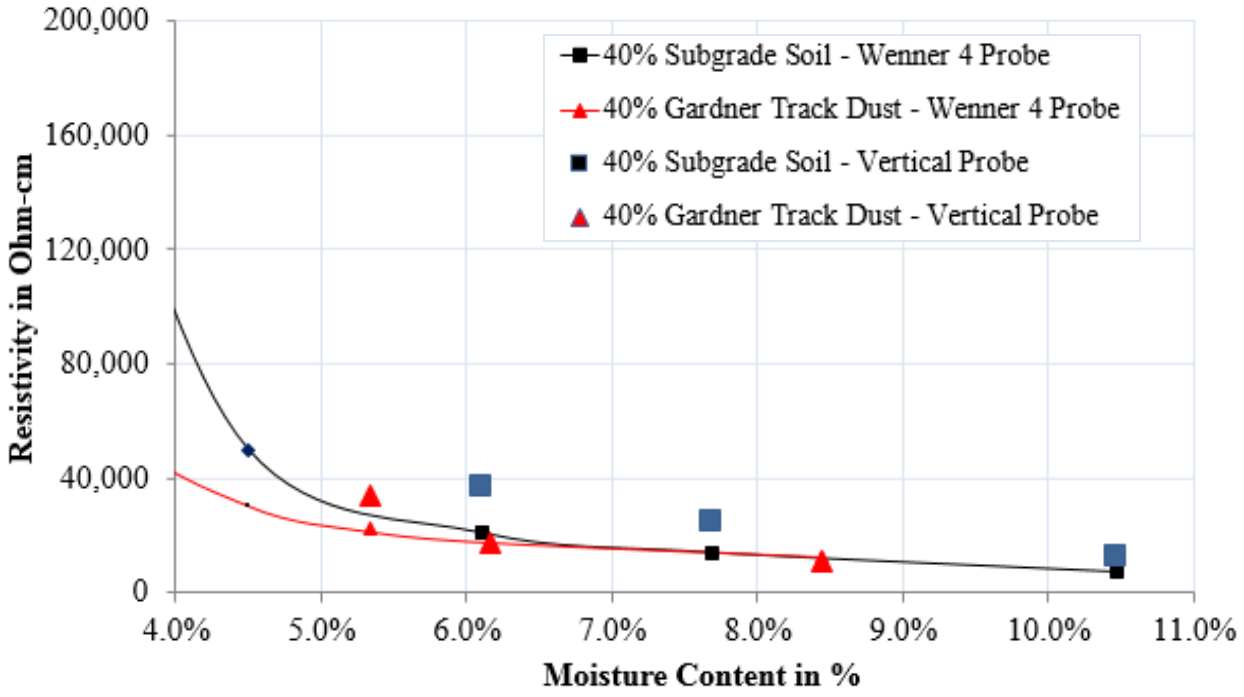

Figure 5-34 Comparison of Resistivity by Horizontal and Vertical Alignments at 40% Fouling

Most of the data on the above four graphs show that resistivity determined using the fall of potential method measured with the help of vertical probe constructed at the Geotechnical Lab at

KU is slightly higher than the resistivity measured by the Wenner 4-point Method. For coal dust fouled ballast, the resistivity is much higher compared to both the subgrade soil and Gardner track ballast dust fouled ballasts.

5.6.3. Discussion of Validity of Vertical Resistivity Tester

The resistance measured by the vertical resistivity probe (tester) constructed at KU showed almost same value for both the vertical and horizontal configuration in subgrade soil. Though it presented the apparent resistance due to its depth limitation, the resistance was reasonably consistent for both types of configuration at different penetration distances.

The resistivity result obtained from fall of potential method was compared with the resistivity data acquired using the Wenner 4 point method. Most of the resistivity data from the vertical probe were higher than the corresponding resistivity data obtained using the Wenner 4 point method. This was likely caused by insufficient contact between the vertical probe and the soil.

5.7. Variation of CBR of Ballast Due to Change in Moisture Content

5.7.1. CBR for Different Percentages of Fouling for Various Fouling Agents

Figures 5.35 to 5.37 present the trend of the CBR obtained from the DCP with various moisture contents for fouled ballast having different percentages of fouling by weight.

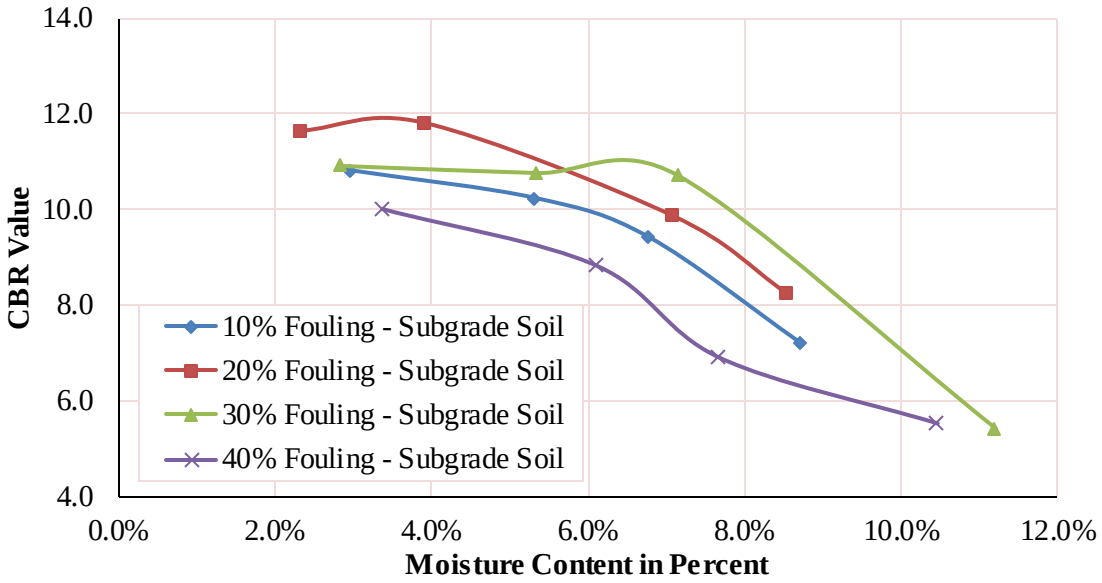

Figure 5-35 Moisture Content versus CBR for Subgrade Soil Fouled Ballast

For ballast fouled with subgrade soil, the structure was approximately stable up to a moisture content of 6% for all amounts of fouling by weight, and is referred to as "optimum moisture content for CBR (OMC_C)" of subgrade soil fouled ballast. It is approximately equal to OMCR. Above OMC_C, the CBR value decreases dramatically. The highest value of CBR for samples with up to OMC_C of subgrade soil was observed in the samples with 20% fouling. For samples with moisture content above OMC_C, the CBR was highest for those with 30% fouling. Samples with fouling of 30% or less experienced a dramatic reduction in strength for moisture contents above 6%. Subgrade soil fouled ballast with 40% fouling had a consistent reduction in strength with increasing moisture content and had the lowest value of the CBR among four percentages.

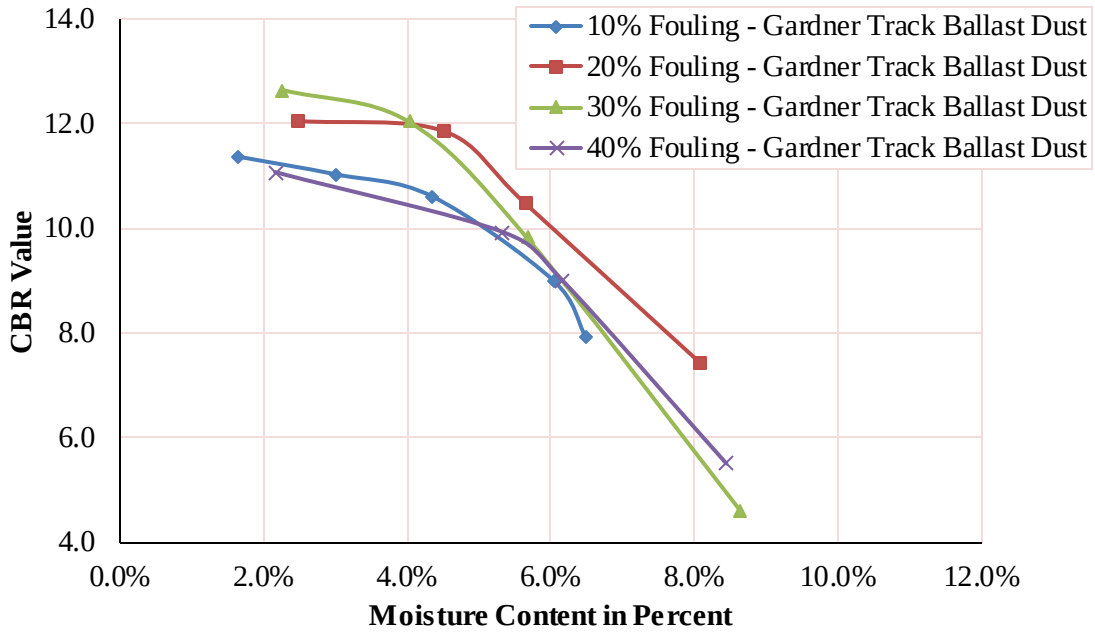

Figure 5-36 Moisture Content versus CBR for Gardner Track Dust Fouled Ballast

Ballast fouled with Gardner track ballast dust was observed to have similar moisture-strength relationships as the ballast fouled with subgrade soil. However, the CBR versus moisture content curves show that ballast shear strength declined dramatically above 5% moisture content and is referred to as "optimum moisture content for CBR (OMC_C)" of Gardner track ballast dust fouled ballast. It is approximately equal to OMCR. All Gardner track ballast dust fouled ballast samples possessed relatively high strength up to OMC_C as compared with the corresponding degree of fouling of subgrade soil fouled ballast. The CBR of all types of Gardner track ballast dust fouled ballast was in the range of 10.3 to 12. For the case of Gardner track ballast dust fouled ballast, the CBR value decreased sharply above OMC_C for all degrees of fouling, which was consistent with the subgrade fouled ballast except the critical moisture content was slightly lower. The highest value of CBR was for 30% fouling and the CBR value was almost 13. For Gardner track ballast dust fouled ballast, the CBR for 20% and 30% fouling was higher than for 10% and 40% fouling. For the case of Gardner track ballast dust fouled ballast, 10% and 40% fouling gave

almost same CBR for a definite amount of moisture content. This was a different result from what was observed for the subgrade soil fouled ballast, because the 40% subgrade soil fouled ballast had a much lower CBR than the 10% subgrade soil fouled ballast.

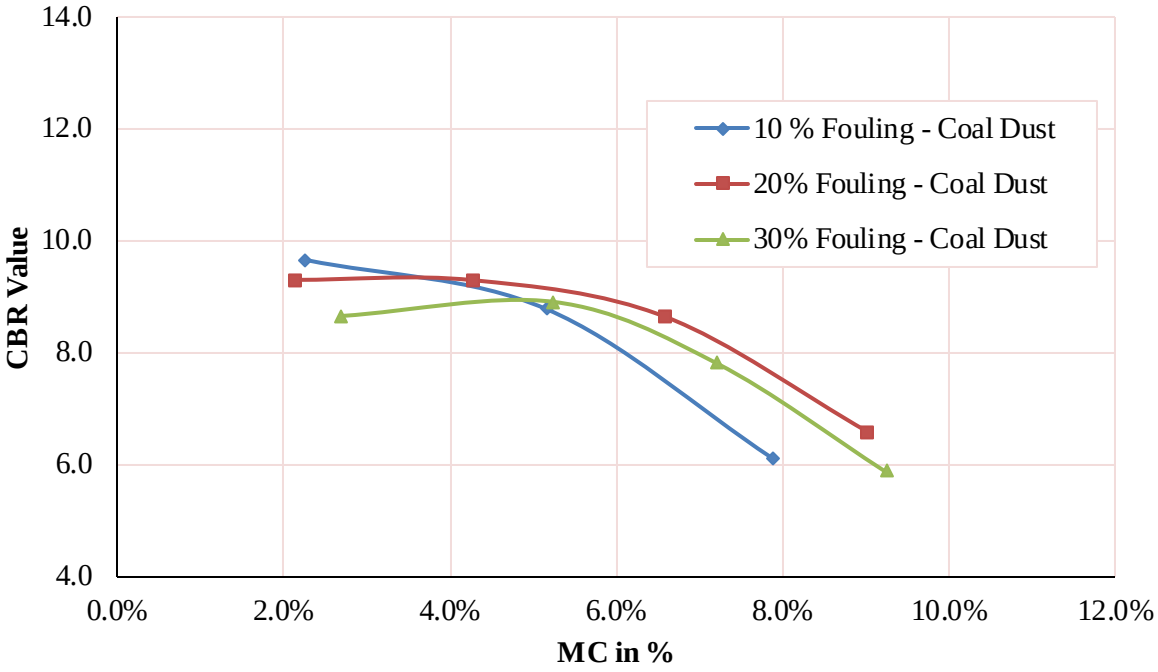

Figure 5-37 Moisture Content versus CBR for Coal Dust Fouled Ballast

Ballast fouled with coal dust showed slightly different behavior than the subgrade soil fouled ballast and the Gardner track ballast dust ballast. The CBR value of coal dust fouled ballast was less than 10 for all samples tested. The shear strength decreased for moisture contents above 5.5% and this boundary moisture content is referred to as OMC_C for coal dust fouled ballast. It is approximately equal to OMCR. However, the decline in strength with increasing moisture was not as steep as for that of the Gardner track ballast dust and the subgrade soil fouled ballast.

5.7.2. CBR Comparison of Different Fouling Agents for the Same Percentage of Fouling

Figures 5.38 to 5.41 show the comparison of CBR for the same percentage of fouling of ballast for different fouling materials. Gardner track ballast dust fouled ballast gives the higher value of

CBR for low moisture contents while ballast fouled with subgrade soil maintains a higher value of CBR for higher moisture contents. The ballast fouled with coal dust shows a lower value of CBR for all water contents and all ballast samples show reduced strength for higher moisture contents.

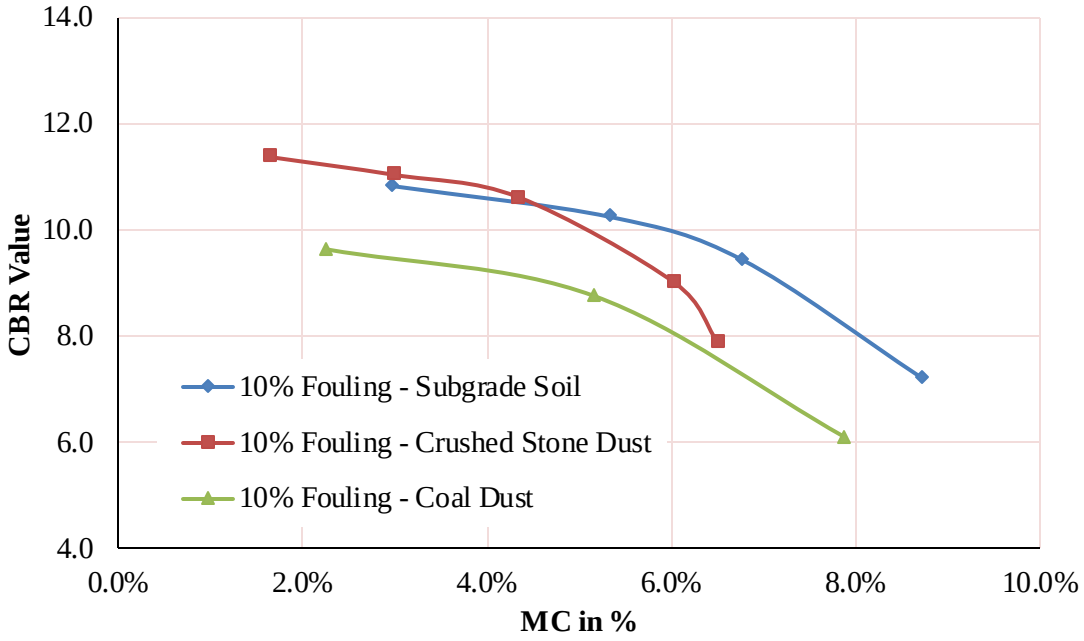

Figure 5-38 Moisture Content versus CBR at 10% Fouling with Different Fouling Agents

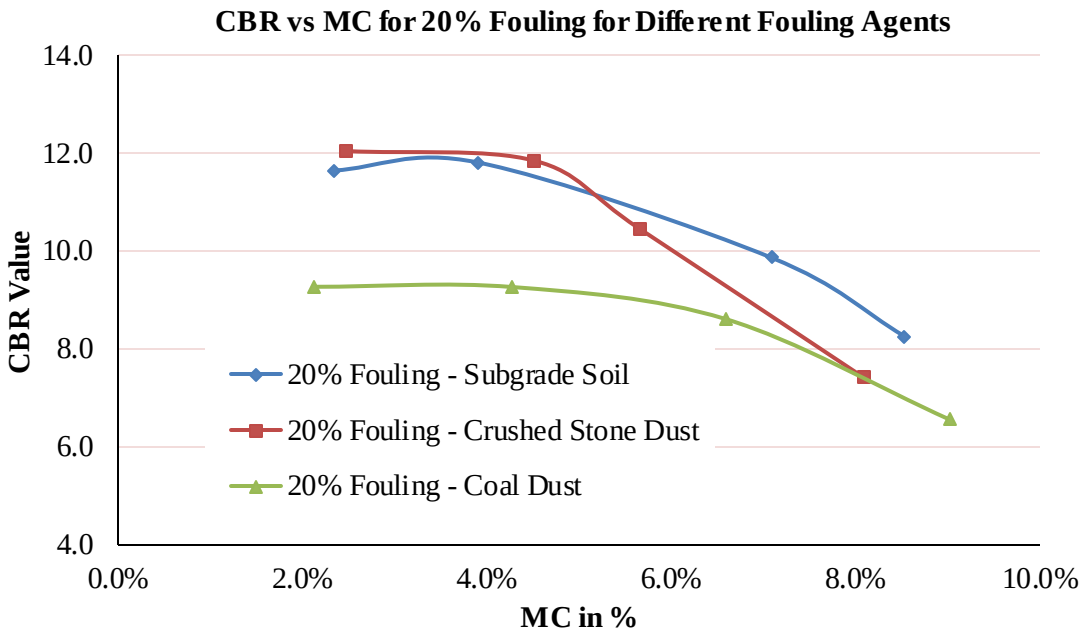

Figure 5-39 Moisture Content versus CBR at 20% Fouling with Different Fouling Agents

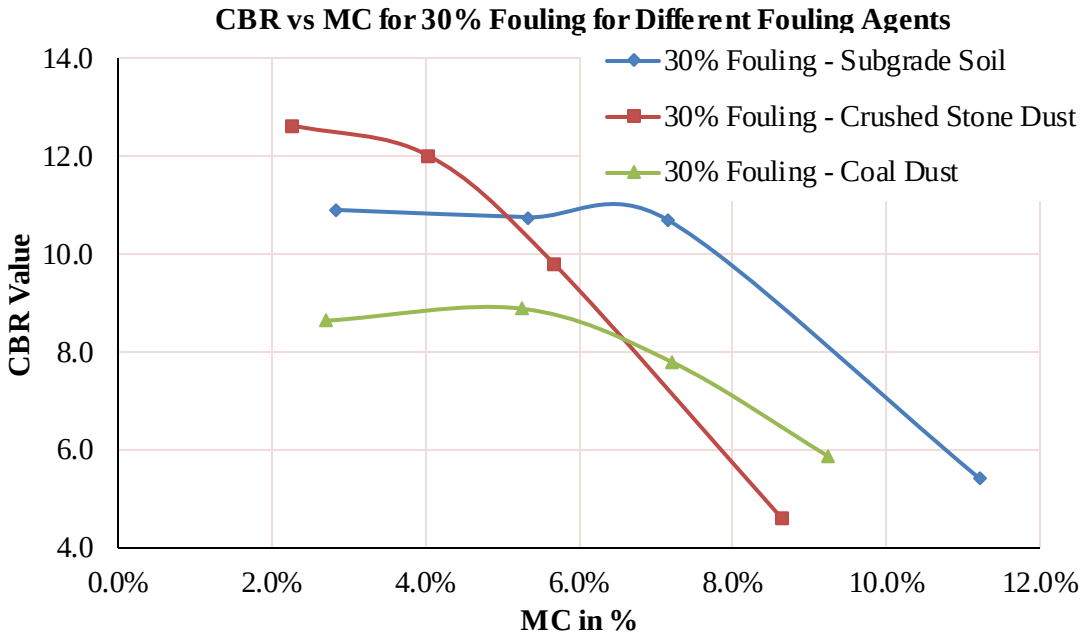

Figure 5-40 Moisture Content versus CBR at 30% Fouling with Different Fouling Agents

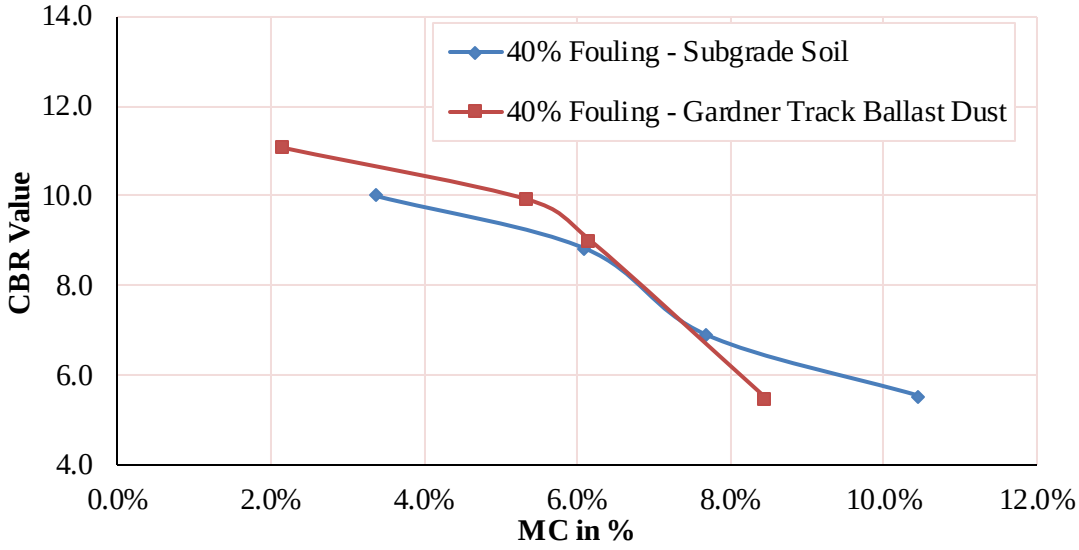

Figure 5-41 Moisture Content versus CBR at 40% Fouling with Different Fouling Agents

5.7.3. Discussion of CBR of Fouled Ballast

Fouled ballast lost a substantial percentage of its shear strength when the moisture content was higher than OMC_C. For moisture contents lower than the OMC_C the fouled ballast layer was relatively strong. This strength was highest for 20% fouling by subgrade soil, 30% fouling by Gardner track ballast dust and 10% fouling by coal dust fouled ballast. The rate of strength loss was highest for Gardner track ballast dust fouled ballast followed by subgrade soil fouled ballast and coal dust fouled ballast. Moreover, due to the lower value of OMC_C of Gardner track ballast dust fouled ballast, it experiences earlier loss of strength with increasing the moisture content when compared with the other fouling agents.

5.8. Resilient Modulus of Fouled Ballast Due to Variations of Moisture

5.8.1. Resilient Modulus for Different Percentages of Fouling for Various Fouling Agents

Figures 5.41 to 5.43 show the resilient modulus versus moisture content of fouled ballast with different fouling agents. The maximum resilient moduli of various percentages of fouling for

subgrade soil fouled ballast, Gardner track ballast dust fouled ballast, and coal dust fouled ballast are approximately 6%, 5%, and 5.5%, and these moisture contents are referred to as "optimum moisture content for resilient modulus (OMC_{MR})" and are approximately equal to OMCR values. However, exact maximum resilient modulus depends on the amount of fouling present in ballast and varies from 5% to 7% for subgrade soil fouled ballast, 4.25% to 5.75% for Gardner track ballast dust fouled ballast, and 5.25% to 6.5% for coal dust fouled ballast. The slope before reaching the maximum resilient modulus is mild while the slope after this point is very steep. If the percentage of fouling materials increases, the maximum resilient modulus moves to the right. The magnitude of the resilient modulus varies with each type of fouling.

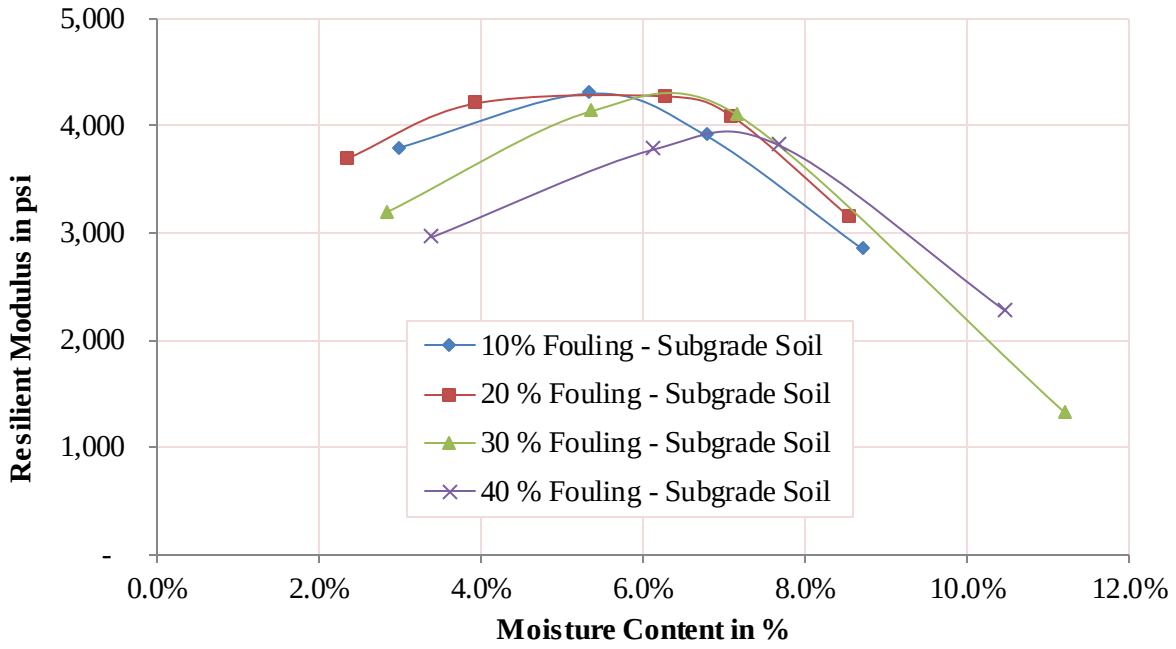

Figure 5-42 Resilient Modulus vs MC for Subgrade Soil Fouled Ballast

Figure 5.42 shows that for low moisture contents the maximum value of resilient modulus was measured at 20% fouling, successively followed by 10% fouling and 30% fouling by weight. The samples with 40% fouling by weight had the lowest maximum resilient modulus. Modulus values were similar at high moisture contents for all amounts of fouling present in the ballast.

Also, for the test of clean ballast, the resilient modulus was found to be very low (approximately 2500 psi) when compared with the maximum resilient modulus for 20% fouling (around 4300 psi). For Gardner track ballast dust fouled ballast and coal dust fouled ballast, moduli decreased with fouling for low moisture contents and were similar at high moisture contents.

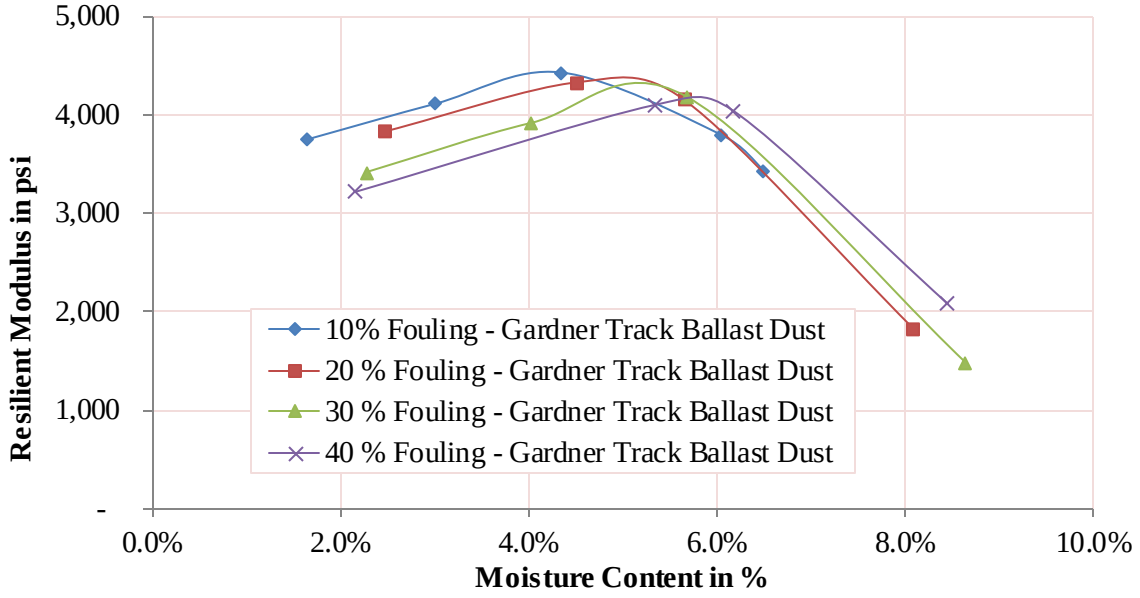

Figure 5-43 Resilient Modulus vs MC for Gardner Track Dust Fouled Ballast

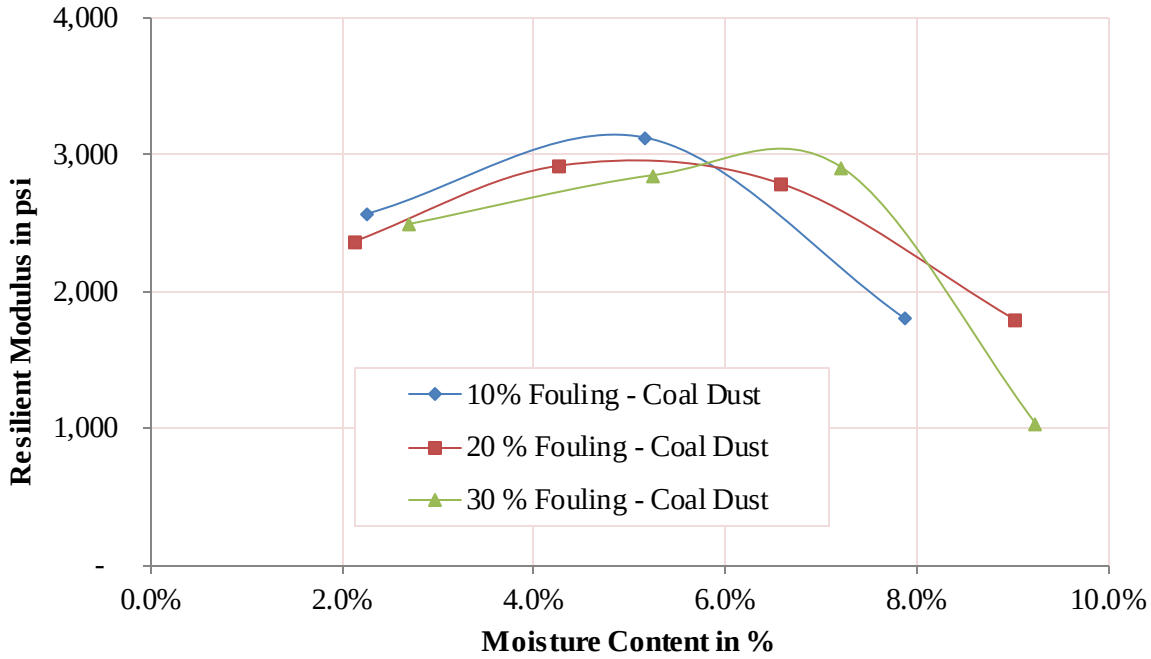

Figure 5-44 Resilient Modulus vs MC for Coal Dust Fouled Ballast

5.8.2. Resilient Modulus Comparison of Various Fouled Ballasts

Figures 5.45 to 5.48 show trends in the resilient modulus versus moisture content for different fouling agents for the same amounts of fouling materials. For all types of fouling the Gardner track ballast dust fouled ballast showed the highest resilient modulus when compared to the other two types of fouling. Also, the maximum resilient modulus of subgrade soil fouled ballast was slightly lower than the resilient modulus of Gardner track ballast dust fouled ballast. However, the maximum modulus of coal dust fouled ballast was significantly lower than the other two types of fouled ballast.

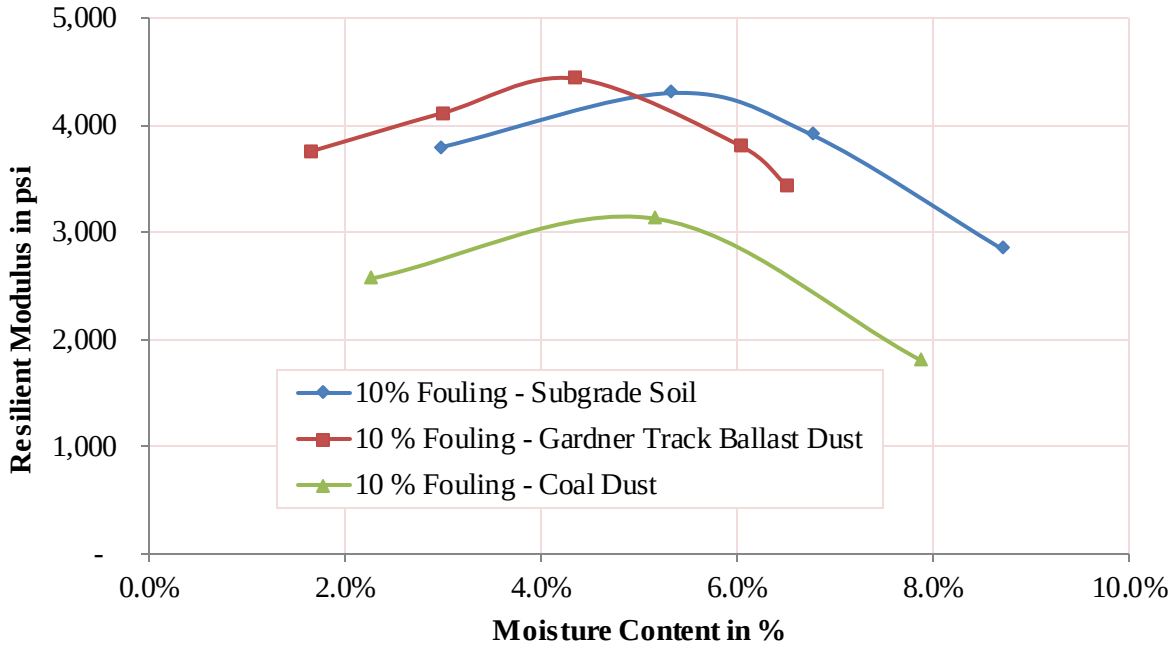

Figure 5-45 Resilient Modulus vs MC for 10% Fouling for Fouled Ballast with Different Agents

Figures 5.45 to 5.48 show that the water content corresponding to the maximum resilient modulus varied depending on the type of fouling. This specific value of water content corresponded closely to the OMC_{MR}. The modulus of the Gardner track ballast dust fouled

ballast decreased more quickly with increasing moisture content above the OMC_{MR} than the moduli for the subgrade soil fouled ballast and coal dust fouled ballast.

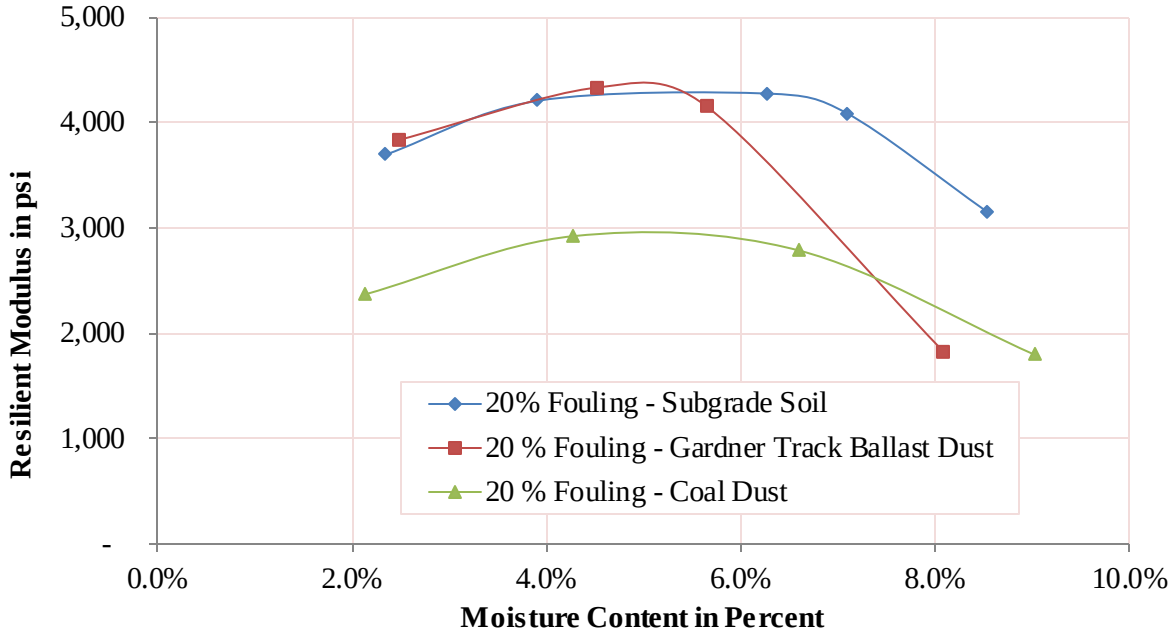

Figure 5-46 Resilient Modulus vs MC for 20% Fouling for Fouled Ballast with Different Agents

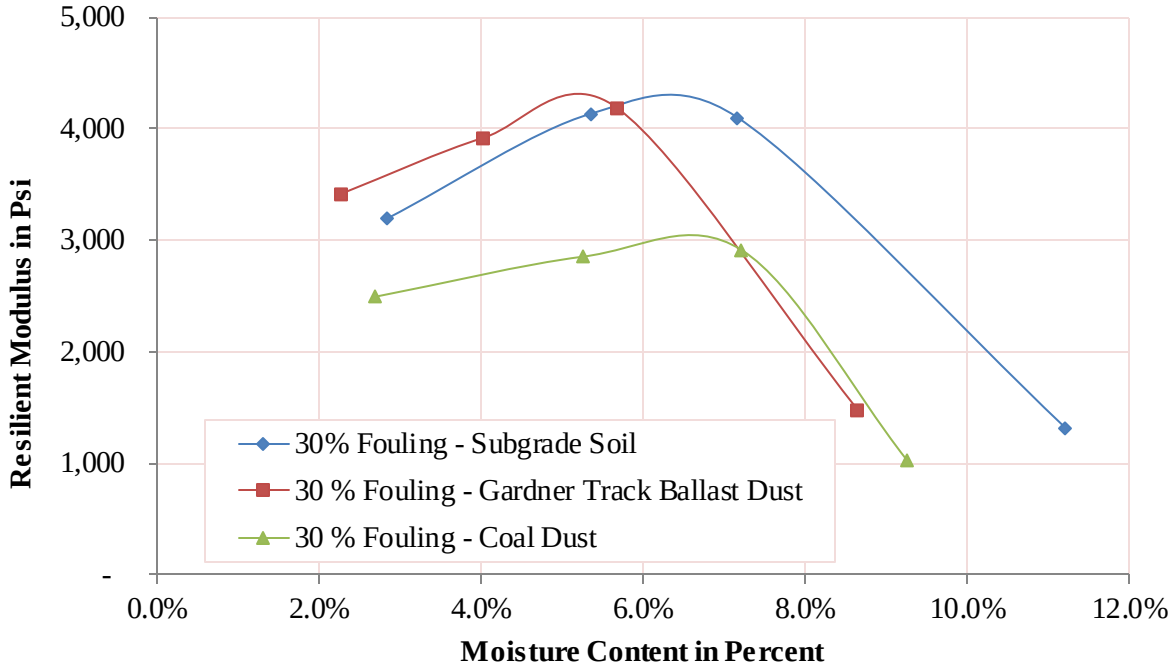

Figure 5-47 Resilient Modulus vs MC for 30% Fouling for Fouled Ballast with Different Agents

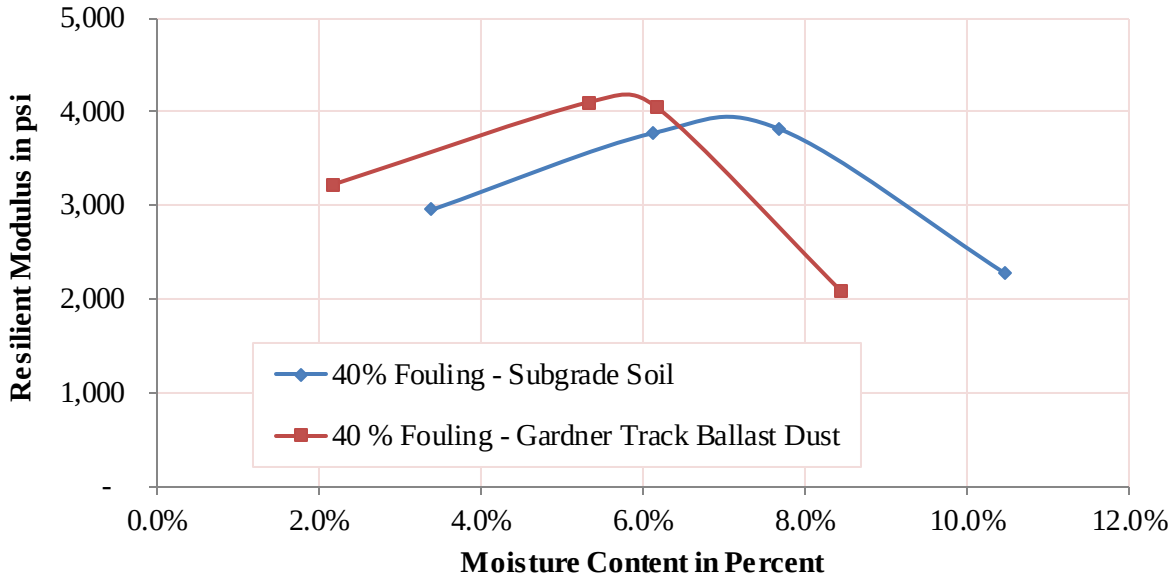

Figure 5-48 Resilient Modulus vs MC for 40% Fouling for Fouled Ballast with Different Agents

5.8.3. Discussion of Resilient Modulus versus Moisture Content

The Resilient moduli behavior was similar to that for CBR for moisture contents greater than OMC_{MR}. Fouled ballast resilient modulus declined significantly when the moisture content was higher than OMC_{MR}. However, unlike CBR, the resilient moduli of fouled ballast with moisture contents lower than OMC_{MR} were also low. So, there was a peak value of resilient modulus of fouled ballast at OMC_{MR}. This maximum value of resilient modulus at OMC_{MR} is termed as "Maximum Resilient Modulus of Fouled ballast ($M_{R\text{-}max\ (FB)}$)". It varied depending on types of fouling and amount of fouling. The increasing slopes of the resilient modului versus moisture content graph were mild for lower moisture contents whereas the decreasing slopes on the same graph for higher moisture contents were steep.

For subgrade soil fouled ballast, $M_{Rmax\ (FB)}$ occurred at a maximum of 20% fouling by weight. $M_{R\text{-}max\ (FB)}$ was highest for 20% fouling by subgrade soil, 30% fouling by Gardner track ballast dust and 10% fouling by coal dust fouled ballast. The rate of resilient modulus loss was highest

for Gardner track ballast dust fouled ballast, followed by subgrade soil fouled ballast and coal dust fouled ballast.

5.9. Static Modulus of Fouled Ballast Relationship with Moisture Content

Unit load versus deflection results obtained from small box plate loading tests were plotted for different moisture contents for different amounts of fouling. The results show that the static modulus (E_s) and hence the stiffness (k) peak at average values of 5% to 6% moisture content, depending on the amount of fouling agents and the type of fouling. The moisture content at this peak is referred to as "optimum moisture content for static modulus (OMC_{MS}) for fouled ballast" and is approximately equal to OMCR. The Elastic modulus (and also the stiffness) for water contents lower than OMC_{MS} is somewhat lower than the peak value but is much lower for moisture contents higher than OMC_{MS}.

5.9.1. Variation of Static Modulus with Moisture Content for Subgrade Soil

Figures 5.49 to 5.52 show the unit load versus deflection curves for 10%, 20%, 30%, and 40% fouling, respectively.

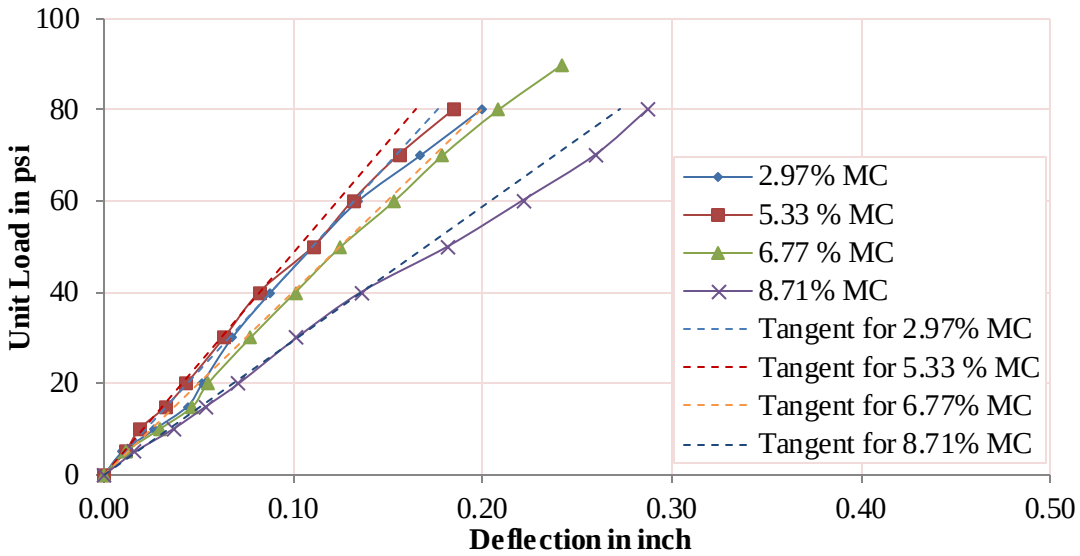

Figure 5-49 Unit Load versus Deflection Curve of 10% Fouled by Subgrade Soil at Various MC

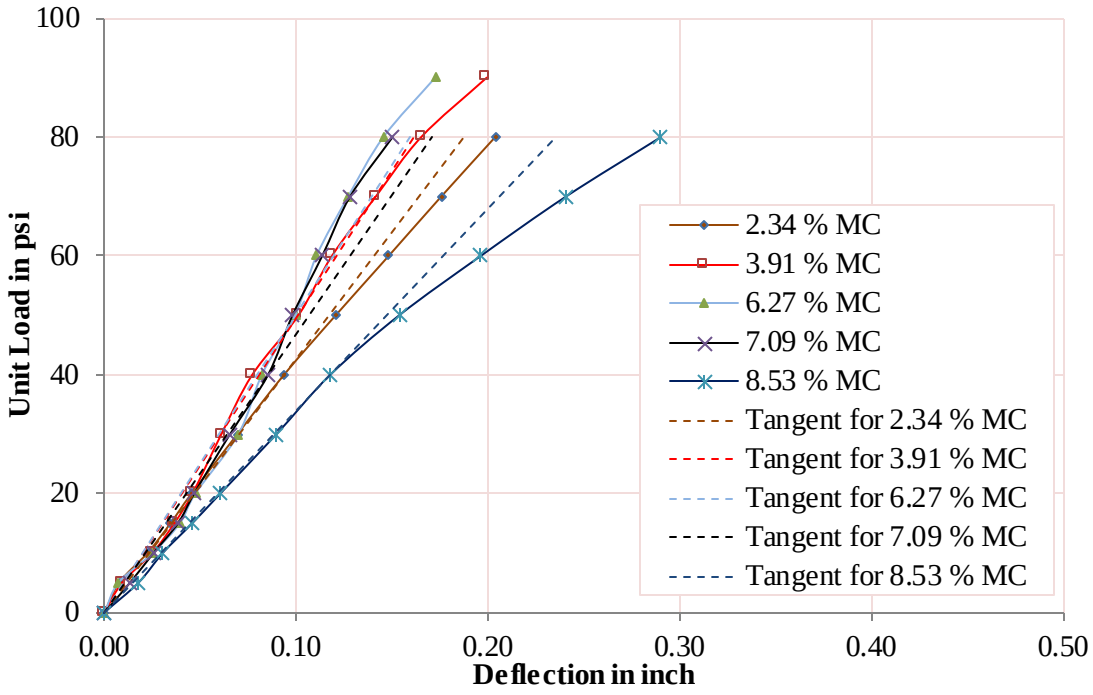

Figure 5-50 Unit Load versus Deflection Curve of 20% Fouled by Subgrade Soil at Various MC

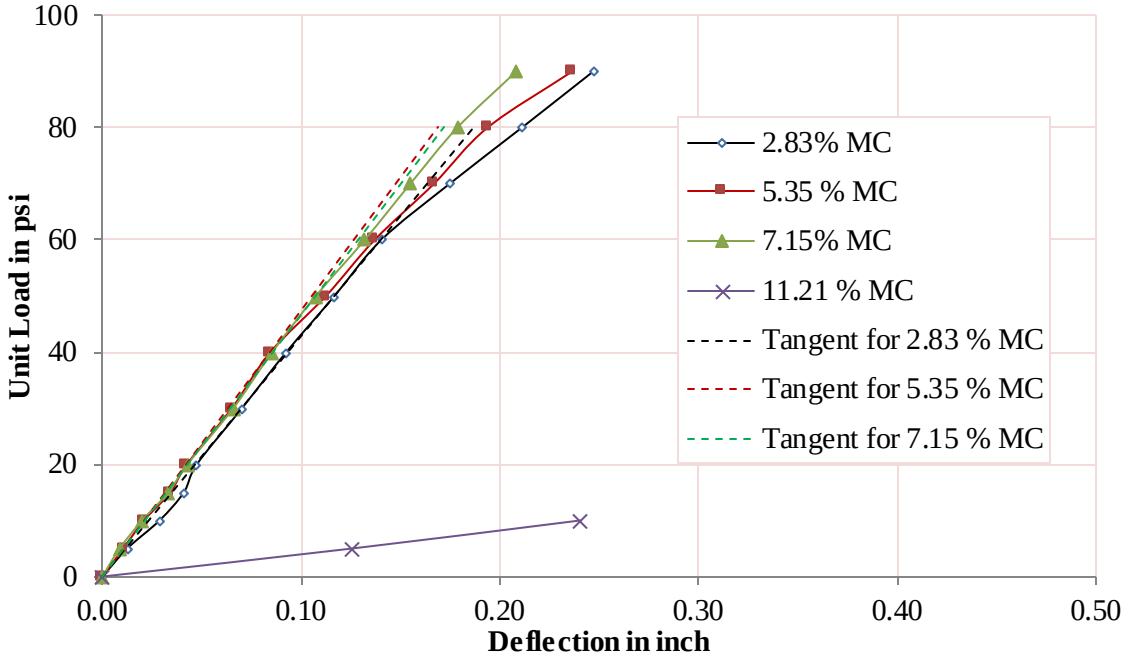

Figure 5-51 Unit Load versus Deflection Curve of 30% Fouled by Subgrade Soil at Various MC

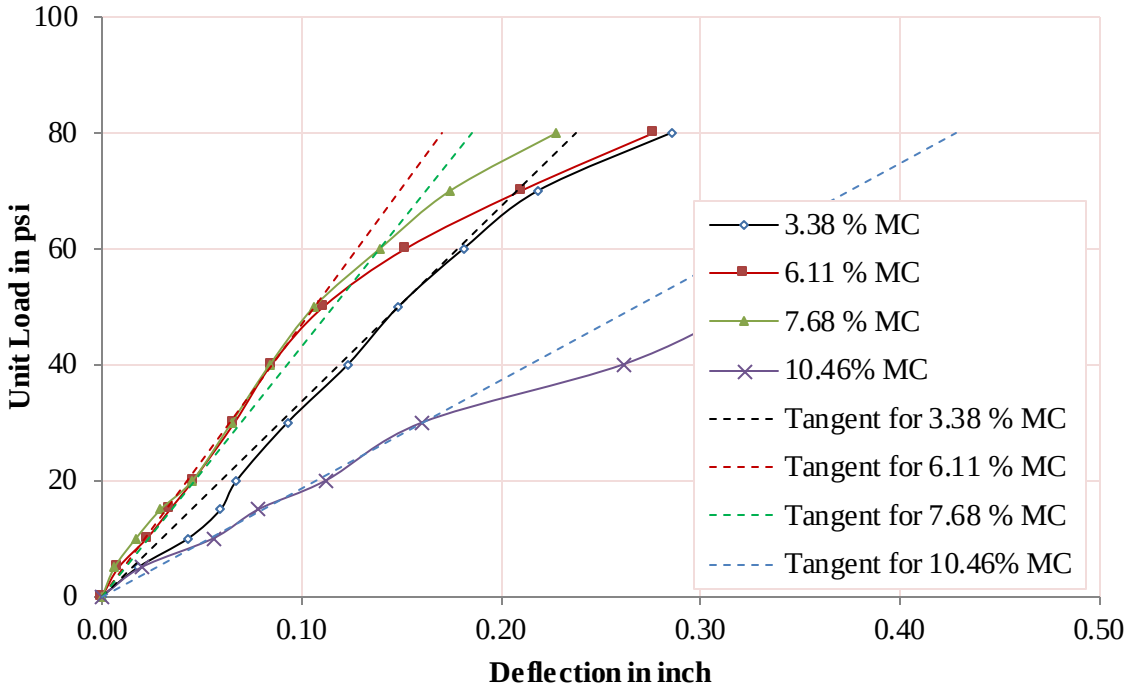

Figure 5-52 Unit Load versus Deflection Curve of 40% Fouled by Subgrade Soil at Various MC

The subgrade reactions of the subgrade soil fouled ballast for different moisture contents are tabulated in Table 5.12, and the corresponding chart is plotted in Figure 5.53:

Table 5-12 Stiffness of Subgrade Fouled Ballast with Various Moisture Contents

Level of Fouling	Items	Sample 1	Sample 2	Sample 3	Sample 4	Sample 5
10% Fouling	Moisture Content	3.0%	5.3%	6.8%	8.7%	
	Stiffness (psi/in)	454	423	486	294	
20% Fouling	Moisture Content	2.3%	3.9%	6.3%	7.1%	8.5%
	Stiffness (psi/in)	427	494	503	469	340
30% Fouling	Moisture Content	2.8%	5.4%	7.2%	11.2%	
	Stiffness (psi/in)	428	473	466	42	
40% Fouling	Moisture Content	3.4%	6.1%	7.7%	10.5%	
	Stiffness (psi/in)	404	471	431	187	

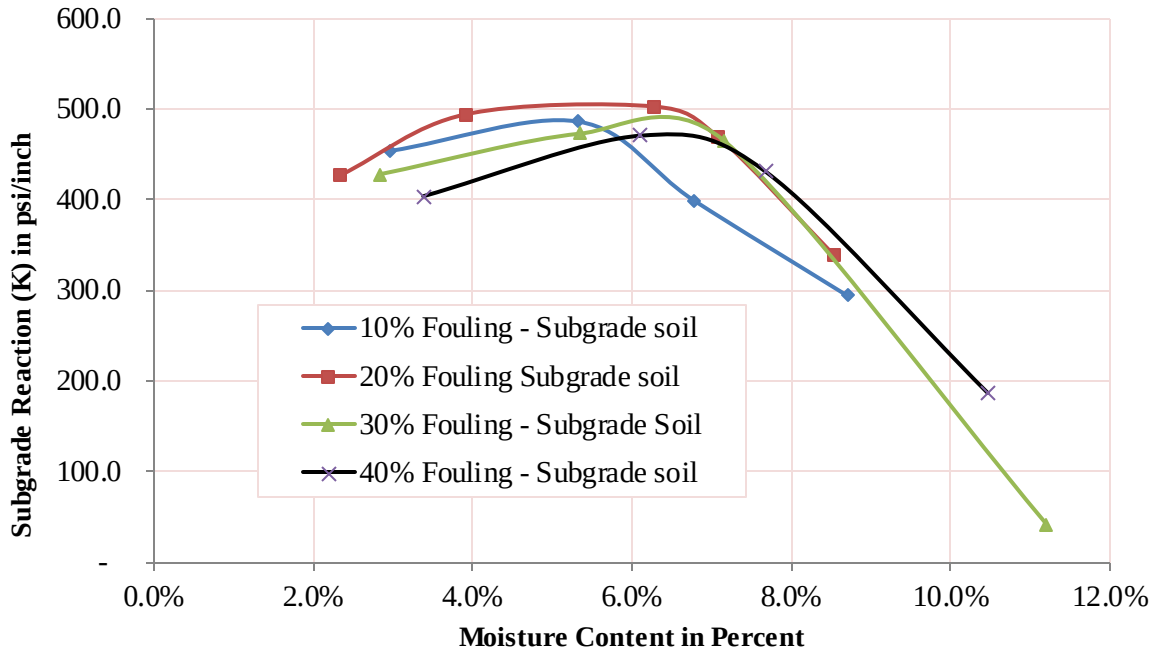

Figure 5-53 Stiffness of Subgrade Fouled Ballast with Various Moisture Contents

The static modulus was calculated based on the initial slope of the load deflection curve. Figure 5.54 depicts the static modulus at different moisture contents for subgrade soil fouled ballast.

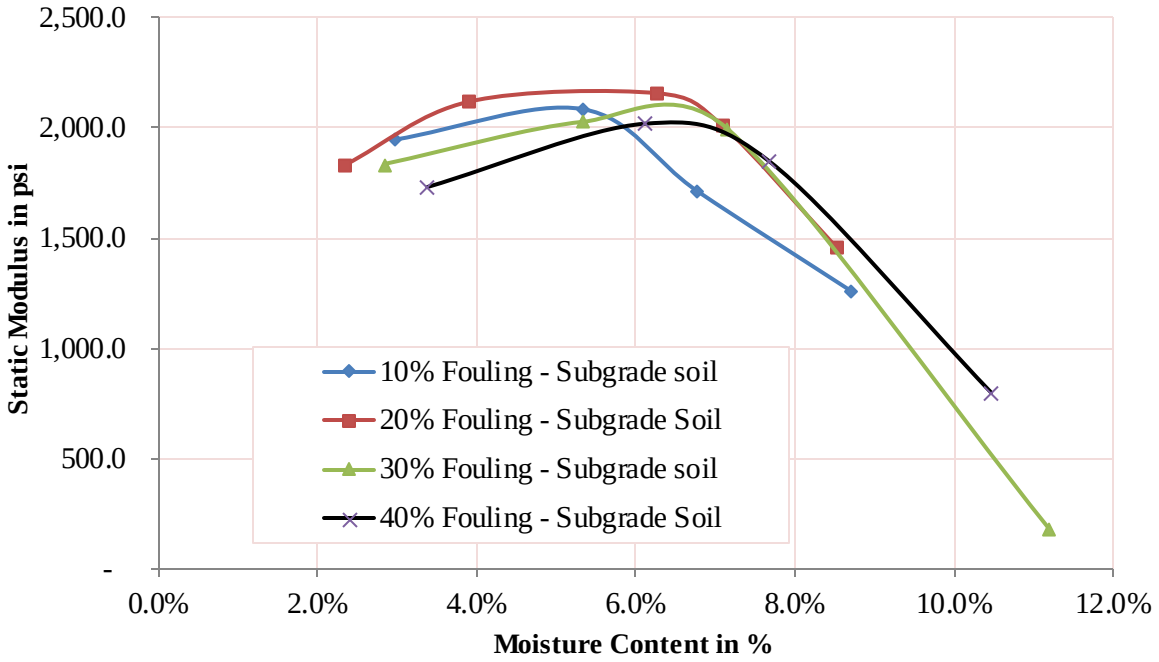

Figure 5-54 Static Modulus of Subgrade Fouled Ballast with Various Moisture Contents

For lower moisture contents the static modulus was slightly higher for 20% fouling with subgrade soil, followed by 10%, 30%, and 40% fouling. For higher moisture contents the static modulus did not vary much for a given moisture content. Also, the moisture content corresponding to the maximum value of the static modulus (OMC_{MS}) was observed to increase slightly as the amount of fouling increased. The maximum values of the static modulus for 10%, 20%, 30%, and 40% fouling by subgrade soil were estimated to be 2080, 2360, 2130 and 2035 psi at moisture contents of 5.60%, 6.25%, 6.30% and 6.40%, respectively. So, the average value of moisture content corresponding to the maximum static modulus is considered to be 6% (between maximum and minimum) and represents the OMC_{MS}.

5.9.2. Variation of Static Modulus with Moisture Content for Gardner Track Ballast Dust

Figures 5.55 to 5.58 present the load per unit area in psi versus the settlement for Gardner track ballast dust fouled ballast with different percentages of fouling material.

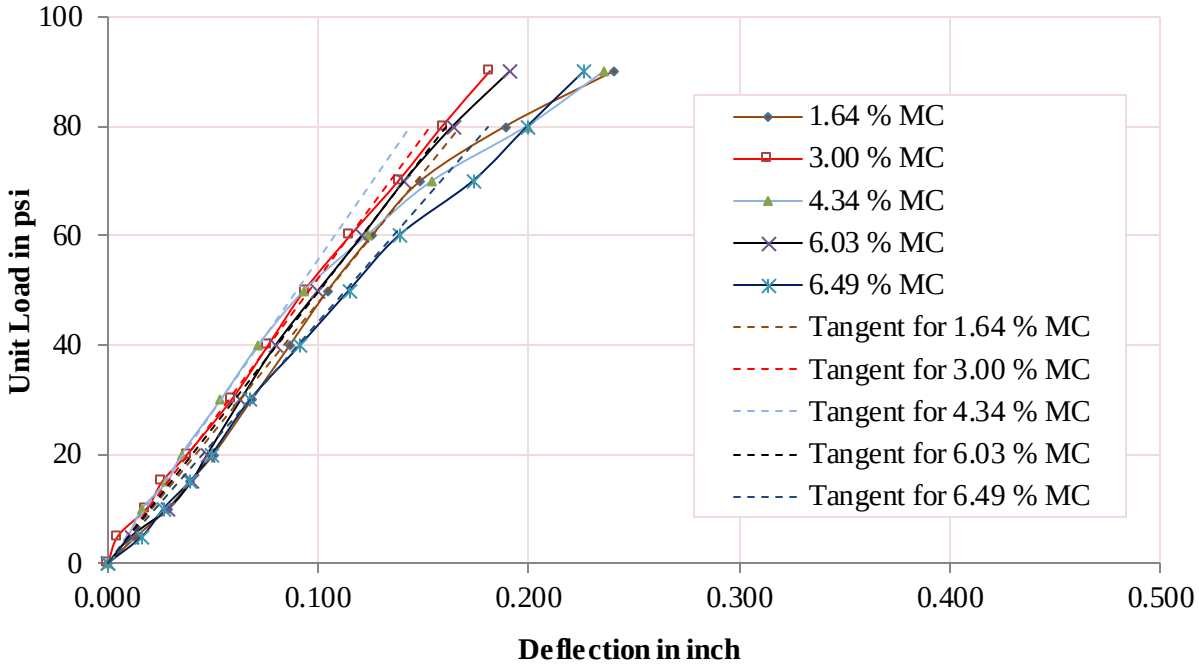

Figure 5-55 Unit Load versus Deflection Curve of 10% Fouled by Gardner Track Dust

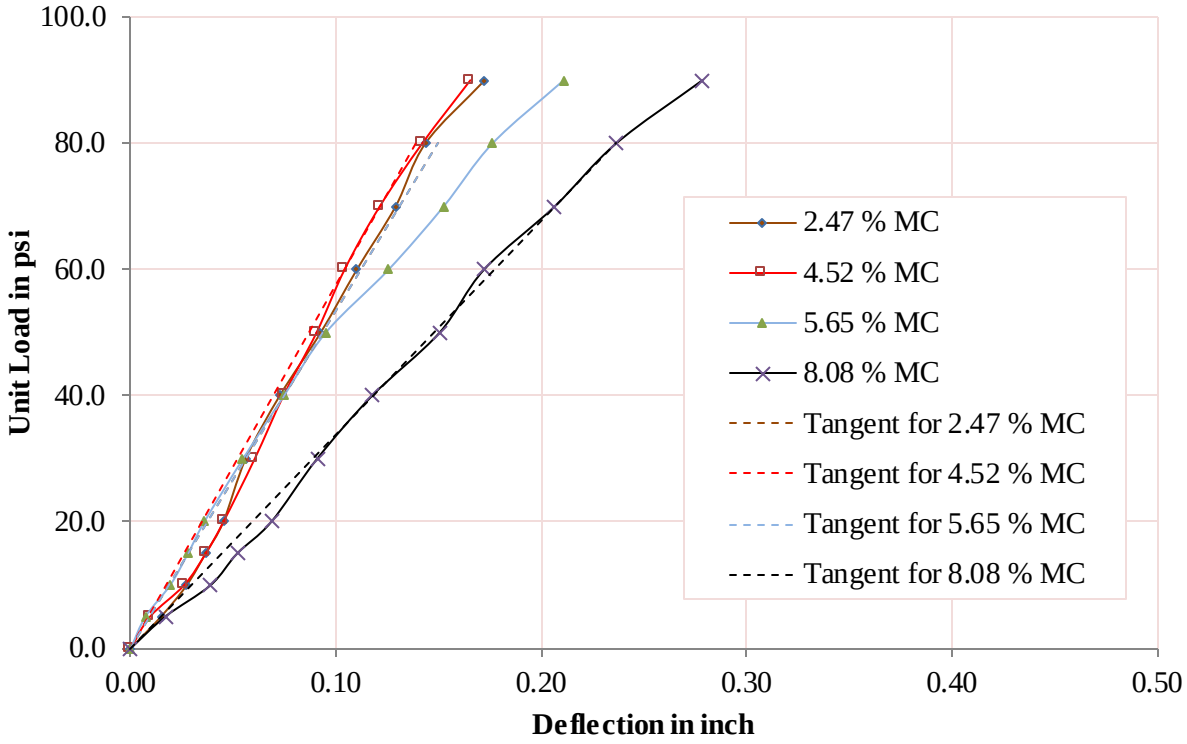

Figure 5-56 Unit Load versus Deflection Curve of 20% Fouled by Gardner Track Dust

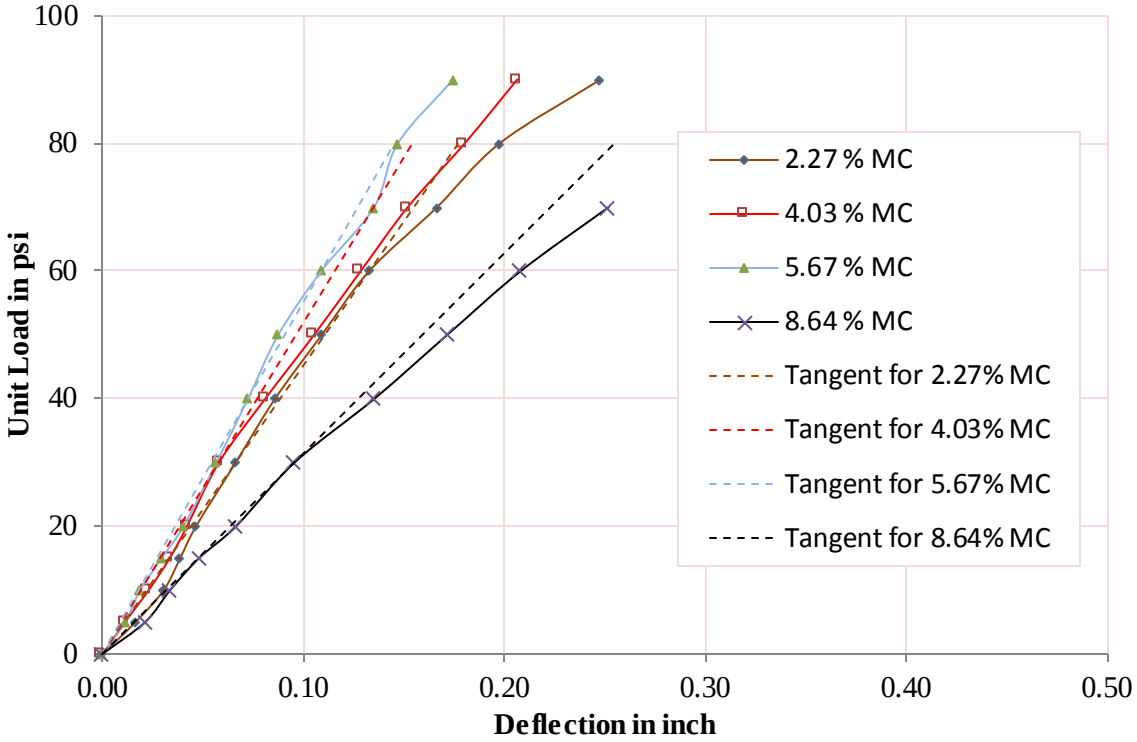

Figure 5-57 Load versus Deflection Curve of 30% Fouled by Gardner Track Dust

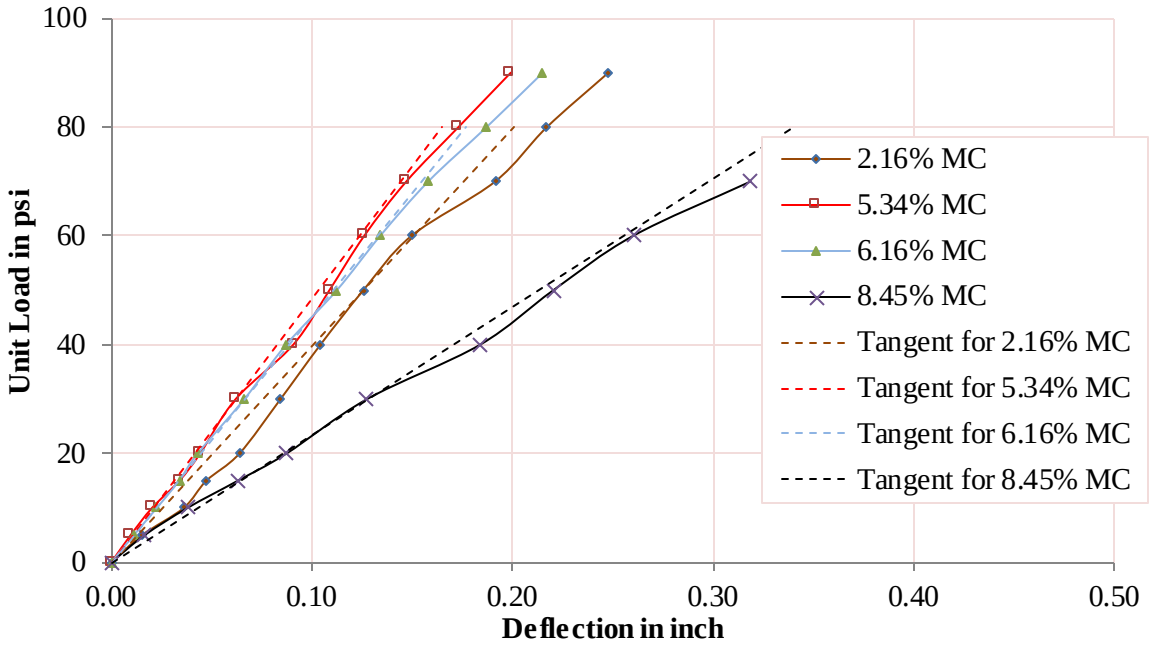

Figure 5-58 Unit Load versus Deflection Curve of 40% Fouled by Gardner Track Dust

The subgrade reactions of the Gardner track ballast dust fouled ballast for different moisture contents are tabulated in Table 5.13, and the corresponding chart is plotted in Figure 5.59:

Table 5-13 Stiffness of Gardner Track Dust Fouled Ballast with Various Moisture Contents

Fouling Level	Items	Sample 1	Sample 2	Sample 3	Sample 4	Sample 5
10% Fouling	Moisture Content	1.6%	3.0%	4.3%	6.0%	6.5%
	subgrade reaction (psi/in)	478	522	558	498	435
20% Fouling	Moisture Content	2.5%	4.5%	5.7%	8.1%	
	subgrade reaction (psi/in)	536	576	536	339	
30% Fouling	Moisture Content	2.3%	4.0%	5.7%	8.6%	
	subgrade reaction (psi/in)	452	519	553	314	
40% Fouling	Moisture Content	2.2%	5.3%	6.2%	8.5%	
	subgrade reaction (psi/in)	398	484	453	236	

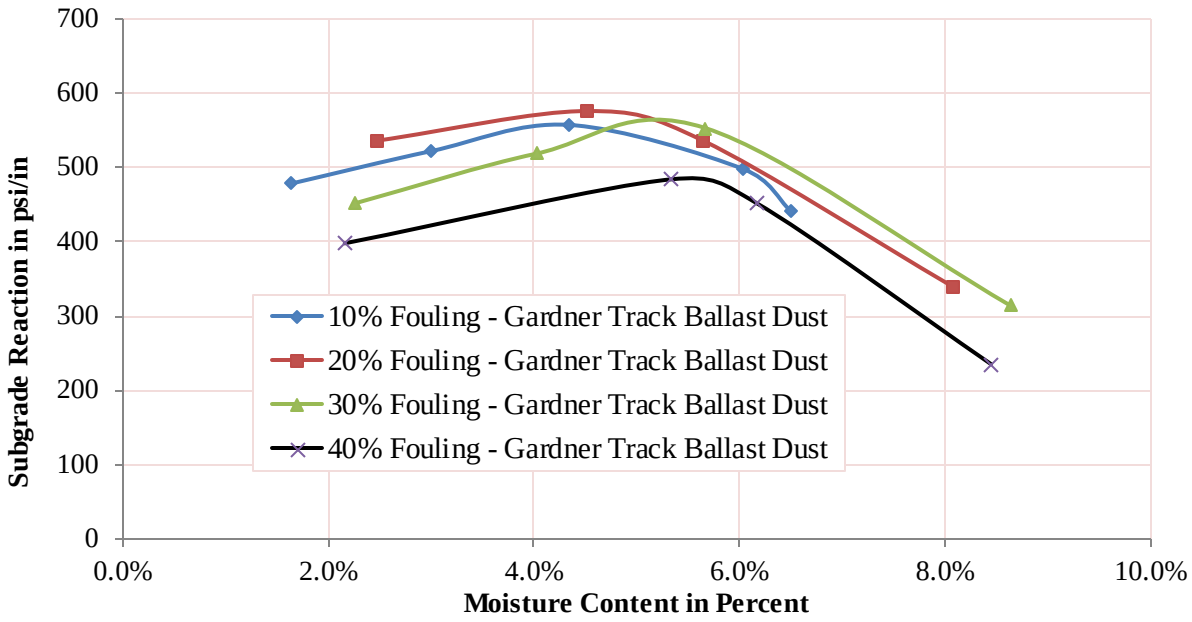

Figure 5-59 Stiffness of Gardner Track Dust Fouled Ballast with Various Moisture Contents

Figure 5.60 represents the static modulus at different moisture contents for Gardner track ballast dust fouled ballast at different degrees of fouling.

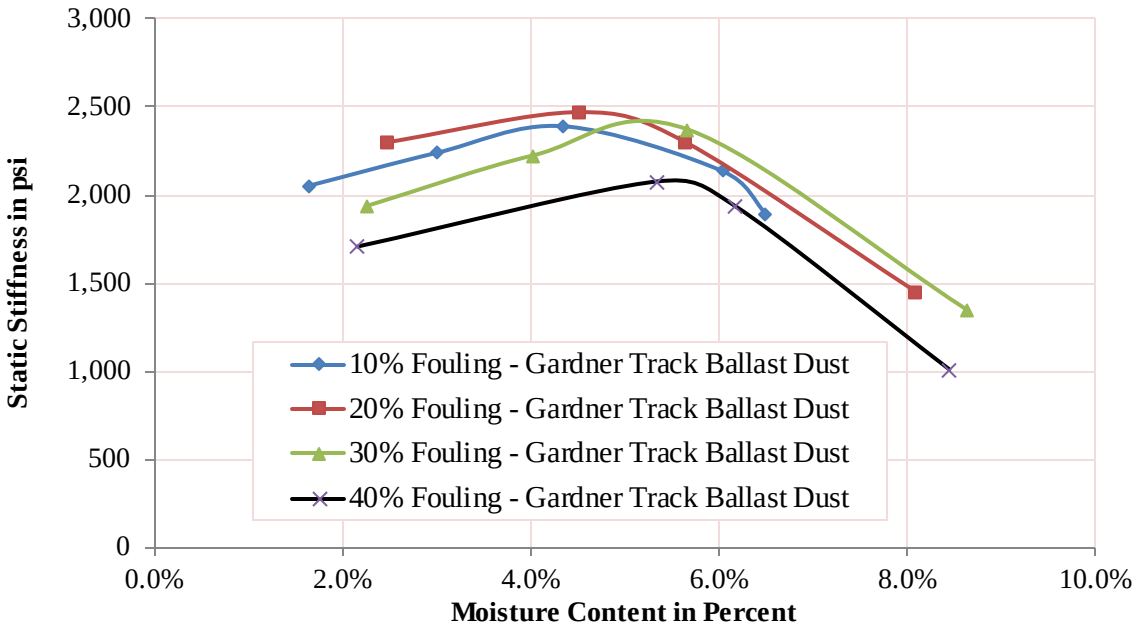

Figure 5-60 Static Modulus of Gardner Track Ballast Dust Fouled Ballast

For low moisture contents the static modulus for Gardner track ballast dust fouled ballast is highest for the samples with 20% fouling, followed by samples with 10%, 30%, and 40% fouling. For higher moisture contents the moduli are closer and the order is changed, with the 30% fouled samples having the highest modulus followed by samples with 20%, 10%, and 40% fouling. Similar to the ballast fouled with subgrade soil, the optimum value of each ratio of fouling can be found for different moisture contents, and shifts from lower to higher with increasing moisture content. The optimum values of static modulus (OMC_{MS}) for 10%, 20%, 30% and 40% fouling by Gardner track ballast dust were found to be 2390, 2470, 2455, and 2080 psi at 4.25%, 4.55%, 5.30% and 5.50% moisture contents, respectively. The average value of the moisture content for the maximum value of the static modulus is about 5%, and hence it is termed as OMC_{MS} for Gardner track ballast dust fouled ballast.

5.9.3. Variation of Static Modulus with Moisture Content for Coal Dust

Figures 5.61 to 5.63 present the load per unit area in psi versus the settlement in inches for different percentages of coal dust fouled ballast.

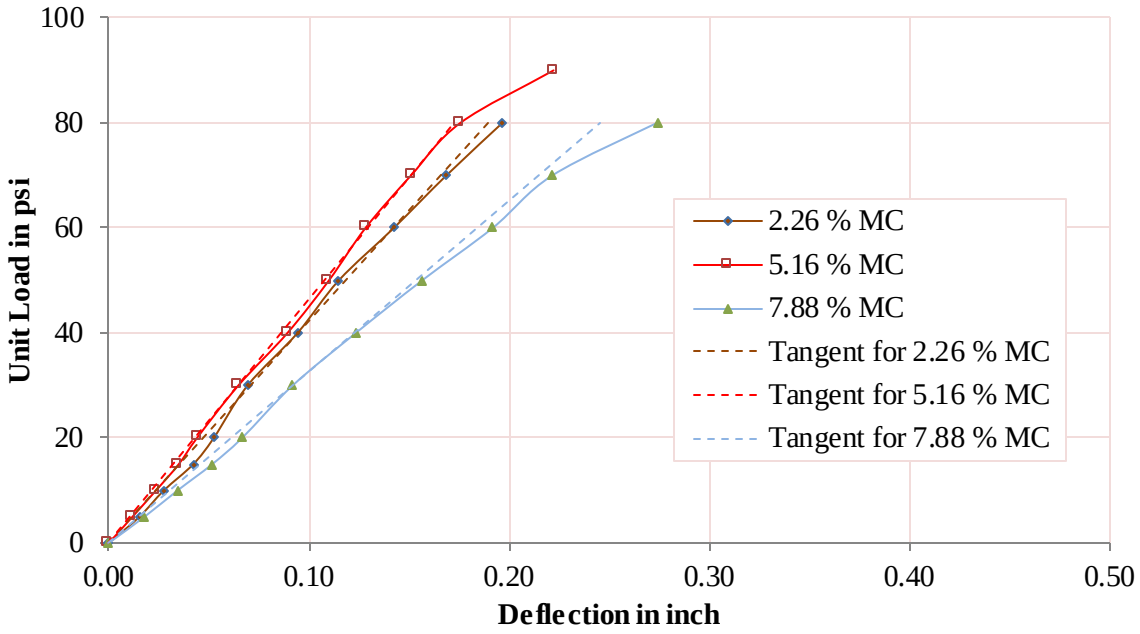

Figure 5-61 Unit Load versus Deflection Curve of 10% Fouled Ballast by Coal Dust

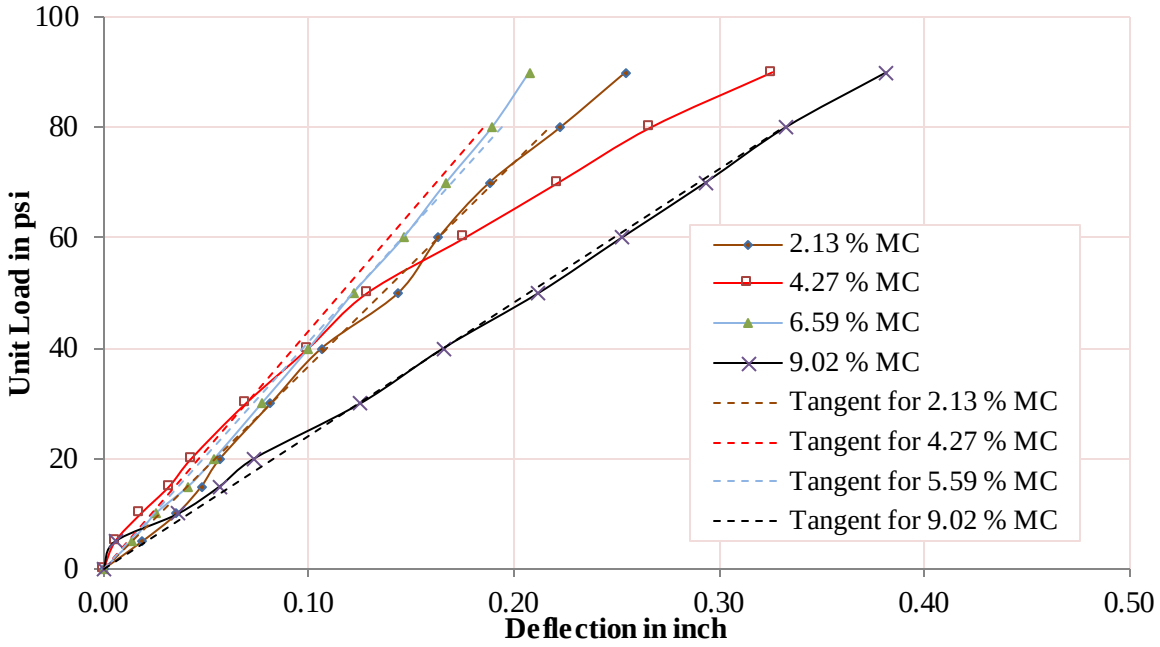

Figure 5-62 Unit Load versus Deflection Curve of 20% Fouled Ballast by Coal Dust

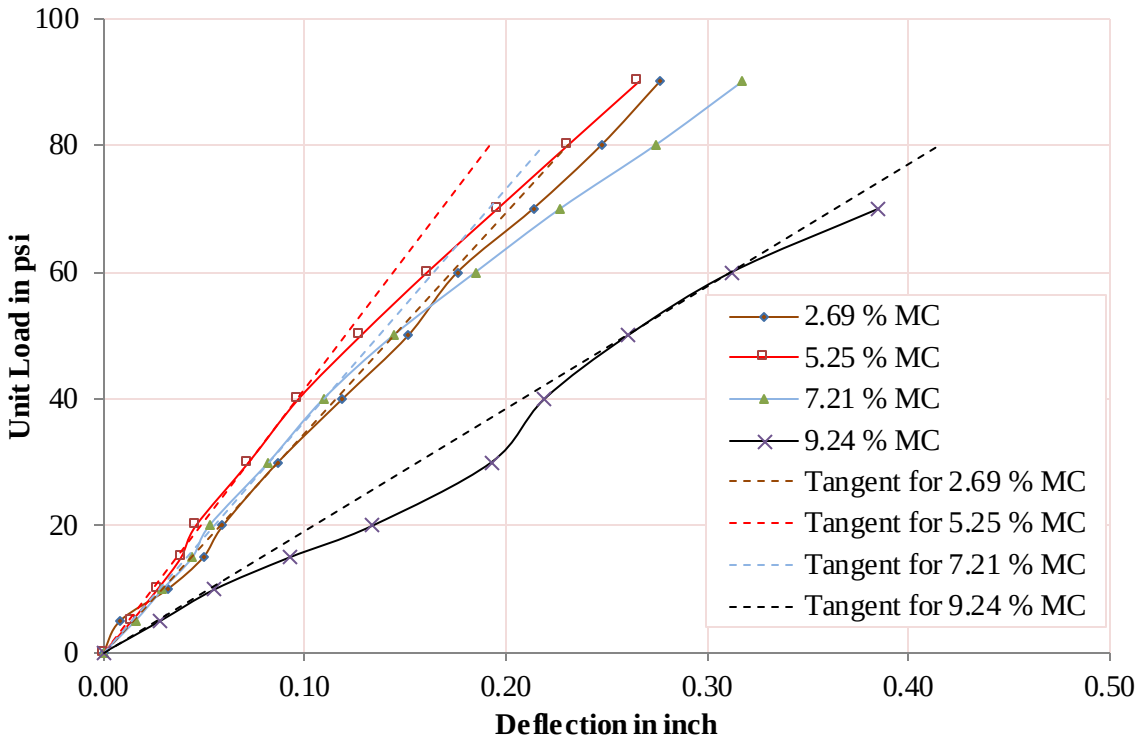

Figure 5-63 Unit Load versus Deflection Curve of 30% Fouled Ballast by Coal Dust

The stiffness of the coal dust fouled ballast for different moisture contents are tabulated in Table 5.14, and the corresponding chart is plotted in Figure 5.64:

Table 5-14 Stiffness of Coal Dust Fouled Ballast with Various Moisture Contents

Fouling Types	Items	Sample 1	Sample 2	Sample 3	Sample 4
10% Fouling	Moisture Content	2.3%	5.2%	7.9%	
	subgrade reaction (psi/in)	421	464	327	
20% Fouling	Moisture Content	2.1%	4.3%	6.6%	9.0%
	subgrade reaction (psi/in)	368	432	411	242
30% Fouling	Moisture Content	2.7%	5.3%	7.2%	9.2%
	subgrade reaction (psi/in)	346	416	366	192

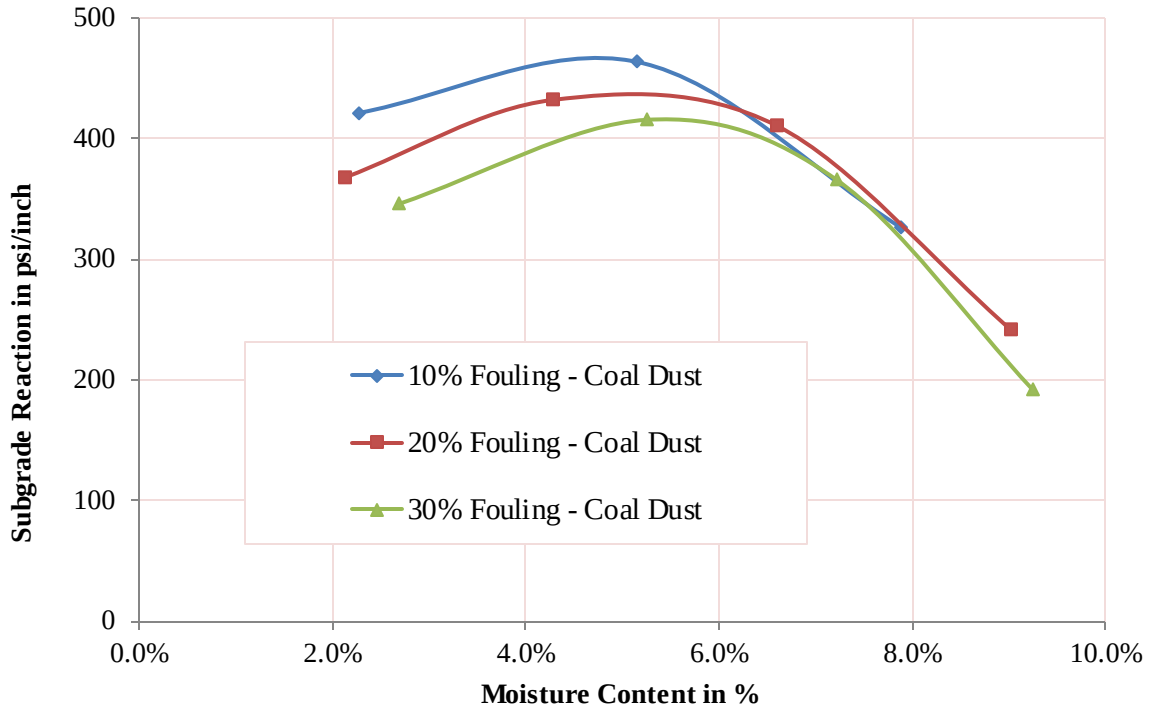

Figure 5-64 Stiffness of Coal Dust Fouled Ballast with Various Moisture Contents

Figure 5.65 represents the static modulus at different moisture contents for Gardner track ballast dust fouled ballast with different degrees of fouling.

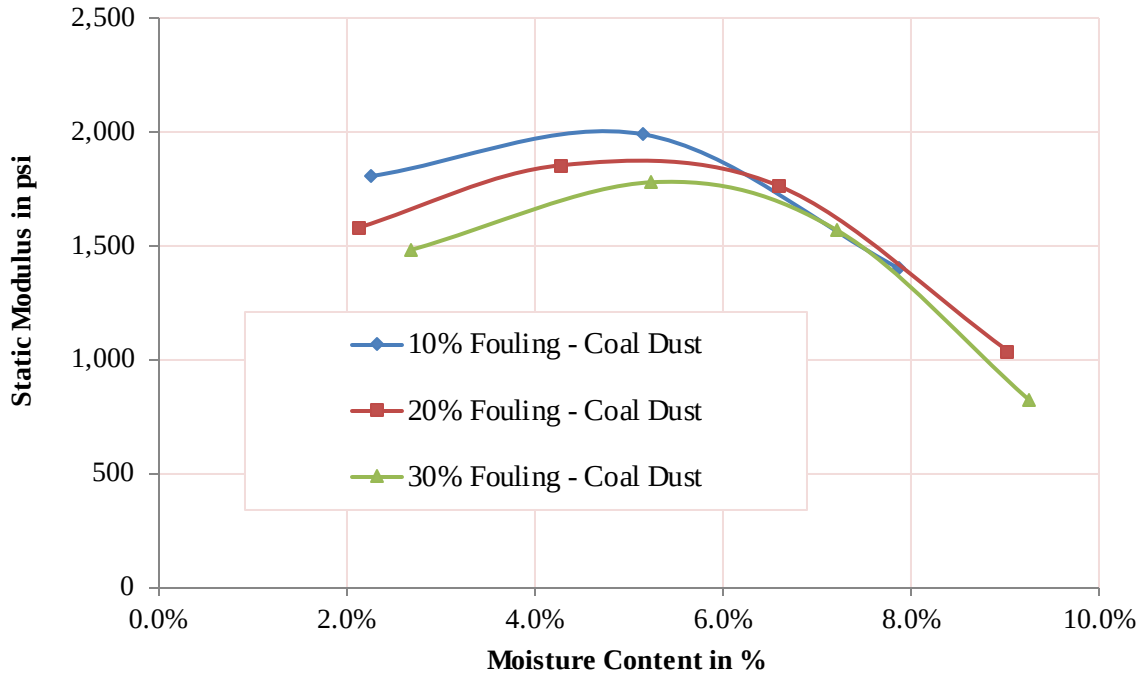

Figure 5-65 Static Modulus of Coal Dust Fouled Ballast with Various Moisture Contents

The highest value of the static modulus was obtained for 10% ballast fouled with coal dust. The optimum moisture content for the static modulus increased as the fouling content increased from 10% fouling toward 30% fouling. The optimum values of static modulus for 10%, 20% and 30% fouling by coal dust were found to be 2,005, 1,870, and 1790 psi at 4.70%, 5.0% and 5.50% moisture contents, respectively.

5.9.4. Comparison of Static Modulus for Different Fouling Agents

Figures 5.66 to 5.69 show the relationships between static modulus and water content for various fouling materials for the same percentages of fouled materials by weight. Similar to the results for resilient modulus, the static modulus of Gardner track ballast dust fouled ballast had the highest static modulus when compared with subgrade soil fouled ballast and coal dust fouled ballast. The static modulus of coal dust fouled ballast is significantly lower than the moduli for the other two types of fouled ballast. The moisture content for the optimum value of static

modulus is the lowest for Gardner track ballast dust fouled ballast and is the highest for subgrade soil fouled ballast.

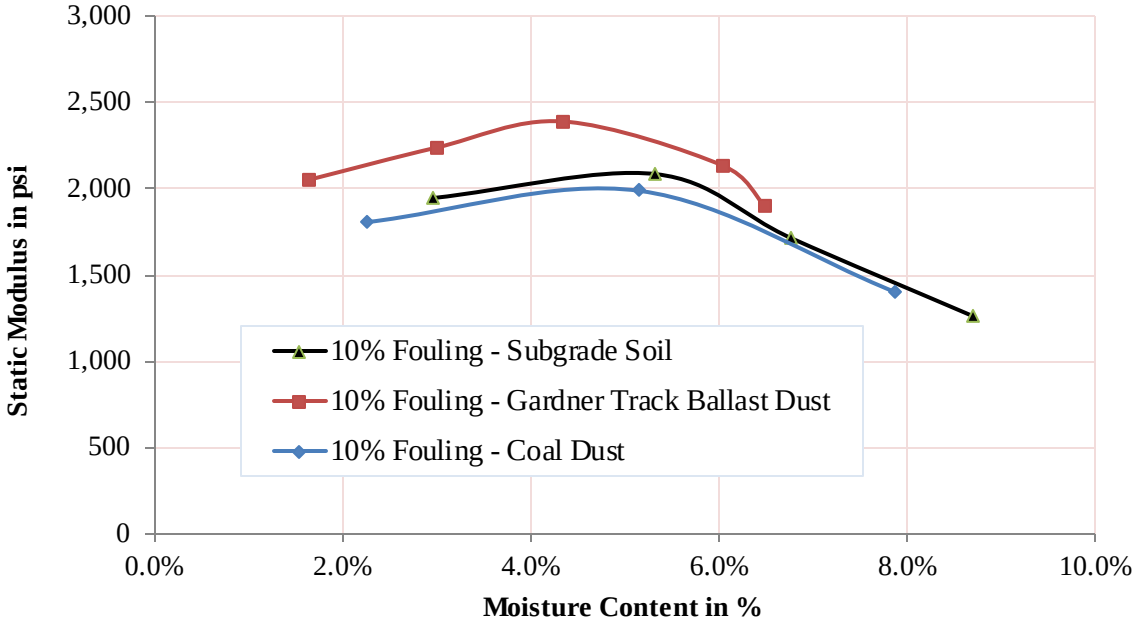

Figure 5-66 Comparison of Static Modulus versus MC at 10% Fouling

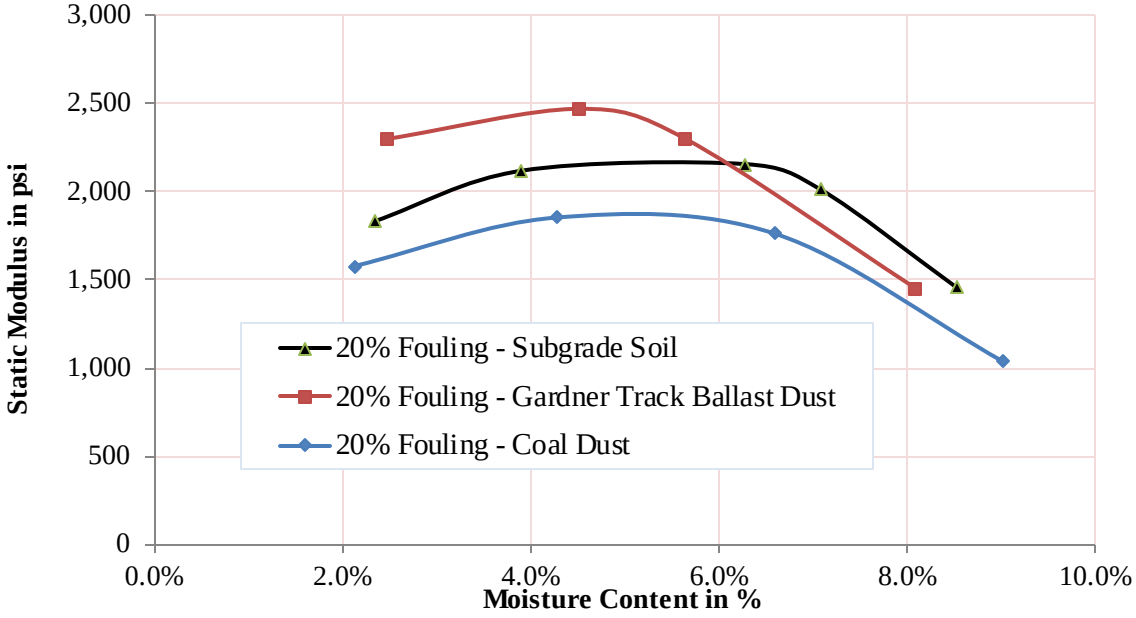

Figure 5-67 Comparison of Static Modulus versus MC at 20% Fouling

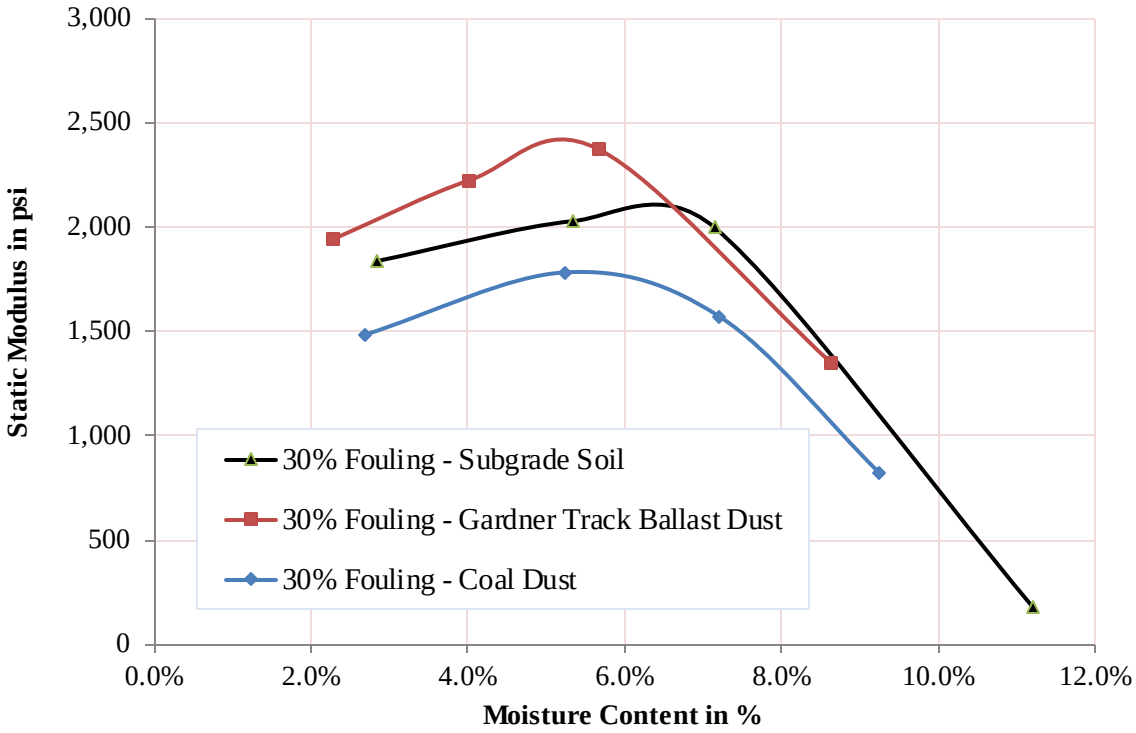

Figure 5-68 Comparison of Static Modulus versus MC at 30% Fouling

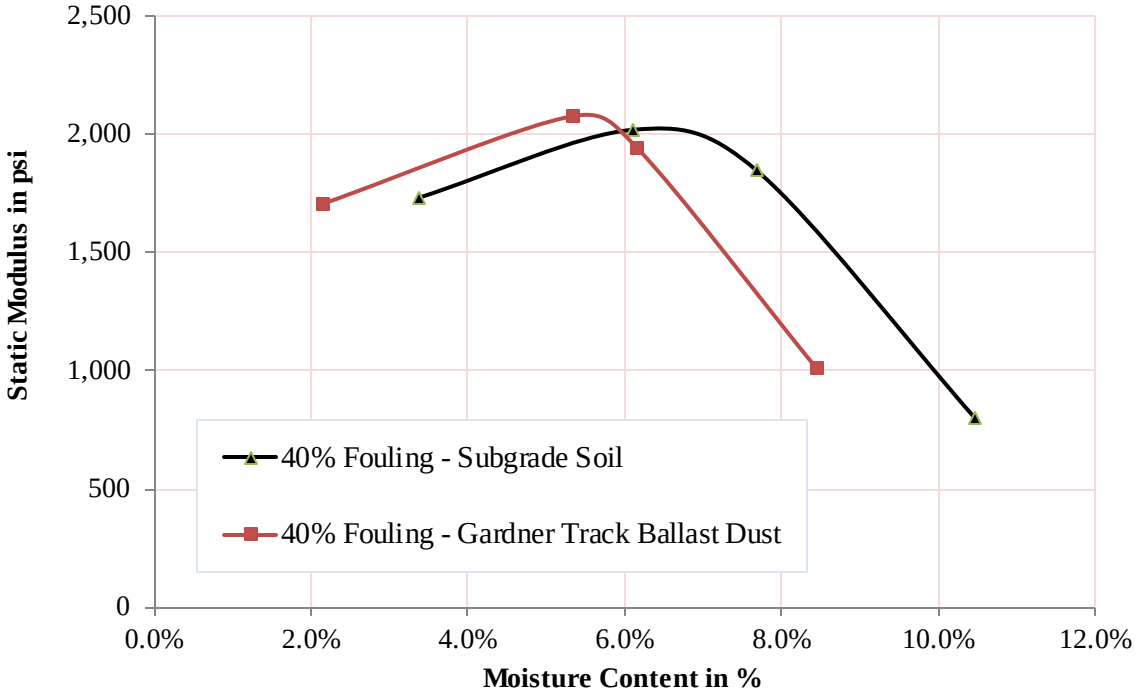

Figure 5-69 Comparison of Static Modulus versus MC at 40% Fouling

5.9.5. Discussion of Static Modulus of Fouled Ballast

The trend for the static modulus of fouled ballast is similar as that of the resilient modulus. The maximum value of static modulus occurred at the OMC_{MS} and these OMC_{MS} values were different for different fouling agents. There was a slight variation of OMC_{MS} depending upon the amount of fouling materials for particular types of fouled ballast, however the average OMC_{MS} were 6% for subgrade soil fouled ballast, 5% for Gardner track ballast dust fouled ballast and 5.5% for coal dust fouled ballast. The variation in OMC_{MS} of coal dust fouled ballast was higher when compared with subgrade soil fouled ballast and the Gardner track ballast dust fouled ballast.

The Gardner track ballast dust fouled ballast had the highest static modulus followed by subgrade soil fouled ballast and coal dust fouled ballast. The maximum static modulus at optimum moisture content was approximately 2000 psi for all types of fouling ratios by weight in subgrade soil fouled ballast; 2400 psi for Gardner track ballast dust fouled ballast, and approximately 1700 psi in coal fouled dust ballast.

5.10. Correlation of Strength Properties of Fouled Ballast

5.10.1. Correlation of Resilient Modulus and Static Modulus of Fouled Ballast

The relationship between resilient modulus and static modulus is plotted in Figure 5-70. Here, the trend lines of the static modulus versus resilient modulus are nearly parallel to each other for all types of fouling. From the data, the variation range (ratio of resilient modulus to the static modulus) of resilient modulus with static modulus for subgrade soil fouled ballast, Gardner track ballast dust fouled ballast and the coal dust fouled ballast are 1.7 to 2.8, 1.7 to 2.1, and 1.3 to 1.9, respectively. The r-squared (r2) value of subgrade soil, Gardner track ballast dust and coal dust

fouled ballast are 0.88, 0.90 and 0.75, respectively. Hence, it can be inferred that a strong correlation exists between resilient and static moduli for Gardner track ballast dust fouled ballast and subgrade soil fouled ballast, and a moderately strong correlation exists for coal dust fouled ballast.

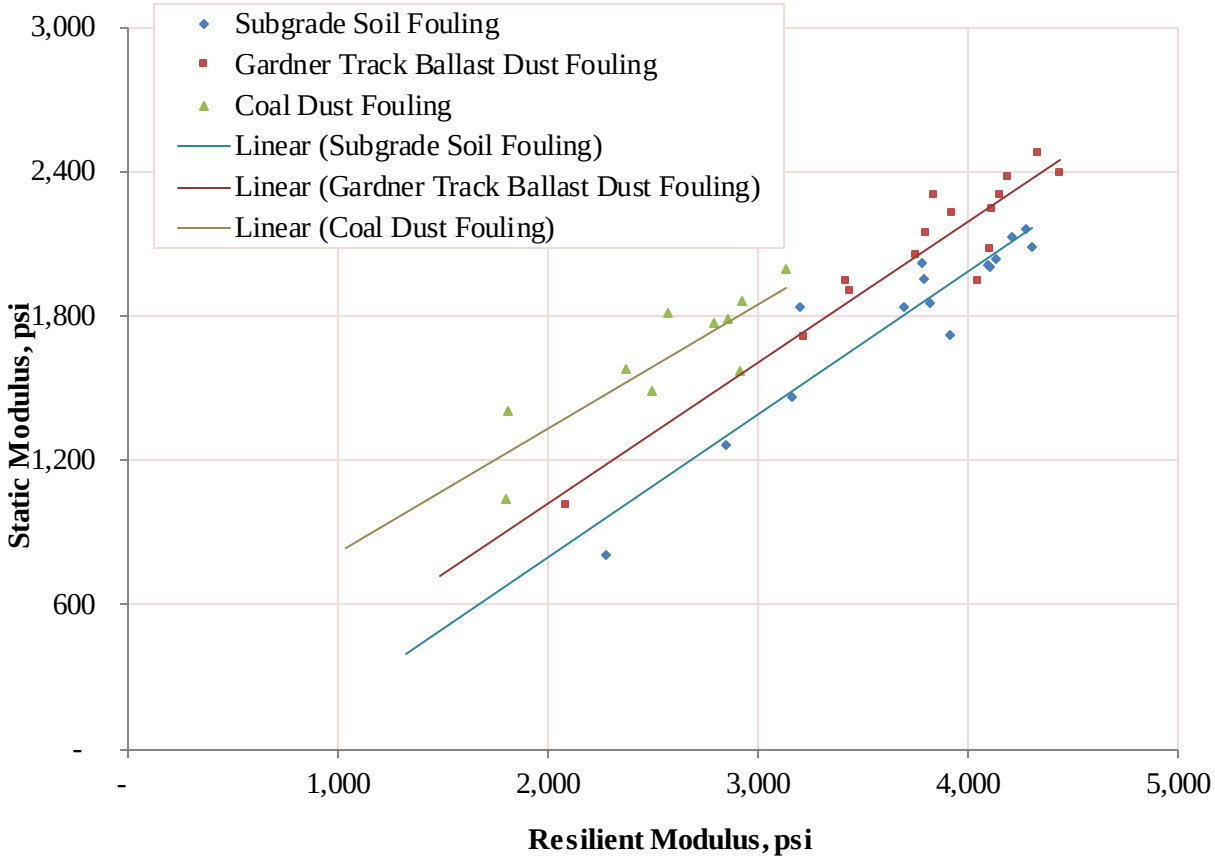

Figure 5-70 Correlation of Resilient Modulus and Static Modulus of Fouled Ballast

5.10.2. Correlation of Resilient Modulus and CBR for Fouled Ballast

Figure 5.71 shows the correlation between resilient modulus and CBR determined using the DCP for different types of fouled ballast. The correlation between CBR and resilient modulus is not as strong as that between static modulus and resilient modulus, as demonstrated by the r-squared (r^2) values of 0.48 for subgrade soil fouled ballast, 0.58 for Gardner track ballast dust fouled ballast and 0.22 for coal dust fouled ballast.

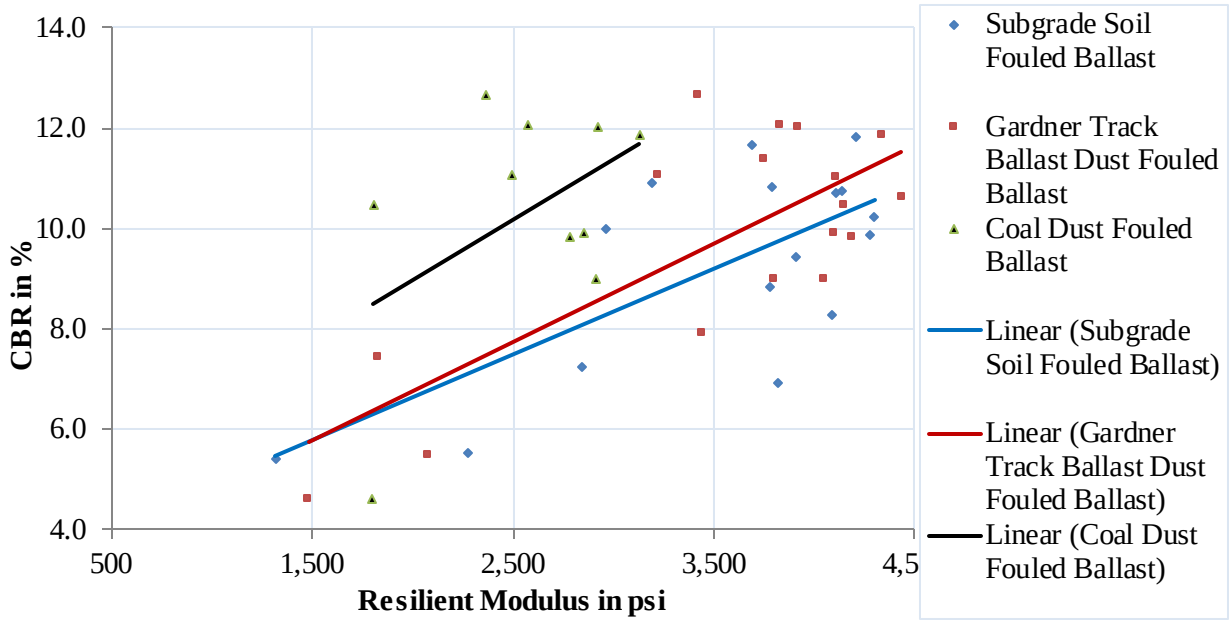

Figure 5-71 Correlation of Resilient Modulus and CBR of Fouled Ballast

5.10.3. Correlation of Static Modulus and CBR of Fouled Ballast

The correlation between the static modulus and the CBR is also relatively weak. Figure 5.72 shows the corresponding correlation data between the CBR and the static modulus. R-squared (r^2) values were 0.51 for subgrade soil fouled ballast, 0.45 for Gardner track ballast dust fouled ballast and 0.55 for coal dust fouled ballast.

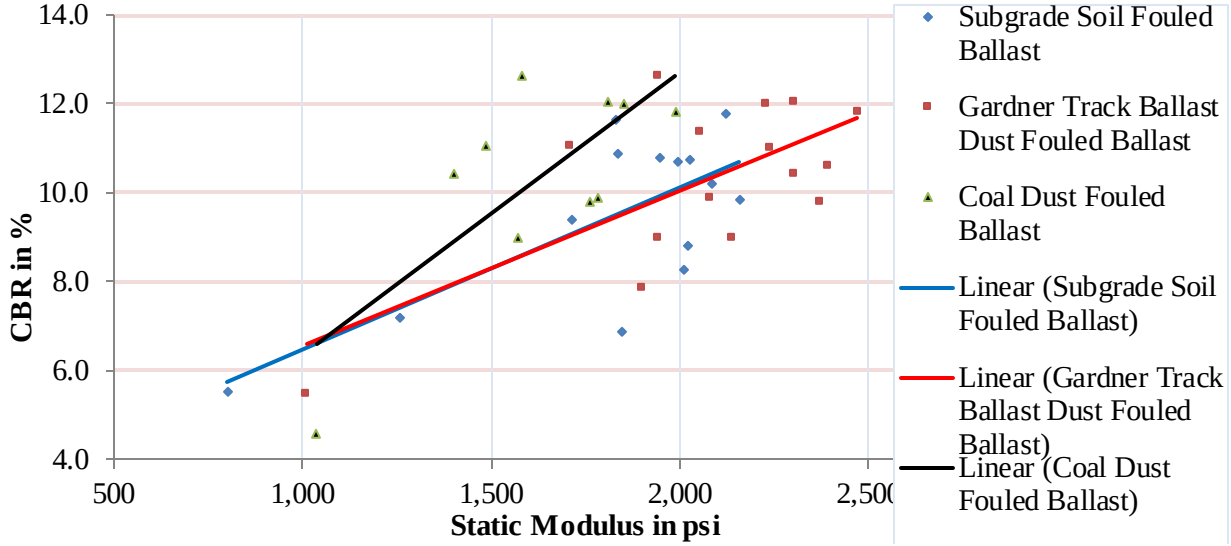

Figure 5-72 Correlation of Static Modulus and CBR of Fouled Ballast

5.10.4. Discussion of Correlation of Strength Properties

The previously mentioned correlations suggested that the static and resilient moduli are well correlated to each other and one parameter can be inferred if another is known. The r-squared values are also near 1.0 for all types of fouled ballast. The slopes of the relationships are also very similar.

The correlation of CBR with either static or resilient modulus was not strongly established as r-squared values were around 0.6 or less.

5.11. Result of Proctor Test

The maximum dry density of the ballast fouled with subgrade soil was found to correspond to 20% fouling by weight, which was higher than the optimum density of the 20% ballast fouling by the Gardner track dust. Ballast fouled with the Gardner track dust had a maximum density at 30% fouling by weight. The coal dust fouled ballast had the maximum dry density at 10% fouling by weight. Figures 5.73 to 5.75 show the results of the optimum moisture contents for maximum dry densities of the test samples.

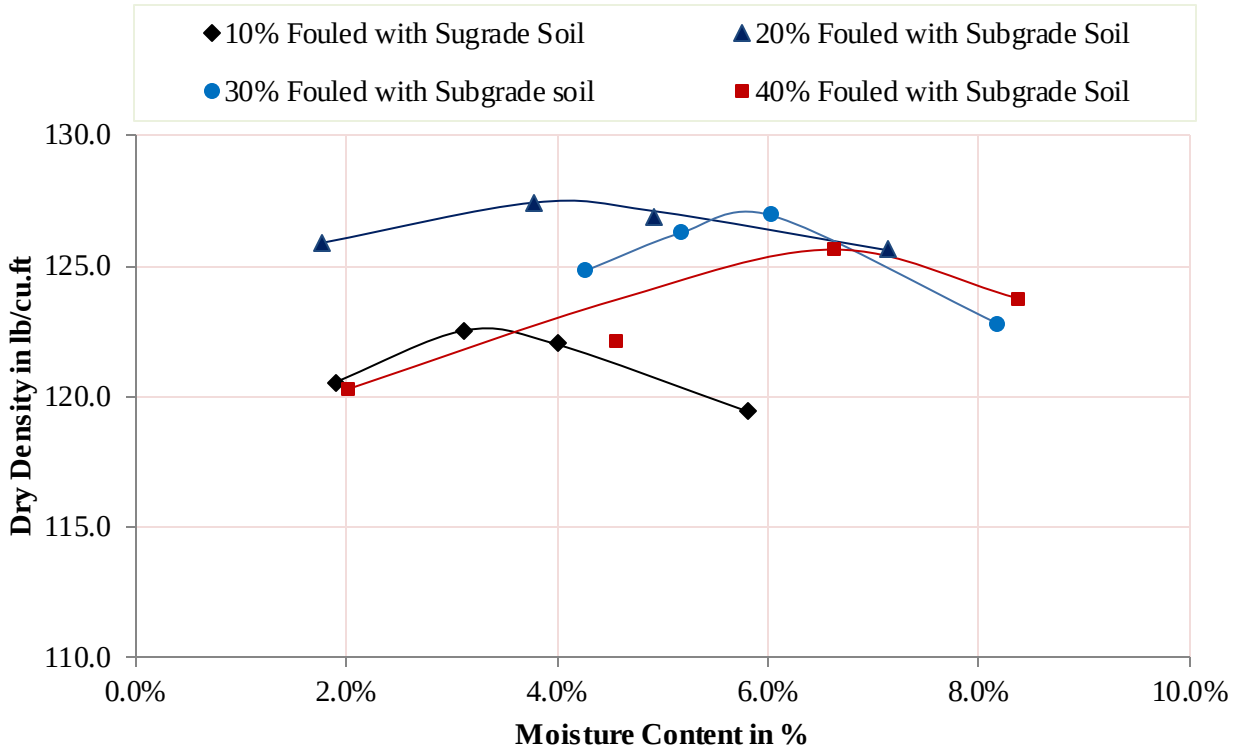

Figure 5-73 Dry Densities versus Moisture Content of Subgrade Soil Fouled Ballast

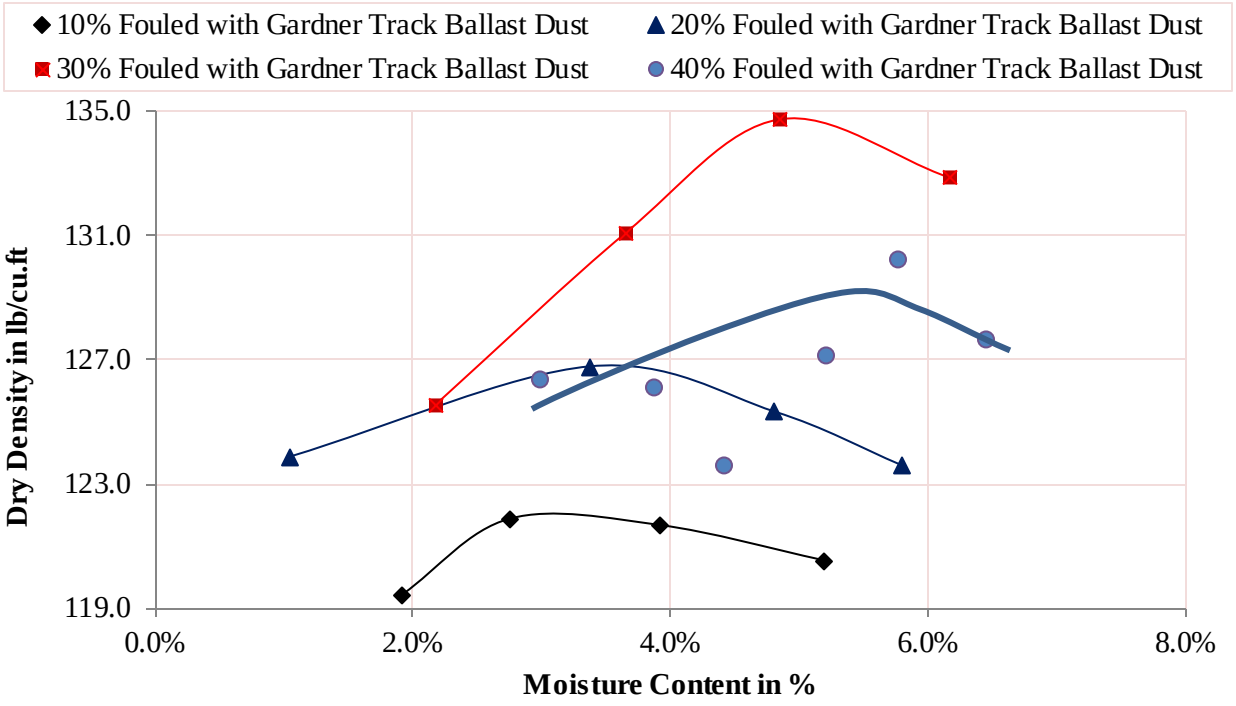

Figure 5-74 Dry Densities versus Moisture Content of Gardner Track Dust Fouled Ballast

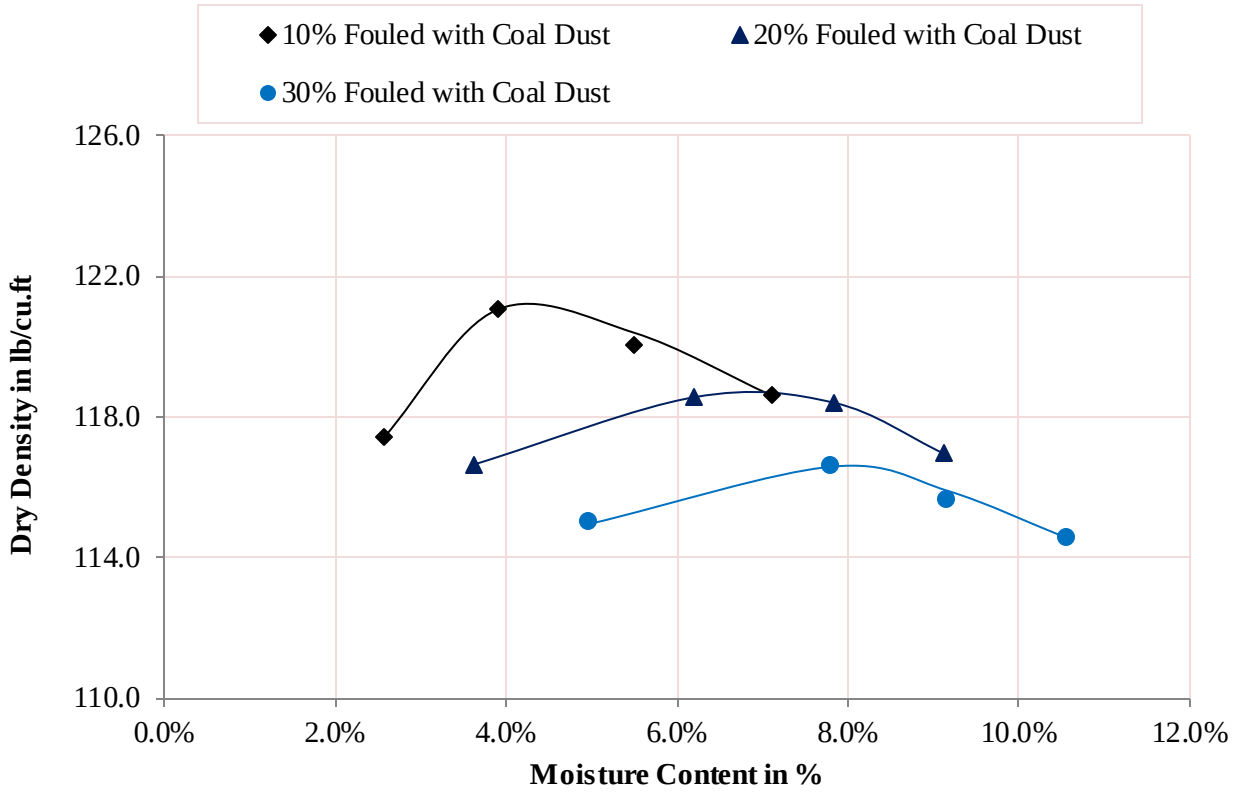

Figure 5-75 Dry Densities versus Moisture Content of Coal Dust Fouled Ballast

From the above figures, the optimum densities for the subgrade fouled ballast, the Gardner track dust fouled ballast, and the coal dust fouled ballast were in the range of 119.4 to 127.4 lb/cu.ft, 119.5 to 134.7 lb/cu.ft, and 114.5 to 121.1 lb/cu.ft, respectively.

The comparison of the optimum dry densities and the corresponding moisture contents are presented in the following figures. The maximum dry density of the subgrade soil fouled ballast occurred at 20% fouling at a moisture content of 3.8%. The highest dry density of Gardner track dust fouled ballast was at 30% fouling and had a moisture content of 4.8%. Coal dust fouled ballast had the highest dry density at 10% fouling with a 3.9% moisture content. Dry densities were almost the same with a range of 120 to 122 lb/cu.ft for all types of fouling with fouling contents of 10% at optimum moisture content.

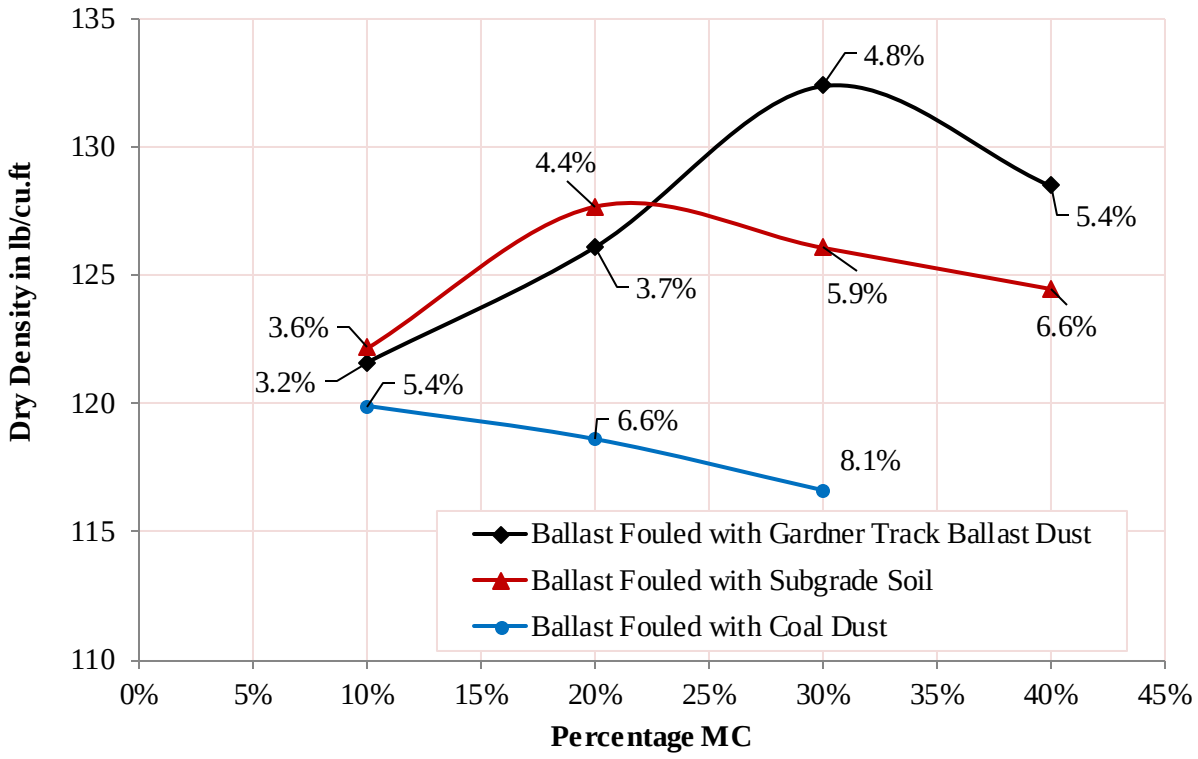

Figure 5-76 Optimum Dry Densities versus Percentage Fouling by Weight

The values reported in figure 5.2 (Average dry densities on text box versus percentage fouling by weight) are similar to the results obtained from the proctor tests (figure 5.76). So, the test samples were compacted almost in the same densities of the optimum dry densities.

5.12. Field Test Results

5.11.1. Resistivity Test Results

Table 5.15 shows the resistivity test results from the Midland Railway Track near Baldwin, Kansas. The tests were conducted at the middle of the track both perpendicular as well as parallel to the track.

Table 5-15 Field Resistivity Data of Midland Railroad Track

Location	Position at Location	Probe Spacing (in)		Resistivity Recorded		Average Resistivity (Ω-cm)
		Test 1	Test 2	Test 1	Test 2	
Site A	Perpendicular to track -middle	12	18	8,400	9,200	8,800
	Parallel to track - middle	12	18	8,200	9,800	9,000
	Parallel to track - shoulder	12	18	17,900	23,100	20,500
Site B	Perpendicular to track - middle	12	18	14,600	13,200	13,900
	Parallel to track - middle	12	18	17,600	16,700	17,150
	Parallel to track - shoulder	12	18	26,900	26,200	26,550

For site A (near the crossing of Montana Road with rail track), the resistivity measurements parallel and perpendicular to the track were almost the same. For site B (near the crossing of US 59 with rail track), the two readings were quite different. Similarly, the resistivity readings of shoulder ballast for the two sites were higher than the corresponding center reading of the resistivity. The resistivity of site B was higher than the resistivity of site A.

5.11.2. Test Results of DCP

Figure 5.77 and 5.78 represents the depth in inches versus penetration index in inches/blow of the DCP test for site locations A and B.

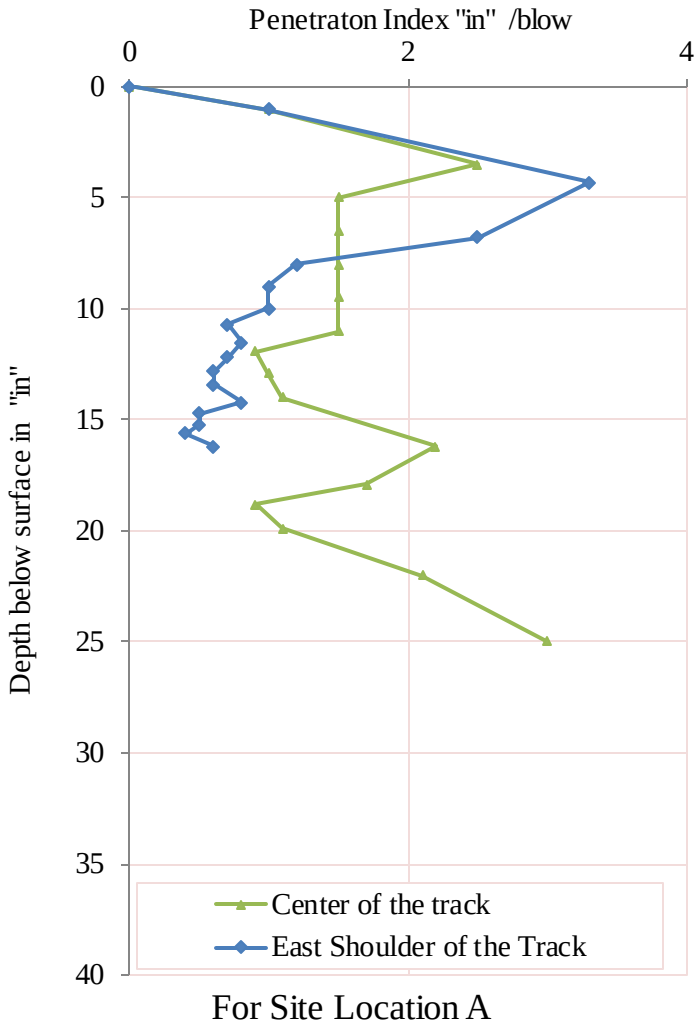

Figure 5-77 Depth versus Penetration Index for Site Location A

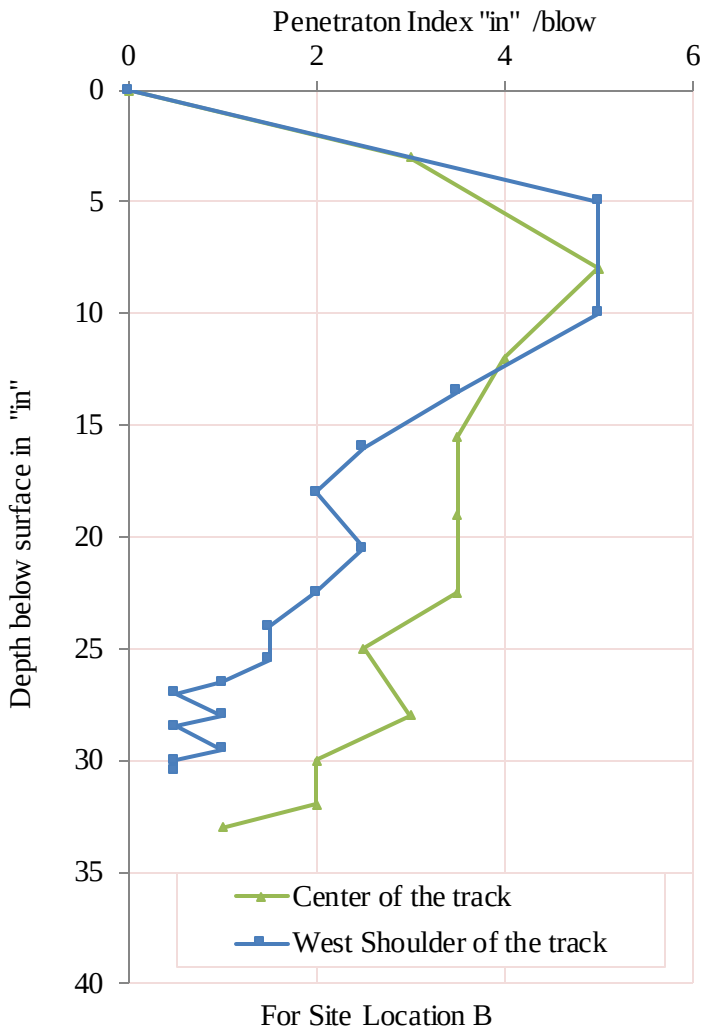

Figure 5-78 Depth versus Penetration Index for Site Location B

From figure 5.77, it can be observed that the depth of the ballast layer for both the center of the track as well as the east shoulder was around 25 inches for site location A. Also, it can be inferred that the ballast depth of the center track was around 20 inches while the depth of the west shoulder was around 10 inches for site location B. From the above two graphs, penetration index as well as the CBR of the four locations are listed in the table 5.16. The CBR value was calculated from average penetration index (PI) of ballast layers.

Table 5-16 CBR of Sites from Field Test by DCP Method

Descriptions of Position at a Location	Penetration Index (mm/blow)		CBR in %	
	Site A	Site B	Site A	Site B
Center of the track	90.7	38.8	1.9	4.8
Shoulder of the track	64.8	33.7	2.7	5.7

So, Site A was very weak as compared to Site B and even Site B was not very strong. The penetration graphs shows that the subgrade soil had a higher CBR than the ballast layer.

5.11.3. Test Result of LWD

Table 5.17 shows the resilient modulus of the different test sites in the field.

Table 5-17 Resilient Modulus of Field Sites from LWD Method

Descriptions of Position at a Location	Resilient Modulus	
	Site A	Site B
Center of the Track	1,700	1,900
Shoulder of the Track	2,090	2,410

As shown in Table 5-17, the resilient modulus data showed that Site A was not as stiff as Site B at the center or the shoulder.

5.11.4. Discussion of Field Test

Since the moisture content of site A was higher than site B (reported in chapter 3.7.5), the resistivity readings of site A were very low as compared to site B. The gradation of the ballast for the two sites shown in figures 3.17 and 3.18 shows that the central track ballast had a high amount of fouling material when compared with the shoulder ballast. Moreover, the gradation

and the resistivity results showed that more fouling was present at Site A when compared with Site B.

The CBR of the track was very low. The subgrade soil of the rail track had a higher CBR than the ballast layer. It was reported that the track was laid on the top of an existing old blacktopped road, however this was not confirmed. During the field visit some chunks of bituminous road top were found at the side of the track.

LWD results were consistent with CBR and resistivity in showing that Site A was comparatively weaker than B. For both sites, the center of track was weaker when compared with the shoulder, this was likely due to the higher percentage of fouling material.

Field test results are comparable to the lab test samples. Field test resistivity data shows that the sample fouling fell between 30% and 40% by weight of subgrade soil fouled ballast for site A and is consistent with 30% fouled by subgrade soil fouled ballast for site B. Similarly, CBR values for both sites were very low due to the high amount of fouling as well as the high water contents. Also, the resilient modulus of the ballast was very low and was likely caused by the highly fouled ballast having higher amount of water content. Hence, it could be concluded from the non-destructive and rapid test methods that this ballast had in excess of 30% fouling. This was confirmed by the soil samples excavated from the sites and the results are presented in chapter 3.7.

Chapter Six: Conclusions and Recommendations

6.1 Introduction

Forty-eight small box tests were carried out to relate resistivity with amount of ballast fouling based on different types of fouling materials. Among the 48 tests, 18 tests were conducted on sample ballast fouled with a series of percentages of subgrade soil, another 17 tests were conducted on sample ballast fouled with a series of percentages of Gardner track ballast dust, and 11 tests were conducted on ballast fouled with a series of percentages of coal dust.

Section 6.2 contains conclusions developed from the results of density tests of the ballast and section 6.3 contains conclusions developed from the resistivity testing with different fouling agents based on different moisture contents. Sections 6.4, 6.5, and 6.6 describe the conclusions of CBR tests carried out by DCP, resilient modulus tests carried out by LWD, and static modulus carried out by plate loading test, respectively. Section 6.7 describes the results from the field test. Section 6.8 contains recommendations for future work on this research topic.

6.2 Dry Density Test of Fouled Ballast

- The average dry density of the clean ballast was 110.1 lb/ft^3. This density was lower than all types of fouled samples tested. All of samples were compacted with the same compaction energy. The average void ratio of the clean ballast was 0.54.
- The proctor test shows that the maximum dry density was for subgrade soil fouled ballast at 20% fouling and is equal to 127.4 lb/ft^3. The Gardner track dust fouled ballast had a maximum dry density of 30% having a value of 134.7 lb/ft^3. However the coal dust fouled ballast has a maximum dry density of about 121.1 lb/ft^3 for 10% fouling by weight.

- The proctor test sample densities and the average dry densities obtained from the test box were consistent.
- For 10% fouling, all types of fouled samples had almost the same average unit weight. This indicates that all types fouling materials settle into the voids of the ballast for 10% fouling by weight.
- The peak of the coal dust fouled ballast decreased as fouling by weight increased from 10% to 30%. The density of the subgrade soil and Gardner track ballast dust increased as fouling by weight increased initially, and then decreased after their optimum values of 20% and 30% fouling by weight, respectively.
- The relationship between moisture content and dry density (Proctor curve) with percentage of fouling was weak to very weak for all types of fouled ballast.

6.3 Resistivity Analysis

6.3.1. Horizontal Probe Resistivity

- The resistivity of the clean ballast was higher than 440,000 Ω-cm for low water contents.
- The resistivity of the fouling agents were very small when compared with the fouled ballast mix.
- When using a test box of 32 inches square and a 7 inch Wenner probe spacing, the resistance should be measured at a distance of more than 8 inches from the boundary parallel to the horizontal probe alignment direction. The current paths are spread almost at equal distance to the probe spacing in the horizontal plane when the array is at least this far from the boundary.
- The resistivity of subgrade soil fouled ballast was low and nearly constant for moisture content levels above 6%. Resistivity values for ballast fouled with the Gardner track

ballast dust were low and nearly constant for moisture content levels above 5%, and for coal dust fouled ballast the resistivity was low and nearly constant for moisture content levels above 5.5%. This moisture content required for resistivity definition is referred to as "optimum moisture content for resistivity" (OMCR).

- The exact value of OMCR varied slightly depending upon the amount of fouling agent present in the mix. The higher the amount of fouling materials, the higher the OMCR observed. OMCR varied most in coal dust fouled ballast, followed by subgrade soil fouled ballast. The least variance was observed in the ballast fouled with Gardner track ballast dust.
- The higher the amount of fouling, the lower the electrical resistance for moisture content levels near the field capacity state. The Gardner track ballast dust fouled ballast has a lower OMCR and hence has a lower resistance than ballast fouled with other fouling agents for moisture contents near its OMCR. For saturated conditions the coal dust has the highest resistance, followed by Gardner track ballast dust and then subgrade soil fouled ballast. Therefore, water content plays an important role for resistivity detection of fouled ballast along with the types and amount of fouling agents.
- Resistivity of fouled ballast is much lower and more stable for soil samples with a moisture content above the OMCR.
- Resistivity values generally decreased with increased fouling and water content and values were generally consistent with those reported by A.J. Rahman (Rahman, Parsons, Han, & Glavinich, 2014).

- Resistivities estimated by the single point method with a simple multimeter were higher than those measured using the Wenner method. Most of the time measurements with a multimeter were inconsistent, hence it was considered as less reliable test.

6.3.2. Vertical Probe Resistivity

- The vertical probe designed and constructed at the KU CEAE department generated values similar to the horizontal array probe. The apparent resistance from both the methods gives almost the same value for similar vertical and horizontal distances, indicating that this probe is valid for measurement of the resistivity.
- The vertical probe measures a higher resistance consistently when compared with the Wenner 4 point method in the box test. This is likely because it also measures the apparent resistance caused by insufficient penetration depth.

6.4 CBR Test

- The highest CBR was found at 20% fouling by weight in subgrade soil fouled ballast, 30% fouling by weight in Gardner track ballast dust fouled ballast, and 10% fouling by weight in coal fouled ballast.
- Strength dropped significantly when moisture content exceeded a threshold value. This threshold value was found at higher moisture content for the samples with more fouling. Samples with less fouling experienced strength loss at lower moisture contents. This threshold moisture was termed as "optimum moisture content for CBR (OMC_C)" and this value was very similar to the threshold value of resistivity (OMCR).
- Gardner track ballast dust fouled ballast lost strength quickly as moisture content increased above OMC_C. Subgrade soil fouled ballast and coal dust fouled ballast also lost strength with increasing moisture above the OMC_C, but at a slower rate.

- As moisture contents decreased below the OMC_C, CBR decreased slightly or approximately constant. However, the slope of the CBR versus moisture content below the OMC_C is very gentle and constant.
- Coal dust fouled ballast always has a smaller value of CBR when compared with subgrade soil fouled ballast and Gardner track ballast dust ballast. However, the coal dust fouled ballast CBR, while it decreases with increasing moisture, is not as sensitive to the moisture content as the other fouling agents.

6.5 Resilient Modulus

- The average maximum values for resilient modulus corresponded to approximately 6%, 5%, and 5.5% for subgrade soil, Gardner track ballast dust, and coal dust fouled ballast, respectively. Actual values varied slightly based on the percentage of fouling. These moisture contents are represented by "optimum moisture content for resilient modulus (OMC_{MR})". This value is similar to the OMCR.
- The maximum resilient modulus of Gardner track ballast dust fouled ballast occurs in a narrower range when compared to the subgrade soil fouled ballast and the coal dust fouled ballast.
- For moisture contents less than OMC_{MR}, the resilient modulus has a positive mild slope (i.e. increasing modulus with increasing moisture). The resilient modulus at moisture contents greater than OMC_{MR} has a steep negative slope (i.e. decreasing with increasing moisture).
- The negative slope after reaching OMC_{MR} of the resilient modulus versus moisture content curve is steeper for Gardner track ballast dust fouled ballast than it is for both subgrade soil fouled ballast and coal dust fouled ballast.

- The Gardner track ballast dust fouled ballast had the highest maximum resilient modulus, followed by subgrade soil fouled ballast and coal dust fouled ballast for the same percentages of fouling by weight.

6.6 Static Modulus

- The average maximum values for static modulus were approximately 6%, 5%, and 5.5% moisture content for subgrade soil, Gardner track ballast dust and coal dust fouled ballast, respectively and these moisture contents are termed as OMC_{MS}. Actual values varied slightly depending on the percentage of fouling. This is similar to the OMCR.
- The maximum static modulus for Gardner track ballast dust fouled ballast varies less when compared with both the subgrade soil fouled ballast and the coal dust fouled ballast.
- For the same percentage of fouling material by weight, the Gardner track ballast dust fouled ballast has the highest stiffness, followed by subgrade soil fouled ballast and then coal dust fouled ballast.

6.7 Correlation of CBR, Static Modulus, and Resilient Modulus

- The static and resilient moduli both showed a high degree of correlation for all types of fouling agents having r^2 values of 0.88, 0.90 and 0.75 for subgrade soil, Gardner track ballast dust and coal dust fouled ballast. The slopes of all correlation lines were very similar.
- There was limited correlation between CBR and either static or resilient moduli since r^2 values were around 0.6 or lower.

6.8 Field Test

- Both field sites had more than 15% of fines and moisture contents greater than OMCR (10% at site A and 6% at site B). Therefore, these sites were suitable for fouling detection by the resistivity method.
- Resistivity test were carried out and very low resistivity values were measured. It was concluded that the sites were highly fouled. The center of the track was highly fouled as compared to the shoulder – which was also supported by the grain size distribution analysis. When comparing the two sites, site A had a higher amount of fouling material and a higher water content.
- The CBR of the ballast layer was lower than the CBR of the subgrade at the test sites. It was reported that the track line was originally a roadway and had very strong subgrade soil, although this was not confirmed.
- The CBR of Site A was very low when compared with Site B, although Site B also had a very low CBR.
- The resilient modulus of Site B was higher than the resilient modulus of Site A.

6.9 Recommendations

The following recommendations are suggested for future research on this topic.

- Since temperature is another major factor for governing the resistivity of fouled ballast, studies on temperature effects on resistivity are recommended.
- The four probe method is recommended instead of fall of potential method for construction of vertical probe.

- A mechanical method of compaction with uniform load application throughout the section is recommended for the compaction of soil in box tests in future works since errors may occur in test results due to non-uniform compaction carried out with the manual rammer.
- It is recommended that extensive field testing be carried out to evaluate the validity of the resistivity method for practical applications.

Bibliography

AAR. (2013). *Total Annual Spending - 2012 Data*. Washington, DC: Association of American Railroads : https://www.aar.org/.

AAR. (2014). *Overview of America's Freight Railroads*. https://www.aar.org/: Association of American Railroads.

Anthony, C. (1996). *Seeing Beneath Soil*. London: Routledge, c/o Taylor & Francis Group LLC.

Archie, G. E. (January 1942). The Electrical Resistivity Log as an Aid in Determining Some Reservoir Characteristics. *Petroleum Technology*.

(2010). *AREMA manual for railway engineering*. AREMA, American Railway Engineering and Maintenance-of-Way Association.

Ayers, M. E., Thompson, M. R., & Uzarski, D. R. (1989). Rapid Shear Strength Evaluation of in situ Granular Materials. *Transportation Research Record 1227*, 134-146.

Blattner, C. J. (1982). Study of Driven Ground Rods and Four Point Soil Resistivity Tests. *IEEE Transactions on Power Apparatus and Systems, Vol. PAS-101, No. 8* .

Campbell, R. B., Bower, C. A., & Richards, L. A. (1948). Change of electrical conductivity with Temperature and the Relation of Osmotic Pressure to Electrical Conductivity and Ion Concentration for Soil Extracts. *Soil Science Society of America, Proceedings 13*, 66–69.

Datta, M., Basu, A. K., & Roy Chowdhury, M. M. (1967). Determination of earth resistance of multiple driven-rod electrodes. *Institution of Electrical Engineers - IEE, Vol. 114, No. 7*.

Ebrahimi, A. (2011). Behavior of Fouled Ballast. *Railway Track and Structures, Aug 2011; 107, 8*, 25.

FRA Annual Report. (2012). *Railroad Safety Statistics - 2010 Annual Report*. Washington, DC: U.S. Department of Tranportation, Federal Railroad Administration (FRA).

Fukue, M., Minatoa, T., Horibe, H., & Taya, N. (1999). The microstructure of clay given by resistivity measurements. *Engineering geology, Volume 54*, 43-53.

Goyan, V. C., Gupta, P. K., Seth, S. M., & Singh, V. N. (1996). *Estimation of temporal changes in soil moisture using resistivity method*. Hydrological Processes, John Wiley & Sons, Ltd.

Harison, J. A. (1987). California Bearing Ratio and Dynamic Cone Penetrometer Strength Measurement of Soils. *Proceedings - Institution of Civil Engineers, Part 2*, 834 - 844.

Hay, W. W. (1982). *Railroad Engineering* (Second ed.). NY: A Wiley - Interscience Publication.

Huang, H., Tutumluer, E., & Dombrow, W. (2009). Laboratory Characterization of Fouled Railroad Ballast Behavior. *Transportation Research Record: Journal of the Transportation Research Board, No 2117*, 93 - 101.

Indraratna, B., Khabbaz, H., Salim, W., & Christie, D. (2006). Geotechnical properties of ballast and the role of geosynthetics in rail track stabilisation. *International Society for Soil Mechanics and Geotechnical Engineering (ISSMGE), Vol. 10(3)* , 91-102.

Lekarp, F., Isacsson, U., & Dawson, A. (2000). State of Art. I: Resilient Response of Unbound Aggregates. *Journal of Transportation Engineering, Vol. 126, No. 1*, 66-75.

Leng, Z., & Al-Qadi, I. L. (2010). Railroad Ballast Evaluation Using Ground - Penetrating Radar - Laboratory Investigation and Field Validation. *Transportation Research Record: Journa lof the Transportation Research Board, No 2159*, 110-117.

Liu, X., Saat, R., & Barkan, C. P. (2012). Analysis of Causes of Major Train Derailment and Their Effect on Accident Rates. *Transportation Research Record: Journal of the Transportation Research Board, No. 2289*, 154–163.

Majidzadeh, K. (2010). Innovative Methodology in Railroad Track Substructure Integrity Investigations. *Ohio Transportation Engineering Conference* . Ohio.

Rahman, A. (2013). *Permiability, Resistivity and Strength of Fouled Railroad Ballast*. Lawrence: Department of Civil Environmental, and Architechtural Engineering, The University of Kansas.

Rahman, A., Parsons, R. L., Han, J., & Glavinich, T. E. (2014). *Permiability, Resistivity and Strength of Fouled Railroad Ballast*. Lincoln, NE: Mid-America Transportation Center, University of Nebraska-Lincoln.

Read, D., Hyslip, J., McDaniel, R., & Lees, H. (2010). Track substructure research - ballast fouling investigations. *Railway Track & Structures; Dec 2010; 106, 12*, 19-24.

Rhoades, J. D., Corwin, D. L., & Lesch, S. M. (1999). GeospatialM easurementso f Soil ElectricalC onductivityt o AssessS oil Salinity and Diffuse Salt Loading from Irrigation. *The American Geophysical Union - Assessment of Non-Point Source Pollution in the Vadose Zone GeophysicaMl onograph1 08* .

Salgado, R., & Yoon, S. (2003). *Dynamic Cone Penetration Test for Subgrade Assessment*. Purdue University, Joint Transportation Research Program. Proj. No. C-36-45S.

Samouelian, A., Cousin, I., Tabbagh, A., Bruand, A., & Richard, G. (2005). Electrical resistivity survey in soil science: a review. *Soil and Tillage Research*, 83, 783-193.

Selig, E. T., & Waters, J. M. (1994). *Track Geotechnology and Substructure Management*. London: Thomas Telford Publications.

Sussmann, T. R., Ruel, M., & Chrismer, S. M. (2012). Source of Ballast Fouling and Influence Considerations for Condition Assessment Criteria. *Transportation Research Record: Journal of the Transportation Research Board, Washington*, 87-94.

Tagg, G. F. (1964). *Earth Resistaces*. New York: Pitman Publishing Corporation.

Wallace, A. J. (2003). *Permiability of Fouled Ballast*. Wollongong, Australia: School of Civil, Mining and Environmental Engineering, University of Wollongong, Wollongong.

Webster, S. L., Brown, R. W., & Porter, J. R. (1994). *Force Projection Site Evaluation Using the Electric Cone Penetrometer (ECP) and the Dynamic Cone Penetrometer (DC)*. Tyndall AFB, FL: Headquarters, U. S. Air Force Civil Engineering Supply Agency.